

CRANFIELD UNIVERSITY

Alhaji Shehu Grema

Optimization of Reservoir Waterflooding

School of Engineering
Process Systems Engineering

PhD
Academic Year: 2011 - 2014

Supervisor: Dr Yi Cao
October 2014

CRANFIELD UNIVERSITY

School of Engineering
Process Systems Engineering

PhD

Academic Year 2011 - 2014

Alhaji Shehu Grema

Optimization of Reservoir Waterflooding

Supervisor: Dr Yi Cao
October 2014

This thesis is submitted in partial fulfilment of the requirements for
the degree of Doctor of Philosophy

© Cranfield University 2014. All rights reserved. No part of this
publication may be reproduced without the written permission of the
copyright owner.

ABSTRACT

Waterflooding is a common type of oil recovery techniques where water is pumped into the reservoir for increased productivity. Reservoir states change with time, as such, different injection and production settings will be required to lead the process to optimal operation which is actually a dynamic optimization problem. This could be solved through optimal control techniques which traditionally can only provide an open-loop solution. However, this solution is not appropriate for reservoir production due to numerous uncertain properties involved. Models that are updated through the current industrial practice of 'history matching' may fail to predict reality correctly and therefore, solutions based on history-matched models may be suboptimal or non-optimal at all.

Due to its ability in counteracting the effects uncertainties, direct feedback control has been proposed recently for optimal waterflooding operations. In this work, two feedback approaches were developed for waterflooding process optimization. The first approach is based on the principle of receding horizon control (RHC) while the second is a new dynamic optimization method developed from the technique of self-optimizing control (SOC). For the SOC methodology, appropriate controlled variables (CVs) as combinations of measurement histories and manipulated variables are first derived through regression based on simulation data obtained from a nominal model. Then the optimal feedback control law was represented as a linear function of measurement histories from the CVs obtained.

Based on simulation studies, the RHC approach was found to be very sensitive to uncertainties when the nominal model differed significantly from the conceived real reservoir. The SOC methodology on the other hand, was shown to achieve an operational profit with only 2% worse than the true optimal control, but 30% better than the open-loop optimal control under the same uncertainties. The simplicity of the developed SOC approach coupled with its robustness to handle uncertainties proved its potentials to real industrial applications.

Keywords:

Optimal control, Receding horizon control, Self-optimizing control, geological uncertainty, controlled variable, Open-loop solution, feedback control, reservoir waterflooding.

ACKNOWLEDGEMENTS

I have to thank the Almighty for making it possible to see this project to completion.

This acknowledgement will never be complete without mentioning my supervisor, in the name of Dr Yi Cao whose academic repute and willingness to impart knowledge make this a successful project. I must appreciate your constructive criticisms, guidance and encouragement at all times. I also have to appreciate the support of the entire staffs of Process Systems Engineering Group.

I am also grateful to SINTEF Applied Mathematics for providing a free license of MATLAB Reservoir Simulation Toolbox (MRST) software.

The financial support of Petroleum Technology Development Fund (PTDF), Abuja throughout my stay in Cranfield University is highly acknowledged. Without their support, this project may not be in existence.

Sincere gratitude and appreciation go to my family and friends whose encouragement and support have been a source of working fluid. Thank you all for making my stay in Cranfield a memorable one.

TABLE OF CONTENTS

ABSTRACT	i
ACKNOWLEDGEMENTS.....	iii
LIST OF FIGURES.....	vii
LIST OF TABLES	xii
LIST OF ABBREVIATIONS.....	xiv
1 Introduction.....	1
1.1 Global Energy Demand.....	1
1.2 Oil and Gas Production Process.....	3
1.3 Waterflooding for Enhanced Oil Recovery.....	5
1.4 Types of Well System	9
1.5 Research Aim and Objectives.....	11
1.6 Thesis Structure.....	12
1.7 Publications	13
1.7.1 Published Work	13
1.7.2 Proposed Publications.....	14
2 Literature Review	15
2.1 Oil and Gas: Origin, Exploration, Development and Production	15
2.1.1 Origin of Oil and Gas.....	15
2.1.2 Exploration and Development of Oil and Gas Fields.....	20
2.1.3 Production of Oil and Gas	21
2.2 Waterflooding Process.....	23
2.2.1 General Principles and Problems.....	23
2.2.2 Design and Operation of Waterflooding Process	25
2.3 General Overview of Optimization Process	29
2.4 Waterflooding Optimization.....	29
2.4.1 Basic Principles	29
2.4.2 Open-Loop Optimization	33
2.4.3 Closed-Loop Optimization	38
2.5 Model Predictive Control for Reservoir Waterflooding	46
2.6 Self-Optimizing Control for Controlled Variables (CVs) Selection.....	49
2.6.1 Basic Definitions and principles.....	49
2.6.2 Manipulated and Controlled Variables	52
2.6.3 Brief Overview of SOC Methods	53
2.7 Performance Evaluation of Optimization Approaches in Counteracting Uncertainties.....	59
2.8 Summary	61
3 Performance Comparison of Smart Wells Design	63
3.1 Introduction	63
3.2 Reservoir and Wells Configurations.....	64
3.3 Optimization Approach.....	67

3.3.1	The Reservoir Dynamic System.....	67
3.3.2	Objective Function	69
3.3.3	Solution Procedure based on Optimal Control Theory	70
3.4	Results and Discussions.....	71
3.5	Conclusions	77
4	Optimization of Reservoir Waterflooding using Receding Horizon Approach.....	81
4.1	Introduction	81
4.2	RHC for Perfect Reservoir Model	82
4.2.1	Optimization with Net Present Value as Objective	82
4.2.2	Optimization with Recoveries as Objective	89
4.3	RHC for Uncertain Reservoir Models.....	95
4.3.1	Approach.....	96
4.3.2	Uncertainty Consideration	99
4.3.3	Results and Discussions	101
4.3.4	Conclusion	112
5	Data-Driven Self-Optimizing Control for Reservoir Waterflooding Process .	115
5.1	Introduction	115
5.2	Development of Data-Driven SOC Methods	116
5.2.1	Static Optimization	116
5.2.2	Dynamic Optimization for Reservoir Waterflooding.....	137
5.3	Sensitivity Analyses	162
5.4	Performance Comparison between SOC and RHC	165
5.5	Conclusions	166
6	Optimal Multivariable Feedback Control for Reservoir Waterflooding	169
6.1	Introduction	169
6.2	Data Collection and Regression	169
6.3	Uncertainty Consideration.....	172
6.4	Results and Discussion.....	176
6.4.1	Regression	176
6.4.2	Case I: Nominal Parameters	177
6.4.3	Case II: Uncertainty in Permeability and Reservoir Size	180
6.4.4	Case III: Uncertainty in the Shape of Relative Permeability Curves.....	183
6.4.5	Case IV: Uncertainty in Reservoir Size, Geometry and Structure ..	184
6.5	Conclusions	188
7	Conclusions and Recommendations	191
7.1	Conclusions	191
7.2	Recommendations.....	196
	REFERENCES.....	197
	APPENDICES	207
Appendix A	Some Basic Concepts	207

Appendix B MATLAB Reservoir Simulation Toolbox (MRST).....	211
--	-----

LIST OF FIGURES

Figure 1-1: Global Population and Economic Growth (ExxonMobil, 2014).....	1
Figure 1-2: Global Energy Demand by Sector (BP plc, 2014)	2
Figure 1-3: Energy Demand by Fuel Type (ExxonMobil, 2014).....	3
Figure 1-4: Waterflooding Process (Johnny, 2012)	6
Figure 1-5: Some Important Reservoir Properties (CO2, 2014)	6
Figure 1-6: Types of Well (Sarma, 2006)	10
Figure 1-7: A Smart Well in Heterogeneous Reservoir (Sarma, 2006).....	11
Figure 2-1: Oil Reservoir Vertical Cross-Section (Brouwer, 2004)	16
Figure 2-2: Relative Permeability Curves for Two-Phase Flow (Ahmed, 2006)	19
Figure 2-3: Petroleum Production System (Guo et al., 2007)	22
Figure 2-4: Heterogeneous Reservoir with Two Smart Wells (Brouwer, 2004)	25
Figure 2-5: Waterflood Well Networks for Repeated Pattern (Muskat and Wyckoff, 1933).....	27
Figure 2-6: Closed-Loop Reservoir Management Process (Jansen et al., 2009)	40
Figure 2-7: Principle of MPC (modified from (Meum et al., 2008))	47
Figure 2-8: Two-Level Strategy to Combine Reservoir Management with Model Predictive Control of Production (van Essen et al., 2013)	48
Figure 2-9: Loss Incurred by Maintaining Constant Setpoint for the Controlled Variable (Skogestad, 2000)	50
Figure 2-10: Feedback operational Strategy (Umar et al., 2012).....	51
Figure 2-11: A Structure of General Control System (Tatjewski, 2007).....	52
Figure 3-1: Permeability Distribution for a Layered Reservoir in mD.....	65
Figure 3-2: Reservoir and Wells Configurations for Case I	66
Figure 3-3: Reservoir and Wells Configurations for Case III	66
Figure 3-4: Cases Design NPV	72
Figure 3-5: Injection Rates for Case II.....	73
Figure 3-6: Oil Production Rates for Case III.....	74
Figure 3-7: Water Saturation Evolution for Case III	74

Figure 3-8: Water Production Rates for Case III.....	74
Figure 3-9: Injection Rates for Case IV	75
Figure 3-10: Oil Production Rates for Case IV	76
Figure 3-11: Injection Rates for Case V	76
Figure 3-12: Oil Production Rates for Case V	76
Figure 4-1: Fixed-End Receding Horizon Strategy	81
Figure 4-2: Moving-End Receding Horizon Strategy	82
Figure 4-3: NPV for Different Strategies (b = 0)	86
Figure 4-4: NPV for ME Strategy for Different Prediction Period (b = 0).....	86
Figure 4-5: Water Injection Rates for Different Strategies (b = 0).....	86
Figure 4-6: Oil Production Rates for Different Strategies (b = 0).....	87
Figure 4-7: Water Production Rates for Different Strategies (b = 0).....	87
Figure 4-8: Total Production for Different Strategies (b = 0).....	87
Figure 4-9: NPV for Different Strategies (b = 10%)	88
Figure 4-10: Water Injection Rates for Different Strategies (b = 10%)	88
Figure 4-11: Oil Production Rates for Different Strategies (b = 10%).....	88
Figure 4-12: Water Production Rates for Different Strategies (b = 10%).....	89
Figure 4-13: Total Production for Different Strategies (b = 10%).....	89
Figure 4-14: Total Production for Rate-Constrained Scenario.....	92
Figure 4-15: Total Production for Pressure-Constrained Scenario	93
Figure 4-16: Injection Rates for Rate-Constrained Scenario	93
Figure 4-17: Oil Production Rates for Rate-Constrained Scenario	93
Figure 4-18: Water Production Rates for Rate-Constrained Scenario.....	94
Figure 4-19: Injection-Pressure for Pressure-Constrained Scenario	94
Figure 4-20: Oil Production Rates for Pressure-Constrained Scenario	94
Figure 4-21: Water Production Rates for Pressure-Constrained Scenario	95
Figure 4-22: A Flowchart for RHC Strategy Applied to Uncertain Reservoir	98
Figure 4-23: Receding Horizon Control Loop	99
Figure 4-24: Reservoir Geometry and Wells for RHC Prediction (Nominal Model).....	100

Figure 4-25: Reservoir and Well Configuration for Case IV.....	101
Figure 4-26: NPVs for Case I	102
Figure 4-27: Injection and Production Rates – Case I.....	102
Figure 4-28: Permeability Sensitivity to NPV	103
Figure 4-29: Total Production for Case II	105
Figure 4-30: Injection Rates for Case II.....	105
Figure 4-31: Oil Production Rates for Case II.....	105
Figure 4-32: Water Production Rates for Case II.....	106
Figure 4-33: NPV for Case II	106
Figure 4-34: Total Production – Case III.....	107
Figure 4-35: NPV for Case III	108
Figure 4-36: Injection Rates - Case III.....	108
Figure 4-37: Oil Production Rates - Case III.....	108
Figure 4-38: Water Production Rates - Case III.....	109
Figure 4-39: NPVs for Case IV	110
Figure 4-40: Injection Rates for Different Strategies – Case IV	111
Figure 4-41: Oil Production Rates – Case IV.....	111
Figure 5-1: Simple CV Implementation.....	120
Figure 5-2: Reference and Neighbourhood Points for Configuration 1	121
Figure 5-3: Reference and Neighbourhood Points for Configuration 2.....	123
Figure 5-4: Reference and Neighbourhood Points for Configuration 3.....	125
Figure 5-5: Offline Determination of CV using Dynamic SOC	139
Figure 5-6: Online Implementation of Feedback Control Law.....	139
Figure 5-7: NPVs for Case I	143
Figure 5-8: Injection and Production Rates for Case I.....	144
Figure 5-9: NPVs for Case II	145
Figure 5-10: Water Injection Rates – Case II.....	146
Figure 5-11: Production Rates - Case II	146
Figure 5-12: NPVs for Different Strategies - Case III.....	147

Figure 5-13: Water Injection Rates – Case III.....	148
Figure 5-14: Production Rates - Case III	148
Figure 5-15: NPVs for Different Strategies- Case IV	149
Figure 5-16: Water Injection Rates - Case IV	150
Figure 5-17: Production Rates - Case IV.....	150
Figure 5-18: NPVs for Case I	154
Figure 5-19: Rates Profiles for Case I	154
Figure 5-20: NPVs for Case II	155
Figure 5-21: Injection Rates for Case II.....	156
Figure 5-22: Production Profiles for Case II.....	156
Figure 5-23: NPVs for Case III	157
Figure 5-24: Injection Rates for Case III.....	158
Figure 5-25: Production Rates for Case III	158
Figure 5-26: NPVs for Case IV	160
Figure 5-27: Injection Rates for Case IV	160
Figure 5-28: Production Rates for Case IV.....	160
Figure 5-29: Sensitivity of CV to Uncertainties	163
Figure 5-30: Sensitivity of Oil Production Rates to Uncertainties	163
Figure 5-31: Sensitivity of Water Production Rates to Uncertainties	164
Figure 6-1: Nominal Reservoir and Wells Configuration.....	170
Figure 6-2: Reservoir and Wells Configuration for Case IV.....	176
Figure 6-3: NPV for Case I – Nominal Parameters.....	178
Figure 6-4: Injection Rates for Nominal Case.....	179
Figure 6-5: Oil Production Profiles for Nominal Case	179
Figure 6-6: Water Production Profiles for Nominal Case.....	179
Figure 6-7: NPVs for Case II	180
Figure 6-8: Injection Rates for Case II.....	182
Figure 6-9: Oil Production Profiles for Case II	182
Figure 6-10: Water Production Profiles for Case II	182

Figure 6-11: NPVs for Case III	183
Figure 6-12: NPVs for Case IV	185
Figure 6-13: Injection Rates for Case IV	186
Figure 6-14: Oil Production Profiles for Case IV	186
Figure 6-15: Water Production Profiles for Case IV.....	187
Figure A-1: Oil Recovery Methods (Adeniyi et al., 2008).....	210
Figure B-1: Pressure Solutions (Sintef, 2014b)	214
Figure B-2: Permeability Field of Realistic Reservoir (Sintef, 2014b)	216
Figure B-3: A Typical Reservoir - Well System (Sintef, 2014b)	217
Figure B-4: Triangular Grid (Sintef, 2014b)	217
Figure B-5: Extruded Triangular Grid (Sintef, 2014b)	218
Figure B-6: GRDECL Structures (Sintef, 2014b).....	218
Figure B-7: Black Oil Simulation (Sintef, 2014b)	219

LIST OF TABLES

Table 3-1: Rock and Fluid Properties	66
Table 3-2: Configurations of Wells for Different Case Design	67
Table 3-3: Performance Comparison of Different Well Designs	72
Table 4-1: Performance Comparison of Optimization Strategies.....	85
Table 4-2: Performance Comparison of Optimization Strategies for Simple Wells System with Recoveries Objective Function.....	92
Table 4-3: RHC and OC Comparison for Case I	102
Table 4-4: Performance Comparison – Case II	104
Table 4-5: Performance Comparison- Case III	107
Table 4-6: Performance Comparison - Case IV.....	110
Table 5-1: Comparison between Data-Driven SOC and other Methods.....	122
Table 5-2: Data-Driven SOC – Configuration 2	124
Table 5-3: Data-Driven SOC – Configuration 3	126
Table 5-4: Data-Driven SOC – Configuration 4	127
Table 5-5: Data-Driven SOC – Configuration 5	128
Table 5-6: Data-Driven SOC – Configuration 6	130
Table 5-7: Data-Driven SOC – Configuration 7	131
Table 5-8: Constrained Data-Driven SOC and NCO Approximation Methods	136
Table 5-9: SOC and OC Comparison for Case I	144
Table 5-10: SOC and OC Comparison for Case II	146
Table 5-11: SOC and OC Comparison for Case III	148
Table 5-12: SOC and OC Comparison for Case IV	150
Table 5-13: Losses and Gains for Various Cases of Uncertainty (Simple Reservoir).....	151
Table 5-14: OC and SOC Performance Comparison for Case I.....	154
Table 5-15: OC and SOC Performance Comparison for Case II.....	156
Table 5-16: OC and SOC Performance Comparison for Case III.....	158
Table 5-17: OC and SOC Performance Comparison for Case IV.....	161

Table 5-18: Losses and Gains for Various Cases of Uncertainty (Realistic Reservoir)	161
Table 5-19: Uncertain Cases for Sensitivity Analyses	162
Table 5-20: Comparison between SOC and RHC Methods	165
Table 6-1: Nominal Rock and Fluid Properties	170
Table 6-2: Case II – Rock and Fluid Properties	173
Table 6-3: Case III – Rock and Fluid Properties	174
Table 6-4: Case IV – Rock and Fluid Properties	175
Table 6-5: CVs Regression Parameters	177
Table 6-6: OC and SOC Performance Comparison for Case II	181
Table 6-7: OC and SOC Performance Comparison for Case III	184
Table 6-8: OC and SOC Performance Comparison for Case IV	186
Table 6-9: Losses and Gains for Various Cases of Uncertainty	187

LIST OF ABBREVIATIONS

API	American Petroleum Institute
BC	Boundary Condition
BHP	Bottomhole Pressure
BM	Bench Mark
CAHM	Computer Assisted History Matching
CLRM	Closed-Loop Reservoir Management
CG	Conjugate Gradient Algorithms
CV	Control Variable
DOF	Degrees of Freedom
EnKF	Ensemble Kalman Filter
EnRML	Ensemble Randomized Maximum Likelihood
EOR	Enhanced Oil Recovery
ESDIRK	Explicit Singly Diagonally Implicit Runge-Kutta
FE	Fixed-End
GA	Genetic Algorithm
ICV	Inflow Control Valve
IP	Integer Programming
KPCA	Kernel Principal Component Analysis
K-L	Karhunen-Loeve
LP	Linear Programming
ME	Moving-End
MPC	Model Predictive Controller
MV	Manipulative Variable
MIP	Mixed Integer Programming
MRST	MATLAB Reservoir Simulation Toolbox
NCO	Necessary Condition of Optimality
NLP	Nonlinear Programming
NCW	Nonconventional well
NPV	Net Present Value
OC	Open-Loop Control
OECD	Organisation for Economic Co-operation and Development
OOIP	Original Oil in Place

PE	Partial Enumeration
PMP	Pontrygin's Minimum Principle
RHC	Receding Horizon Control
RO	Robust Optimization
SA	Steepest Ascent
SOC	Self-Optimizing Control
SPSA	Simultaneous Perturbation Stochastic Approximation
SQP	Sequential Quadratic Programming
STB	Stock Tank Barrel
STO	Switching Time Optimization

1 Introduction

1.1 Global Energy Demand

The world's population is estimated to increase from 7 billion to 9 billion between the years 2010 – 2040. This population growth will be associated with growth in economies and hence improvement in the living standards of people. To maintain such standards, global demand in energy is projected to increase by about 35%. Economic growth and energy development is not uniform across the globe (Figure 1-1) but varies from one region or country to the other. For example, the growth in countries belonging to the Organisation for Economic Co-operation and Development (OECD) is estimated to be at an average of 2.0% annually through 2040 while for non-OECD countries, the rise is expected to be 4.4% per year over the same period (ExxonMobil, 2014).

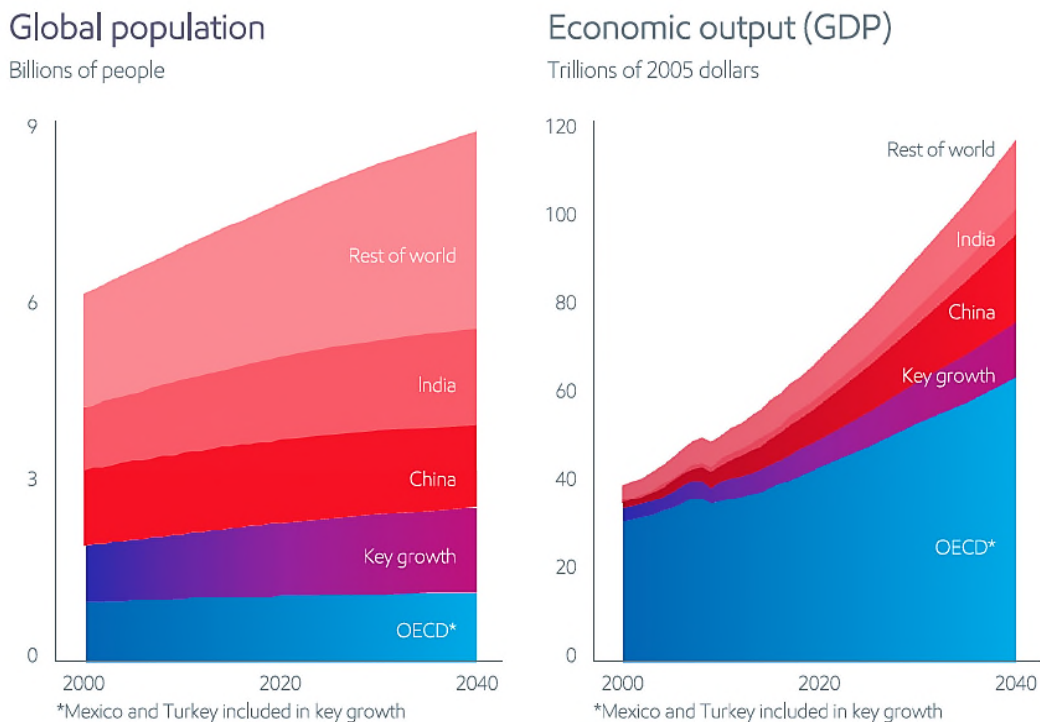


Figure 1-1: Global Population and Economic Growth (ExxonMobil, 2014)

Energy is needed in various aspects of human endeavours for industrial, residential, agricultural and transportation usage. Among these sectors, industries will account for more than half of the energy growth from 2012 to 2035 according to BP Energy Outlook 2035 (BP plc, 2014), see Figure 1-2.

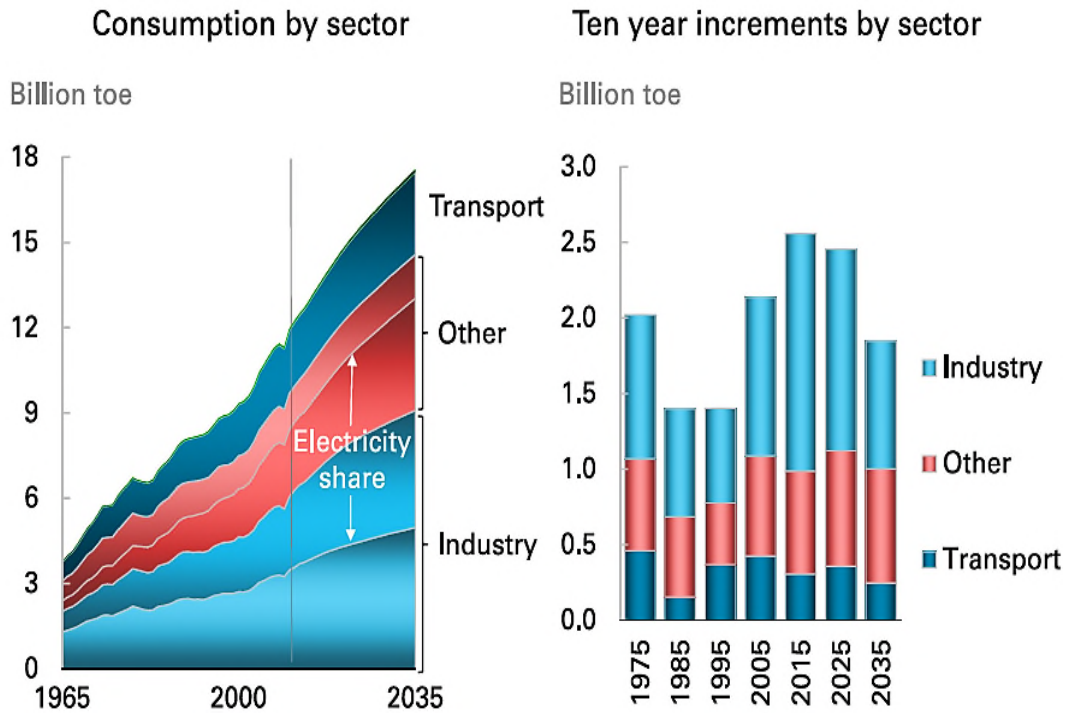


Figure 1-2: Global Energy Demand by Sector (BP plc, 2014)

There are many sources to support such demand for example, fossil fuels such as oil, gas and coal, renewables which include wind, solar, and hydro, and nuclear sources. However, oil is the top energy source globally and remains the preferred fuel for transportation. Its demand is projected to increase by 25% by the year 2040. Similarly the demand of natural gas will increase by 65% and will account for more than 25% of the global energy requirement (Figure 1-3). It is one of the cleanest energy sources with CO₂ emission level that is 60% less than coal when used for power generation (ExxonMobil, 2014).

Energy expansion to meet the global needs will require investments on infrastructure to the tune of approximately \$1.6 trillion on the average annually up to 2035. Almost half of these investments will go into oil and natural gas projected needs while about 45% will be spent on power generation (ExxonMobil, 2014). Therefore, the need for the search for an efficient method of oil recovery or improvement of existing ones can never be over emphasised.

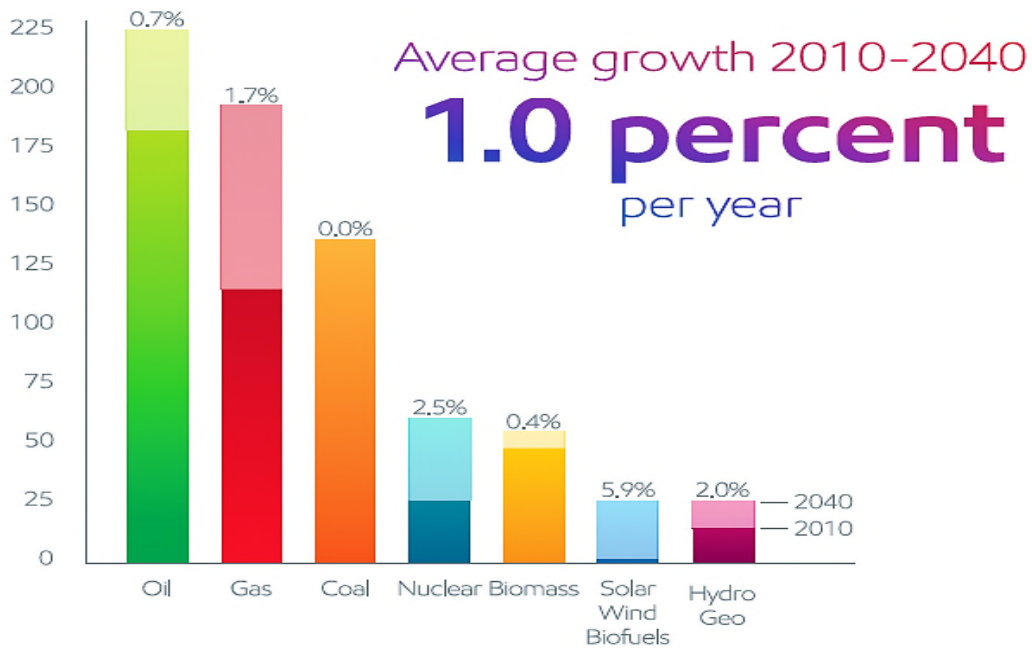


Figure 1-3: Energy Demand by Fuel Type (ExxonMobil, 2014)

1.2 Oil and Gas Production Process

Oil and gas are naturally occurring hydrocarbons which are found several kilometres beneath the earth surface in a structure called reservoir. Oil and gas reservoirs are porous which allow the oil to be stored, and permeable that enables fluids transmission. Usually, hydrocarbons are trapped in the reservoir by an impermeable rock or water formation which prevents it from escaping to a nearby structure. Based on its initial pressure condition, reservoirs can be oil, gas condensate, or gas reservoirs (Guo et al., 2007).

Oil and gas are produced from reservoirs by drilling wells to intersect the hydrocarbon bearing zone(s). The fluid moves into the wells and get produced at the surface by virtue of its hydrostatic pressure. Usually for a new discovered oil field, the reservoir pressure is very high and can support production for some period of time. This production phase is called **primary production**. As production progresses, the reservoir is depleted of its fluid and the pressure starts to decrease with a corresponding decline in production. As this continues, the production is affected severely. To maintain a target production capacity, the reservoir pressure is artificially boosted by injection of fluid into the reservoir during **secondary production phase**. Due to its availability, water is the common injecting fluid and the process is called **waterflooding**. In waterflooding process, a separate well is drilled or an existing one is converted to be an injection well where water is pumped through into the reservoir with the aim to flood the oil in place to a production well which gets produced to the surface. Water is also produced in association with the oil. However, the amount of water production increases with time until a point where the process is considered uneconomical. At this point secondary recovery methods will fail to yield any significant incremental oil. A third production stage is then employed to increase the productivity which is known as **tertiary production phase**. This is more complex technically and expensive than secondary recovery methods. It involves injection of more sophisticated fluids into the reservoir such as steam, polymers, cheap hydrocarbon gases and so on. In situ combustion is also regarded as a tertiary recovery method where a burnt air in the reservoir is used to drive the production (Brouwer, 2004).

Production from gas reservoirs is relatively easier than oil. Due to high compressibility of gas, pressure decline is not that severe and only a single phase exists throughout the production period (Brouwer, 2004).

Waterflooding being one of the cheapest means of enhancing production (Asheim, 1987) will be the focus of this work.

1.3 Waterflooding for Enhanced Oil Recovery

Waterflooding as stated earlier involves injection of water into the reservoir with the aim of boosting a depleted reservoir pressure and sweeping the available oil toward a production well (Figure 1-4). It is one of the cheapest means of recovery (Asheim, 1987). It is also the dominant means of production among secondary recovery methods which leads to present high production rate (Adeniyi et al., 2008). The popularity of this mechanism can be attributed to the following (Adeniyi et al., 2008):

1. the availability of water
2. ease of injection
3. the high tendency of water spreading out in the oil bearing formation and
4. the displacement efficiency possessed by water

Unfortunately, even with the employment of waterflooding only about one-third of the original oil in place (OOIP) is recovered and the rest is left to be produced through a more complex and expensive means.

As water is injected into the reservoir, it is expected that it will sweep the oil uniformly. However, it is not that easy in reality, the simple reason is reservoirs are highly heterogeneous in nature. Properties that determine fluid flow directions such as porosity and permeability vary significantly in space. Porosity is the fraction of reservoir rock that can be covered by fluids (pore space) while permeability is the interconnection of these pore spaces that determines fluid conductivity (Figure 1-5). So, when water is injected into the reservoir, it will preferentially flow through easier paths which are conductive fractures and high permeability zones, and therefore bypass pools of oil. This phenomenon results to premature water break-through and hence reduced sweeping efficiency which are serious hiccups to waterflooding operations. Many solutions to these problems have been suggested in the past which include use of polymeric materials, mechanical isolation or squeeze cementing (Mody and Dabbous, 1989). Recently, the use of smart or intelligent wells in mitigating the shortcomings of high water cut is receiving a great attention (Brouwer et al.,

2001; Brouwer, 2004; Brouwer and Jansen, 2004a; Meum et al., 2008). See Section 1.4 for description of smart wells.

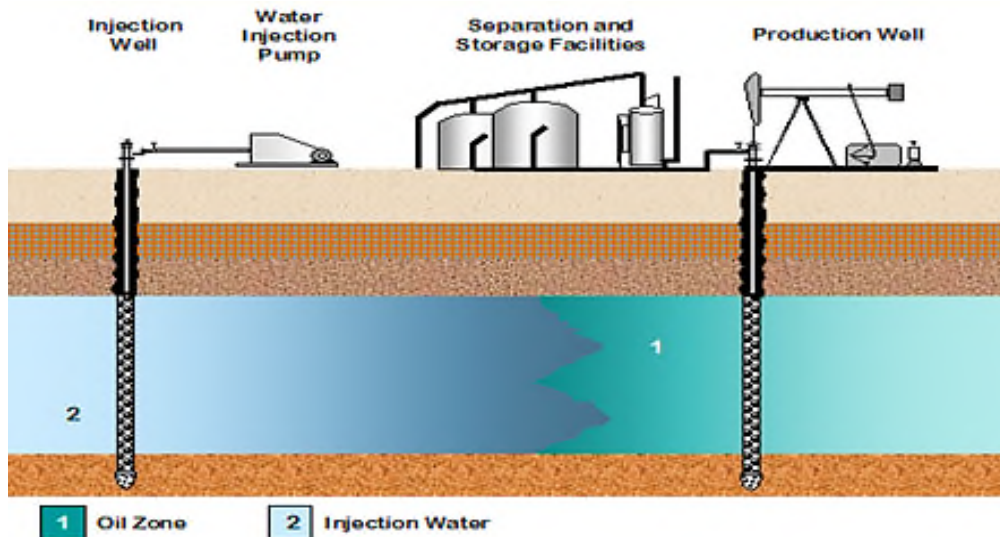


Figure 1-4: Waterflooding Process (Johnny, 2012)

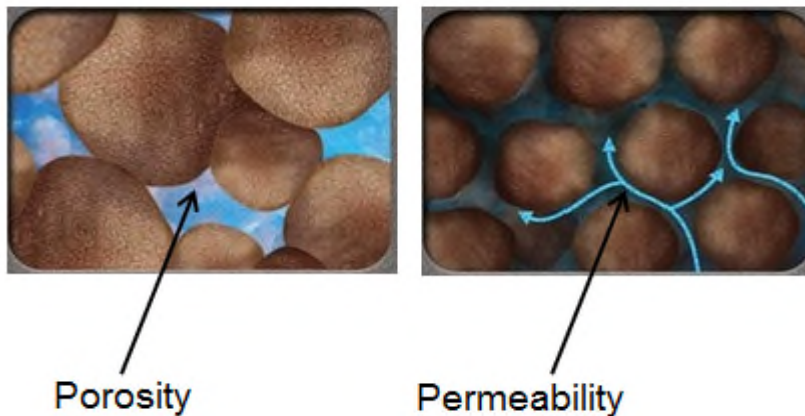


Figure 1-5: Some Important Reservoir Properties (CO2, 2014)

Reservoir production is a long term process that runs for decades. However, reservoir states such as pressures and saturations are dynamic; they quite change significantly along the production horizon; and with each change of

states, different injection and production rates will be required to lead to optimal operation. This problem is usually formulated as optimization tasks and is receiving a great attention (Brouwer et al., 2001; Durlofsky and Aziz, 2002; Brouwer, 2004; Jansen et al., 2005; Jansen et al., 2008; Dilib and Jackson, 2013a; Dilib et al., 2013b). The optimization is normally carried out by considering a combination of injection and production rates, and bottomhole pressures of wells as manipulative variables with an objective to maximize either an economic index such as profits, net present value or production recoveries and flooding efficiencies. The objective can also be to minimize some factors with detrimental effects such as water-cut.

Waterflooding optimal operation is a dynamic optimization problem and many authors attempted to solve it via the traditional optimal control approaches (Brouwer, 2004; Asadollahi and Naevdal, 2009) with the assumption that the reservoir model is perfect and captures all reservoir behaviours and characteristics. However, oil reservoirs are extremely heterogeneous and its properties can only be known with some degrees of certainty around the well vicinity only. Some basic properties such as shape or geometry which ought to be known with perfection are uncertain because they are deduced from seismic data (Jansen et al., 2008). Other properties require high model resolution to be captured, for example thin, high permeability zones. Similarly, there are some production behaviours like coning that are rarely captured well through simulation models (Dilib and Jackson, 2013a). So, approaches based on optimal control theory can only provide open-loop solutions and lack robustness to handle such uncertainties.

A lot of efforts have been geared toward finding a solution algorithm that can handle reservoir uncertainties for optimal waterflooding process. To this regard, robust optimization (RO) technique for instance has been reported by van Essen and co-workers (van Essen et al., 2009) which involves the use of a set of reservoir realizations to account for geological uncertainty within the optimization framework. The procedure assumes that all possible reservoir characteristics and production behaviours are captured by the realizations,

which however is not possible in reality. The performance of this technique is mostly conservative which hardly leads to optimal solution because it is designed to account for all possible uncertainties.

The current practice in oil and gas industries is employment of one of these approaches for optimization using available reservoir model. As new data such as production data, well logs, seismic data and data from core analysis become available the reservoir model is updated through a procedure called history matching. History matching activities are performed periodically on a campaign basis and new optimized strategies are obtained based on the updated model. However, the prediction of history-matched models may still be substantially different from reality (Tavassoli et al., 2004).

Other dynamic optimization methods available are either too complicated or inappropriate for waterflooding problems. For instance, parametric optimization techniques (Fotiou et al., 2006) are too complex for reservoir system. Stochastic optimization methods (Collet and Rennard, 2007) on the other hand are not efficient and require high computational power. A practical approach, repeated learning was developed for batch processes (Ganping and Jun, 2011; Ahn et al., 2014), unfortunately, petroleum production from reservoirs is not repeatable. So this method is not applicable to waterflooding problems.

In view of this, many authors are of the opinion that there should be a shift from present practice of periodic model and strategies updating for every history matching exercise to a more efficient utilization of production measurements where control strategies are implemented in a closed-loop fashion (Jansen et al., 2008; Foss and Jensen 2011). Introducing a direct feedback strategy into the optimization scheme can add robustness to the control performance so as to counteract the effect of model errors that are inevitable in any real system (Dilib and Jackson, 2013a).

A fundamental task that has not been given attention for waterflooding operation optimization is, determination of a controlled variable (CV) in a feedback structure which is not sensitive to geological and operational uncertainties so that when the CV is maintained at a constant setpoint the

operation is automatically optimal or near optimal. A lot of researches are ongoing for continuous processes in that direction through a concept called self-optimizing control (SOC). The principle involves selection of CVs among available measurements (Skogestad, 2000) so that when they are controlled at setpoints through a feedback control, the plant operation becomes automatically optimal or near optimal (Skogestad, 2004). There are several methods developed for CV selection over the years (Halvorsen et al., 2003). Some of these methods require process models and linearization of nonlinear systems around a nominal point leading to local solutions. To overcome this shortcoming of local solutions, Ye et. al. (2013a) came up with a method to approximate necessary condition of optimality (NCO) globally. However, their method still requires process model for NCO evaluation. Recently, a regression-based data driven method which approximates the NCO or compressed reduced gradient from either operation or simulated data was developed (Girei et al., 2014). It is worth to note that above mentioned SOC approaches for continuous processes are static; however this has been extended to batch processes, hence dynamic SOC (Dahl-Olsen et al., 2008; Dahl-Olsen and Skogestad, 2009). Unfortunately, these approaches also have the listed shortcomings above of localness and complexity which makes it difficult to be applicable to any practical applications, such as the waterflooding problem. So, it is motivating to extend the method presented in (Girei et al., 2014) to dynamical systems with particular attention to waterflooding operations.

1.4 Types of Well System

Traditionally, the most common types of well are the conventional wells which are vertical or slightly deviated. These have the advantages of being easier and cheaper to be drilled. A shortcoming to conventional wells is that they provide small contact area with the reservoir, thereby limiting the well productivity. Furthermore, they are not good candidates for optimization because of insufficient installed instrumentation and control gadgets (Sarma et al., 2006).

Nonconventional wells (NCWs) on the other hand, are horizontal, highly deviated or multilateral wells. These are also referred to as advanced wells.

They are more cost effective than conventional wells because drilling a single NCW is equivalent in efficiency to drilling many conventional wells. Apart from this, NCWs provide more drainage area and therefore exploit the reservoir more efficiently. However, despite the benefits mentioned above, NCWs have no much provision for controllability (Sarma et al., 2006). See Figure 1-6 for different types of well.

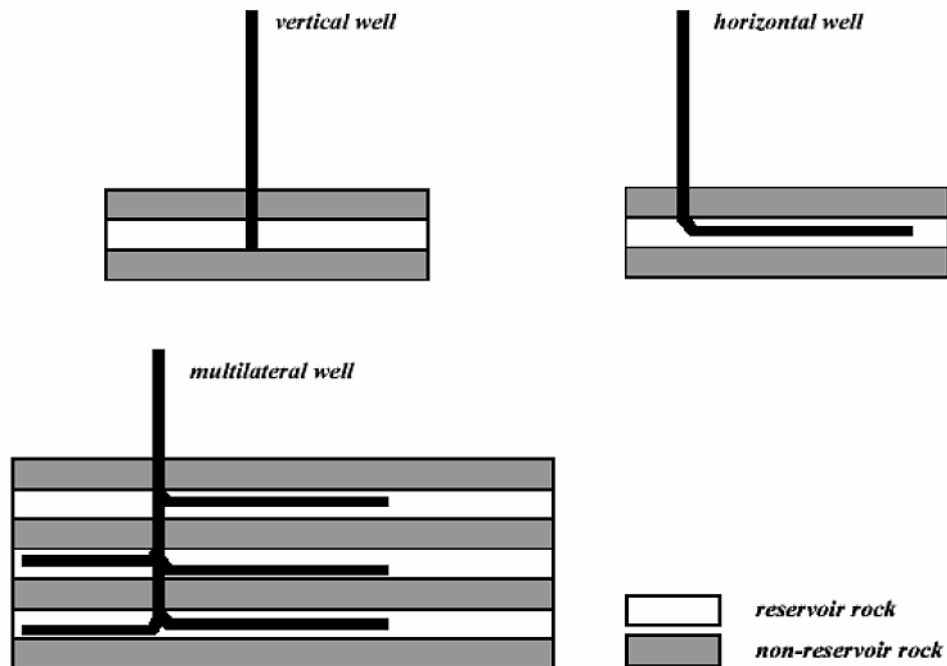


Figure 1-6: Types of Well (Sarma, 2006)

Smart wells are designed and installed with instrumentation which includes sensors and valves for real time measurements and control. Downhole measurements are provided by smart wells so that production monitoring is improved and therefore real time control and optimization are possible (Sarma et al., 2006). The control gadgets (inflow control valves, ICVs) divide the reservoir into segments where variables such as flow rates, pressure or temperature can be controlled independently (Meum et al., 2008) as shown in Figure 1-7. This enables the shut in of the part of the production well that has the potential of producing high volume of water remotely without affecting other

producing zones. The benefit of this technology is particularly high for difficult terrains where well intervention is expensive (Brouwer, 2004).

The basic principle behind smart well technology lies on the fact that oil sweeping in various zones of reservoir under waterflooding depends on injection rate and pressure and therefore by optimally controlling these variables, the flooding efficiency can be improved (Brouwer et al., 2001). Therefore, controlling these variables in addition to production, delay or avoid water break-through whenever possible (Meum et al., 2008).

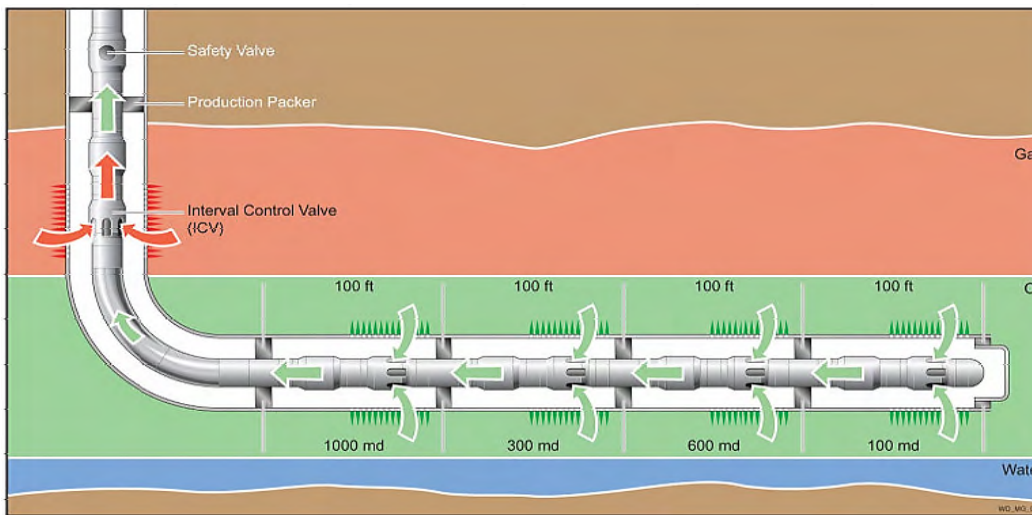


Figure 1-7: A Smart Well in Heterogeneous Reservoir (Sarma, 2006)

1.5 Research Aim and Objectives

The aim of this research project is to formulate reservoir waterflooding optimization strategy for efficient oil recovery. To achieve this aim, the following objectives are pursued:

1. Carry out systematic optimization study on a reservoir system with different well configurations to lay a strong foundation of the subject.

2. Develop feedback optimization strategies based on the concept of receding horizon control with the aim of counteracting the effects of geological uncertainties that are inevitable to reservoirs.
3. Develop a data-driven self-optimizing control method where gradient of objective function with respect to control is obtained entirely from simulation or production data such that an analytical expression of the gradient is not required. The gradient formulated from data is proposed to be used as the controlled variable which will be tested for robustness against various uncertainties.
4. Apply the method developed in 3 above to solve waterflooding optimization problem.
5. Compare the efficacies of these two methods mentioned above in terms of uncertainty handling based on simulated reservoirs.

1.6 Thesis Structure

The thesis is organised as follows:

A detailed literature review is given in Chapter 2. The review is opened with an overview of the activities involved in oil and gas production starting from search of the resources to production stage. Description of some reservoir properties is also given which can help with understanding of the subject. This is followed by a detailed review of optimization where emphasis is given to waterflooding optimization methods.

In Chapter 3, a comparative study is carried out on different configurations of smart well. Here, a particular reservoir system is considered while the performances of different well designs are optimized and compared. A method based on optimal control theory is used for the optimization. The chapter also serves as an insight into the optimization process of reservoir waterflooding.

A feedback optimization approach based on the principle of receding horizon control is developed in Chapter 4. The method is initially applied to cases without model/system mismatches the performance of which is compared to

that of open-loop optimal solution. It is then extended to annul the effects of geological uncertainties in terms of mismatches between a nominal model and some assumed real reservoir models.

A novel method based on the principle of self-optimizing control that is purely data driven is presented in Chapter 5. The formulation starts with static optimization problem which is then extended to dynamic problem with particular attention to waterflooding operation. However, only cases with single manipulative variable are considered.

The method presented in Chapter 5 is extended to solve multivariable waterflooding optimization problems in Chapter 6.

Chapter 7 gives conclusions of the work done and summary of results obtained. Recommendations and future work direction are also given.

In the Appendices, explanations to basic reservoir fluid properties that have not been covered in Chapter 2 are given. Classifications of oil and gas recovery methods are also covered. Finally, fundamental aspects of MRST software are covered in the Appendices.

1.7 Publications

List of publications arising from this work are given below. These are categorised into two; those that have been published already and those proposed to be published.

1.7.1 Published Work

Chapters 3 and 4

Grema, A. S. and Cao, Y. (2013) "Receding Horizon Control of Reservoir Waterflooding using Sequential Quadratic Programming". A paper presented at IET Control and Automation Conference 2013, Birmingham, U.K.

Grema, A. S. and Cao, Y. (2013) "Optimization of Petroleum Reservoir Waterflooding using Receding Horizon Approach". A paper presented at the 8th IEEE Conference on Industrial Electronics and Applications (ICIEA 2013), 19-21 June 2013, in Melbourne, Australia.

Chapter 5

Girei, S. A., Cao, Y., Grema, A. S., Ye, L., and Kariwala, V. (2014) 'Data-Driven Self-Optimizing Control'. A paper presented at 24TH European Symposium on Computer Aided Process Engineering (ESCAPE 24) June 15-18, 2014, Budapest, Hungary.

Grema, A. S. and Cao, Y. (2014) "Optimal Feedback Control for Reservoir Waterflooding". A paper presented at the 20th International Conference on Automation and Computing (ICAC 2014), 12-13 September 2014, Cranfield, Bedfordshire, U.K. The paper has received the best student paper award from the conference programme committee.

1.7.2 Proposed Publications

Four journal papers are proposed to be published which are drawn from Chapters 3, 4, 5 and 6. A conference paper was also submitted to the '2nd IFAC Workshop on Automatic Control in Offshore Oil and Gas Production', which will be held in Florianopolis, Brazil from 27-29, May, 2015, based on the work reported in Chapter 6.

2 Literature Review

2.1 Oil and Gas: Origin, Exploration, Development and Production

2.1.1 Origin of Oil and Gas

Oil and gas which are generally referred to as petroleum are naturally occurring hydrocarbon composed of mainly carbon and hydrogen with possible traces of impurities such as oxygen, nitrogen and sulphur. Process of hydrocarbon generation takes a very long period of time which begins with deposition of microscopic remains of plants and animals in deltaic, marine, and lake environments. Agents for the transportation of these organic materials into the depositional environments may include rivers, streams or sea. Sometimes, the organic materials may originate from the environment itself. Transportation and origination processes can also occur within the same formation. Silts and/or clay which are fine clastic sediments are generally deposited with the organic remains. The sediments serve the purpose of protecting the organic materials during burial and creating oxygen depleted environments which allow the later to accumulate without being destroyed by aerobic microorganisms.

The accumulated remains are subjected to intense temperature and pressure, and over time (tens of thousands of years) are converted into oil and gas. The generated petroleum in the sediments (**source rock**) usually migrates into a **reservoir rock** and gets accumulated. The reservoir rock is sealed by a **cap rock** to avoid further migration of the petroleum accumulation. It can be said that, petroleum system is made up of source rock, migration route, reservoir rock, seal rock and trap (Halliburton Corporation, 2001).

Oil fields can cover from a few to hundred square kilometres in area while reservoir rock thickness can be just from few to hundreds of metres. Figure 2-1 shows a vertical cross-section of an oil reservoir. The impermeable cap rock is seen over the oil-bearing formation. The oil reservoir may be bounded by a less porous and permeable rock and/or by a water bearing rock (aquifer).

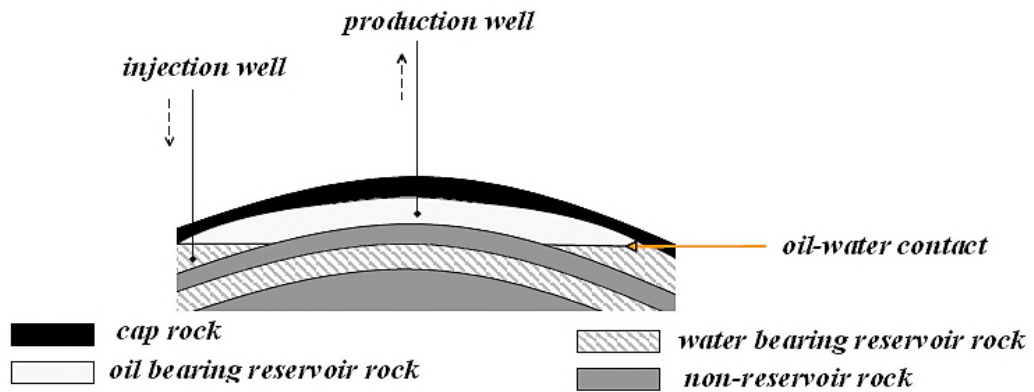


Figure 2-1: Oil Reservoir Vertical Cross-Section (Brouwer, 2004)

The separation zone between the oil and water bearing formations is referred to as oil-water contact (Brouwer, 2004).

Reservoirs can generally be classified based on the type of fluids they contain. So, based on this classification we can have oil, gas condensate or gas reservoirs depending on the initial reservoir conditions of pressure and temperature (Guo et al., 2007). To help with the understanding of the basic concepts, some properties of reservoir rock and fluids are briefly reviewed below:

- **Porosity** – this measures the storage capacity of a rock. It is a ratio of the pore volume to the total volume (bulk volume) given as

$$\phi = \frac{\text{pore volume}}{\text{bulk volume}} \quad (2-1)$$

where ϕ is the porosity (Ahmed, 2006).

- **Saturation** – the fraction of the pore volume occupied by a particular fluid (oil, gas or water)

$$\text{fluid saturation} = \frac{\text{total volume of fluid}}{\text{pore volume}} \quad (2-2)$$

Oil, water and gas saturations are usually denoted by S_o , S_w , and S_g respectively. For a reservoir rock containing oil, water and gas

$$S_o + S_w + S_g = 1.0 \quad (2-3)$$

as given by Ahmed (2006). It is generally assumed that reservoir fluids are in a state of equilibrium and will therefore separate into distinct layers according to individual fluid densities (Ahmed, 2006).

- **Connate Water Saturation (S_{wc})** – as shown in Figure 2-1 there may be edge or bottom water associated with oil bearing formation, and in addition to that, there is connate water that is distributed throughout the oil and gas bearing zones. Connate water is the distributed water in the reservoir that has been reduced to an irreducible amount which is retained by capillary forces on pore scale. The saturation of connate water S_{wc} is an important factor for consideration because it reduces the available pore space for oil and gas. Most times, connate water saturation, critical water saturation and irreducible water saturation are used interchangeably (Ahmed, 2006).
- **Critical Oil Saturation (S_{oc})** – this is the saturation of oil phase that must be exceeded for it to flow. At S_{oc} , the oil remains in the pores and cease to flow for all applications (Ahmed, 2006).
- **Residual Oil Saturation, (S_{or})** – the saturation of oil remaining in the pores after been displaced by fluid injection or encroachment. At residual saturation, the oil phase can still move but cannot be recovered by the displacement process employed. Therefore, the value of S_{or} is larger than S_{oc} (Ahmed, 2006).
- **Wettability** – is the preferential tendency of one fluid to adhere to a solid surface over the other. This is important in that reservoir fluids are distributed based on their wettability to the rocks in the porous media. Usually, the wetting phase occupies the smaller pores of the rock while the nonwetting phase are found in the more or less open channels (Ahmed, 2006).
- **Permeability** – this measures the ability of the rock to transmit fluid. It is an important property of the reservoir rock formation that defines the

direction and rates of fluids. Conventionally, permeability is denoted by k with a unit of millidarcy (mD). One mD is equivalent to $9.8692 \times 10^{-16} m^2$. The above definition of permeability is for a situation when there is only one fluid phase present in the porous medium, the rock is 100% saturated with the fluid, k is therefore referred to as **absolute permeability**. In reality however, there are two or more phases present in reservoir rocks. Therefore, the concept is modified for multiphase flow in reservoir where effective permeability is used to describe the permeability of the rock to a particular fluid in the present of others. Thus, effective permeabilities to oil, gas and water are denoted respectively by k_o , k_g and k_w . Effective permeability of a phase decreases with a decrease in its saturation (Ahmed, 2006).

- **Relative Permeability** – for a multiphase flow in a porous medium, relative permeability of a phase at a given saturation is the ratio of the effective permeability of the phase to the absolute permeability, which is given mathematically by Ahmed (2006) as

$$\begin{aligned} k_{ro} &= \frac{k_o}{k} & (2-4) \\ k_{rg} &= \frac{k_g}{k} \\ k_{rw} &= \frac{k_w}{k} \end{aligned}$$

where k_{ro} , k_{rg} and k_{rw} are relative permeabilities to oil, gas and water respectively. Generally, relative permeability of a wetting phase can be denoted by k_{wt} and that of a nonwetting phase as k_{nw} . For a two-phase flow in porous media, the presence of a nonwetting phase at even small saturation value will drastically reduce the permeability of the wetting phase since the former occupies the larger pore spaces. Typical relative permeability curves for two-phase flow of oil and water in a porous medium is shown in Figure 2-2. Here oil is the nonwetting phase and water the wetting phase (Ahmed, 2006).

Relative permeability curves are usually obtained from core analyses on actual reservoir samples. However, most of the times, these relative permeability data are not readily available for a particular field or for future use. To overcome these shortcomings, correlations were developed to generate relative permeability curves (Ahmed, 2006). One of the most common correlations in use is that developed by (Corey and Rathjens, 1956). Corey's equations are generally written as (Ahmed, 2006).

$$k_{ro} = \left(\frac{1 - S_w}{1 - S_{wc}} \right)^n \quad (2-5)$$

$$k_{rw} = \left(\frac{S_w - S_w}{1 - S_{wc}} \right)^m$$

where n and m are referred to as oil and water Corey exponents respectively.

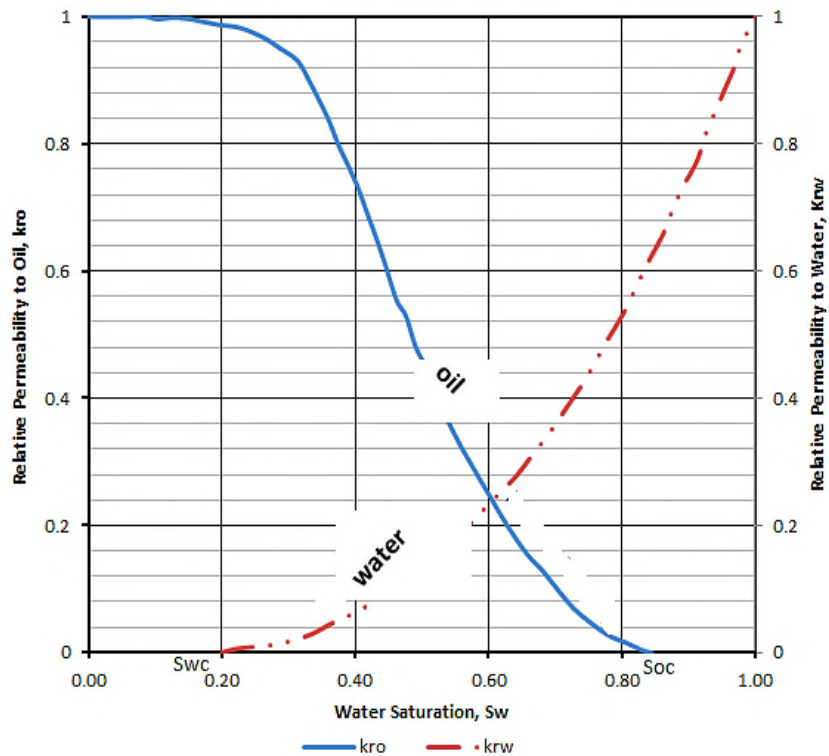


Figure 2-2: Relative Permeability Curves for Two-Phase Flow (Ahmed, 2006)

Other rock properties include surface and interfacial tension, rock compressibility and net pay thickness. Reservoir fluid properties of interest include density, viscosity, compressibility, formation volume factor, etc. (Ahmed, 2006). See A.1 for details.

Rock properties are usually determined in the laboratory from samples of the reservoir to be evaluated. The rock samples are referred to as cores while the analyses that are performed to obtain the properties in question are termed core analyses. Certainly, reservoir properties are highly heterogeneous, and cores obtained by drilling just few wells are hardly true representative of the whole field. The cores after been removed from reservoir conditions must have been subjected to some changes that might have substantial effects on the properties. Typical properties that might be affected include the core pore volume, bulk volume, wettability and fluid saturations. So, this makes the determined properties to be highly uncertain. Another source of uncertainty in determining reservoir properties are the errors that are inherent with handling experimental data. Apart from core analyses, reservoir properties can be obtained through other means. For example, rock porosity can be determined from wire-line logs. Although this is not accurate as core analyses, it can however provide continuous information on porosity values (Ahmed, 2006).

2.1.2 Exploration and Development of Oil and Gas Fields

2.1.2.1 Exploration Surveying Phase

Hydrocarbon-bearing rock search starts with a critical review of geological maps with the aim of identifying the possibility of the presence of sedimentary basins. Identification of promising structural formations such as faults or anticlines may then be carried out using aerial photography. More detailed geological information is assembled at field geological assessment stage. One of three main methods of survey, namely, magnetic, gravimetric and seismic is carried out to obtain information on structural geological formation (Environmental Management in Oil and Gas Exploration and Production, 2004).

2.1.2.2 Exploration Drilling Phase

In this phase, an exploratory well, known as a 'wild cat' is drilled to confirm the presence of hydrocarbons from the identified promising structures. The internal pressure and reservoir thickness can also be confirmed at this stage.

Initial well tests are carried out if hydrocarbon formation is found so as to determine maximum flowrate and formation pressure (well potential). If presence of hydrocarbon in commercial quantities is proven by the test, a wellhead assembly is installed, or the site is decommissioned if otherwise (Environmental Management in Oil and Gas Exploration and Production, 2004).

2.1.2.3 Appraisal Phase

At this stage, 'appraisal' or 'outstep' wells are drilled to determine the size and extend of the commercially proven field. Evaluations of the actual number of wells required and the need of further seismic are carried out (Environmental Management in Oil and Gas Exploration and Production, 2004).

2.1.2.4 Development Phase

After the size of the field has been established, development or production wells are drilled, the number of which depends on the field size (Environmental Management in Oil and Gas Exploration and Production, 2004).

2.1.3 Production of Oil and Gas

Oil or gas production system will primarily consist of the reservoir, well, flowlines, separator, pumps and transportation lines (Figure 2-3). The reservoir as was explained earlier serves as a store for the hydrocarbon fluids. The well functions as a flow path for the movement of the fluids from bottomhole to the surface. It also provides a means of control. The fluids are transferred from the well to separator in flow lines. Water and/or gas are removed from the oil in the

separator. The oil and gas are sent to storage tanks or sales points via transportation lines (Guo et al., 2007).

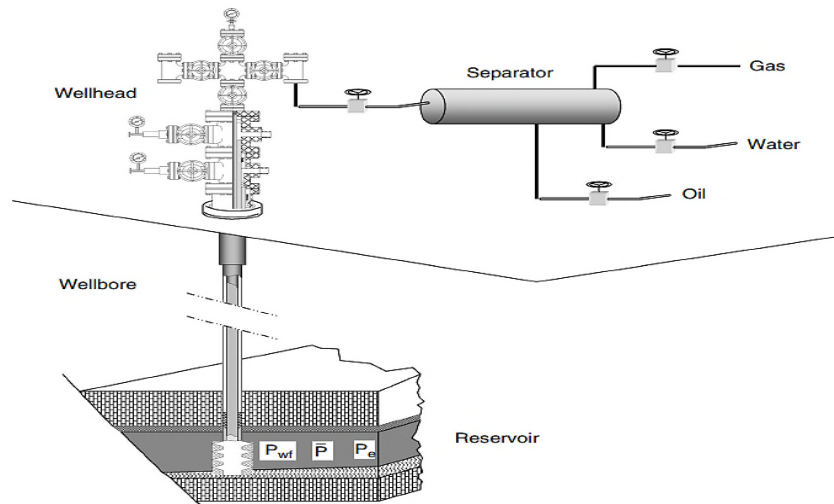


Figure 2-3: Petroleum Production System (Guo et al., 2007)

As mentioned earlier, reservoirs can be oil or gas reservoirs depending on the kind of fluid it contains. Production processes from gas reservoirs consist of only one phase and the flow from reservoir to the surface is relatively easy owing to low density and viscosity of gas. Due to the fact that the reservoir is depleted of its contents as production continues, its pressure declines progressively; although this is not severe for a gas reservoir due to high compressibility of gas.

Production from oil reservoirs is more complicated than from gas reservoirs. Oil production typically will consist of a number of phases based on the reservoir pressure. At the time of discovery, the reservoir pressure is usually high and the production is characterised with high flow rates. So, transportation of oil from underneath to the surface is relatively easier. This phase of production is called **primary recovery**. The decrease in reservoir pressure from continuous depletion makes flow of oil to the surface more difficult than for gas due to low oil compressibility and high density. During the production process, a time will

eventually reach where the natural reservoir pressure will not be sufficient to move the oil from ground to the surface. At this point, some techniques are usually employed to aid the oil flow. One of such techniques involves installation of pumps or gas lifting gadgets. Other means of aiding the production is by boosting the depleted reservoir pressure through liquid and/gas injection. This process of improved oil recovery is termed **secondary recovery** (Brouwer, 2004). Secondary recovery mechanisms will generally require drilling of an injection well near the vicinity of production well. Due to its availability, water is commonly used as one of the injecting fluids. The process is called **waterflooding**. Waterflooding is globally used and was sometimes responsible for increased flow rates in the U.S. and Canada (Craig, 1971). The present work will focus on this secondary recovery method and therefore will be reviewed in the following sections. When secondary recovery methods ceased to produce any significant incremental hydrocarbon, **tertiary recovery** techniques are then employed. Similar to secondary recovery, tertiary recovery involves injection of fluids such as steam (Ali and Meldau, 1979; Dietrich, 1990; Wei et al., 1993; Joshi et al., 1995; Gonzalez et al., 2009), carbon dioxide (Mungan, 1981; Holm, 1987; Martin and Taber, 1992; Shaw and Bachu, 2002; Odi and Gupta, 2010), and cheap hydrocarbon gases (Verma and Giesbrecht, 1985; Bowers et al., 1996; Pingping and Wen, 1998), polymers (Needham and Doe, 1987; Van Doren et al., 2011; Let et al., 2012). Others include in situ combustion and surfactant flooding (Capolei et al., 2012). These recovery operations are also called **enhanced oil recovery (EOR)**. Refer to A.3 for classifications of recovery mechanisms.

2.2 Waterflooding Process

2.2.1 General Principles and Problems

Waterflooding involves injection of water through an injection well into the reservoir and production of flushed oil through a production well. This process of secondary recovery has been in used for more than 100 years back, but gained popularity in the 1950's. It is one of the simplest and perhaps

economical means of increasing oil recovery (Asheim, 1987). Water is injected into the reservoir for two main purposes (Singh and Kiel, 1982):

- I. To increase oil recovery from semi-depleted and depleted reservoirs.
- II. To maintain pressure in new or partially depleted reservoirs with an aim to sustain the production rate.

Ideally, the injected water supposed to sweep oil from the point of injection towards the production well which get produced to the surface. But in reality, this does not happen so easily. Reservoir is heterogeneous in terms of properties. Meaning, reservoir properties vary spatially, the degree of variability depends on depositional environments and events that led to reservoir formation such as compaction, dolomitization, solution and cementation. These properties with high heterogeneity may include porosity, permeability, saturation, thickness, fractures and faults, and rock facies (Ahmed, 2006). So, the injected water will naturally flow through the easiest paths with less resistance which are typical high permeability zones and conductive fractures, as a result it (injected water) bypasses pools of oil and get its way into the production well. This phenomenon reduces the efficiency of the process as well as the ultimate recovery. The amount of water that is produced increases with time until a point is reached where the cost of injection and treatment of produced water outweighs the proceeds realisable from oil sales. At this point, the process is regarded as uneconomical. Unfortunately, due to poor sweep efficiency only about one-third of the original oil in place is recovered even with employment of waterflooding. Remedies to poor sweep efficiency have been suggested in the past which include mechanical isolation, squeeze cementing and use of polymeric materials (Mody and Dabbous, 1989). Another alternative which is receiving a great attention is the installation of smart injection and production wells (Brouwer et al., 2001). A smart well is an unconventional well with multi-segment completion. Each segment is equipped with inflow control valves (ICVs) so that flows can be controlled independently. The technology has the ability to delay or avoid early water break-through (Meum et al., 2008). This is shown in Figure 2-4.

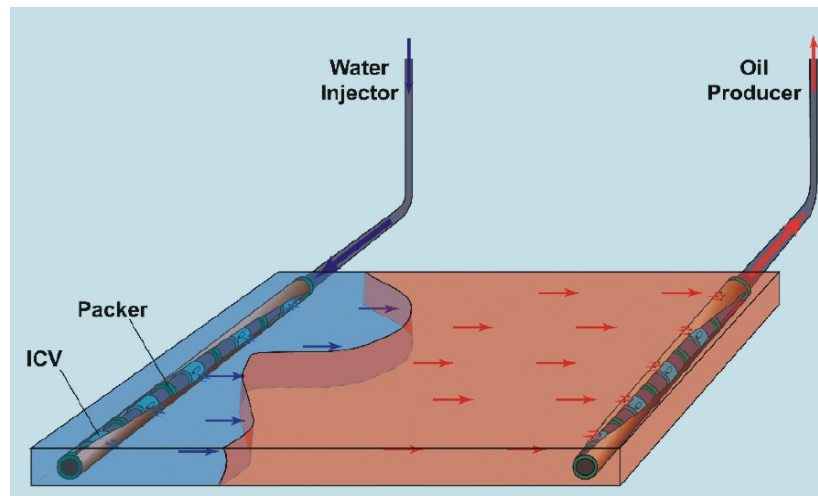


Figure 2-4: Heterogeneous Reservoir with Two Smart Wells (Brouwer, 2004)

2.2.2 Design and Operation of Waterflooding Process

The design of waterflooding process will require consideration of some critical factors as highlighted by Singh and Kiel (1982). These include geology, reservoir and fluid properties, primary production mechanisms, well spacing and waterflood patterns.

The first step in the design is however, a proper understanding of the reservoir geology. This entails knowing the reservoir structure and geometry. The structure will dictate wells location and waterflood methods to be employed. Other geological features of equal importance include faults, shale layers and other permeability barriers.

Rock and fluid properties of most important may include permeability, relative permeability, formation volume factor, and oil viscosity. The relative flowability of oil and water during waterflooding is usually characterised by factor, M called mobility ratio given by Ahmed (2006) as

$$M = \frac{k_{rw}}{\mu_w} \times \frac{\mu_o}{k_{ro}} \quad (2-6)$$

where μ_o and μ_w are oil and water viscosities respectively. It is obvious from Equation (2-6) that the fluids viscosities and relative permeabilities control its mobilities in the reservoir.

The natural supplies of energy that enable oil and gas to flow from the underground structure to the surface are called primary drive mechanism. These are categorised into depletion drive (dissolved gas drive), gas cap drive and gravity drainage. A combination of these forces may be present in a reservoir system in which the drive mechanism is referred to as combination drive (Guo et al., 2007). These drive mechanisms will actually indicate the requirement and extend of waterflood to a particular field. For instance, a reservoir with a very strong natural water drive or good gravity drainage will normally not require waterflood. On the other hand, reservoirs with depletion drive, small gas cap or inefficient water drive are good candidates for waterflooding (Singh and Kiel, 1982).

Flood patterns and well spacing have been found to directly affect the efficiency of waterflooding process. Pattern is the arrangement of injection and production wells. There are two broad categories of waterflooding patterns. These are repeated and peripheral patterns. Repeated pattern as the name implies, involves sequential repetition of a particular geometrical arrangement of wells. Common arrangement is square-spacing. Various types of repeated pattern include: (i) direct line drive (ii) staggered line drive (iii) five spot (iv) nine spot and (v) seven spot patterns. These are shown in Figure 2-5. Inverted networks are also possible where the positions of injection wells are interchanged by production wells and vice versa.

In peripheral flooding, injection wells are assembled along the flanks of a reservoir. This type of pattern is mostly applied to dip reservoirs so as to take advantage of the formation dip in order to have a more or less uniform flood front (Singh and Kiel, 1982).

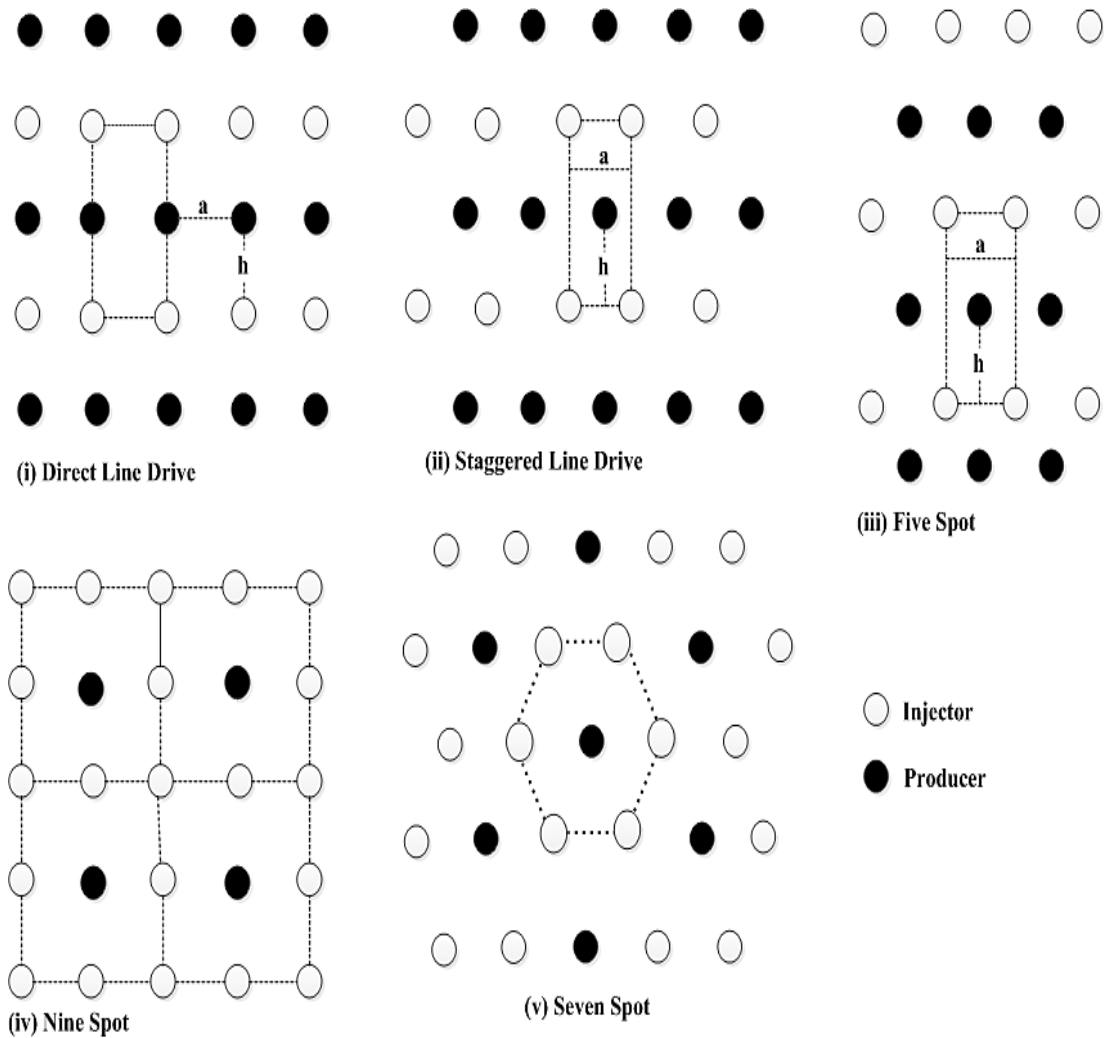


Figure 2-5: Waterflood Well Networks for Repeated Pattern (Muskat and Wyckoff, 1933)

Generally, reservoir engineering design of waterflooding encompasses specifying water injection rates, selection of a flood pattern and estimate of production rates and expected oil recovery. Specification of water injection rates is a difficult task and hardly accurate using analytical techniques. Injection requirements depend on the reservoir states at any particular point in time. Prediction of reservoir states however involves a lot of uncertain parameters to deal with. So, the best approach is continuous determination of injection settings throughout the operational period. Recently, this has been formulated as an optimization problem and is receiving a lot of attention; it will be the focus

of the present work. Therefore, optimization procedure and waterflood operation optimization are reviewed in Sections 2.3 and 2.4 respectively.

The amount of oil recovered by waterflooding is a function of three efficiency factors as described by (Singh and Kiel, 1982):

1. Areal sweep efficiency, E_a is the fraction of the pattern area that has been displaced by water.
2. Vertical sweep efficiency, E_i is the fraction of the cross-sectional area of the reservoir contacted by the injected water
3. Unit displacement efficiency, E_d is the fraction of initial oil in place displaced by injected water given by Singh and Kiel (1982)

$$E_d = \frac{S_{oi} - S_{or}}{S_{oi}} \quad (2-7)$$

where S_{oi} is the initial oil saturation. Volumetric efficiency, E_v is the combination of E_a and E_i given by (Singh and Kiel, 1982)

$$E_v = E_a \times E_i \quad (2-8)$$

The overall recovery efficiency, E_R is (Singh and Kiel, 1982)

$$E_R = E_v \times E_d \quad (2-9)$$

The traditional approach to operating waterflood fields is to design one of the symmetrical patterns described above and allocating equal rates to the injection wells based on the assumption that the permeability is homogeneous. If this assumption is to be true, then the flow streamlines will have the symmetry of the well pattern. Unfortunately, a realistically sized reservoir can hardly be homogeneous, therefore, constant and equally partitioned injection rates have been found not to be optimal (Sudaryanto and Yortsos, 2000). Another approach of finding operational injection and production settings is through a trial and error method by employing numerical reservoir simulation to compare performance of different injection/production schemes. The possibility of getting an optimum scheme via such a method is quite minimal (Asheim, 1987).

2.3 General Overview of Optimization Process

Optimization is a technique of determining the inputs to a system in order to maximize or minimize its output(s) so as to make it better (Haupt and Haupt, 2004). Application of optimization processes in upstream sector of oil and gas industry can be traced as far back as 1950's with new algorithms being explored. Several fields of interest within the industry are optimized which include planning, drilling, history matching, well placement, recovery processes, facility design and operation, etc. Different optimization techniques have been employed depending on the nature of the problem (Wang, 2003).

An optimization problem can be generally represented as

$$\begin{aligned} \min_u \quad & f(u) \\ \text{s.t.} \quad & g(u) = 0 \\ & lb_i \leq c_i(u_i) \leq ub_i \end{aligned} \tag{2-10}$$

where f is an objective function, u is given names as variable, decision variable, decision parameter, control variable and so on, g and c_i are equality and inequality constraint functions respectively. lb_i and ub_i are lower and upper bounds respectively for i th variables. Optimization problems are usually classified based on the nature of either the control variables, objective or constraints function. These include linear programming (LP), nonlinear programming (NLP), integer programming (IP), mixed integer programming (MIP), constrained and unconstrained problem. Detailed review of these classifications and their solution techniques can be found in Wang (2003).

2.4 Waterflooding Optimization

2.4.1 Basic Principles

In waterflooding optimization, the usual control variables are water injection rates, oil production rates and/or well bottomhole pressures (BHP). The objective to be maximized is either net present value (NPV) of the venture or oil recovery. Sometimes, delay in water break-through or water-cut can be set as

an objective. To visualize the problem better, it will be helpful to consider the reservoir model first.

Reservoir model equations are obtained for multiphase flow in porous media from mass balance equations, Darcy's law, equations of state and some initial and boundary conditions (Jansen et al., 2009). Combining these laws yields a set of ordinary differential equations after discretization in space which were presented in a compact form by Jansen et al. (2008) as

$$\mathbf{g}(\mathbf{u}, \mathbf{x}, \dot{\mathbf{x}}, \boldsymbol{\theta}) = 0 \quad (2-11)$$

where \mathbf{g} is a nonlinear vector-valued function, \mathbf{u} is the control vector (or input vector), \mathbf{x} is the vector of states, and $\boldsymbol{\theta}$ is vector of model parameters. Typically, for an isothermal reservoir system \mathbf{x} consists of reservoir pressure, saturation or components compositions. \mathbf{u} may contain those elements as bottom hole or tubing head pressure, wells choke settings that penetrated grid blocks, and parameters such as permeabilities, porosities and other reservoir and fluid properties make up the vector, $\boldsymbol{\theta}$ (Jansen et al., 2009). After discretising Equation (2-11) in time, we have (Jansen et al., 2009)

$$\mathbf{g}_{k+1}(\mathbf{u}_{k+1}, \mathbf{x}_k, \mathbf{x}_{k+1}) = 0, \quad k = 0, \dots, K - 1 \quad (2-12)$$

where the subscript, k is a discrete time-step while K is the end time. For the model to be complete, initial conditions are usually specified as (Jansen et al., 2009)

$$\mathbf{x}_0 = \check{\mathbf{x}}_0 \quad (2-13)$$

Outputs are combined in an output vector, \mathbf{y} , which are functions of \mathbf{x} and \mathbf{u} (Jansen et al., 2009)

$$\mathbf{y}_{k+1} = \mathbf{h}(\mathbf{u}_{k+1}, \mathbf{x}_{k+1}) \quad (2-14)$$

The optimization may be to maximize an objective of the form (Jansen et al., 2009)

$$J = \sum_{k=1}^K J_k(\mathbf{u}_k, \mathbf{y}_k) \quad (2-15)$$

where J is the objective function and J_k is the contribution to J in each time step.

Constraints can be imposed to the optimization in terms of state variables like pressures in the wells or input variables such as the injection rates. It can also be inequality or equality constraints and can take the form (Jansen et al., 2009)

$$\mathbf{C}(\mathbf{u}_k, \mathbf{x}_k) \leq 0 \quad (2-16)$$

The optimization problem can then be formulated as (Jansen et al., 2009)

$$\begin{aligned} \min_{\mathbf{u}_k} \quad & J = \sum_{k=1}^K J_k(\mathbf{u}_k, \mathbf{y}_k) \\ \text{s. t.} \quad & \mathbf{g}_{k+1}(\mathbf{u}_{k+1}, \mathbf{x}_k, \mathbf{x}_{k+1}) = 0 \\ & \mathbf{y}_{k+1} = \mathbf{h}(\mathbf{u}_{k+1}, \mathbf{x}_{k+1}) \\ & \mathbf{C}(\mathbf{u}_k, \mathbf{x}_k) \leq 0 \end{aligned} \quad (2-17)$$

We can therefore identify two types of well constraint, rate and pressure constraints. These are briefly described as follows (Brouwer and Jansen, 2004a).

Rate-Constrained Wells

When wells or segments of wells are constrained by rate, the control variables, \mathbf{u} are water injection and liquid production rates. In this case, no well inflow model is required. For an injection well or segment, i , the liquid rate, u_i equals the water injection rate, $u_{w,i}$ (Brouwer and Jansen, 2004a)

$$u_{w,i} = u_i \quad (2-18)$$

In a case where oil and water are produced from a production well or segment, j , the liquid rate, u_j is the sum of oil and water rates. The phase rates can then

be expressed in terms of the liquid rate and fractional flow (Brouwer and Jansen, 2004a)

$$u_{w,j} = u_j \frac{\lambda_{w,j}}{\lambda_{o,j} + \lambda_{w,j}}, \quad u_{o,j} = u_j \left(1 - \frac{\lambda_{w,j}}{\lambda_{o,j} + \lambda_{w,j}} \right) \quad (2-19)$$

where the water and oil mobilities are respectively given by (Brouwer and Jansen, 2004a)

$$\lambda_w = \frac{\rho_w K_a k_{rw}}{\mu_w} \quad (2-20)$$

and

$$\lambda_o = \frac{\rho_o K_a k_{ro}}{\mu_o} \quad (2-21)$$

The subscripts w and o refer to water and oil phases respectively. Parameters $\rho, \mu, K_a,$ and k_r are density, viscosity, absolute and relative permeability respectively. Relative permeabilities depend on saturations while densities and viscosities on pressure. It can be concluded therefore, that the phase rates, u_w and u_o are functions of state variables.

Pressure-Constrained Wells

Here, a well inflow model is required to link the flowing wellbore pressures and liquid rates for injectors and producers. The relationship can be expressed as (Brouwer and Jansen, 2004a)

$$u = \alpha_p (p_{wf} - p_{gb}) \quad (2-22)$$

where u is the injector or producer liquid rate, p_{wf} is the flowing wellbore pressures, p_{gb} is the grid block pressure in which a well is completed, and α_p is termed well productivity index which is not constant for two-phase flow region. It depends on the reservoir states, and fluid and rock properties. So the relationship in Equation (2-22) is not linear (Guo et al., 2007).

Having laid a foundation on waterflooding optimization, a review in this field is given next. Two approaches to the solution of the problem are discussed, the open- and closed-loop optimization.

2.4.2 Open-Loop Optimization

With reference to waterflooding, open-loop optimization (Jansen et al., 2008; Jansen et al., 2009) is when optimal injection and production profiles are computed over a horizon without taking the advantage offered by measurements in a feedback fashion. This is usually employed during the early stage of field development studies when production measurements are not available and the field plan has to be done from static and dynamic reservoir models built from outcrop studies, well tests, seismic data and so on (Jansen et al., 2005). Most of the optimization studies conducted in earliest times are open-loop.

Asheim (1987) considered two vertical injectors and a single producer in simplified reservoir systems to maximize NPV with well rates as the optimization variables. A finite difference reservoir simulator was used. The gradient of the objective function with respect to well rates was computed using implicit differentiation algorithm. Both artificial water drive and natural aquifer were studied. Improvement in NPV in the range 2-11% was recorded. This study was followed by work that considered two vertical producers (Asheim, 1988).

In the work of Virnovsky (1988), well rates were optimized for a waterflooding operation for both single-and multi-phase fluids in a one-dimensional reservoir. The optimization problem was solved by method of successive linearization with oil recovery as objective function. This work was extended to cover two-dimensional reservoir (Virnovsky, 1991). Sudaryanto and Yortos (2000, 2001) carried out their optimization studies considering two extremes of well control, that is either fully opened or closed (bang-bang control approach) when water break through is experienced. They used switching time optimization (STO) algorithm to find optimum location of switch times. Two injectors and one

producer were considered in a rectangular bounded reservoir. Homogenous and heterogeneous reservoir systems were studied. The heterogeneity was in the form of non-uniformity in permeability and presence of impermeable fault. This approach was compared to a case where injection rates are kept constant. The bang-bang control approach gave better displacement efficiencies than the constant rate case with improvements of up to 13.7%.

Yeten et al. (2003) optimized location, trajectory, number of laterals of nonconventional well, and well pressures and rates to maximize NPV and total oil recovery. They used hybrid of algorithms in their work. Specifically, genetic algorithm (GA) was used as a master optimization engine with simple hill-climbing procedure to enhance the search within the solution region. A near-well upscaling method was used to speed up the finite difference simulation. Realistic reservoir cases were treated.

In the work of Brouwer et al. (2001), optimization was performed for fully penetrating, smart horizontal wells in two dimensional horizontal reservoirs with simple large-scale heterogeneities. A black-oil commercial reservoir simulator, IMEX was used to simulate two-phase of oil and water in the reservoir system. The optimization was set for time-independent variables that were allowed to depend only on the spatial reservoir heterogeneity. Application of this optimization procedure results in improvement in oil recovery from 0-20% and delay in water break-through time from 7-168%.

Brouwer and Jansen (2004a) optimized valve settings of smart horizontal injection and production wells using optimal control theory with adjoint formulations for gradient computation. Steepest descent algorithm was used for calculation of improved controls. Three horizontal 2-D reservoir models with different levels in permeability heterogeneity were simulated using an in-house semi-implicit simulator. Either oil recovery or NPV was maximized. Both purely rate- and purely pressure- constrained were investigated. They concluded that the benefit of using smart wells under pressure-constraint conditions is to mainly reduce water production while wells operated under rate constraints

have the potential for accelerated oil production as well as a drastic cut in water production.

One shortcoming of adjoint-based technique (that is, using Lagrange multipliers) is that it requires a detailed knowledge of the reservoir simulator. For this reason, Lorentzen and others (2006) optimized discrete choke settings of smart wells using ensemble Kalman filter (EnKF) technique. The model equations were treated as a black box so there is no need for adjoint equations. A simplistic layered reservoir was used to demonstrate the efficacy of the approach. Both oil recovery and NPV were used as objective functions. The technique was found to be robust and superior when compared to partial enumeration (PE) method. For the particular case studied, PE utilized 440 Eclipse simulations with six months duration while EnKF used 3100 Eclipse simulations for five years duration. Therefore, the authors concluded that EnKF approach was relatively slow.

Apart from the complexity in coding adjoint formulation, the codes need to be updated whenever the forward simulation model is updated. For this reason, Sarma and colleagues (2005) proposed a method to overcome this short coming by developing new algorithm that makes the adjoint codes entirely independent of the simulation model. Also, two methods of handling nonlinear path constraints were proposed. The algorithm was applied to both simplistic and a complex reservoir system. The problems with these constraint handling methods are that, they are either applicable to small problems or do not satisfy some of the constraints. The constraint handling algorithm was improved in a later study by Sarma and others (2008a) through developing an approximate feasible-direction NLP algorithm which combines a feasible-direction algorithm and constraint lumping with a feasible-line search. This leads to a computationally efficient procedure. After applying the methodology on two reservoir structures of different complexities, improvements in NPV and oil recovery were recorded.

In the work of Asadollahi and Naevdal (2009) the effects of initial starting point and type of optimization variables on gradient-based optimization were

investigated. Three optimizing variables were tested, oil and liquid production rates, and bottomhole pressure. Two line-search methods, steepest descent and conjugate gradient were considered and compared in the adjoint-based optimization approach. Reservoir realizations reported in Lorentzen et al. (2009) were used for these comparative analyses. Well liquid rates were found to be the best optimization variables. It was also found that conjugate gradient is slightly faster than steepest descent algorithm (difference in time duration was not specified by the authors) but the effect of initial guess is far more important on performance of the optimization methods.

A new algorithm was developed by Völcker et al. (2011) for the solution of the model equations, which is Explicit Singly Diagonally Implicit Runge-Kutta (ESDIRK) method while the gradients were computed by adjoint methods. The constrained optimization was solved using a quasi-Newton Sequential Quadratic Programming (SQP). The reservoir models used in Brouwer and Jansen (2004a) was adopted in this study to test the efficacy of the proposed method. Water injection rates and producer bottomhole pressure were used as variables to maximize NPV of the waterflooding process. An improvement of up to 10% was recorded over a non-optimized scenario. The main advantage of this high-order scheme is that, larger time steps are possible with minimal error and therefore an improved computational time can be achieved.

In all of the above mentioned adjoint procedures, the gradients were computed using discrete adjoint. Capolei et al. (2012) improved the method presented in Völcker et al. (2011) by including continuous time adjoint formulation for faster simulation. This formulation was applied to a five-spot pattern of waterflooding process where heterogeneity in reservoir permeability was considered. Both increases in NPV and oil recovery were achieved.

The model-based optimization schemes mentioned above were carried out using single reservoir models whose properties were assumed to be known with perfection. However, reservoir properties are highly heterogeneous and uncertain. These properties are only known with some degrees of certainty near the well region only. Reservoir geometry is usually deduced from seismic data.

As a result, its boundaries are highly uncertain (Haupt and Haupt, 2004). Some properties such as thin, high-permeability zones may not be captured within the given model resolution. Similarly, productions can be dominated by some near-well effects for example, coning which is rarely captured well in simulation models (Dilib and Jackson, 2013a). Apart from well coning, there are other possible operational uncertainties such as reservoir formation damage which occurs as a result of injecting incompatible water. There may also be uncertainty in the reservoir fluid description. For this reason, basing the open-loop optimal control on a single reservoir model may be suboptimal or entirely non optimal. Optimal control can therefore be said lacks robustness to handle geological uncertainties. Several attempts have been made in the past to come up with optimization methods which result to injection and production settings that are less sensitive to these uncertainties. One of these methods is robust optimization (RO) where ensemble of geological realizations is used. The main assumption underlying this technique is that, the geological realizations are able to capture all possible reservoir and production characteristics. In the work of Yeten et al. (2002), five geostatistical realizations of reservoir with different channelized permeability fields were used. Conjugate gradient algorithm was applied to optimize oil recovery. Each of these realizations was used separately to determine the optimum profiles. The effect of the permeability variations was seen in the amounts of oil recovered from each reservoir model. The total oil recoveries vary significantly with a standard deviation of 0.95 MMSTB, minimum of 2.48 MMSTB and a maximum of 4.27 MMSTB.

Van Essen et al. (2009) successfully implemented 100 ensemble of reservoir realizations into the optimization scheme using expected value E of the objective function J over the set of realizations given by

$$E_{\theta}[J(\mathbf{q}_{1:K}, \boldsymbol{\theta})] \approx E_{\theta_d}[J(\mathbf{q}_{1:K}, \boldsymbol{\theta}_d)], \boldsymbol{\theta}_d := \{\theta_1, \dots, \theta_{N_r}\} \quad (2-23)$$

where $\boldsymbol{\theta}_d$ is the deterministic set of realizations parameters and \mathbf{q} its outputs. N_r is the total number of realizations. When the realizations are assumed to be

equiprobable, E is simply the average of J_s as in Equation (2-24) (Van Essen et al., 2009)

$$E_{\theta_d}[J(\mathbf{q}_{1:K}, \theta_d)] = \frac{1}{N_r} \sum_{i=1}^{N_r} J(\mathbf{q}_{1:K}, \theta_i) \quad (2-24)$$

An adjoint technique was used to obtain the gradient. The RO scheme was compared to a nominal case where optimal strategies were found on each individual model, and a reactive control case which strategy is to shut-in any production well that is not profitable. The results from RO approach indicated a smaller variance than the two alternatives with improved NPV. Only a simple linear constraint was considered. This indicates robustness in handling uncertainty. In a similar work (Chen et al., 2012), linear, nonlinear and bound constraints were incorporated. The linear and nonlinear constraints were augmented into the objective function (expected value of NPV) via augmented Lagrangian method while the bound constraint was enforced using a gradient-projection trust region method. An adjoint solution was used to compute the gradient of the Lagrangian function. The method was applied to a synthetic reservoir where it was found that optimal controls obtained on the basis of a single uncertain reservoir may not achieve optimality and is associated with high risks whereas results from RO demonstrated that an improved NPV could be realised.

2.4.3 Closed-Loop Optimization

Closed-loop optimization (Jansen et al., 2008; Jansen et al., 2009) involves the use of uncertain reservoir models in the optimization process and continuous updates of these models using production measurements and other data in a systematic fashion. As mentioned above, reservoir properties are quite uncertain and power of models to predict production characteristics is usually low. Traditionally, predictive value of such models is usually improved through a process called 'history-matching'. This involves the use of available production data, well logs, seismic data and data from core analysis to update the reservoir

model(s). Then new optimized production and injection strategies are obtained based on the updated models. However, history-matching is performed periodically on a campaign basis. Apart from this, many draw-backs are associated with this technique as mentioned in Jansen et al. (2005). One of these shortcomings is that, it involves manual tuning of parameters instead of systematic approach. The resulting updated models may not have even a predictive capacity because of over-fitting.

In view of this, several authors are of the opinion that there should be a shift from present practice of periodic updating of model and strategies for every history matching activity to a more efficient utilization of production measurements where control strategies are implemented in a closed-loop fashion (Brouwer et al., 2004b; Jansen et al., 2005; Sarma et al., 2005; Sarma et al., 2008b; Foss and Jensen, 2011; Dilib and Jackson, 2013a). This led to studies on methodologies for automatic model updating (data assimilation) integrated with optimization of production systems in a closed-loop. The concept is receiving a great attention which is termed 'closed-loop reservoir management (CLRM)', 'real time reservoir management', 'self-learning reservoir management', 'e-fields' or 'smart field'. The key components of CLRM are model updating and optimization. Model upscaling/downscaling is also considered as an integral element of the system (Jansen et al., 2005). The aim is to increase reservoir performance using measurement and control techniques. The source of inspiration was driven from measurement and control theory in the process industries and data assimilation as used in meteorology and oceanography (Jansen et al., 2009). Figure 2-6 shows the concept of CLRM described by Jansen et al. (2009).

The loop consists of physical system, such as reservoir(s), wells and facilities. The system models may involve static geologic model, reservoir dynamic model and well model. Sometimes, a number of reservoir models are used to counteract the effect of uncertainties as mentioned in Section 2.4.2. The sensors by the right of the figure can be devices for real-time measurements of production data such as rates, wellhead pressures and so on; it can also be

regarded as sources of other data types. The optimization algorithms produce the actual optimal production variables such as choke settings, injection and production rates, or can be thought as a decision making tool where decisions such as optimal well locations are taken. The effect of system uncertainties is taken care of by data assimilation block where system model(s) is/are continuously updated via computer assisted history matching (CAHM). This is done by comparing the model parameters and measured output until the difference is minimised. This has been explained in detail (Jansen et al., 2005; Jansen et al., 2008; Asadollahi and Naevdal, 2009; Jansen et al., 2009).

One of the earliest works to combine optimization with model updating in a closed-loop frame work is that of Aitokhuehi et al. (2004). Optimal well type, location and trajectory were first optimized using genetic algorithms (GA). Optimization of valve settings was then performed using conjugate gradient

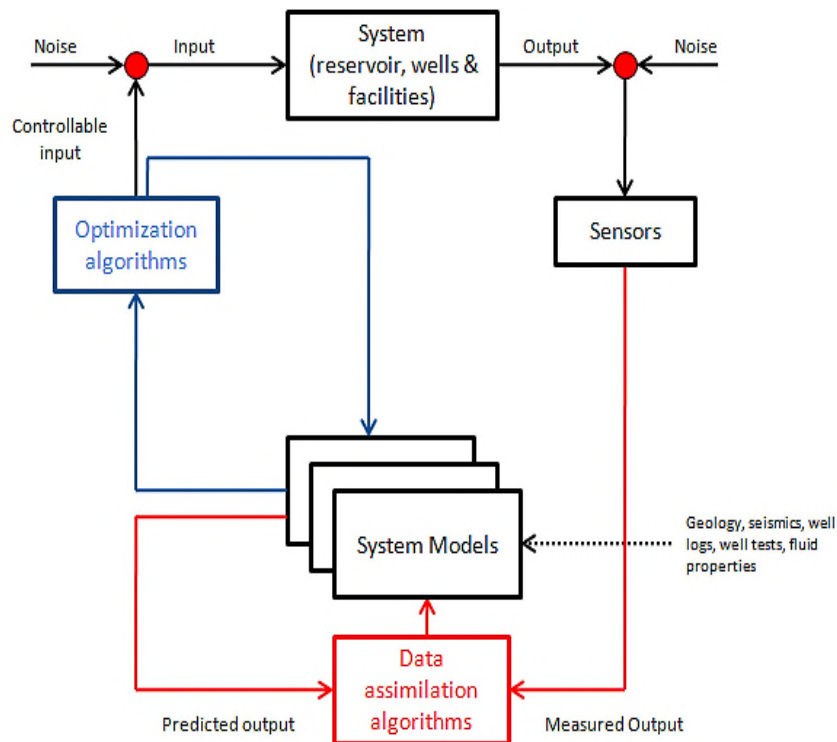


Figure 2-6: Closed-Loop Reservoir Management Process (Jansen et al., 2009)

algorithms (CG) with continuous model updating using probability perturbation method to maximize oil recovery. Downhole pressures and phase flow rates were used for history matching. Both single and multiple realizations were used for the optimization and the results obtained showed benefits of continuous model updating and use of ensemble of realizations to counteract effects of geological uncertainties. The algorithms were applied to a quad-lateral well system and a channelized reservoir with a gas cap and aquifer simulated using a commercial simulator. The advantage of using CG is that it does not require access into the simulator like adjoint formulation; though, it was reported that it is too slow; about 100 simulations were required for gradient calculations for valve settings optimization.

New concepts and algorithms developed for reservoir management are only tested on virtual asset, not on real reservoir fields. This is because reservoir management procedures are in the orders of years to decades (Jansen et al., 2005).

In the work of Brouwer et al. (2004b), adjoint-based technique was used to optimize NPV of waterflooding process which was integrated with automatic history matching that was configured using ensemble Kalman filter method. An ensemble of 100 geological realizations was used. Pressure and saturations data at well grid blocks were utilized for model updating. Both static parameters (permeability fields) and dynamic variables (pressures and saturations) are updated. The optimization procedure was started by using a homogenous reservoir model to determine the optimal control strategy. The model was then continuously updated once new production data become available. The algorithms were tested on two different synthetic reservoirs. Improvements in NPV, acceleration of oil production, cumulative oil recovery and reduction in water production were realized. In one of the cases, improvement in oil recovery was found to be very close to a case where the reservoir description is assumed to be known perfectly. A similar work was conducted by Overbeek et al. (2004). Here, a higher-order reservoir model simulated with a commercial simulator was used to represent real reservoir while a low-order model was

used for optimization which was updated when new production measurements become available. But in the case of Brouwer et al. (2004b), low-order models were used to represent reality, and for optimization and updating. A related work was reported in Jansen et al. (2005) where 100 random geostatistical realizations with differing permeability fields were used. A good result was obtained which is closer to the one obtained using open-loop with perfect reservoir knowledge. However, the optimization was not performed on all the ensemble members, but on their average. Similar result was discussed in Naevdal et al. (2006). In a follow-up study by Sarma et al. (2006), model updating was performed using Bayesian inversion theory which is combined with adjoint models and parameterization of uncertain permeability fields in terms of Karhunen-Loeve (K-L) expansion. Bayesian inversion is a statistical method of estimating model parameters from measurements. Here, posterior probability density of model parameters was determined by combining prior probability densities of observed data and model parameters. Typically, the method was used for the inversion of production data such as well flow rates and pressures to estimate uncertain values of porosity and permeability (Sarma et al., 2006). The representation of the unknown parameter in terms of K-L expansion enables the updating procedure to use adjoint techniques while maintaining the two-point geostatistics of the reservoir descriptions. The optimal control optimization was also performed using adjoint-based formulations. Again, the closed-loop procedure yielded results that are close to those obtained from an open-loop optimal control with reservoir descriptions assumed to be known a priori. Non-linear path constraints were considered in the closed-loop configuration by Sarma et al. (2008b) using adjoint-based configuration. An NLP algorithm based on objective function gradient and combined gradient of the active constraints was applied to handle the constraints. An example of such constraint is constraint on injection rate when BHP is used as the control. Parameterization for model updating was based on kernel principal component analysis (KPCA) that allows the maintenance of high-degree geological realization with gradient-based algorithm for history-matching. The configuration was applied to a complex realistic reservoir case with three injection wells and

four production wells. An improvement of about 25% was achieved over a base case and this is closer to that of a theoretical open-loop in which the reservoir is assumed to be known.

Three optimization algorithms were compared in the CLRM arrangement by Wang et al. (2009). These are EnKF, steepest ascent (SA) and simultaneous perturbation stochastic approximation (SPSA). These were tested on two simple case studies where BHP was used as the control. About 90 ensemble members of porosity and log-permeability fields were generated and optimization was performed on the updated central model only. They defined central model as “the updated model obtained by assimilating measurements without perturbation using the prior mean as its initial realization”. The results showed SA as the most efficient algorithm even though the gradient was computed by finite difference method. EnKF was found to be very slow as an optimization algorithm with poor estimates of the controls. SPSA also converges very slow but gives reasonable controls. In one of the case studies, SA required only 20 equivalent reservoir simulation runs while SPSA and EnKF reached convergence after 1000 and 2500 simulation runs respectively.

A novel ensemble-based CLRM scheme was reported by Chen et al. (2009) where a robust optimization was performed using EnKF. The optimization scheme they named EnOpt. Model updating was done via ensemble randomized maximum likelihood (EnRML) procedures. The main advantages of this approach is that it is adjoint-free, can be used with any reservoir simulator and more importantly it is fairly robust. This configuration was tested on a synthetic reservoir model reported in Brouwer and Jansen (2004a) and was compared to three production scenarios; wells with no control, reactive control where wells are shut-in based on the production water oil ratio and optimization with known geology. The closed-loop method used 60 ensembles of reservoir realizations based on uncertain permeability fields. An improvement in NPV was obtained that is similar to the case with known reservoir properties. In Chen and Oliver (2010), the methodology was also applied to Brugge field, a large and complex synthetic reservoir field designed to mimic reality so that different

CLRM techniques can be tested and compared. It was used as a benchmark in a workshop; see for example Jansen et al. (2009). An NPV which is worst by less than 1% of the actual value obtained by the organisers of the workshop based on known geology (benchmark) was found. The benchmark NPV is $\$4.63 \times 10^9$ while that obtained by the novel scheme is $\$4.59 \times 10^9$.

A control algorithm was proposed to be included in multi-level structure of CLRM (Saputelli et al., 2006; Foss and Jensen, 2011; van Essen et al., 2013). In the work of van Essen et al. (2013), the loop consists of a synthetic reservoir model representing the truth reservoir, a coarser reservoir model in time-step and space used for life-cycle optimization and a model predictive controller (MPC). A simple data-driven model developed with sub-space identification method was used for prediction in conjunction with the MPC. No noise was added to the data so that state estimation became less complex that was carried out using Luenberger observer. In the work however, neither CAHM nor robust optimization was used to handle uncertainty. The only method used to alleviate the effect of uncertainty is through tracking effort of the controller even though the model mismatch considered is not much; grid refinements around wells and slight variation in permeability were the only mismatches introduced. One advantage of using a data-driving model in the loop is its ability to capture some operational issues such as gas or water conning and effects of unforeseen activities that may include well intervention and maintenance which will otherwise be difficult to be covered by physics-based reservoir simulator and handled during life-cycle optimization. On the other hand, the data-driven model formulated can never predict water saturations; it can however, predict pressures over a short period of time during which saturations do not change appreciably. Therefore, they concluded that rejection of larger disturbances that can cause a change in water saturations can only be possible through CAHM and/or geological model revision. Unfortunately, CAHM is very slow which renders the whole process of CLRM time consuming and therefore, frequency of model updating is reduced drastically.

The processes proposed for CLRM are very complex and will be difficult to be implemented to real life scenario. The search for a simple feedback control capable of counteracting the effects of uncertainties in reservoir behaviour can never be over emphasized. There have been attempts in the past to this regard, although the control actions were determined using ad hoc models for e.g. Grebenkin and Davies (2010). Recently, Dilib and Jackson (2013a) designed their feedback configuration by optimizing feedback control relationship between measured data and inflow control settings. Typically, the relationship was constructed from measured water-cut and valve openings of smart well which is given as (Dilib and Jackson, 2013a).

$$\pi_i = \max \left[A - \left(\frac{W_i - W_m}{W_l - W_m} \right)^c, B \right] \quad (2-25)$$

where $c \geq 0$ and $B \leq A$; π_i is inflow setting, W_i is measured completion water cut, W_l is maximum well water-cut limit, and W_m is smallest completion water cut. The parameters A , B and C were obtained via model-based optimization with the assumption that the reservoir description is perfectly known. Four uncertain parameters that include width of shale-free zone of high vertical permeability, strength of aquifer, horizontal permeability and shape of oil/water relative permeability curves were considered in the feedback strategy. The benefit of feedback control application was seen from improved NPV similar to that obtained with an open-loop optimal solution based on perfect reservoir descriptions. As was mentioned by the authors, apart from its relative simplicity that has a very high potential to be implemented in practice, direct feedback strategy implements control decisions that are not based on model predictions which most often are characterised by uncertain behaviours. Furthermore, model-based optimal strategies may not have the possibility to be implemented in practice. Although, in their work (Dilib and Jackson, 2013a), the feedback control relationship was formulated from model predictions and gradient-based optimization technique, the real-time implementation of the controls is based on production measurements. It is worth to note that only a single model was used in the derivation of the relationship and robustness was due to the feedback implementation. The method was applied to a simplistic reservoir with a

horizontal well; it was then applied to a more realistic, synthetic reservoir, the Brugge field (Dilib et al., 2013b).

A fundamental task that needs to be addressed is the design of such a simple feedback strategy that is robust enough to counter the effects of uncertain reservoir and production behaviours. An interesting aspect will be in determining controlled variables (CVs) in the configuration that is insensitive to uncertainties which when kept constant at a set point the process is optimal or near-optimal. This concept which is termed 'self-optimizing control (SOC)' is receiving a great attention for continuous processes and it will be worth exploring for waterflooding processes. For this reason, SOC is reviewed in Section 2.6.

2.5 Model Predictive Control for Reservoir Waterflooding

According to Mayne et al. (2000), "model predictive control (MPC) or receding horizon control (RHC) is a form of control in which the current control action is obtained by solving online, at each sampling instant, a finite horizon open-loop optimal control problem, using the current state of the plant as the initial state; the optimization yields an optimal control sequence and the first control in this sequence is applied to the plant". It can be seen from Figure 2-7 that the "control law is calculated for a given control horizon, T_N , and the dynamic behaviour of the system is calculated over the prediction horizon T_k where $T_N \leq T_k$ and $r(t)$ is the reference trajectory that the system is to be controlled to" (Meum et al., 2008). MPC has received a great attention over the years and different industrial implementations exist (Qin and Badgwell, 2003). It operates on the basis of the principle of optimality and is robust due to its closed-loop control; it can also handle efficiently system's constraints, a reason that gives it a widespread acceptance (Meum et al., 2008). Traditionally, MPC is implemented in real-time optimization mode which makes it complicated because there is a requirement for data reconciliation, model update and optimization that all are to be performed online (Alstad, 2005).

van Essen et al. (2013) have proposed a consideration of MPC in combination with a data-driven model as a lower-level tracking in the CLRM configuration shown earlier in Figure 2-6. So by adopting the proposed approach, reservoir models are continuously updated using field measurements and life cycle optimization is carried out based on the updated models.

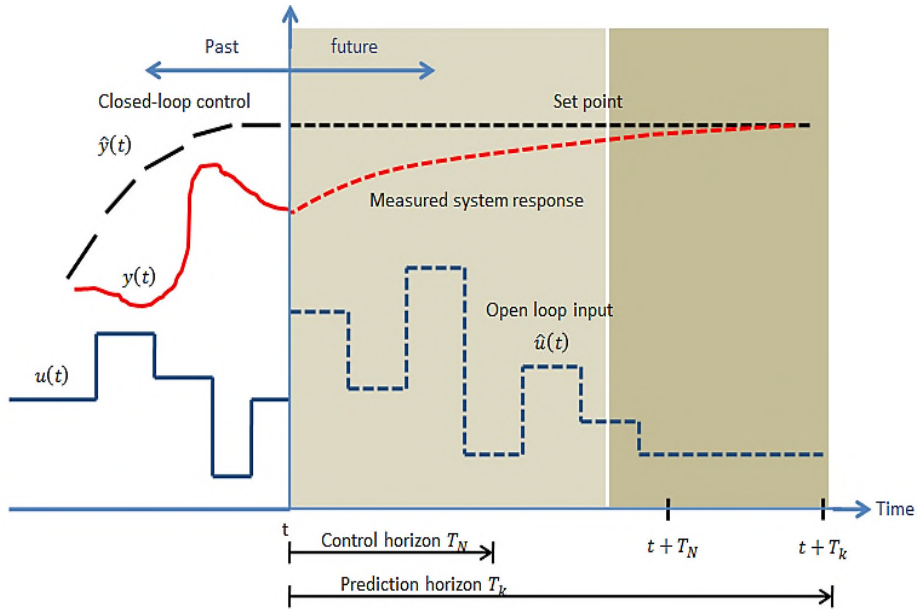


Figure 2-7: Principle of MPC (modified from (Meum et al., 2008))

The measurements are also used to estimate the data-driven prediction model. The optimum production profiles $\hat{y}_{1:k}$ obtained at the optimization stage are used as reference trajectory for the MPC which serves to track these optimum variables. The controller determines optimum well settings \tilde{u} by minimizing the difference between the actual measured outputs y and optimal \hat{y} (Figure 2-8). This is solved as an optimization problem where the objective function, Equation (2-26) is minimized over a short period of time (Jansen et al., 2009).

$$V(\tilde{u}_{1:N}) = \sum_{k=1}^N (\mathbf{y}_{k+1} - \hat{\mathbf{y}}_{k+1})^T \mathbf{W}_1 (\mathbf{y}_{k+1} - \hat{\mathbf{y}}_{k+1}) + (\tilde{\mathbf{u}}_k - \hat{\mathbf{u}}_k)^T \mathbf{W}_2 (\tilde{\mathbf{u}}_k - \hat{\mathbf{u}}_k) \quad (2-26)$$

where N is number of time steps over the control horizon and \mathbf{W}_1 and \mathbf{W}_2 are weighting matrices.

In addition, Foss and Jensen (2011) have advocated the use of MPC in CLRM. They first described four different control hierarchy based on the time scale used to make decision and implementation. This four-level structure includes asset management, reservoir management, production optimization, and control and automation. In CLRM, control inputs are implemented between sampling times, and because of this, the authors argued that in reality it (CLRM) will be a mix of closed-loop and open-loop strategies; and going by the principles of MPC discussed above, it can be said that it balances the two strategies in such a way that it can be the right choice for reservoir management. They have however, pointed out that MPC is computationally intensive due to the necessity of reoptimization at every control time. Furthermore, prediction and control horizons have a great effect on its performance.

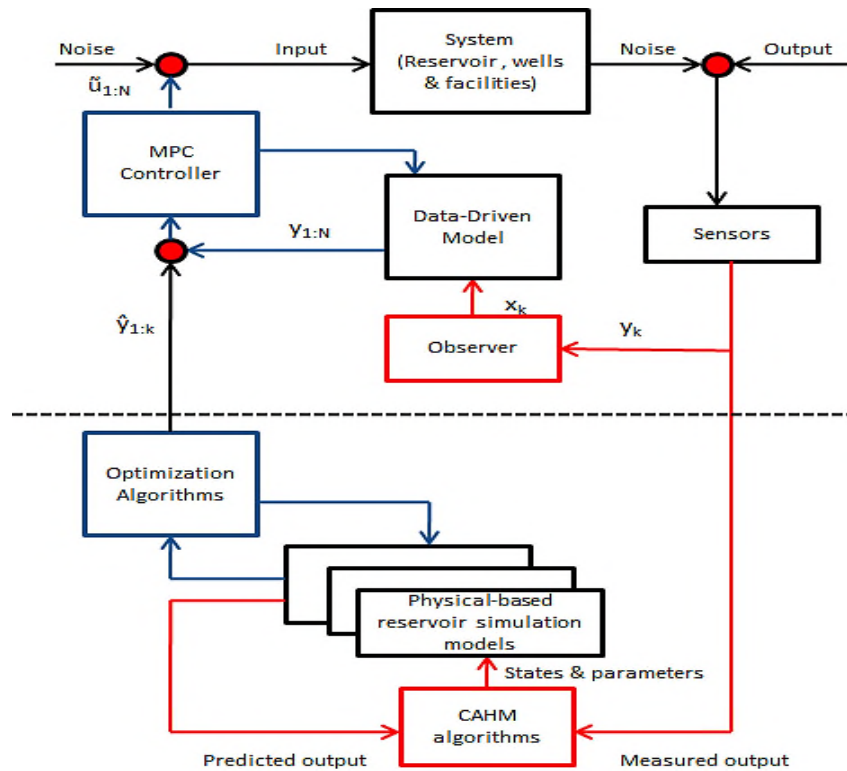


Figure 2-8: Two-Level Strategy to Combine Reservoir Management with Model Predictive Control of Production (van Essen et al., 2013)

2.6 Self-Optimizing Control for Controlled Variables (CVs) Selection

2.6.1 Basic Definitions and principles

A critical stage in any control structure design is the selection of CVs and manipulated variables (MVs), and the linkage of these variables. This stage affects to a larger extent the economy and the safety of any plant operation (Umar et al., 2012). In CLRM studies, very little attention has been given to selection of CVs. Skogestad (2000) proposed a method of CV selection that places an emphasis on optimal operation of plant. This concept is called self-optimizing control (SOC). As stated by Umar et al. (2012), the main idea of this method is to find CVs which can be controlled despite the presence of uncertainties and disturbances keep the operation of the process near-optimal. That is to say, the process becomes 'self-optimizing' with the control of the selected CVs at constant setpoints. Skogestad (2000) had this to say about SOC:

Self-optimizing control is when we can achieve an acceptable loss with constant setpoint values for the controlled variables (without the need to reoptimize when disturbances occur).

There are two important points that can be inferred from above definition:

- The ability to control the selected CVs at their setpoint.
- The above control should result to a minimum acceptable loss.

The concept may be well understood by considering one of our daily activities as an example, this is, the process of cake baking. Here, by appropriately controlling the oven temperature and baking time at the setpoints, the baking operation is indirectly kept close to its optimum which is 'well-baked cake' (Skogestad, 2000).

The principle can be illustrated further by observing Figure 2-9, where it can be seen that a loss is incurred by keeping a constant setpoint instead of reoptimization with occurrence of a disturbance which takes the process away from its nominal operating point (denoted by *). In the figure, c_1 and c_2 are the

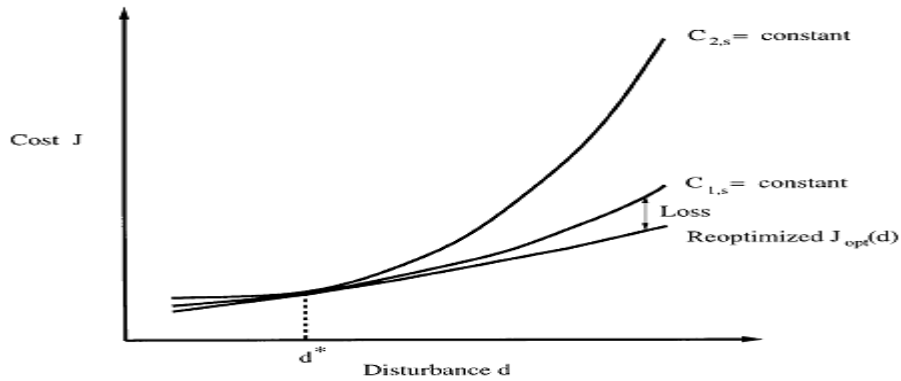


Figure 2-9: Loss Incurred by Maintaining Constant Setpoint for the Controlled Variable (Skogestad, 2000)

CV alternatives with respective setpoints, c_{1s} and c_{2s} . The setpoints are the optimal values of the CVs for nominal disturbance, d^* . At a point where $d = d^*$, the loss is zero for both CVs. But as the disturbance, d deviates from d^* , it will be better to maintain constant the setpoint, c_{1s} instead of c_{2s} (Umar et al., 2012).

For easier referencing, the optimization problem can be stated as follows for steady state processes (Umar et al., 2012)

$$\begin{aligned} \min_u \quad & J(u, d) \\ \text{s. t.} \quad & g(u, d) \leq 0 \end{aligned} \quad (2-27)$$

where the objective function J is scalar, $u \in \mathbb{R}^{n_u}$ are manipulative variables, $d \in \mathbb{R}^{n_d}$ are the disturbances or uncertainties and $g: \mathbb{R}^{n_u} \times \mathbb{R}^{n_d} \Rightarrow \mathbb{R}^{n_g}$ are the constraints.

To maintain the CVs at setpoints, a feedback controller is used to update the manipulated variables (degrees of freedom, DOF) as can be seen from Figure 2-10. In the diagram u_{fb} is the feedback control law, e is the implementation or measurement error, \tilde{y} is the outputs, c_s is the set point while y is the summation of \tilde{y} and e . The loss is incurred from the use of a feedback-based strategy in comparison with the truly optimal operation. The truly optimal operation is the desirable which can be obtained if only the optimization problem in Equation

(2-27) can be solved online for every change in d . This is not realistic in practice. The loss is written as (Umar et al., 2012)

$$L = J(u_{fb}, d) - J_{opt}(d) \quad (2-28)$$

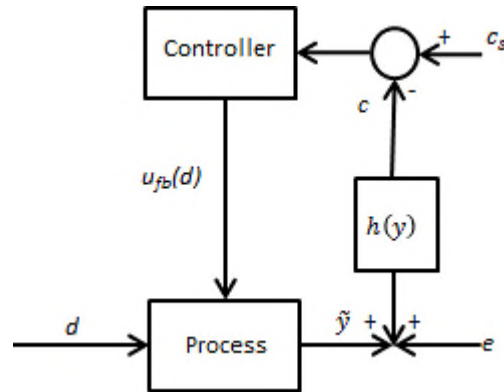


Figure 2-10: Feedback operational Strategy (Umar et al., 2012)

Ideally, as $u_{fb}(d)$ changes with disturbance, the setpoint should be updated based on the disturbances. Thus, the use of a constant setpoint results to an error known as setpoint error. The loss presented in Equation (2-28) is a combination of losses due to implementation and setpoint errors. Due to the effect of implementation error as a result of measurement error, the CVs shift from the setpoints even though the disturbances do not change (Umar et al., 2012). For this reason, Skogestad (2000) listed the following qualitative rules for CV selection:

- Optimal value of CV should be insensitive to disturbances.
- To reduce the effects of implementation error, the CV should be easy to measure and control.
- The CVs should be sensitive to manipulative variable changes.
- CVs should not have interlinked effect for cases with more than one CV.

Since, the main concern of SOC is the selection of appropriate CVs, a brief description of MVs and CVs is given in the next section.

2.6.2 Manipulated and Controlled Variables

A manipulated variable, control variable or control input according to Janert (2013) is a quantity that can be adjusted directly which hopefully influences the output in a favourable way. The controlled variable or process variable is the quantity that is to be controlled. The controlled variable is needed to track a certain setpoint. A simple example to illustrate the concept of MV and CV is the process of maintaining the temperature of a vessel containing some material at a specific value. Here, the MV may be the flow of heating oil or the voltage applied to a heating element. The temperature of the vessel is CV (Janert, 2013).

Furthermore, Tatjewski (2007) had this to say to distinguish between CVs and MVs: a controlled process undergoes a controlled influence through a control unit for example, a control algorithm executed by a computer. It can also be influenced by uncontrolled environmental factors which are referred to as disturbances. The process input variables at the disposal of the control unit are called manipulated variables or control variables. The state of a controlled process is evaluated on the basis of measurements. These measurements should be variables that have features that can characterise the process behaviour which are called process output variables. Figure 2-11 shows the structure of a control system with manipulated and output variables (Tatjewski, 2007). For waterflooding process, water injection and total liquid production rates can be the MVs while oil and water production rates can be output variables.

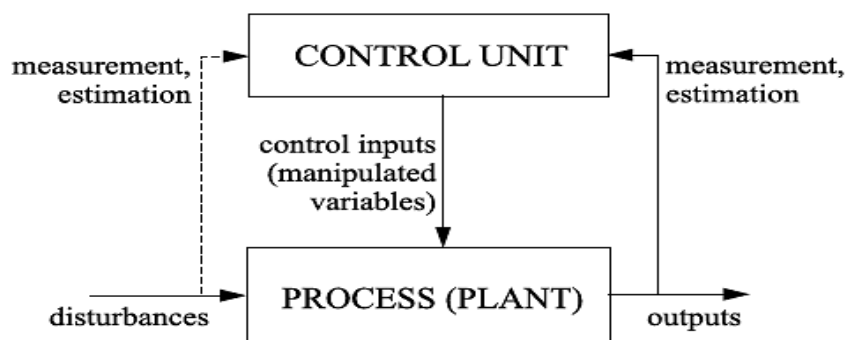


Figure 2-11: A Structure of General Control System (Tatjewski, 2007)

2.6.3 Brief Overview of SOC Methods

An overview of the methods developed for CV selection using SOC is given in this section. This review is not meant to be exhaustive but to give a flavour of the general methodologies that were adopted over the years so that a basis of comparison can be established with our developed methods given in Chapters 5 and 6. For detailed review readers are referred to Skogestad (2000) and Umar et al. (2012). Basically, SOC methods can be classified into local and global methods. These were developed for either static or dynamic processes.

Local Methods

These methods depend on linearizing a non-linear model around a nominal operating point and quadratic approximation of the loss function; this renders the solution to be local (Umar et al., 2012). A linearized model between y , u and d is given below (Ye et al., 2013a)

$$y = G^y u + G_d^y W_d d + W_n e \quad (2-29)$$

where G^y and G_d^y are steady-state gain matrices of input and disturbance respectively. W_d and W_n are magnitude diagonal matrices to normalize d and e respectively. Again y and u are respectively the measurements and manipulated variables while d and e are disturbances and errors respectively. Equation (2-29) is a linearized form of a certain nonlinear model. The CV is given as a function of the measurements, y as (Ye et al., 2013a)

$$c = Hy \quad (2-30)$$

where H is a combination or selection matrix. In the latter, individual elements of measurements are selected as CVs while measurements are linearly combined in the former to form the CV function.

One of the first local methods for CV selection is based on minimum singular value (MSV) rule presented by Skogestad and Postlethwaite (1996) and Halvorsen et al. (2003). The main idea relies on the CV that maximizes the

MSV of a scale gain matrix (Halvorsen et al., 2003; Umar et al., 2012). Unfortunately, this method can lead to wrong identification of CVs (Hori and Skogestad, 2008).

A method based on the assumption that 'the setpoint around which linearization is done to obtain the approximate model is optimal' was developed to overcome the shortcoming of MSV rule by Halvorsen et al. (2003). This is termed exact local method. Obtained loss expressions are used to screen CVs (Umar et al., 2012).

The above two local methods are used to select CVs as a subset of measurements. A lower loss and therefore improved self-optimizing properties can be obtained by selecting CVs as linear combination of measurements. One of such methods that were developed to obtain optimal combination matrix is null space method (Alstad and Skogestad, 2007). Here, the implementation error is ignored and the setpoint error is considered. The idea is to have an optimal value of CVs which is not affected by disturbance so that loss due to setpoint error is reduced to zero. The method is suboptimal since implementation error is ignored, although this can be beneficial to complex systems where consideration of implementation error will be difficult to solve. There is also a requirement for minimum number of measurements to be satisfied in order to obtain the combination matrix which may sometimes lead to a complex control structure (Umar et al., 2012).

The selection of a subset of measurements as CV alternatives or their combination is regarded as a combinatorial optimization problem. Branch and bound methods for efficient solution of such problem has been proposed (Cao and Kariwala, 2008; Kariwala and Cao, 2009; Kariwala and Cao, 2010).

Two expressions for loss in objective function have been defined (Ye et al., 2013a) that are used as criteria for CV selection. These are worst case and average losses for uniformly distributed disturbance given as follows (Ye et al., 2013a):

$$L_{worst} = \frac{1}{2} \sigma_{max}^2(M) \quad (2-31)$$

$$L_{average} = \frac{1}{6(n_y + n_d)} \|M\|_F^2 \quad (2-32)$$

where $\sigma_{max}(\cdot)$ and $\|\cdot\|_F$ are the maximum singular value and Frobenius norm of a matrix, respectively. The matrix M was defined as

$$M = [J_{uu}^{1/2}(J_{uu}^{-1}J_{ud} - G^{-1}G_d)W_d \quad J_{uu}^{1/2}G^{-1}HW_n] \quad (2-33)$$

where $G = HG^y$, $G_d = HG_d^y$ and the Hessian matrices are given as (Ye et al., 2013a)

$$J_{uu} = \frac{\partial^2 J}{\partial u^2} \quad (2-34)$$

$$J_{ud} = \frac{\partial^2 J}{\partial u \partial d}$$

The loss expressions given by Equations (2-31) and Equations (2-32) are used to select the right CV as a subset of measurements defined in Equation (2-30) (Umar et al., 2012). It can then be said that CV selection procedure involves minimizing the loss expressions with respect to H (Ye et al., 2013a). Expressions for H have been derived as stated by Ye et al. (2013a).

Global Methods

The methods described above depend on linearizing a nonlinear system around a nominal point to obtain a local solution which introduces losses in the SOC framework. To avoid this shortcoming, gradient functions were proposed to be used as the CVs directly so as to achieve a global optimal operation. In the work of Cao (2003; 2005), the gradient function was proposed to be determined analytically and be used directly as the CV. For cases where the gradient is not available or difficult to be obtained, the idea was extended to select CVs based on sensitivity of the gradient function to disturbances and implementation errors. The major drawback of this method is that finding the analytical gradient of

some systems is not trivial. The gradient may also be nonlinear in state variables and unknown disturbances. In a related work, chain rule differentiation was used to explicitly express the gradient function in terms of system's Jacobian (Cao, 2004). The gradient function was used as CV for a constrained optimization problem. A cascade control structure was proposed to handle the active constraint.

Methods were also developed to select CVs to approximate necessary condition of optimality (NCO) with zero setpoints to achieve near-optimality globally (Ye et al., 2012; Ye et al., 2013a). This is similar to NCO tracking technique where the NCO is selected as controlled variables. The difference is for SOC, CVs are selected offline based on output measurements and then a feedback controller with an integral action track the selected CVs online at their setpoints. On the other hand, the components of NCO which are active constraints and reduced gradients are computed online and chosen as CVs in NCO tracking (Ye et al., 2013a). In the work of Ye et al. (2012), a two-step regression approach was used. In the first step, the economic objective was approximated using operational data while CVs were determined in the second step by incorporating NCO. The main advantage of this approach is that CVs are obtained that cover a wide operational range based on data; process model is not required. However, a shortcoming to this is the large error that results from the two regression steps.

A one-step regression approach was reported where CVs were used to approximate the NCO or reduced gradient with zero setpoints (Ye et al., 2013a). The NCO was split into two parts: active constraint, \mathbf{g}_a (constraint with strict equality) and reduced gradients $\nabla_r J$ given as (Ye et al., 2013a)

$$\mathbf{g}_a = 0, \quad \mathbf{g}_a \in \mathbb{R}^{n_a} \quad (2-35)$$

and

$$\nabla_r J = \frac{\partial J}{\partial \mathbf{u}} \left[I - \left(\frac{\partial \mathbf{g}_a}{\partial \mathbf{u}} \right)^+ \frac{\partial \mathbf{g}_a}{\partial \mathbf{u}} \right] = 0 \quad (2-36)$$

The reduced gradient has n_u components which is compressed to $n_u - n_a$ dimensions using singular value decomposition and is given by (Ye et al., 2013a)

$$\nabla_{cr}J = \frac{\partial J}{\partial \mathbf{u}} \mathbf{V}_2 = 0, \quad \nabla_{cr}J \in \mathbb{R}^{n_u - n_a} \quad (2-37)$$

where $\nabla_{cr}J$ is the compressed reduced gradient, and \mathbf{V}_2 are $n_u - n_a$ right singular vectors. An assumption made in the work is that the active constraints are measurable and are controlled perfectly with an aim to control the remaining compressed reduced gradient at zero setpoint. Despite the fact that a global optimal operation is achievable with this approach, a system model is still required to evaluate the NCO. This is actually a hiccup to systems with unknown or complicated model.

Dynamic Optimization Methods

The local and global methods listed above were developed for continuous processes at steady state. Having recognised the impacts of batch processes in chemical plant operation, some authors (Dahl-Olsen et al., 2008; Dahl-Olsen and Skogestad, 2009; Hu et al., 2012; Ye et al., 2013b) strived to develop CV selection methodologies of dynamic processes applicable to batch process. In the work of Dahl-Olsen et al. (2008) for instance, the principle of maximum gain rule for the selection of CV is extended to batch process tracking problems. With this approach, poor controls can be screened out which leads to selection of only good ones according to scaled gains.

Ye et al. (2013b) extended the technique of NCO approximation (for static optimization of continuous processes) to approximating invariants. The invariants are also modelled as functions of output measurements. They considered a case of unconstrained dynamic optimization of batch processes with a single input which is formulated as (Ye et al., 2013b)

$$\begin{aligned} \min_{u(t)} \quad & J = \phi(\mathbf{x}(t_f), \mathbf{d}) \\ \text{s. t.} \quad & \dot{\mathbf{x}} = g(\mathbf{x}, u, \mathbf{d}), \quad \mathbf{x}(0) = \mathbf{x}_0 \end{aligned} \quad (2-38)$$

where all variables have their usual meaning. The problem is then formulated as minimizing the Hamiltonian function $H(t)$ using Pontrygin's Minimum Principle (PMP) as (Ye et al., 2013b)

$$\begin{aligned} \min_{u(t)} \quad & H(t) = \lambda^T g(\mathbf{x}, u, \mathbf{d}) \\ \text{s. t.} \quad & \dot{\mathbf{x}} = g(\mathbf{x}, u, \mathbf{d}), \quad \mathbf{x}(0) = \mathbf{x}_0 \\ & \dot{\lambda}^T = -\frac{\partial H}{\partial \mathbf{x}}, \quad \lambda^T(t_f) = \frac{\partial \phi}{\partial \mathbf{x}} \Big|_{t_f} \end{aligned} \quad (2-39)$$

where λ is a non-zero, n -dimensional vector of adjoint variables. After some manipulations, the invariant was analytically derived as (Ye et al., 2013b)

$$c \equiv \det(\Gamma) = 0 \quad (2-40)$$

Where Γ is defined as (Ye et al., 2013b)

$$\lambda^T [g_u \quad \Delta g_u \quad \dots \quad \Delta^{n_x-1} g_u] = \lambda^T \Gamma = 0 \quad (2-41)$$

and (Ye et al., 2013b)

$$\begin{aligned} g_u &= \frac{\partial g}{\partial u} \\ \Delta v &:= (\partial v / \partial x)g - (\partial g / \partial x)v + (\partial v / \partial u)\dot{u} \\ \Delta^k v &= \Delta(\Delta^{k-1} v) \end{aligned} \quad (2-42)$$

In Equation (2-40), the invariant c contains some unmeasured states and disturbances and therefore its control online is not possible. To this regards c is approximated using available measurements including the manipulated variable, u so that a linear control law is automatically obtained which avoids the further need of a feedback controller and the difficulty in its tuning. So, the input is given in a linear feedback form as (Ye et al., 2013b)

$$u = -\frac{1}{\theta_u} [\theta_0 \quad \theta^T] \begin{bmatrix} 1 \\ \mathbf{y} \end{bmatrix} \quad (2-43)$$

The approach was applied to a fed batch reactor and results similar to optimal solutions were found. Although, the application to a simplistic case was successful, the method will be cumbersome to be applicable to complex processes. More importantly, it is not applicable to processes with unknown models. A better approach is to approximate the NCO with measurements based on data only without the need of process equations. This type of data-driven SOC will be explored in the present work.

2.7 Performance Evaluation of Optimization Approaches in Counteracting Uncertainties

In this section, a review of approaches employed by different authors in evaluating the performance of their proposed solution methods towards uncertainties treatment is given. Various methodologies reviewed in previous sections are considered.

Starting with RO approaches, in the work of Yeten et al. (2002), although optimization was carried out considering uncertainties in some properties, the methodology does not cover counteracting of such uncertainties but illustrated the impacts geological characterization has on oil recovery and how smart wells are useful for increased recovery. However, in the work reported by van Essen et al. (2009), the methodology was aimed at annulling the effects of geological uncertainties through ensemble of geological realization. The method was validated by applying the optimal strategies on a separate set of realizations where similar responses were obtained for both sets, an indication of a good representation of the considered uncertainty. Nevertheless, the validation has yielded a positive result; the method would have been regarded as so robust if other forms of uncertainties were incorporated in the validation exercise. Furthermore, the set of realizations has to be a true representation of reality before it can be applicable in practice. In a related work (Chen et al., 2012), the robustness of the method was illustrated only through two case studies, no formal analysis was carried out for that purpose.

Looking at some closed-loop approaches, for instance, Aitokhuehi et al. (2004) assessed the performance of combined model updating and optimization against two reference procedures. The first is a strategy obtained based on known geology and non-optimized valve settings while the second reference was based on known geology and optimized valve settings (ideal case). Although, the methodology was tested on two different reservoir systems, the uncertainties considered are the same for both cases, which are uncertainties in permeability and porosity. It would be interesting to see how the proposed methodology will perform when more mismatches are introduced into the loop.

In the work reported by Brouwer et al. (2004b), performance of a closed-loop configuration was evaluated through two case studies where the methodology was compared to traditional and optimized (based on certain reservoir properties) approaches. Permeability was the only uncertain property that was focused on. Almost same pattern of performance evaluation was followed by other researchers (Overbeek et al., 2004; Jansen et al., 2005; Naevdal et al., 2006; Sarma, 2006; Sarma et al., 2008b; Wang et al., 2009) with uncertainty in either permeability or a combination of permeability and porosity. Comparison was basically made among the developed closed-loop method, a benchmark based on known geology, and an open-loop solution or a reactive control method.

The MPC configuration of van Essen et al. (2013) however, considered mismatches in permeability and grid refinement around the well. Similar to other work, the efficacy of the constructed closed-loop was evaluated by comparing its performance to an open-loop based solution.

However, in the work of Dilib and Jackson (2013a), the robustness of their direct feedback relationship (formulated from a base model) was tested on more unexpected reservoir behaviours which include shape of relative permeability curves, horizontal permeability, width of shale-free zone and aquifer strength. Although more uncertainties were introduced in this work than the previous ones, the approach of performance evaluation is basically the same. It would be

more helpful had the paper presented sensitivities of the feedback relationship to the various uncertainties.

2.8 Summary

This chapter started by briefly reviewing how oil and gas are formed where it was stated that their origin is from plants and animals remains which are buried under intense temperature and pressure condition over thousands of years in an oxygen depleted environment. For the formation and subsequent storage of petroleum resources underneath the ground to take place, there must be presence of source rock, migration route, reservoir rock, seal rock and trap. The chapter then continued with basic definition of some reservoir rock and fluid properties that are critical in the design and operation of any oil and gas fields. These include porosity, saturation, wettability, permeability and relative permeability. Various stages of exploring and developing oil and gas fields were highlighted to give a flavour of the activities carried out in the fields. Production of these valuable resources then followed after field development. The production is categorised into three phases based on the reservoir pressure. These are: primary, secondary and tertiary or enhanced oil recovery phases. Waterflooding falls into secondary recovery phase where it is employed to boost the pressure of a depleted reservoir. Here water is injected into the reservoir to sweep the oil so as to increase its recovery. However, due to the heterogeneous nature of the reservoir, the sweeping is most often not uniform, and therefore the efficiency of the process is very low. Smart wells have been proposed to overcome this problem which divide production zone into segments; each segment is equipped with ICVs for measurement and control purposes.

Oil recovery depends on the dynamic states of the reservoir, as such optimal injection and production settings will depend on these states. The search for the optimal trajectories was traditionally done via trial and error methods where different well configurations and rate settings are tested on numerical reservoir simulators. The optimal solutions are hardly found through this tedious means.

Because of this shortcoming, a lot of researches have been reported to formulate the problem as a well-structured optimization problem. Early studies focused on model-based open-loop optimal solutions, robust optimization, and recently receding horizon control was proposed. However, these approaches are either found to be sensitive to model/system mismatches or too conservative to lead to optimal solutions. In lieu of this, the optimization process was proposed to be conducted in a closed-loop fashion where production measurements are directly used to update reservoir models on regular intervals from which optimum production and injection settings are obtained. Several literatures have reported this proposal with different terminologies such as 'closed-loop reservoir management (CLRM)', 'real term reservoir management', 'self-learning reservoir management', 'e-fields' or 'smart field'. Although, the concept of CLRM sounds promising, it is very complicated and will be computationally prohibitive for a real reservoir system because of the requirement of online re-optimization.

In this thesis a simple optimal feedback approach that is robust to uncertainties will be proposed. The concept is based on the principle of self-optimizing control where optimal or near optimal operation is automatically achieved by keeping properly selected CVs at set points despite the presence of uncertainties and disturbances. The gradient of the objective function with respect to control is proposed to be selected as the CV which is obtained from regression based on simulated or production data. Optimal feedback control relationship can therefore be obtained by setting the CV function to zero.

3 Performance Comparison of Smart Wells Design

3.1 Introduction

One of the common operational problems encountered during waterflooding is non uniformity in oil sweep as a result of reservoir heterogeneity. The consequence of this is reduced sweep efficiency, early water break-through and eventually reduced oil recoveries. A reservoir property of significant importance in determining directional flow of fluids is reservoir permeability to the fluids. Heterogeneity in permeability alone is enough to cause aforementioned problems (Sudaryanto and Yortsos, 2000). As was mentioned in Chapter 2, one of the solutions to such problems that are receiving great attention is the use of smart wells.

In this chapter, different well configurations are considered in a heterogeneous reservoir with variations in vertical permeability. Five cases of well design were compared. The first case is the conventional well completion where the control is done at well level (Figure 3-2). Cases II and III (Figure 3-3) have combination of smart and conventional wells. In Cases IV and V, both the injection and production wells have smart completions and well control is performed at perforation level. The distinguishing feature between these two cases is, in Case IV the production well is horizontal and the injector is vertical while both wells are vertical in Case V. Performance comparison of these different designs was done by optimizing a performance index using injection and production settings as control variables. Waterflooding optimization is a dynamic optimization problem; as such optimal control theory with adjoint formulation using Lagrange multipliers (Brouwer and Jansen, 2004a; Jansen et al., 2008) was employed to carry out the task.

The performance of different smart configurations was compared against the conventional design. Based on net present value (NPV) of the process, the best case design was found to be Case IV with an improvement of 11.38% over the conventional design. However, with the same cost function, Case V has the highest improvement in terms of total oil production with an increase of 7.92%

while water production was best reduced with Case III design. The reduction in this case is up to 17.18%. Generally, improvement in NPV was found to increase with total number of well control (ICVs) put in place. On the other hand, oil production increase is favoured when ICVs (both for injection and production) are installed in each layer of reservoir with different rock properties.

3.2 Reservoir and Wells Configurations

The actual reservoir size is 100 m x 100 m x 10 m but modelled with 20 x 20 x 5 grid cells. Each cell is therefore 5 m x 5 m x 2 m. This reservoir model was adopted from MRST package (Sintef, 2014b) and modified to suit our purpose. The reservoir was assumed to have five vertical layers each of 2 m thickness and with different permeability. The permeability in each layer is log-normally distributed with mean values of 200 mD, 500 mD, 350 mD, 700 mD and 250 mD from top to bottom as shown in Figure 3-1. Reservoir porosity was assumed uniform with a value of 0.3. Only two-phase of incompressible oil and water was assumed to be flowing in the reservoir with properties given in Table 3-1.

Five cases of well configuration were considered. For the first case, conventional well control was used where a single choke valve was assumed for control action. A vertical injection and a horizontal production wells were located arbitrarily as shown in Figure 3-2. The injection well was perforated in each layer (that is five perforations) while the production well has 20 perforations. The two wells are rate-controlled and an assumption of voidage replacement was made. That is, total injection must equal total production at all time-steps.

In Case II, the vertical injector was completed as a smart well. Each of the five perforations was modelled to have an ICV so that it can be controlled independently from others. The number of control variables is therefore six as against two in Case I. Case I was taken as a reference case from which the performance of other cases are compared.

Case III also has same well locations as in I and II but the horizontal producer was completed as a smart well with all the 20 perforations equipped with ICVs. The injector was however modelled as a conventional well with only one choke valve. The number of optimizing variables is therefore 21, which is, 20 for the producer and one for the injector. Figure 3-3 shows the wells configurations for this set up. The injector is labelled W1 while the 20 perforations for the producer W2 – W21.

However, both injection and production wells in Case IV were completed with ICVs. The injection well has five ICVs in each completion layer while the producer has 20 ICVs, in total, 25 optimizing variables were used for performance optimization. The ICVs are named ICV1 – ICV5 for injection well and ICV6 – ICV25 for production wells. For Case V both the injection and production wells are vertical with smart completions, 10 optimizing variables that represent the rate settings of the wells are therefore used for the optimization purpose. Similarly, injection ICVs are denoted by ICV1 – ICV5 while ICV6 – ICV10 for producer. These design configurations are summarised in Table 3-2.

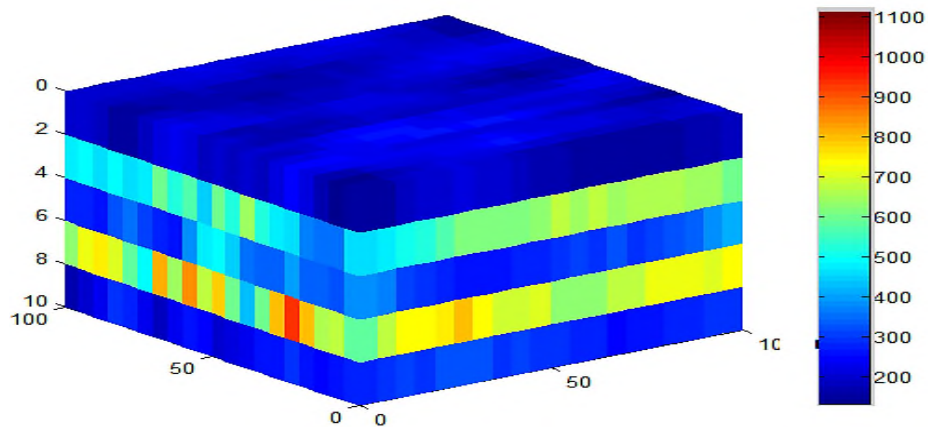


Figure 3-1: Permeability Distribution for a Layered Reservoir in mD

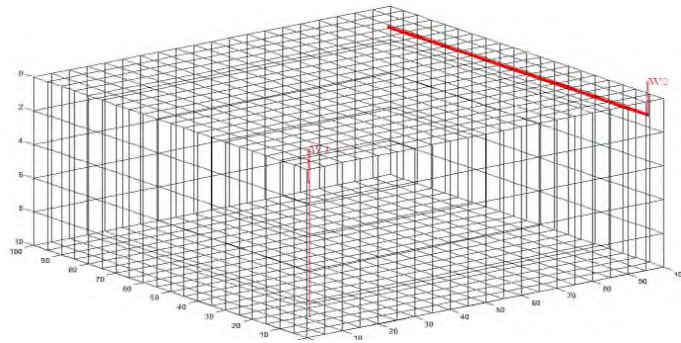


Figure 3-2: Reservoir and Wells Configurations for Case I

Table 3-1: Rock and Fluid Properties

Property	Value	Unit
Porosity	0.3	-
Oil viscosity	5	cp
Water viscosity	1	cp
Oil density	859	Kg/m ³
Water density	1014	Kg/m ³
Oil Corey exponent	2	-
Water Corey exponent	2	-

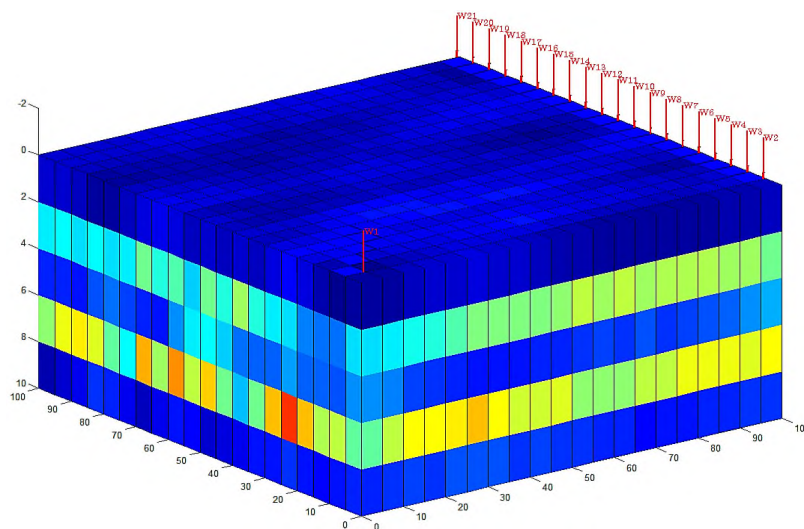


Figure 3-3: Reservoir and Wells Configurations for Case III

Table 3-2: Configurations of Wells for Different Case Design

Case	Injector			Producer		
	Orientation	Completion	No. of ICVs	Orientation	Completion	No. of ICVs
I	Vertical	conventional	1	horizontal	conventional	1
II	vertical	smart	5	horizontal	conventional	1
III	vertical	conventional	1	horizontal	smart	20
IV	vertical	smart	5	horizontal	smart	20
V	vertical	smart	5	vertical	smart	5

3.3 Optimization Approach

The optimal performance of the five configuration cases was obtained through dynamic optimizations of the flooding process. A gradient-based algorithm was used to carry out the optimization which requires computation of derivative of the objective function, J given in (2-15) with respect to the control, $\mathbf{u}_{1:k}$. Optimal control theory which is very efficient for this purpose was used (Brouwer, 2004; Jansen et al., 2008; Jansen, 2011). For this type of problem, J is a function of the states, \mathbf{x} which depend on \mathbf{u} . Some intermediate steps are taken to solve the problem which are summarised in Section 3.3.3. The reader is referred to Brouwer (2004) and Brouwer and Jansen (2004a) for details.

3.3.1 The Reservoir Dynamic System

As discussed in Section 2.4.1, the reservoir model equation can be given in a discretized form (Jansen et al., 2009) as

$$\mathbf{g}_{k+1}(\mathbf{u}_{k+1}, \mathbf{x}_k, \mathbf{x}_{k+1}) = 0, \quad k = 0, \dots, K - 1 \quad (3-1)$$

where \mathbf{g} is originally a nonlinear vector-valued function, \mathbf{u} is a control vector comprising injection and production rates of each well or perforation, \mathbf{x} is a vector of states (pressures and saturations in each grid block) and the subscript, k is a discrete time-step while K is the end time. The optimization procedures considered control of total production and injection rates for the wells with the assumption of voidage replacement. That is, total injection must equal total production at all time-steps. This form of well constraint was discussed in Section 2.4.1 and represented as (Brouwer et al., 2004b)

$$\sum_{i=1}^{N_{inj}} (u_{w,i})_k = y_{tot} \quad , \quad \sum_{j=1}^{N_{prod}} \left((y_{w,j})_k + (y_{o,j})_k \right) = -y_{tot} \quad (3-2)$$

where

N_{inj} = number of injection wells

N_{prod} = number of production wells

$u_{w,i}$ = water injection rates in wells $i = 1, \dots, N_{inj}$ (control variables)

$y_{w,j}$ = water production rates in wells $j = 1, \dots, N_{prod}$ (output variables)

$y_{o,j}$ = oil production rates in wells $j = 1, \dots, N_{prod}$ (output variables)

y_{tot} = field total production rates

The injection rate is required to remain positive while the production rate negative at all time-steps, so we have (Brouwer et al., 2004b)

$$(u_{w,i})_k \geq 0 \quad (3-3)$$

and

$$(y_{w,j})_k \leq 0, \quad (y_{o,j})_k \leq 0 \quad (3-4)$$

3.3.2 Objective Function

The objective is maximization of NPV of the waterflooding process. NPV is the difference between the present values of the expected cash inflows and outflows over the production period. A positive NPV indicates a profitable venture while a negative one means the cost incurred outweighs the inflow. For the present work, water injection and production costs are the two sources of cash outflow while oil production represents revenue generation. NPV is given as (Brouwer and Jansen, 2004a)

$$J_k = \left\{ \frac{\sum_{i=1}^{N_{inj}} r_{wi}(u_{w,i})_k + \sum_{j=1}^{N_{prod}} [r_{wp}(y_{w,j})_k + r_o(y_{o,j})_k]}{(1+b)^{\frac{t_k}{\tau}}} \right\} \Delta t_k \quad (3-5)$$

where

r_{wi} = negative valued water injection cost

r_{wp} = negative valued water production cost

r_o = oil production unit income

b = discounting factor

τ = reference time for discounting

t_k = time at k step

$\Delta t_k = t_{k+1} - t_k$

Oil price was taken as \$100/bbl while water injection and production costs were both \$10/bbl. Discounting factor of 0% per annum was used so as to ascertain that any improvement in NPV for a particular case is as a result of the design configuration in question. The optimization procedures considered control of total production and injection rates for the two wells with the assumption of voidage replacement. That is, total injection must equal total production at all time-steps. A total of two years production period with two months (60 days) time-step was used.

3.3.3 Solution Procedure based on Optimal Control Theory

Optimal control theory was used to compute the optimal injection and production settings that maximize the NPV. It is a very efficient method of computing the gradient of the objective function with respect to controls irrespective of the number of variables involved; a forward integration of the reservoir dynamic system Equation (3-1) and a backward integration of adjoint systems are all that is required to compute the gradients (Brouwer et al., 2004b).

Here, the reservoir system is regarded as an equality constraint by summing it to the objective function using a set of Lagrange multipliers which gives rise to a modified objective function written as

$$\bar{J} = \sum_{k=0}^{K-1} J(k) + \lambda(k+1)^T g(k) = \sum_{k=0}^{K-1} \mathcal{H}(k) \quad (3-6)$$

where $\mathcal{H}(k)$ is called the Hamiltonian. The following constitutes the optimal control of waterflood optimization (Brouwer et al., 2004b)

- the reservoir dynamic system Equation (3-1)
- initial conditions of the dynamic system (Brouwer et al., 2004b)

$$\mathbf{x}_0 = \check{\mathbf{x}}_0 \quad (3-7)$$

- a set of injection and production rates, \mathbf{u}
- time steps, $k = 0, \dots, K - 1$
- adjoint equation (Brouwer et al., 2004b)

$$\lambda(k)^T = \left[-\frac{\partial J(k)}{\partial \mathbf{x}(k)} - \lambda(k+1)^T \frac{\partial \mathbf{g}(k)}{\partial \mathbf{x}(k)} \right] \left[\frac{\partial \mathbf{g}(k-1)}{\partial \mathbf{x}(k)} \right]^{-1} \quad (3-8)$$

where $\frac{\partial J(k)}{\partial \mathbf{x}(k)}$ is a vector of partial derivatives of the objective function with respect to the states, \mathbf{x} while $\frac{\partial \mathbf{g}(k)}{\partial \mathbf{x}(k)}$ and $\frac{\partial \mathbf{g}(k-1)}{\partial \mathbf{x}(k)}$ are the Jacobians of the reservoir dynamic system with respect to the states.

- Final conditions of the adjoint systems, and for a free terminal state problem is given by (Brouwer et al., 2004b)

$$\lambda(K)^T = \mathbf{0}^T \quad (3-9)$$

With the above ingredients, the solution procedure of the waterflooding optimization problem involves repeating the following steps until a set of optimal controls is obtained (Brouwer et al., 2004b):

- Forward numerical simulation of the reservoir dynamic system by numerical integration of Equation (3-1) over entire time interval 0 to K while taking the initial conditions, Equation (3-7) into consideration as well as initial or updated \mathbf{u}
- Backward numerical simulation of the adjoint system by numerical integration from time K to 0 starting with the final condition expressed by Equation (3-9)
- The gradients of the Hamiltonian with respect to the controls are computed which are (Brouwer et al., 2004b):

$$\frac{\partial \mathcal{H}(k)}{\partial \mathbf{u}(k)} = \lambda(k)^T \frac{\partial \mathbf{g}(k)}{\partial \mathbf{u}(k)} + \frac{\partial J(k)}{\partial \mathbf{u}(k)} \quad (3-10)$$

- Improvement in \mathbf{u} is calculated using a line search technique and obtained derivatives in Equation (3-10).

3.4 Results and Discussions

Table 3-3 gives a summary of the performance for different well design with Case I (conventional design) served as a reference design. Based on NPV, Case IV with the highest number of controls is the best design with an improvement of 11.38% over the conventional case design. On the other hand, the worst design was found to be Case II with the least number of ICVs. In general, performance based on NPV increases with number of ICVs irrespective of well's orientation (see also Figure 3-4).

Table 3-3: Performance Comparison of Different Well Designs

Cases	Total Oil (m ³)	Total Water (m ³)	NPV x10 ⁶ (\$)	Increase in NPV (%)	Increase in Oil (%)	Decrease in Water (%)
I	15,082.11	10,864.82	7.2137	-	-	-
II	15,202.29	11,171.44	7.2387	0.35	0.80	-2.82
III	15,993.39	8,998.70	8.0001	10.90	6.04	17.18
IV	16,092.50	9113.00	8.0347	11.38	6.70	16.12
V	16,276.15	10,638.83	7.9128	9.69	7.92	2.08

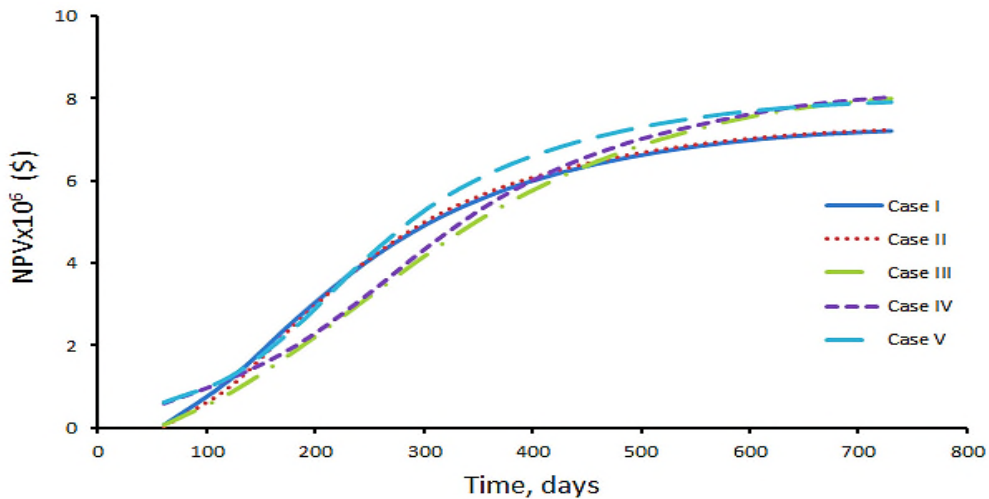


Figure 3-4: Cases Design NPV

It can also be seen that, although Case V with only 10 ICVs has the highest improvement in terms of oil production but least in terms of water production after the worst case. This has to do with the well orientation, as both are vertical wells and the ICVs were exactly placed at the vertical layers with permeability variations.

The permeability distribution has led to different behaviours of ICV settings. For instance, in Case II the injection rates for various perforations are distinguishable up to 300 days of production period after which it became uniform (Figure 3-5). It can also be seen that ICV1 and ICV5 were allocated with higher injection rates at all time-steps. This was due to low permeability associated with their corresponding layers; doing so will create a more or less uniform sweeping and delay in water break-through which unfortunately led to high water production because the production at these two layers were not controlled separately as in Case V.

Considering Case III, It is worth to note that, most of the producer perforations that are closer to the injection well are relatively shut-in. For instance perforations W13 – W21 can be seen opened throughout the production period. Those perforations that are prone to experience early water breakthrough, were closed (Figure 3-6). This is to allow proper flooding of the reservoir at the vicinity of injection with minimal production of the injected water. Figure 3-7 shows evolution of water saturation at different times of production. The figure has confirmed at grid level how the section of the reservoir that is further away from point of injection was first depleted to control water production. The benefit of the smart well design can further be observed from water production profiles (Figure 3-8). For this case, only perforations W16 – W21 experienced appreciable water production which was actually after around 230 days of production start-up.

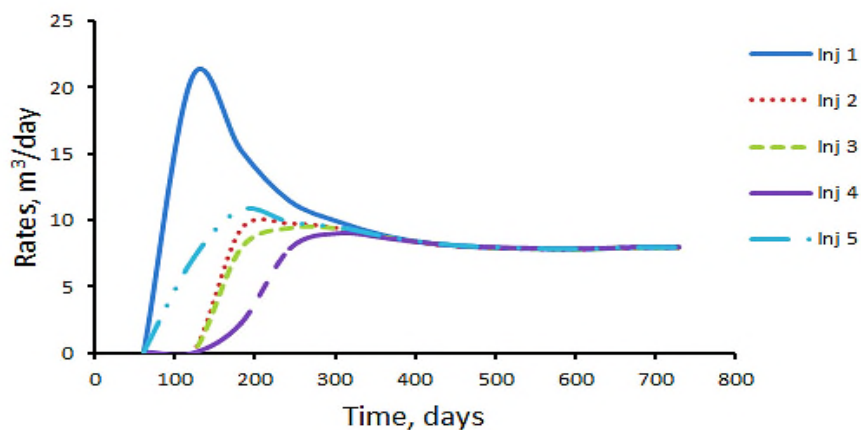


Figure 3-5: Injection Rates for Case II

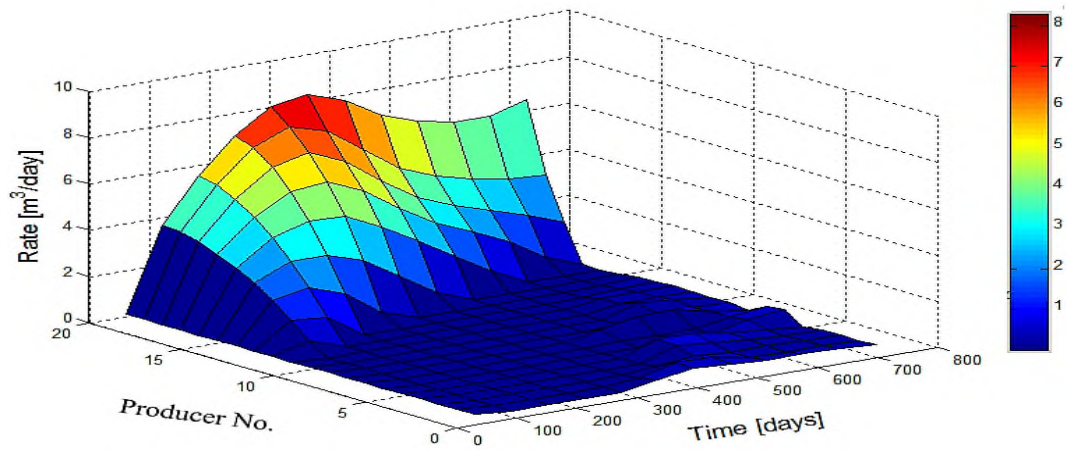


Figure 3-6: Oil Production Rates for Case III

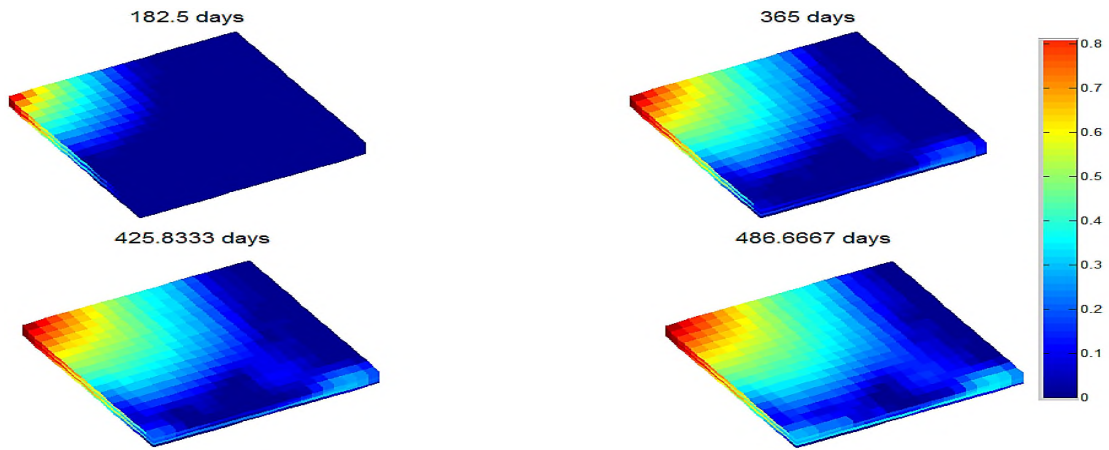


Figure 3-7: Water Saturation Evolution for Case III

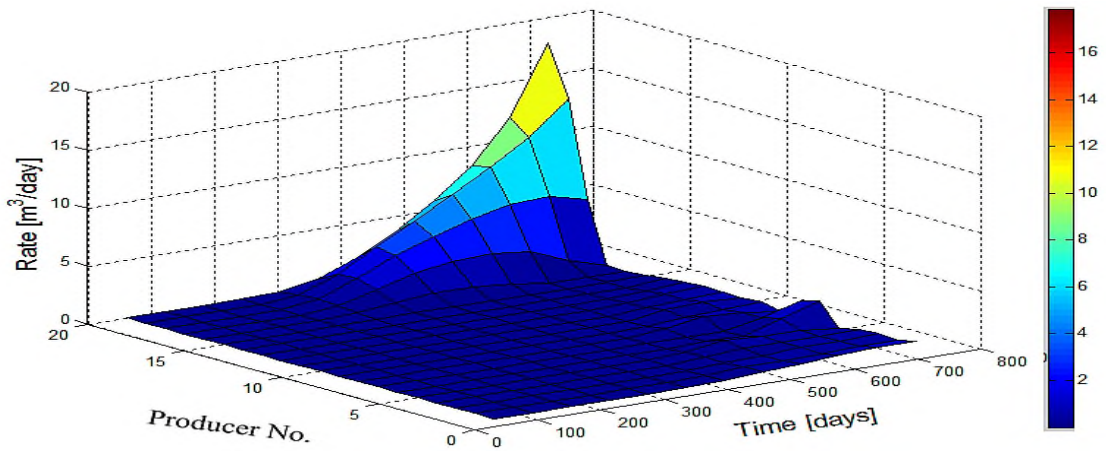


Figure 3-8: Water Production Rates for Case III

Having the two wells with smart completions in Case IV, all design advantages associated with Cases II and III explained above can be seen with this case (Case IV). Typically, water can be seen to be injected prudently in low permeability layers (layers 1 and 5) at the beginning of production period (Figure 3-9) to maximize oil recovery. Similarly, producer ICV's closer to injection points were more or less shut-in for the production period to prevent early water break-through and for even oil sweeping (Figure 3-10). With Case IV design configuration, higher volume of water was injected than with Case III design, this causes increased oil and water productions of about 0.48% and 1.06% respectively with the former over the latter. This increase in production resulted to a corresponding increase of 0.48% in NPV in favour of Case IV (Table 3-3).

A similar injection pattern can be observed with design Case V (Figure 3-11). The initial high injection rates for ICV1 and ICV5 allowed equal oil productions from all the layers for the first 200 days and even higher afterwards from the lower permeability layers (Figure 3-12). This gave rise to highest amount of total oil production among all the case designs although with a corresponding increase in water production, a situation that saw the NPV decreased slightly from the best case design (Table 3-3).

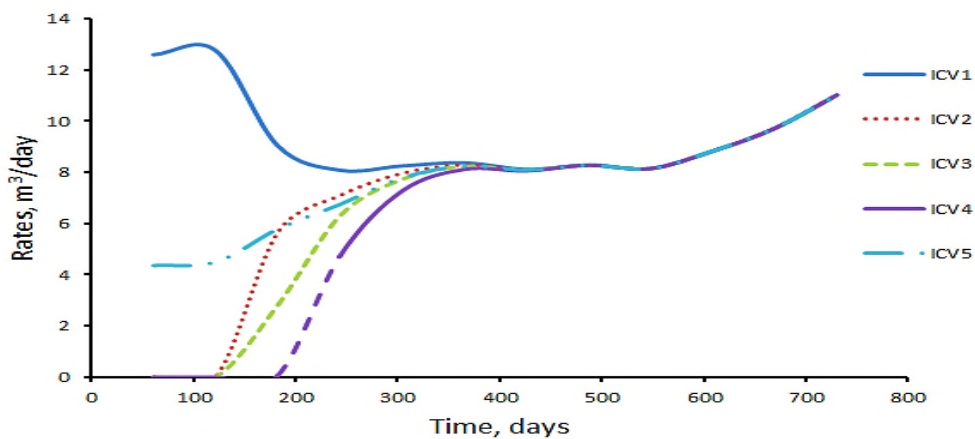


Figure 3-9: Injection Rates for Case IV

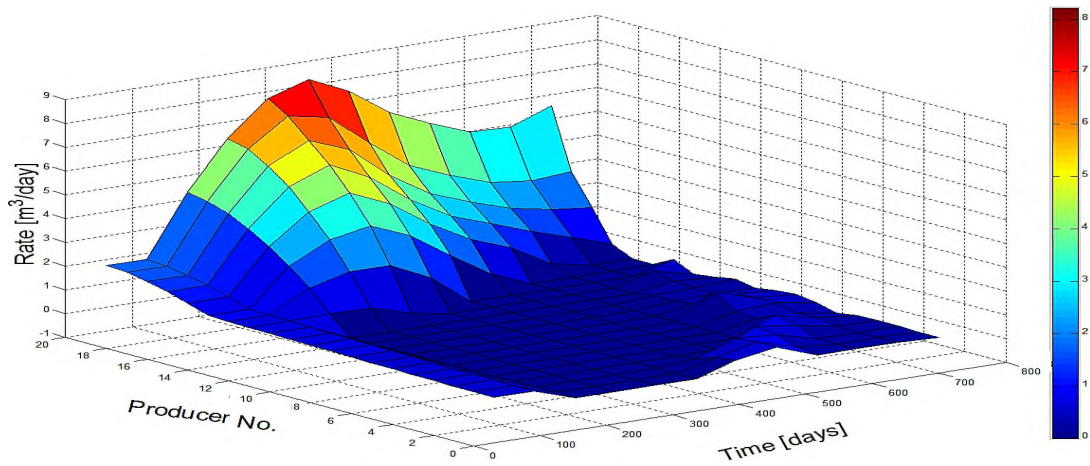


Figure 3-10: Oil Production Rates for Case IV

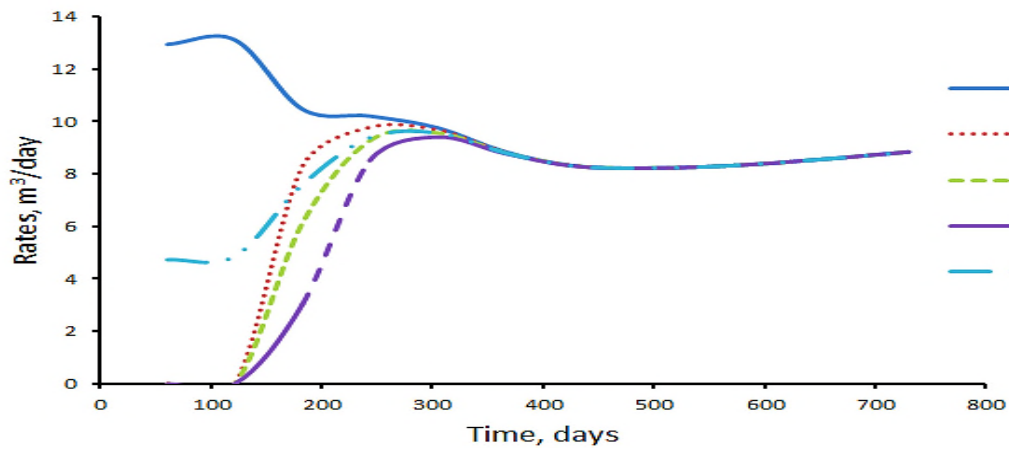


Figure 3-11: Injection Rates for Case V

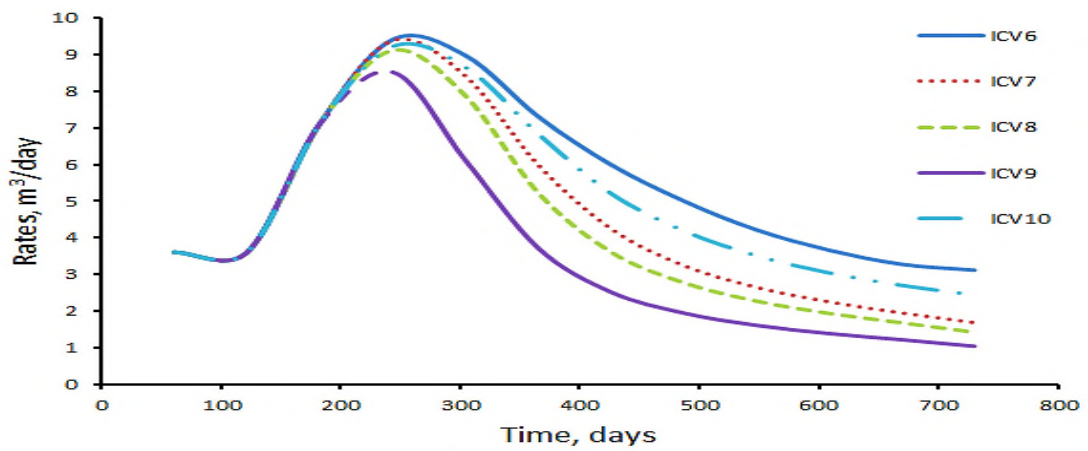


Figure 3-12: Oil Production Rates for Case V

It is worth to note that the total oil recovery for each case is more than 50% of the initial oil in place which is difficult to achieve in practice. This high production record was possible due the prolific properties that characterise the reservoir as well as some simplifying assumptions. These are adopted for the sake of analyses and clarity of the concept. For instance, the homogeneous porosity of 30% considered throughout the reservoir is not realistic. Apart from this, the relatively high permeability values assigned to the various reservoir layers with absence of non-producing zones such as shale or any other permeability barrier is also responsible for these promising recoveries. For this type of property consideration, the reader is referred to the work of Foss and Jensen (2011). Furthermore, the optimization study has considered a fixed time horizon whereas in practice the reservoir is allowed to produce till its economic life time.

3.5 Conclusions

In this chapter, performance comparison of different smart well design configurations was carried out. The study was done on a heterogeneous reservoir with five vertical layers each has distinct permeability distribution. Because of this property variation, each layer may require different injection and production settings at each point in time for optimum oil recovery. Wells with smart completions will be able to provide such control capability. However, the number of control gadgets and the actual orientation of wells in the reservoir will have an influence on the fluid flow profile. For this reason performance of various design configurations of smart wells were compared against that of conventional well. The comparison was formulated as an optimization study where economic performance (NPV) of each design was maximised with injection and production rates as control variables. A gradient-based algorithm was used to solve the dynamic optimization problem where the gradients of the objective function with respect to control were computed via adjoint formulations using Lagrange multipliers. The results can be summarised as follows:

1. In terms of NPV, the best design is Case IV with five injection ICVs and 20 ICVs for the horizontal producer which records an improvement of

11.38% over the conventional design (Case I). The worst performance however, was obtained from Case II design where only the vertical injection well has smart completions with five ICVs. The improvement in NPV in this case is only 0.35%. Because the producer was not controlled at perforation level, high water production is a bottleneck with this configuration; an increase in water production of about 2.82% was observed. Switching this control structure in Case III, where the horizontal producer was completed with ICVs (20 in number) while the vertical injector was controlled at well level a tremendous improvement has been recorded especially with cut in water production to the tune of 17.18% and 10.90% increase in NPV. On the other hand, when vertical wells were drilled in Case V both with smart completions (five ICVs for each well), a tremendous increase in oil production of about 7.92% was seen but with an increased water production. Comparing to the reference case, the decrease in the amount of produced water is only 2.08%.

2. In general, it can be said that NPV was found to increase with increase in number of ICVs. This was possible due to the fact that, as the number of ICVs is increased, more suitable flow profiles along the wells are imposed and therefore, sweeping efficiency is improved.
3. For maximum total oil recovery, each producing layer should be controlled independently from injection and production points. This was demonstrated through design Case V, although this has the tendency of high water production.
4. It has also been seen how optimization technique coupled with smart completion technology was able to take reservoir properties and states into consideration in deciding optimum flow trajectories for added economic value. For instance, high volume of water was injected into low permeability layers when compared to the amount injected to relatively high permeability layers. This was to ensure uniform oil sweeping throughout the reservoir. On the horizontal producer side, the ICVs that are closer to the point of injection were mostly closed while production

was made possible from ICVs on the other end to prevent excessive water production.

5. It can be concluded that the most important determining factor in maximizing the economic gain of waterflooding project is the number of controls associated with wells; hence smart well technology coupled with appropriate control algorithm is just the right candidate for solving waterflooding problems.
6. The above conclusions drawn for the considered reservoir can be applicable to other reservoir systems as long as various regions of the reservoir and their corresponding properties are identified. Having considered the performance of design alternatives of smart wells based on open-loop optimization, an approach based on the principle of receding horizon is presented in the next chapter. This is a closed-loop approach, and hence will consider geological uncertainties in the optimization framework.

4 Optimization of Reservoir Waterflooding using Receding Horizon Approach

4.1 Introduction

In this chapter, dynamic optimization of reservoir waterflooding using the concept of receding horizon control (RHC) is reported. The first part treated the optimization with the assumption of perfect reservoir knowledge. In the second part, the feedback strategy was used to counter the effects of uncertainties in reservoir properties. These include uncertainties in permeability, porosity, geometry, size and structure. Reservoir simulation was carried out using MATLAB Reservoir Simulator Toolbox (MRST). The objective is to either maximize economic indicator such as net present value (NPV), or maximization of total oil production and minimization of produced water. For the first part, two forms of RHC are compared against a benchmark strategy, open-loop control (OC). However, three strategies were compared in the second part where uncertainties were considered; a RHC approach, OC solutions based on a nominal model and a benchmark (BM) case which assumes perfect knowledge of the reservoir. The two forms of RHC strategies developed in this work are named fixed-end (FE) and moving-end (ME). The difference is in scheduling of the prediction horizon. For FE as shown in Figure 4-1, the initial prediction period, T_p , is set to be equal to the total production time (divided into n sampling periods) which then decreases subsequently by one sampling period as production advances. For ME on the other hand, the length of the prediction time remains constant, see Figure 4-2.

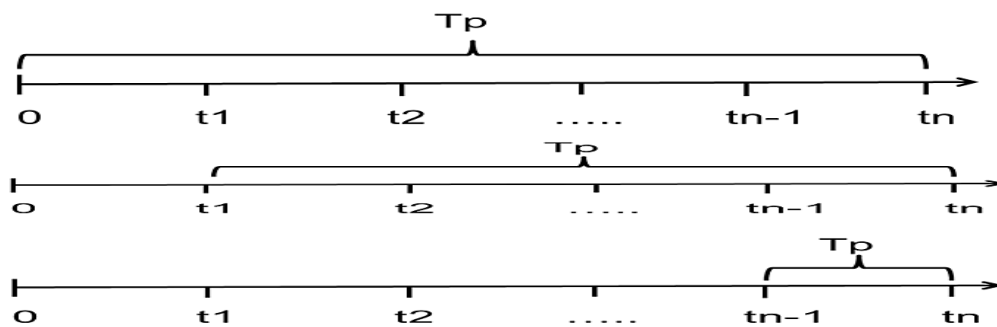


Figure 4-1: Fixed-End Receding Horizon Strategy

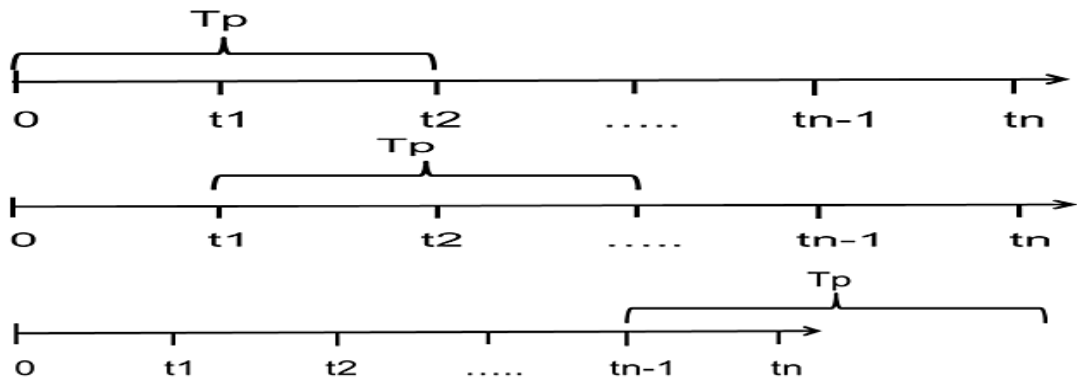


Figure 4-2: Moving-End Receding Horizon Strategy

4.2 RHC for Perfect Reservoir Model

In this section, perfect reservoir model was assumed, so there is no mismatch between the reservoir model used for control predictions and the actual reservoir for which the predicted controls are implemented. The aim is to first test the efficacy of the method through a comparative analysis with optimal control solutions; and secondly to compare the two RHC approaches in which a better option is chosen for uncertainties treatment. In this section, maximization of NPV and recoveries are considered. Two types of well control were also treated when recovery is the objective function vis-a-vis, rate- and pressure-control.

4.2.1 Optimization with Net Present Value as Objective

Reservoir and Well Configurations

The simple reservoir model adopted from MRST package (Sintef, 2014b) and used in Chapter 3 is employed here. However, the actual size of the reservoir was kept at $20 \times 20 \times 5 \text{ m}^3$ to make the concept clear. Another distinguishing feature is the reservoir has a uniform permeability of 100 mD, see Table 3-1 for other rock and fluid properties.

Approach

Three optimization strategies were carried out and compared, an open-loop control solution, OC and two feedback strategies, FE and ME. Although, no reservoir uncertainty was considered, this methodology will give an idea of the relative performance of the two feedback methods and their deviations from the truth optimal solutions. The objective is maximization of NPV of the waterflooding process Equation (3-5).

The optimization procedures considered control of total production and injection rates for the two wells with the assumption of voidage replacement. That is, total injection must equal total production at all time-steps. A total of two years production period with two months (60 days) sampling period was used. So with this set up, for FE, optimization is initially performed for two years and the optimal rates found are implemented for two months. Then, the current reservoir state is used as an initial state for another 22-month optimization with the optimal rate applied for one sampling period. This process is continued for 20-, 18-,.....2-month optimization and the corresponding optimal rates being implemented. For the case of ME, the prediction period is fixed. However, the length of this period will greatly influence the performance of the strategy. For this reason, different periods were tested and compared in this work. Typically, prediction periods of two, four, six and twelve months were compared. So, setting the prediction period to two months for example, optimal rates are predicted over this length of time and then implemented for one sampling period. The current reservoir state is used as a starting point for another two-month optimization with optimal rates implemented. The procedure is continued till the end of the optimization window. The optimal control problem is solved through the methodology outlined in Section 3.3.

Results and Discussion

A summary of the optimization results is given in Table 4-1 for two cases of discount factor, b of 0% and 10%. For the two cases, OC gave the highest NPV than the two RHC strategies (Figure 4-3) due to the absence of model/system mismatch as expected. However, between the two feedback strategies, FE appears to be better than ME. In the ME approach, effect of prediction horizon is well pronounced. For the case where $b = 0$, NPV increases with increase in prediction period (Figure 4-4) with variation that has a standard deviation of \$2,054 and a mean of \$140,990. Despite the fact that, OC generated the highest NPV, the difference is not significant. It is only 0.14% higher than FE and 1.88% in the case of ME (for $T_{pr} = 12$ months).

The high NPV gain associated with OC can be attributed to a steady rise in water injection from the beginning of production to about 300 days which was maintained afterwards till the end of production time (Figure 4-5). This also corresponds to a similar rise in oil production as shown in (Figure 4-6) with a more or less flattened plateau period and a delayed water production (Figure 4-7) which results to a higher total oil production (Figure 4-8).

A similar trend can be observed when $b = 10\%$. Here, variations in NPV with T_{pr} for ME strategy record a standard deviation of \$19,591 and a mean of \$139,010. The relative increase in NPV for the case of OC over FE and ME is 0.68% and 1.41% respectively. See profiles in Figure 4-9 - Figure 4-13.

It can also be seen that the discounting factor does not affect appreciably the injection and production settings for RHC (Figure 4-10 - Figure 4-12). This causes the total oil and water productions to remain the same for the two factors considered. However, NPV was seen to vary greatly when b was changed from 0 to 10%. The relative change in NPV for the benchmark case is 2.69%. The changes are respectively 3.22% and 2.23% for FE and ME approaches.

Table 4-1: Performance Comparison of Optimization Strategies

Discount Factor (%)	Strategy		NPV x 10⁵ (\$)	Total Oil (m³)	Total Water (m³)
0	OC		1.5920	325.22	206.51
	FE		1.5898	321.79	195.80
	ME				
	T_{pr} (Months)	2	1.1115	369.05	777.85
		4	1.4401	347.12	417.97
		6	1.5259	343.35	333.09
		12	1.5620	315.07	181.36
10	OC		1.5491	319.55	191.96
	FE		1.5386	321.79	195.80
	ME				
	T_{pr} (Months)	2	1.1037	369.05	777.85
		4	1.4246	347.12	417.97
		6	1.5047	341.61	333.09
		12	1.5272	315.07	181.36

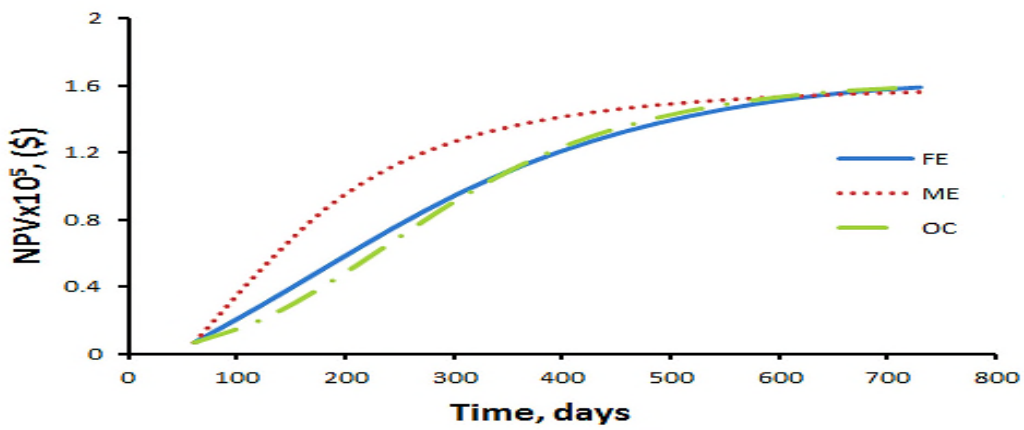


Figure 4-3: NPV for Different Strategies (b = 0)

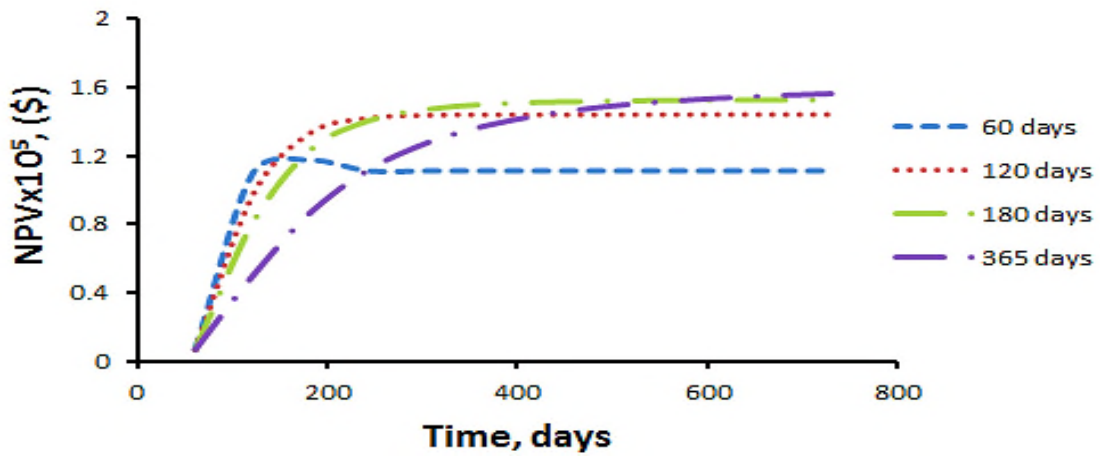


Figure 4-4: NPV for ME Strategy for Different Prediction Period (b = 0)

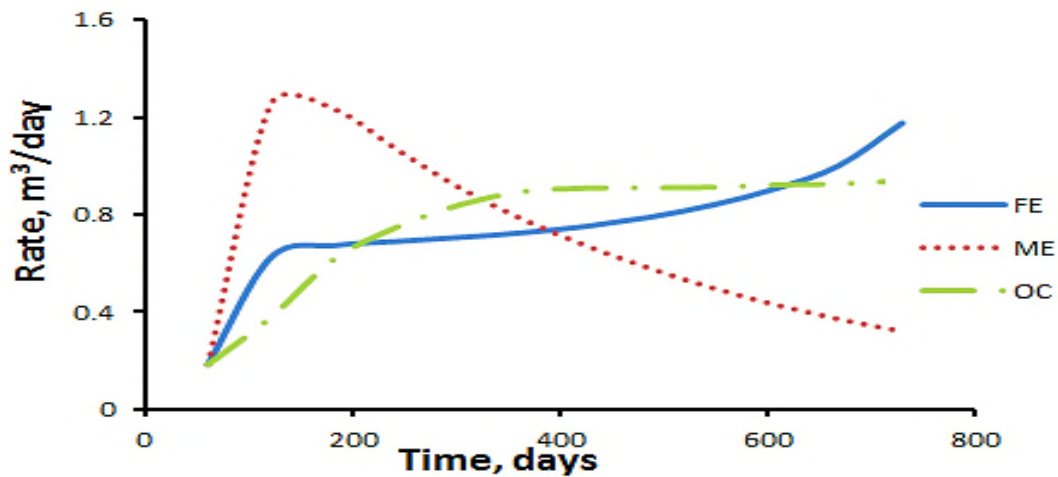


Figure 4-5: Water Injection Rates for Different Strategies (b = 0)

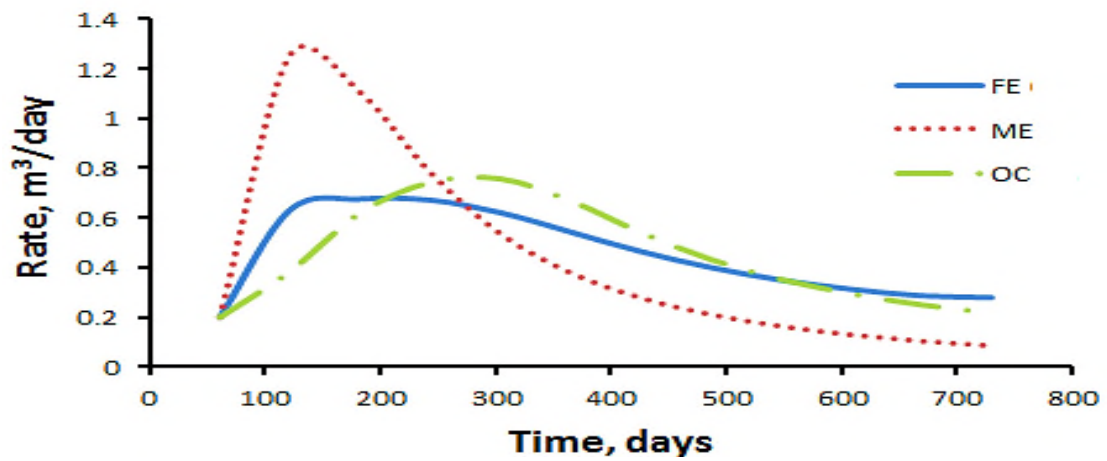


Figure 4-6: Oil Production Rates for Different Strategies (b = 0)

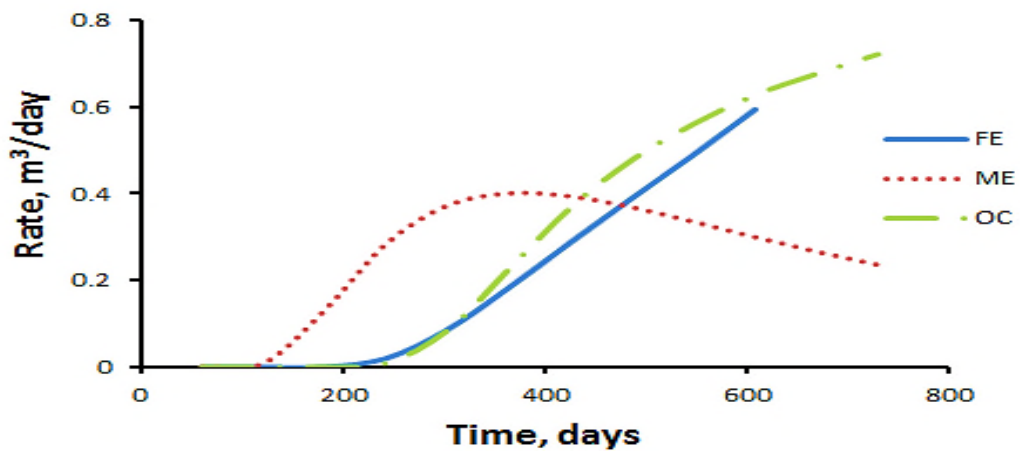


Figure 4-7: Water Production Rates for Different Strategies (b = 0)

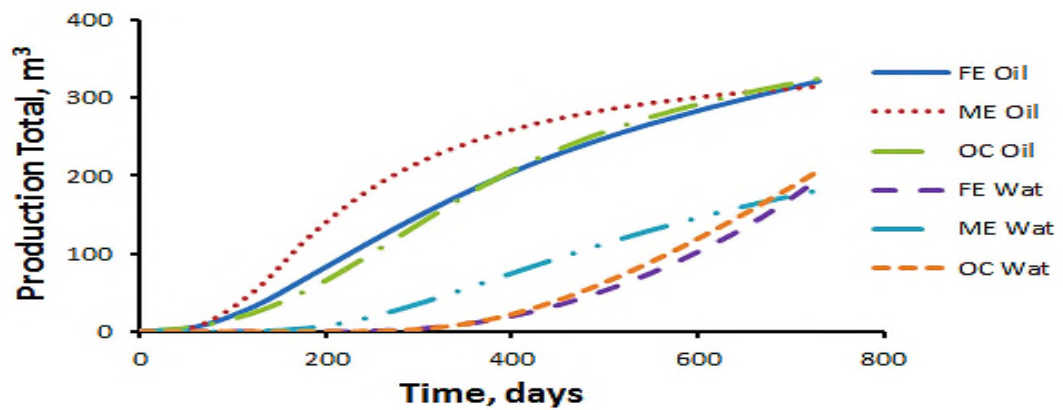


Figure 4-8: Total Production for Different Strategies (b = 0)

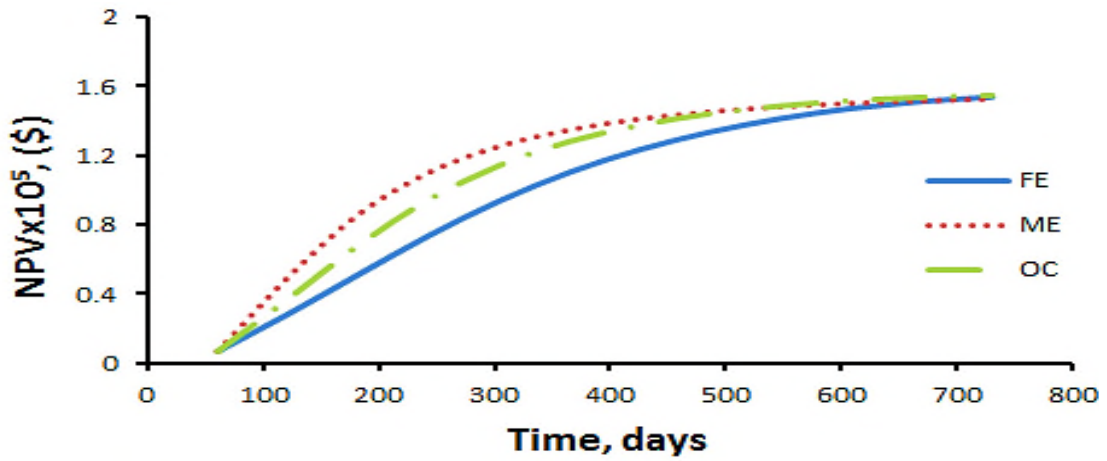


Figure 4-9: NPV for Different Strategies (b = 10%)

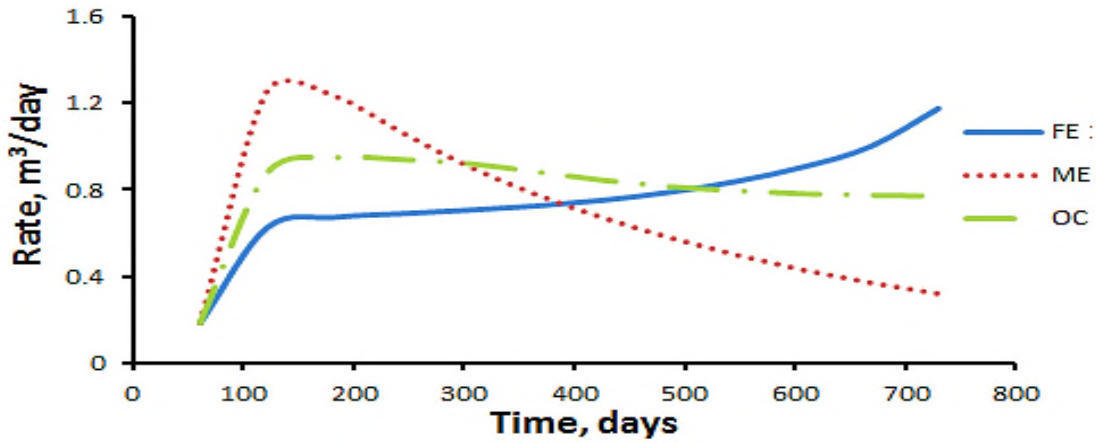


Figure 4-10: Water Injection Rates for Different Strategies (b = 10%)

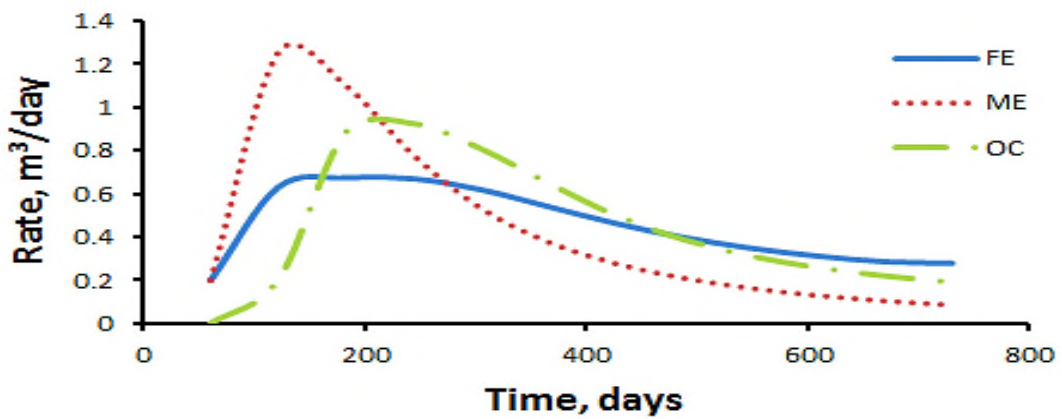


Figure 4-11: Oil Production Rates for Different Strategies (b = 10%)

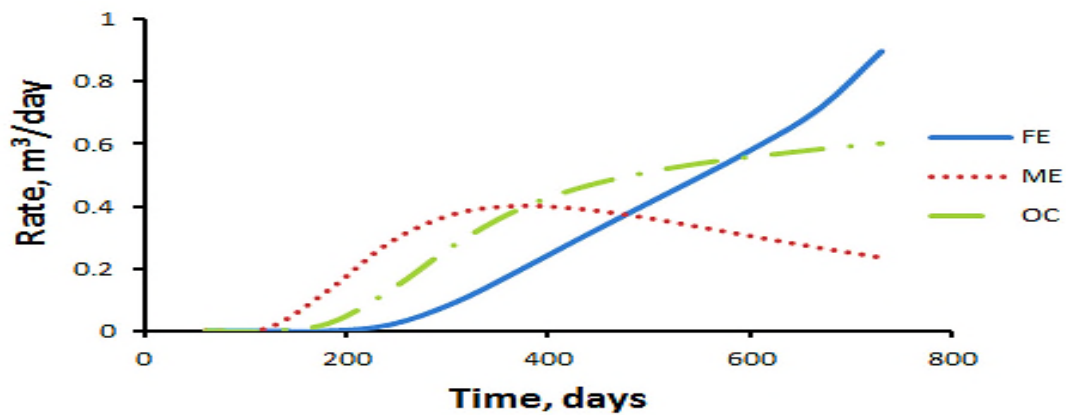


Figure 4-12: Water Production Rates for Different Strategies (b = 10%)

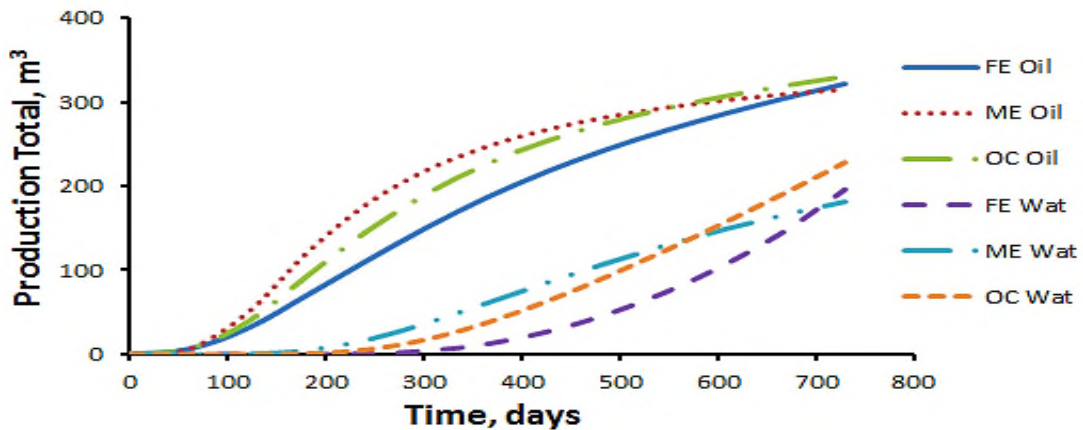


Figure 4-13: Total Production for Different Strategies (b = 10%)

4.2.2 Optimization with Recoveries as Objective

In this section, optimization study will focus on maximization of total oil recovery and minimization of water production. The reservoir and well configurations used in Section 4.2.1 are adopted here with the same rock and fluid properties. As in the previous section, two RHC strategies, FE and ME are compared against a benchmark approach, OC to ascertain if earlier conclusion can also be made here. In addition to rate-controlled wells, a case of pressure-constrained scenario is included. Again, a voidage replacement was assumed for the rate-constrained case.

For the pressure-constrained case, the optimization variables are bottomhole pressures (BHP) of injection and production wells. The injector and producer BHPs were bounded in the range [1.5 5] bars and [1 2] bars respectively. As discussed in Section 2.4.1, a mathematical relationship such as Equation (2-22) is needed to link the BHPs with the liquid rates. An important factor to be determined in order to make use of such relationship is well productivity index (α_p). Here, a simple Peaceman's well index is adopted (Guo et al., 2007).

As mentioned above, the objective function is maximization of total oil recovery and minimization of water production given in Equation (4-1).

$$J_k = \left(\sum_{j=1}^{N_{prod}} [(y_{o,j})_k - (y_{wp,j})_k] \right) \Delta t_k \quad (4-1)$$

The total production period was as well fixed to two years. The best prediction window of 12 months was selected with respect to ME approach. Sampling rate of two months was maintained here.

Results and Discussion

The simulation results are shown in in Table 4-2. With respect to oil production, OC has the highest performance followed by FE. In the rate constrained-case, the relative increase in total oil production for OC strategy in comparison to FE and ME are 4.52% and 7.97% respectively. Similarly, increase in performance in the case of pressure-controlled scenario is 6.23% and 8.93% for FE and ME respectively. However, increase in oil production is associated with a corresponding increase in water production as can be seen in Figure 4-14 and Figure 4-15.

High performance by OC can be explained based on injection-production relationship as follows: Take for instance, in the case of rate-controlled wells, intermediate injection rates were applied right from the beginning of production which were maintained till the end of the period (Figure 4-16). This resulted to a longer much-needed plateau period in oil production (Figure 4-17) with a delay

in water production that is in between the two RHC methods (Figure 4-18). Comparing this to the worst case of ME approach, a sudden rise in water injection rates which was followed by a sharp decline can be observed in (Figure 4-18). A similar phenomenon can be explained for oil production shown in Figure 4-17.

Now, considering pressure-constrained case, for the OC approach, intermediate injection pressures were found which are little bit higher than those found with FE approach but much lower than for the case of ME RHC as clearly shown in Figure 4-19. The production BHPs were also relatively low for the cases of OC and FE in comparison to those found using ME approach. The effects of these are translated in the production profiles of oil and water given in Figure 4-20 and Figure 4-21 respectively. Again, a much longer plateau period was created by OC approach with water production been delayed till about 400 days. Water break-through was further delayed with FE RHC while early water production can be seen with ME approach (occurred just after 200 days of production commencement).

As stated earlier, the relative performances of the three strategies in terms of total oil production increases in the order of ME, FE and OC. This order is however reversed when the performance is based on water production. The reason was explained in detail above. So performing optimization with this type of objective function will require the decision of the operator in choosing appropriate settings that will suit market demand, current oil price, and processing cost and capacity. Therefore, it can be concluded, that, NPV of the venture is the best performance index that can be used in conducting optimization studies because it takes into consideration the aforementioned factors in addition to time value of money.

Table 4-2: Performance Comparison of Optimization Strategies for Simple Wells System with Recoveries Objective Function

Control	Strategy	Total Oil Production (m ³)	Total Water Production (m ³)
Rate	OC	231.63	30.03
	FE	221.16	23.23
	ME	213.16	18.01
Pressure	OC	240.76	38.13
	FE	225.75	26.11
	ME	219.27	22.14

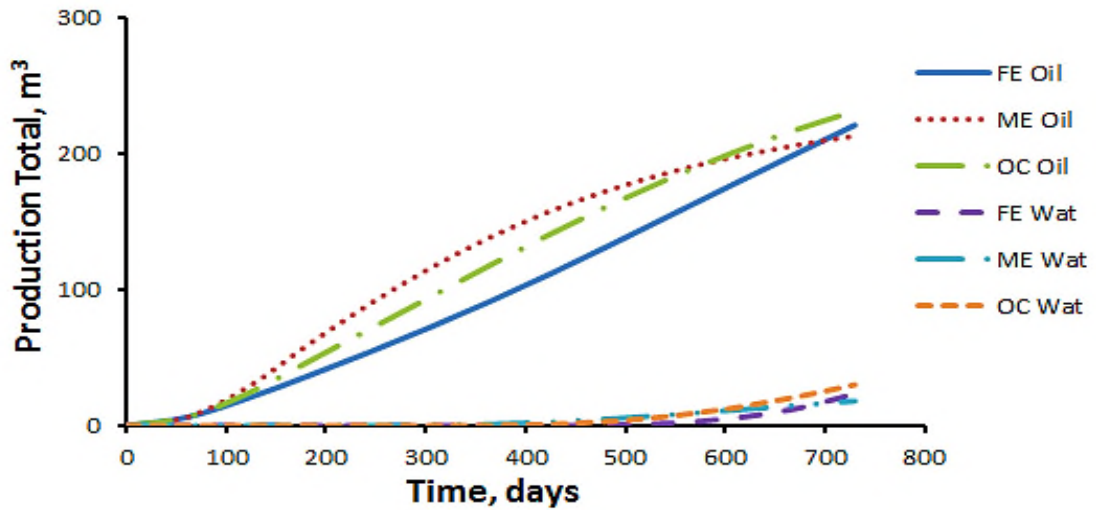


Figure 4-14: Total Production for Rate-Constrained Scenario

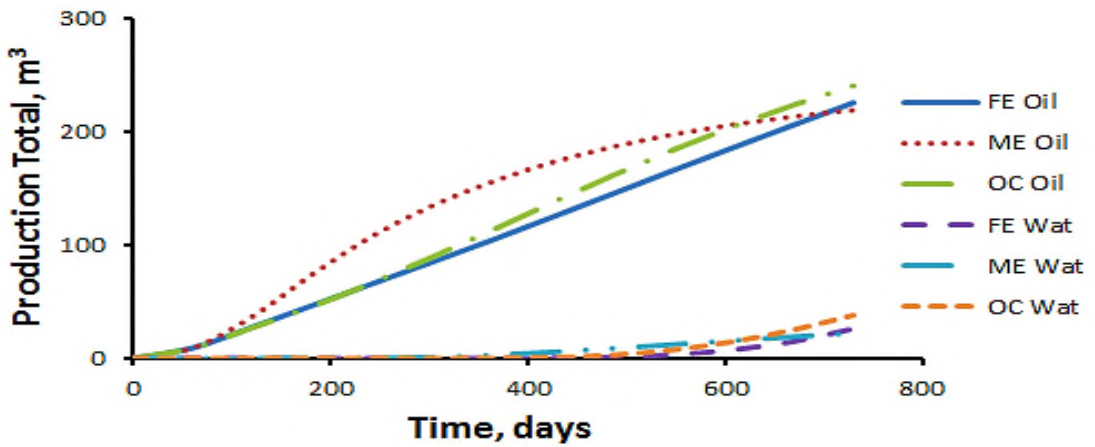


Figure 4-15: Total Production for Pressure-Constrained Scenario

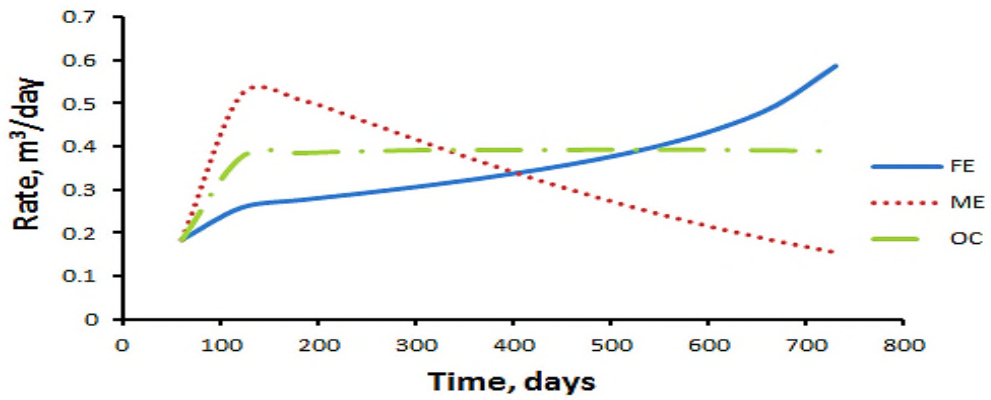


Figure 4-16: Injection Rates for Rate-Constrained Scenario

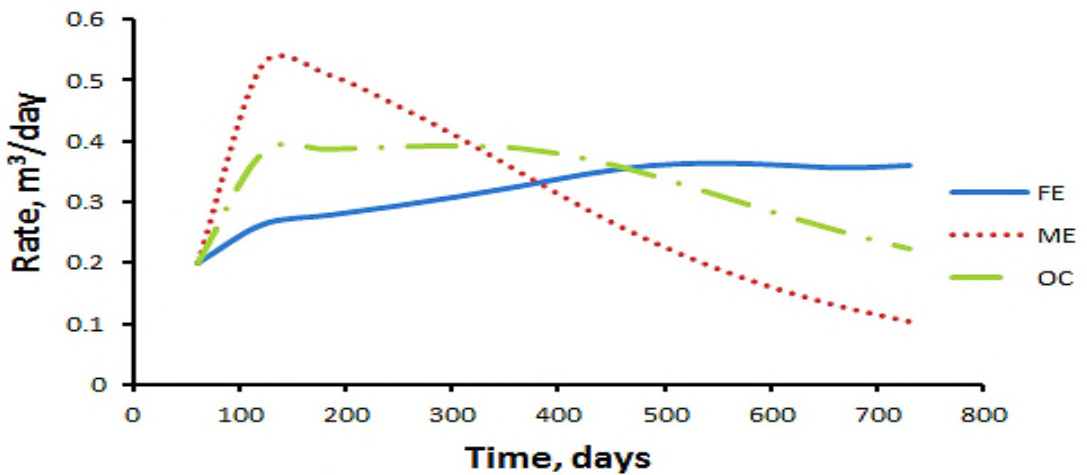


Figure 4-17: Oil Production Rates for Rate-Constrained Scenario

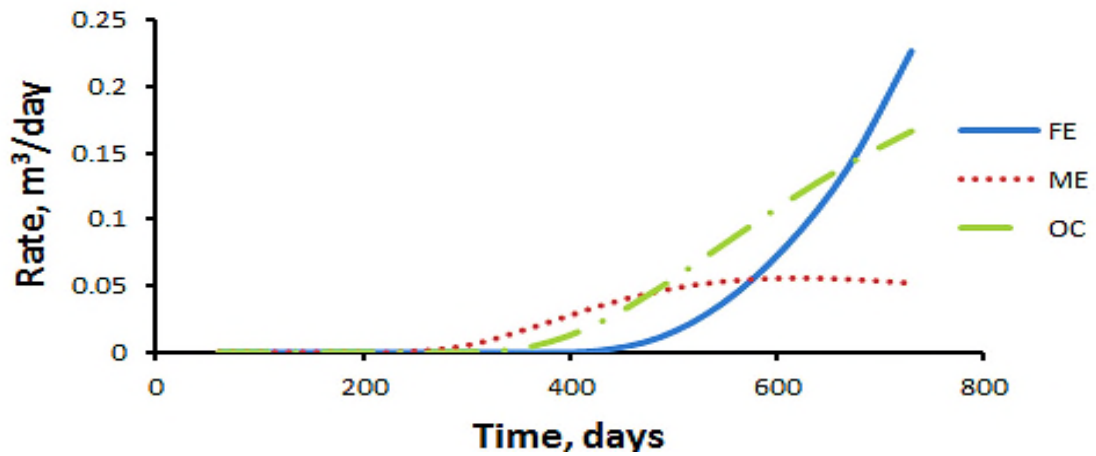


Figure 4-18: Water Production Rates for Rate-Constrained Scenario

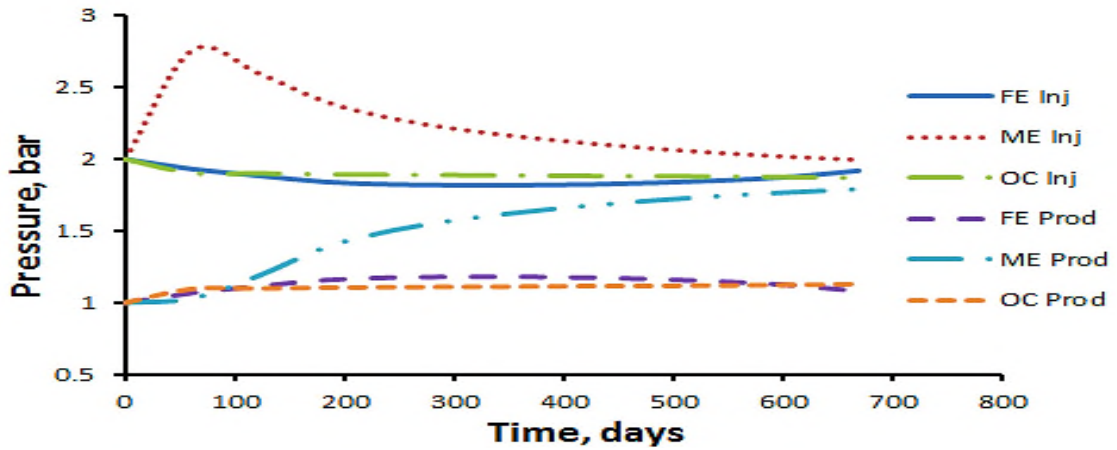


Figure 4-19: Injection-Pressure for Pressure-Constrained Scenario

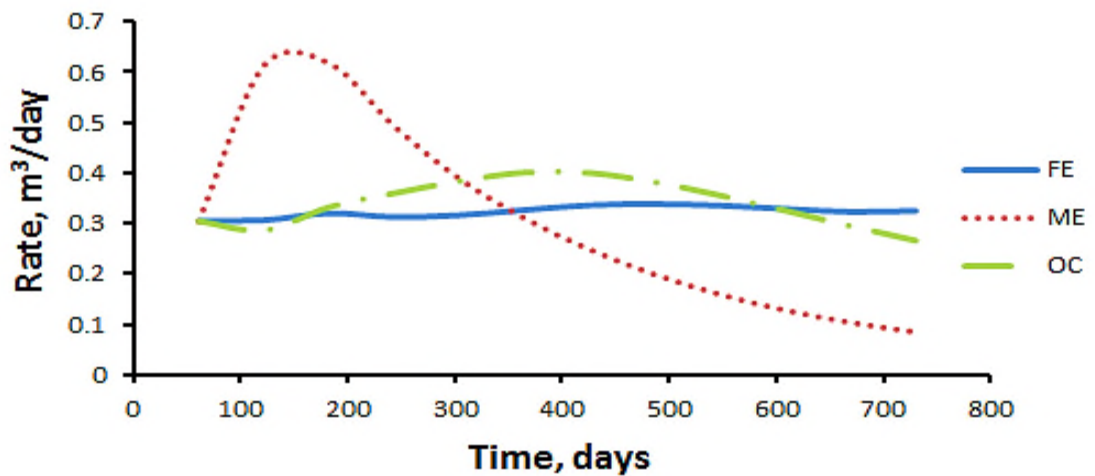


Figure 4-20: Oil Production Rates for Pressure-Constrained Scenario

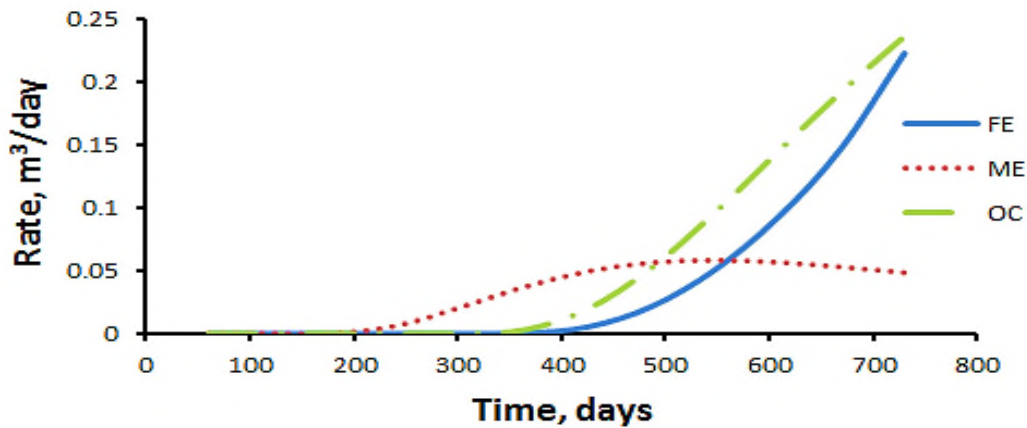


Figure 4-21: Water Production Rates for Pressure-Constrained Scenario

4.3 RHC for Uncertain Reservoir Models

RHC is applied here to deal with uncertainties in reservoir properties such as permeability, porosity and structure. Two different reservoir models were used for the study; a prediction model to determine optimal well settings and implementation model where these well settings are implemented. The implementation model was assumed to be the real reservoir with uncertain properties that are different from those of the prediction model. The prediction model also served as a nominal model for determination of open-loop optimal control. A benchmark (BM) solution case was also developed with assumption of a perfect reservoir model and properties known a priori.

The real reservoir provides synthetic measurements while the RHC reservoir was used to perform optimal control predictions. A physics-based reservoir model was used for the prediction in this work instead of data-driven model as is common with MPC for the simple reason that, data-driven models can never predict water breakthrough or saturations. They (data-driven models) can only predict pressures over a very short time for which saturations do not change appreciably (van Essen et al., 2013). Although, very time consuming, physics-

based reservoir models provide more accurate predictions and better optimization performance over a long prediction horizon as was shown in Section 4.2.

4.3.1 Approach

A simple methodology adopted to counteract the effects of system/model mismatch is highlighted below:

1. Based on initial measurements from the real reservoir, initial states are chosen for the prediction model so that difference in real and predicted measurements is minimized.
2. An optimization is carried out with the adjusted initial states to determine control inputs for the starting step.
3. These optimal inputs \mathbf{u}_{opt} are applied to both the RHC and real reservoir models where two sets of measurements are obtained, predicted, \mathbf{Y}_p and real, \mathbf{Y} measurements respectively.
4. Output disturbance, \mathbf{d} is taken as the difference between \mathbf{Y} and \mathbf{Y}_p which is added to \mathbf{Y}_p for an update. The disturbance is assumed constant over the prediction horizon.
5. Optimization is carried out based on the updated measurements to obtain control inputs for the second time-step which are applied to both models.
6. Steps 3 – 5 above are repeated till the end of production time.

Figure 4-22 shows algorithms for implementation of the above steps. A simplified diagram for such closed-loop system is given in Figure 4-23. Rate-controlled wells are considered. The measurements that are updated in step 3 above are oil and water production rates given as

$$\mathbf{Y} = [y_o \ y_w]^T \quad (4-2)$$

To evaluate the efficacy of this approach, its performance was compared against OC strategy where the optimal control inputs obtained based on the nominal reservoir model are implemented on the true reservoir model; and a benchmark case in which open-loop optimal controls were determined from the truth reservoir model whose properties were assumed to be known a priori. For all approaches, NPV, Equation (3-5) was used as the objective function with zero discount factor and other economic parameters as given in Section 4.2. Two simple indices were chosen for the comparative analyses:

- The loss which is a deviation from the benchmark performance as a result of implementing either RHC or OC solution and computed from

$$Loss = \frac{J_{BM} - J_{RHC/OC}}{J_{BM}} \times 100\% \quad (4-3)$$

where J_{BM} is NPV obtained from the benchmark case and $J_{RHC/OC}$ the NPV obtained from either RHC or OC approach.

- The gain which measures the benefit realisable through RHC implementation as compared to OC given by

$$Gain = \frac{J_{RHC} - J_{OC}}{J_{RHC}} \times 100\% \quad (4-4)$$

Based on the results from Section 4.2 where it was shown that FE is better than ME for all cases, it was then decided to adopt the former approach here to deal with uncertainties. A sampling time of one day was used for this analysis. Therefore, for a two-year production period, the initial prediction horizon is fixed to 730 days which then decreases subsequently by one day after every control implementation (see Figure 4-1). For the prediction of optimum well control, an adjoint formulation was applied for gradient computation, see previous chapter (Section 3.3).

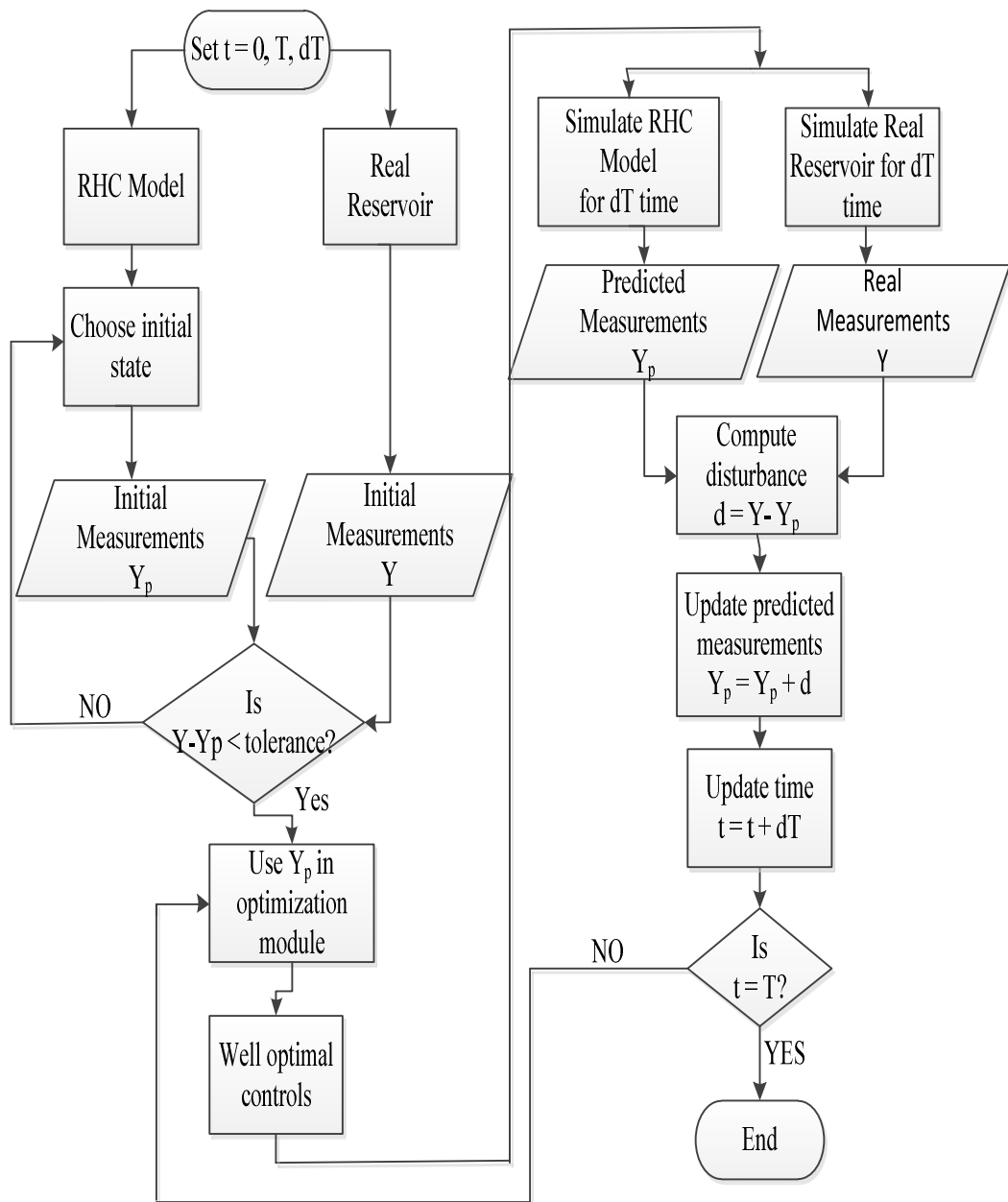


Figure 4-22: A Flowchart for RHC Strategy Applied to Uncertain Reservoir

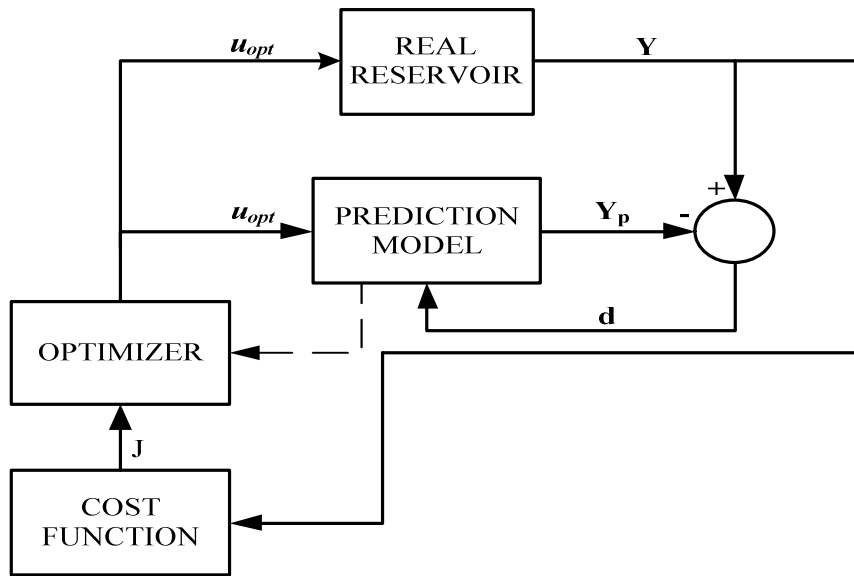


Figure 4-23: Receding Horizon Control Loop

4.3.2 Uncertainty Consideration

Four different cases were considered. For the first case, uncertainty has not been introduced; both real and prediction models are the same (nominal model was used). The reservoir used in Section 4.2.1 is adopted here as the nominal model which is a reservoir of size 20 m x 20 m x 5 m and homogenous in all fluid and rock properties. Specifically, the porosity and permeability are 0.3 and 100 mD respectively. However, both injection and production wells are vertical as shown in Figure 4-24 and are rate-constrained. As stated earlier, it is expected that RHC solution for this case would not be as good as open-loop optimal control due to the absence of model/system mismatch. However, the case would serve as a basis of comparison with other uncertainty cases and to a novel methodology developed in the next chapter.

In Case II, the prediction reservoir model differed from the real reservoir in permeability. All other properties of rocks, fluid, geometry and well configuration remain the same. The prediction reservoir model therefore, has a uniform permeability of 100 mD. The truth reservoir however, has five layers each with

different permeability which is log-normally distributed with mean values of 200 mD, 500 mD, 350 mD, 700 mD, and 250 mD from top to bottom. See Figure 3-1 in the previous chapter for this type of permeability distribution.

In addition to uncertainty in permeability, rock porosity was also assumed to be uncertain in Case III. The setup is the same as in Case II but the porosity of the truth reservoir and prediction model differs. Here, the nominal porosity remains at 0.3 while the real reservoir has a porosity of 0.45.

A lot of geological uncertainties were incorporated in Case IV which range from uncertainties in reservoir size, geometry and structure. The real reservoir was considered to be appreciably larger than the predictive reservoir whose size is 225 m x 22.5 m x 1 m. It was modelled with 30 x 3x 1 cells using a corner point gridding system (predictive reservoir was modelled using a Cartesian grid). It also has a structural fault with width of 0.12 m. The fault can transmit fluids if the pressure drop across it is sufficient (Figure 4-25). Other rock and fluid properties are the same for both reservoirs.

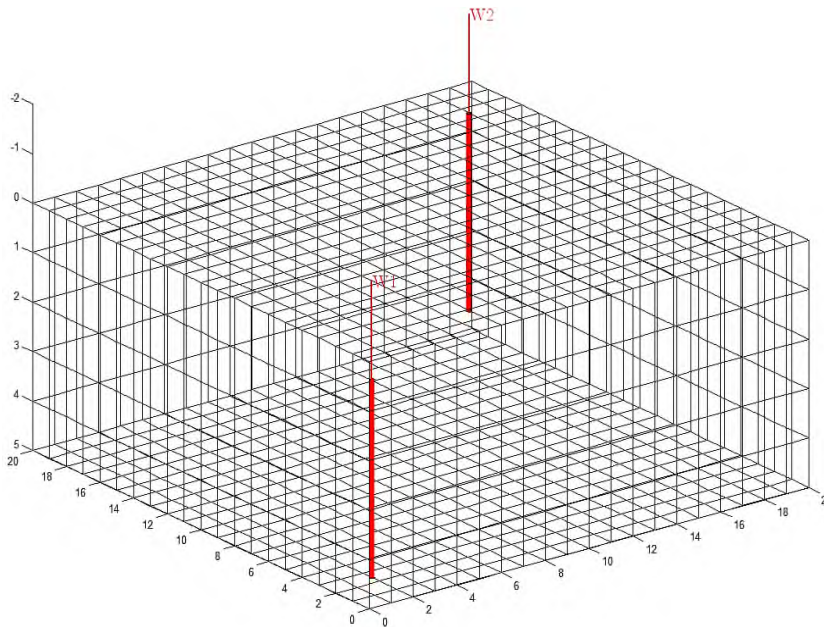


Figure 4-24: Reservoir Geometry and Wells for RHC Prediction (Nominal Model)

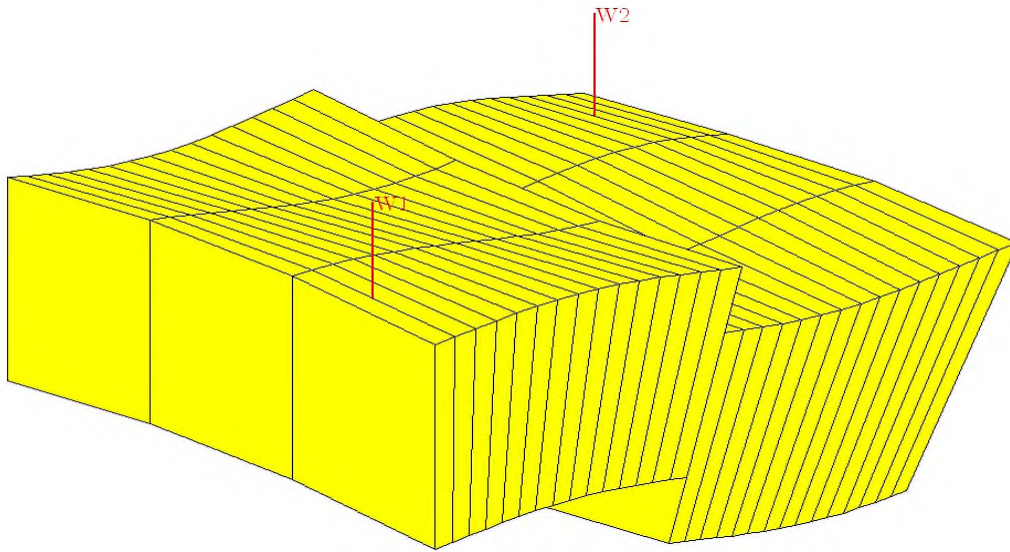


Figure 4-25: Reservoir and Well Configuration for Case IV

4.3.3 Results and Discussions

The results for different cases are now presented and discussed.

4.3.3.1 Case I: Nominal Reservoir Parameters

For the case where nominal parameter values were used (both real and prediction models are the same), NPVs for RHC and OC approaches are respectively \$182,274.70 and \$182,775.04 which indicates a loss of only 0.27%. The two NPVs are indistinguishable right from beginning of production to the end as shown in Figure 4-26. This resemblance was as a result of identical injection and production trajectories found by the two methods (Figure 4-27). A brief summary of the results obtained is given in Table 4-3 where the similarities are further confirmed in total productions and water break-through time.

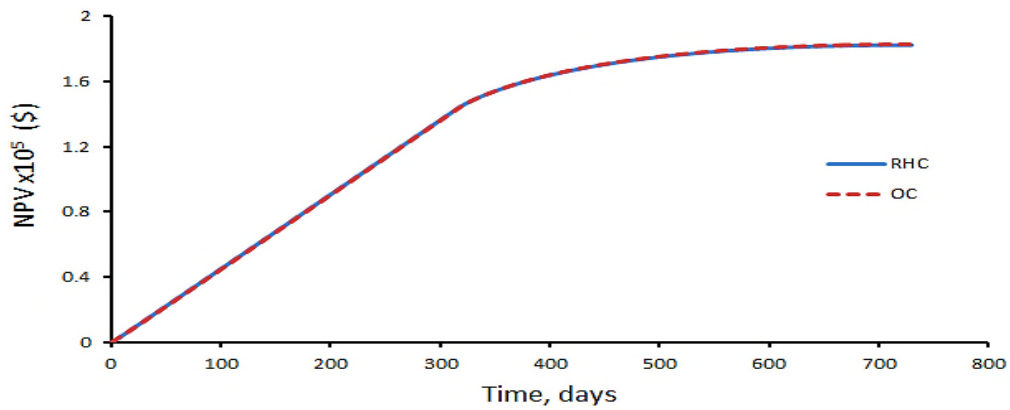


Figure 4-26: NPVs for Case I

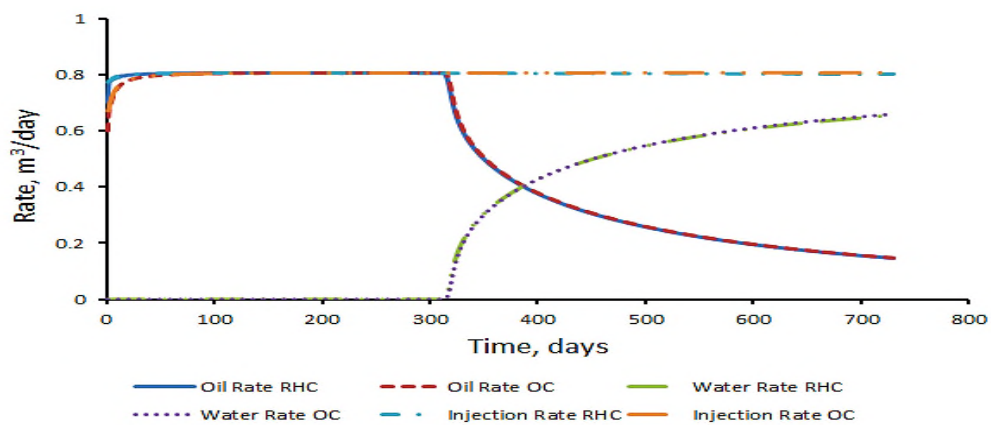


Figure 4-27: Injection and Production Rates – Case I

Table 4-3: RHC and OC Comparison for Case I

Strategy	Total Oil (m ³)	Total Water (m ³)	Time of Water Break-Through (days)	NPV (\$)
RHC	368.62	218.63	324	182,274.70
OC	370.69	215.91	317	182,775.04

4.3.3.2 Case II: Uncertainty in Reservoir Permeability

Here, the prediction reservoir model has a uniform permeability of 100 mD while the truth reservoir has five layers with different permeability which is log-normally distributed with mean values of 200 mD, 500 mD, 350 mD, 700 mD, and 250 mD from top to bottom.

To investigate the extent to which error in the actual value of permeability can affect waterflooding performance, the sensitivity of the objective function, NPV to reservoir permeability was first studied. About 50 reservoir realizations were generated each with different permeability distributions. These realizations were simulated using open-loop optimal control obtained based on the nominal model.

It can be seen from Figure 4-28 that NPV is greatly affected by changes in permeability values. A minimum value in NPV of \$155,440.00 was obtained with a maximum value of \$159,700.00. The variation has a standard deviation of \$1,141.20 and a mean of \$157,540.00. Hence, a feedback configuration such as RHC strategy can play a big role in counteracting the effects of such modelling error. Table 4-4 summarises the performance of the three approaches.

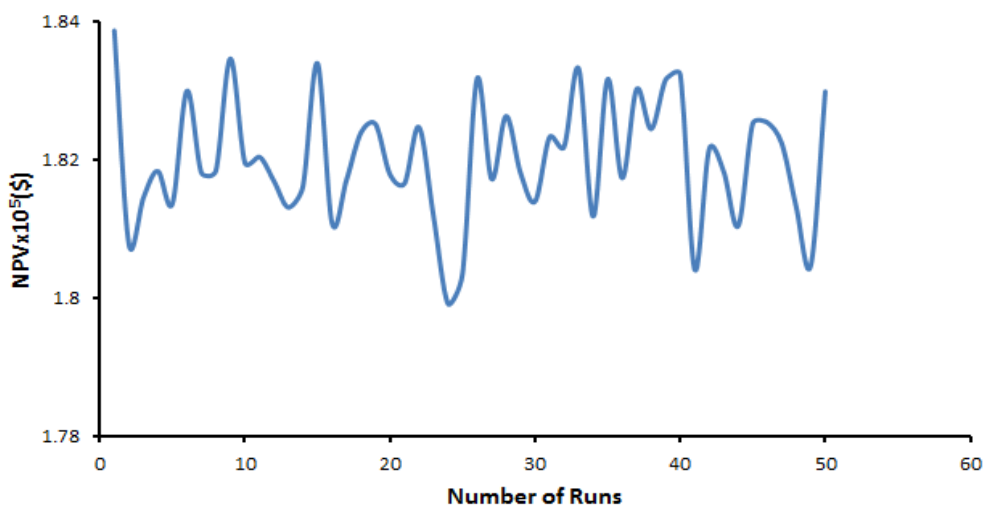


Figure 4-28: Permeability Sensitivity to NPV

Table 4-4: Performance Comparison – Case II

Strategy	Total Oil (m³)	Total Water (m³)	Time of Water Break-Through (days)	NPV (\$)
RHC	336.91	249.33	186	159,320
OC	336.47	250.17	187	159,096
BM	344.28	280.33	142	159,724

The use of RHC in mitigating against the considered modelling error has incurred a loss in NPV of 0.25% as compared to 0.39% for the case of OC based on BM. Furthermore, the gain obtained in introducing feedback into the optimization process via RHC is 0.14% over OC approach. The slight improvement obtained is due to a slight increase in oil production (0.13%) and a corresponding decrease in water production (0.34%) which is also evident from difference in water break-through time (one day). The above trend can be confirmed from total production profiles shown in Figure 4-29. It can be observed from the figure that the total productions for RHC and OC strategies are indistinguishable on the scale of the graph. This occurs because the optimal solutions found by the two strategies are only slightly different which can be observed from plots of water injection, oil and water production rates shown in Figure 4-30 - Figure 4-32 respectively. This indistinguishable trend can also be attributed to the size of reservoir considered and the prediction horizon used (FE). Another reason may be from the scale of uncertainty, as can be seen the BM approach also found solution with similar profiles. However, an improvement in NPV has been achieved which is shown in Figure 4-33.

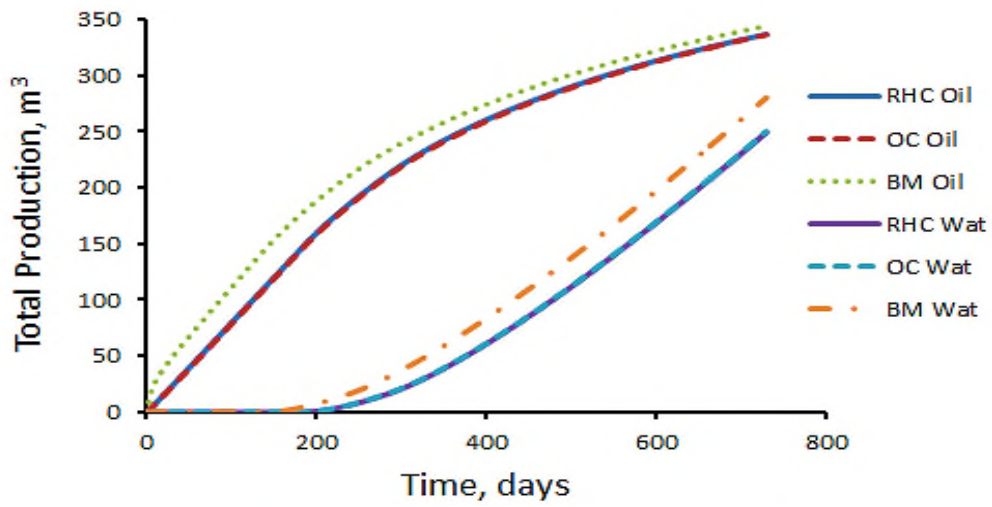


Figure 4-29: Total Production for Case II

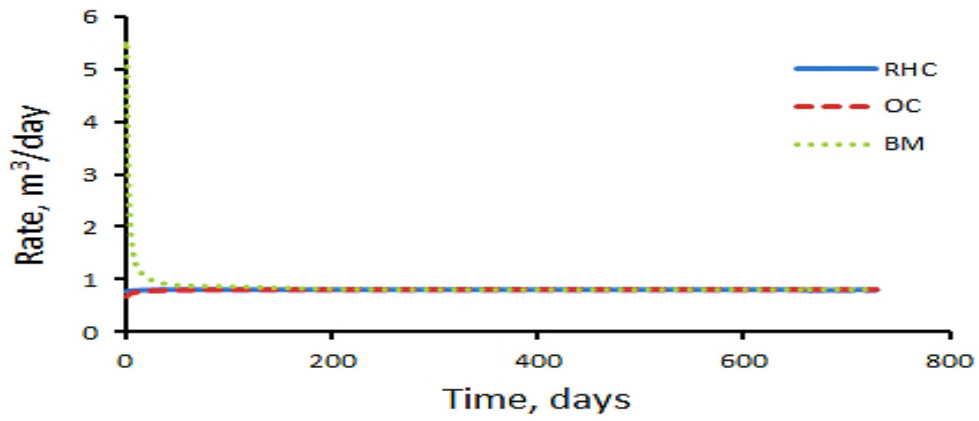


Figure 4-30: Injection Rates for Case II

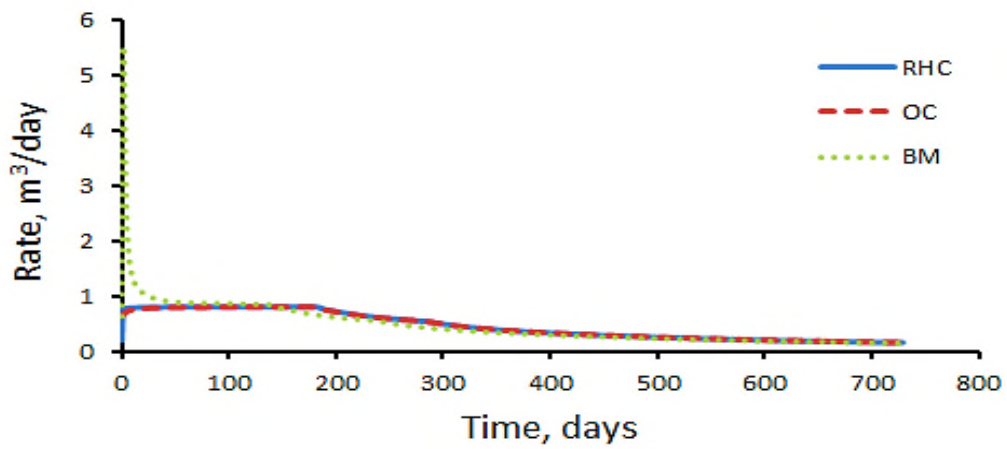


Figure 4-31: Oil Production Rates for Case II

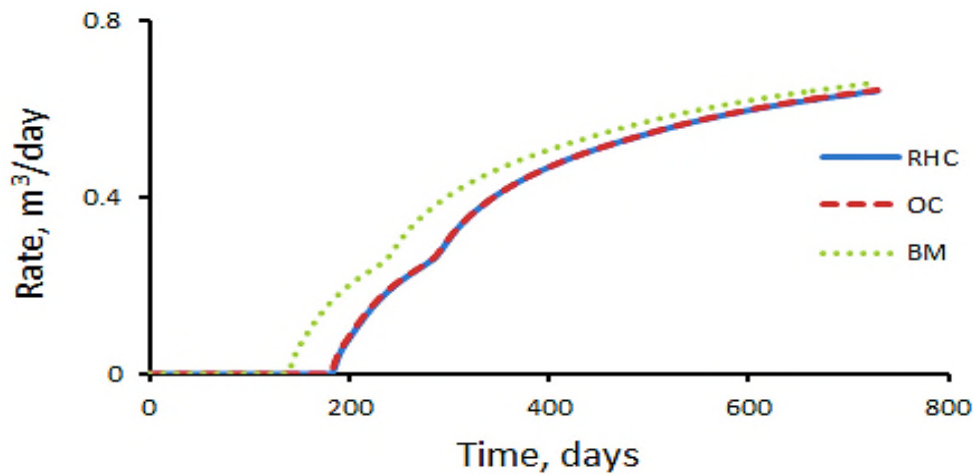


Figure 4-32: Water Production Rates for Case II

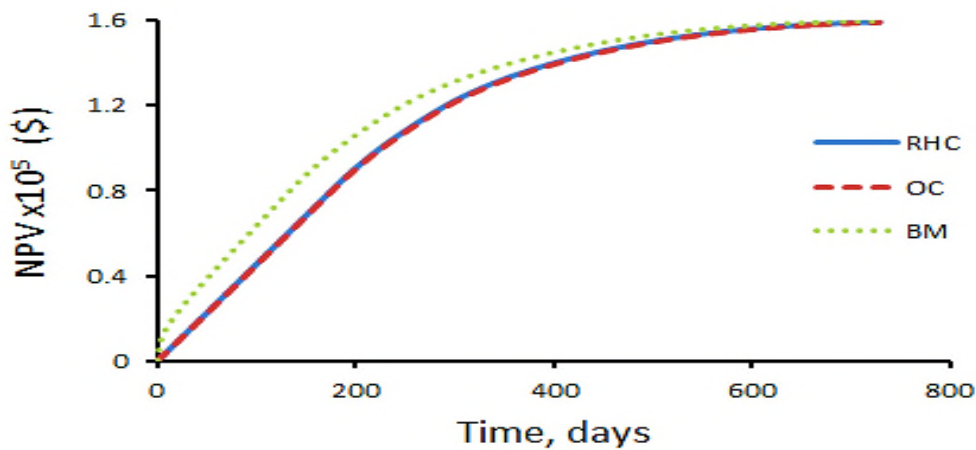


Figure 4-33: NPV for Case II

4.3.3.3 Case III: Uncertainty in Reservoir Permeability and Porosity

In addition to log-normal distribution in permeability as in Case II, the truth reservoir has a porosity of 0.45 as against 0.3 for the prediction model. With the increase in scale of uncertainty, the performance of RHC has further improved in relation to OC. Here, the gain achieved is 0.67% as compared to 0.14% in Case II. A summary of performance is given in Table 4-5. However, the losses recorded have increased to 7.10% in the case of RHC and 7.67% for OC. The superior performance by RHC strategy is attributed to a higher production in oil

(0.67%) and lower water production (1.58%) which can be visualised from Figure 4-34. A wide gap is observed between the BM approach and the two strategies which translated to a corresponding gap in NPV (Figure 4-35). This wide difference was caused as a result of disparity between injection (Figure 4-36) and production (Figure 4-37 and Figure 4-38) settings of the two strategies and BM. Although a good plateau period was seen with all the strategies; that of the BM is quite higher at the beginning of production period but became almost similar eventually after around 300 days. As in Case II, RHC and OC profiles are still indistinguishable.

Table 4-5: Performance Comparison- Case III

Strategy	Total Oil (m ³)	Total Water (m ³)	Time of Water Break-Through (days)	NPV (\$)
RHC	427.87	158.38	280	222,286.10
OC	425.70	160.93	274	220,918.20
BM	520.05	439.30	166	239,271.50

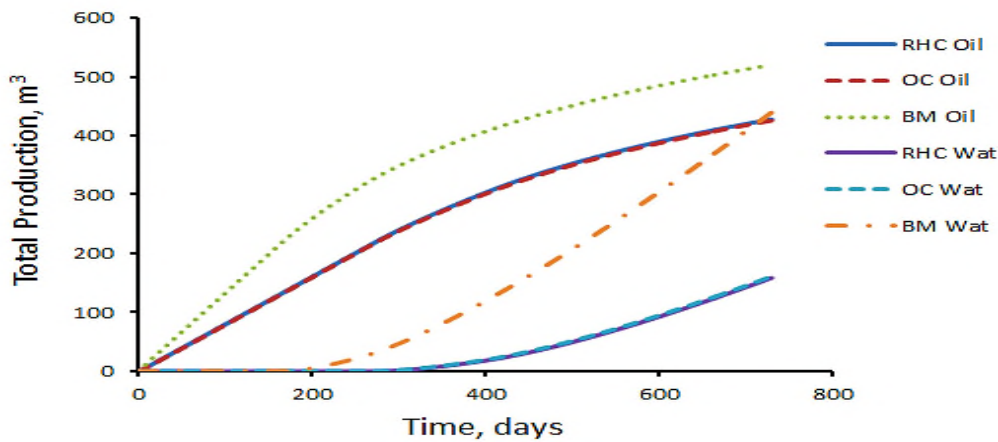


Figure 4-34: Total Production – Case III

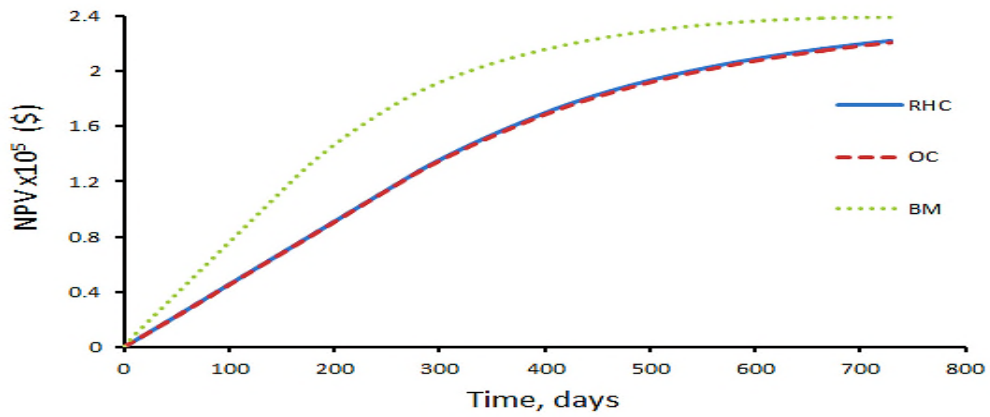


Figure 4-35: NPV for Case III

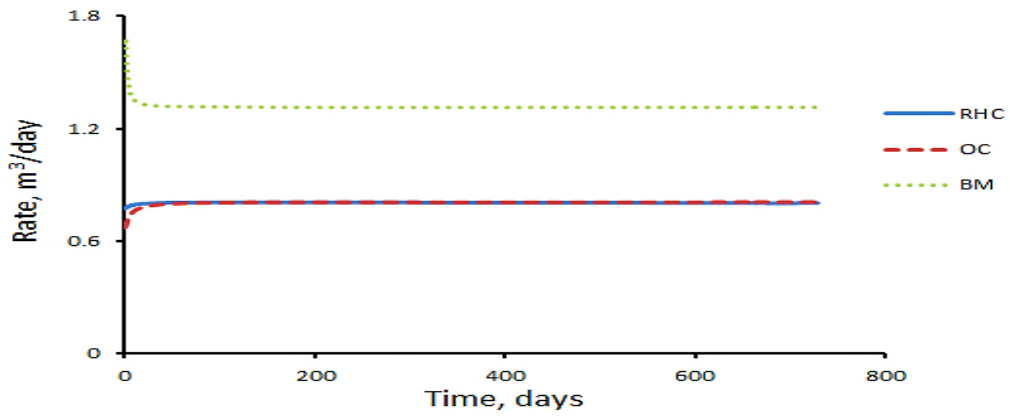


Figure 4-36: Injection Rates - Case III

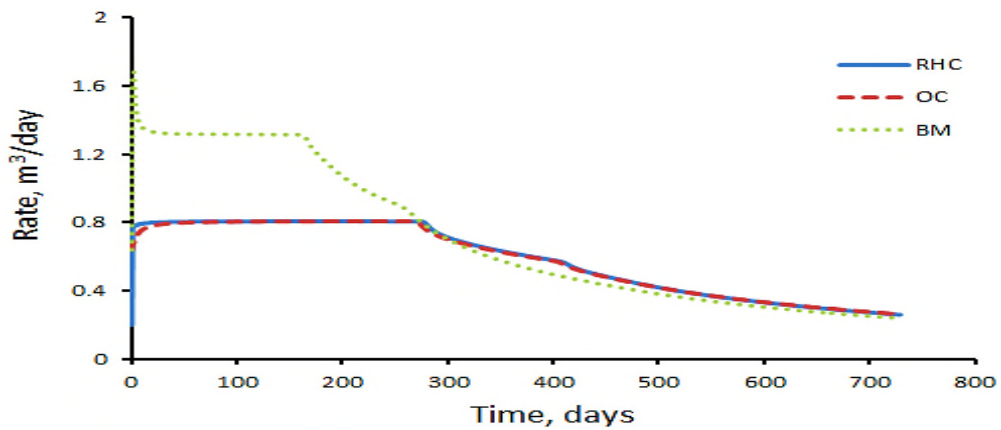


Figure 4-37: Oil Production Rates - Case III

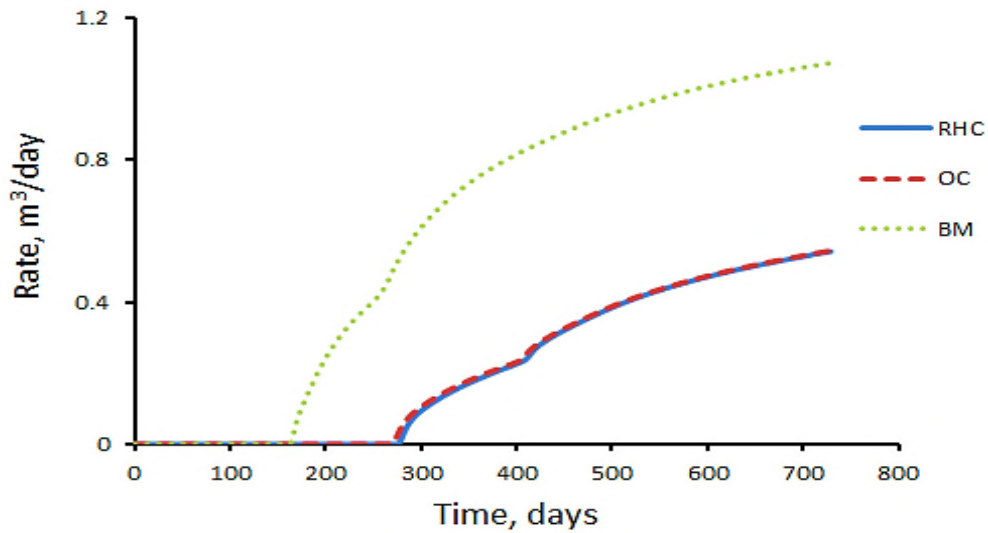


Figure 4-38: Water Production Rates - Case III

4.3.3.4 Case IV: Uncertainty in Reservoir Size, Geometry and Structure

With the introduction of high degree of uncertainty in this case which includes uncertainties in reservoir size (real size of 225 m x 22.5 m x 1 m while nominal is 20 m x 20 m x 5 m), geometry (real geometry is corner point and Cartesian grid for the prediction model) and structure (presence of fault in the real reservoir), a very huge loss was incurred as a result of implementing an open-loop optimal solution with a value of 31.51%. However, the loss was drastically reduced by almost half through the use of measurements by RHC (loss of 15.21%). The gain in this case is 19.22% in favour of RHC. The significant improvement of the feedback strategy can be visualised graphically from the plots of NPVs in Figure 4-39. The open-loop NPV is not close in any way to the RHC performance index which indicates a total failure of the former in the presence of these uncertainties.

Table 4-6 summarises the obtained results where it can be seen that a reasonable amount of oil was produced via RHC implementation which is comparable to the ideal amount (8.45% less), although the production was associated with high volume of water production; a reason that affected the

NPV significantly. For the OC case however, a very low production was experienced. The zero-level water production is not a plus to this strategy; it is indeed an indication of inefficient reservoir sweeping. This can be further confirmed by observing the injection profiles of the three approaches in Figure 4-40. As it was shown, an average of 1.8 m³/day of water is required for an optimum flooding operation (BM), a requirement that has not been satisfied with open-loop solution whose injection trajectory averages at 0.8 m³/day. In the case of RHC, the optimum flooding requirement has been exceeded where the average injection rates throughout the production period is 2 m³/day. This is one of the reasons for the excessive water production which characterises RHC solution method for the considered reservoir system.

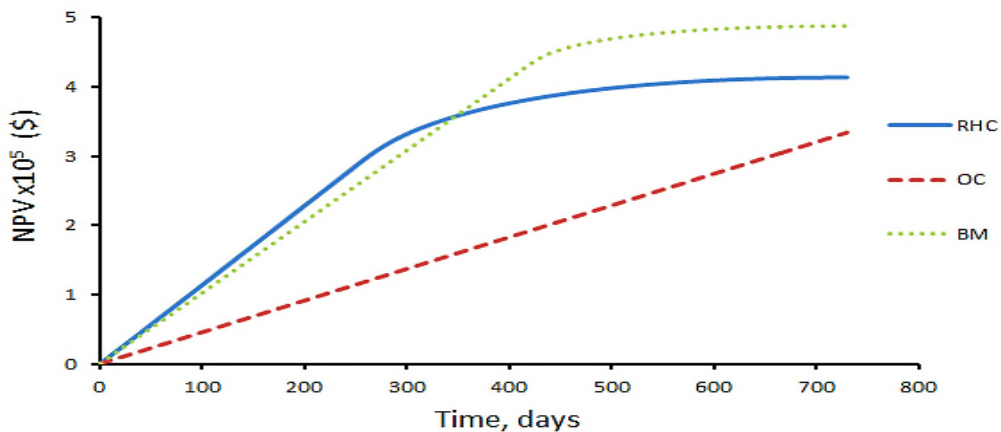


Figure 4-39: NPVs for Case IV

Table 4-6: Performance Comparison - Case IV

Strategy	Total Oil (m ³)	Total Water (m ³)	Time of Water Break-Through (days)	NPV (\$)
RHC	865.68	609.54	264	413,365.02
OC	587.73	0	-	333,904.67
BM	944.12	381.11	424	487,520.08

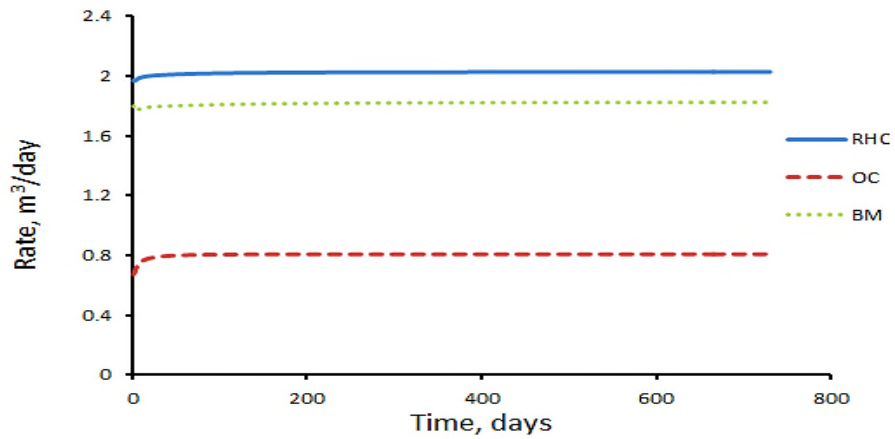


Figure 4-40: Injection Rates for Different Strategies – Case IV

The inefficiency of OC solution on this uncertain system can be further observed from oil production profiles shown in Figure 4-41. For a reservoir that has a potential to produce at a peak of 1.8 m³/day for a period of 424 days will in no way be produced profitably at an average of 0.8 m³/day throughout the set period of two years.

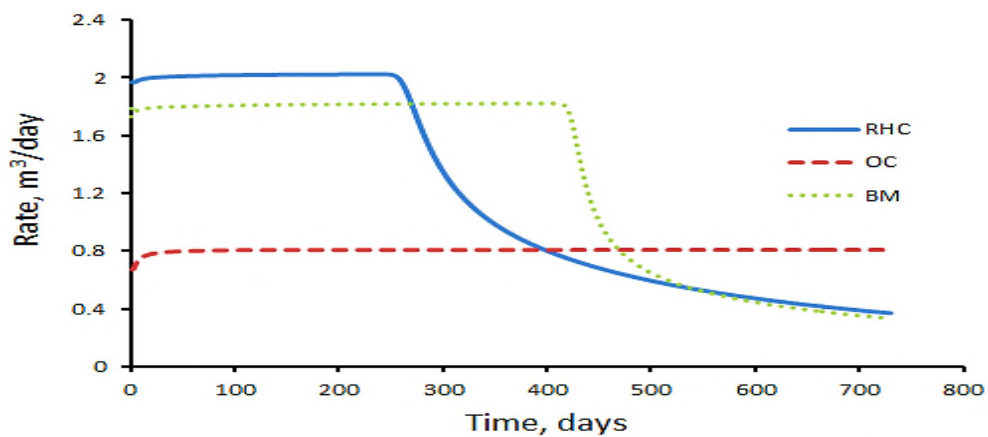


Figure 4-41: Oil Production Rates – Case IV

4.3.4 Conclusion

In this chapter, a feedback control approach based on receding horizon strategy was used for optimization of reservoir waterflooding. The aim was to counteract uncertainties in reservoir properties. The chapter started the optimization study by assuming a perfect reservoir modelling where two forms of RHC were exploited. Different forms of objective functions and well controls were also investigated. Based on the findings from this initial work, model/system mismatch was then introduced into the feedback configuration. The following conclusions were drawn:

1. For all cases considered, FE strategy performed better than ME.
2. Length of prediction horizon affects the performance of ME approach. So, a considerable effort is needed to determine an optimum prediction period which will depend on the nature of the reservoir in question. As reservoir production is not repeatable, determination of optimum prediction period may not be realistic. Therefore, FE is preferable than ME for the case of waterflooding process.
3. The rate of discounting has insignificant effect on optimum injection and production settings found by RHC strategies.
4. NPV was found to be more appropriate performance index than recoveries because the former takes into consideration actual value of assets at a point in time.
5. The application of RHC strategy to counteract the effect of uncertainties has yielded gains that vary from 0.14% to 19.22% over the traditional open-loop approach. The gain increases with introduction of more uncertainties into the configuration. The losses incurred as a result of the effect of feedback is in the range of 0.25% - 15.21% in comparison to 0.39% - 31.51% for the case of OC approach.
6. Although, an improvement has been achieved by applying RHC strategies to annul the effect of model/system mismatch, it will be worth investigating other feedback approaches that may result to higher gains and less sensitive to uncertainties.

7. The use of RHC approach is very time consuming as optimization is required at every sampling time. For this reason and that mentioned in 6 above, application of self-optimizing control is recommended to deal with uncertainties with less computational power requirement.

5 Data-Driven Self-Optimizing Control for Reservoir Waterflooding Process

5.1 Introduction

The benefits and necessity of feedback control in counteracting uncertainty and disturbances during waterflooding operation were highlighted in Chapters 2 and 4. To this regard, RHC strategy was developed and applied in previous chapter. Although, improvements have been recorded for various cases considered when comparing with traditional open-loop approach, RHC was found to be not only complicated and time-consuming, but sensitive to reservoir uncertainties. For this reason in the present chapter, a novel self-optimizing control (SOC) methodology for controlled variable (CV) selection is proposed and applied to waterflooding optimization considering various degrees of uncertainty in reservoir and fluid properties.

As was discussed in Section 2.6.3, the best CV is the gradient of the cost function if it is available online. Recently, a method was developed to approximate necessary condition of optimality (NCO) or reduced gradient through regression using measurements (Ye et al., 2012; Ye et al., 2013a). The approximation is over entire operation region which makes the solution global. However, the method requires explicit analytical expression of the process which is difficult or impossible to obtain for complex processes such as waterflooding of reservoir. The SOC approach developed in this chapter is entirely based on data, and does not require gradient expression; it is calculated through finite difference. The method can be applicable to commercial simulators where the gradient information is not available but the cost function can be computed.

The chapter starts with development of data-driven SOC where methodologies for static optimization were first derived and applied to simplified theoretical case which is termed *Toy Problem*. Both unconstrained and constrained optimizations were considered. After laying a strong foundation through the

static optimization procedure, the method was extended to dynamic optimization which was applied to waterflooding process.

5.2 Development of Data-Driven SOC Methods

The derivation of data-driven SOC given in this section will begin with static optimization case for both constrained and unconstrained systems. The idea is then extended to dynamic optimization with particular application to waterflooding problems.

5.2.1 Static Optimization

5.2.1.1 Unconstrained Static Optimization

For this case, the optimization problem is of the form

$$\min_u J(u, d) \quad (5-1)$$

where J is the objective function, u the manipulative variable and d the disturbance. Here, we assume the target CVs be measurement functions, $C = C(\mathbf{y}, \boldsymbol{\theta})$ with parameters, $\boldsymbol{\theta}$ to be determined through regression using measurements, \mathbf{y} . The CV can be expressed as

$$\frac{dJ}{du} = C(\mathbf{y}, \boldsymbol{\theta}) \quad (5-2)$$

Equation (5-2) can be approximated using finite difference. For a reference point k and using forward difference, the approximation is given as

$$C(\mathbf{y}_k, \boldsymbol{\theta}) = \frac{J_{k+1} - J_k}{u_{k+1} - u_k} \quad (5-3)$$

Using backward difference, we have

$$C(\mathbf{y}_k, \boldsymbol{\theta}) = \frac{J_k - J_{k-1}}{u_k - u_{k-1}} \quad (5-4)$$

For central difference, the approximation is written as

$$C(\mathbf{y}_k, \boldsymbol{\theta}) = \frac{J_{k+1} - J_{k-1}}{2(u_{k+1} - u_{k-1})} \quad (5-5)$$

The above formulations are for one degree of freedom (DOF). For DOF other than one, Equations (5-3) - (5-5) are respectively written as

$$J_{k+1} - J_k = C^T(\mathbf{y}_k, \boldsymbol{\theta})(\mathbf{u}_{k+1} - \mathbf{u}_k) \quad (5-6)$$

$$J_k - J_{k-1} = C^T(\mathbf{y}_k, \boldsymbol{\theta})(\mathbf{u}_k - \mathbf{u}_{k-1}) \quad (5-7)$$

and

$$J_{k+1} - J_{k-1} = 2C^T(\mathbf{y}_k, \boldsymbol{\theta})(\mathbf{u}_{k+1} - \mathbf{u}_{k-1}) \quad (5-8)$$

Various types of model such as polynomials, neural network model and so on can be used to approximate the target CV function, C depending on the complexity of the system.

The performance of the method is evaluated using average loss (Ye et al., 2013a) defined by

$$\bar{L} = \frac{1}{d^+ - d^-} \int_{d^-}^{d^+} L dd \quad (5-9)$$

for which the loss, L is given by

$$L = J(u_{fb}, d) - J_{opt}(d) \quad (5-10)$$

In Equation (5-10), u_{fb} is the feedback control law and J_{opt} the theoretically obtainable optimum value of the cost function.

The developed methodology will now be tested on a hypothetical problem, named toy example (Umar et al., 2012).

Toy Example

The objective function is

$$J = \frac{1}{2}(u - d)^2 \quad (5-11)$$

with two available measurements

$$\begin{cases} y_1 = u \\ y_2 = \frac{1}{4}u^2 + d \end{cases} \quad (5-12)$$

The disturbance, d is assumed to vary in the range $d \in [-1, 1]$. The manipulative variable, u is also bounded in this range. With this set up, optimum operation is achieved if the gradient

$$\frac{dJ}{du} = u - d \quad (5-13)$$

is maintained at zero.

Two sets of polynomials were used for regression purposes to approximate the target CV:

1. First-order polynomial

$$C_1(\mathbf{y}_0, \boldsymbol{\theta}) = \theta_1 y_{1,0} + \theta_2 y_{2,0} + \theta_3 \quad (5-14)$$

2. Second-order polynomial

$$C_2(\mathbf{y}_0, \boldsymbol{\theta}) = \theta_1 y_{1,0}^2 + \theta_2 y_{1,0} y_{2,0} + \theta_3 y_{1,0} + \theta_4 y_{2,0} + \theta_5 \quad (5-15)$$

where the subscript, 0 in Equations (5-14) and (5-15) indicates measurements taken at reference points. The following steps are followed to determine the CV parameters, $\boldsymbol{\theta}$ through linear regression:

1. A set of data is collected by sampling the whole space of manipulative variables and disturbances.
2. At each reference point, the gradient of the objective function with respect to manipulative variable, $\frac{dJ}{du}$ is computed using one of the finite

difference schemes presented in Equations (5-3) - (5-5), and the measurements, y_1 and y_2 .

3. Regressions were performed by minimizing the value of squared 2-norm of the residual with the parameters, θ being adjusted to fit in the computed gradient to either of the measurement functions in Equations (5-14) - (5-15); If we let the right-hand sides of Equations (5-3) - (5-5) to be q , the regression problem can be expressed as

$$\min_{\theta} \frac{1}{2} \|C(y_k, \theta) - q\|_2^2 \quad (5-16)$$

R-squared value is used to measure the performance of the regression. This is sometimes referred to as coefficient of determination which is an indicator for goodness of fit. It ranges from 0 to 1 with 1 indicating best regression fit (Ye et al., 2013a). If N samples of x_i , $i = 1, 2, \dots, N$ is approximated, then,

$$R^2 = \frac{S_T - S_E}{S_T} \quad (5-17)$$

where

$$S_T = \sum_{i=1}^N (x_i - \bar{x}_i)^2 \quad (5-18)$$

is total sum of squares and

$$S_E = \sum_{i=1}^N (x_i - \hat{x}_i)^2 \quad (5-19)$$

is error sum of squares. In the above equations, \hat{x}_i are the approximated x_i and \bar{x}_i the mean of x_i for which $i = 1, 2, \dots, N$.

The CV implementation can simply be visualised in Figure 5-1. Measurements obtained from the process are used to evaluate the CV, $C(y, \theta)$ while a feedback controller with a simple integral action is used to update the feedback control, u_{fb} for every disturbance, d so that the CV is kept at a setpoint, C_s .

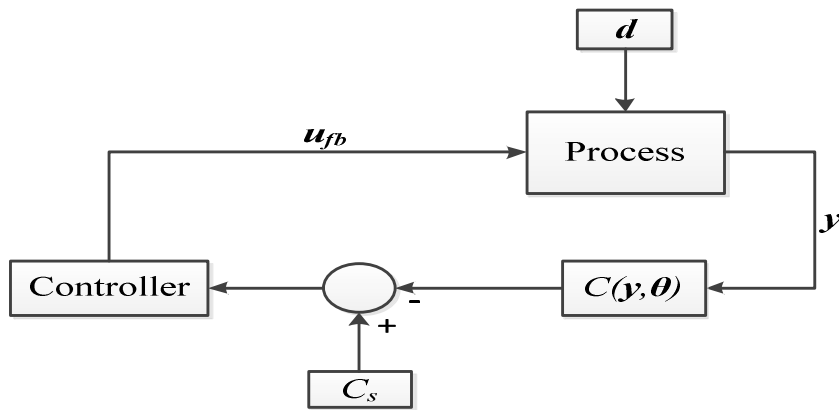


Figure 5-1: Simple CV Implementation

Different configurations with respect to number of sampling points, neighbourhood points and finite difference schemes are tested next.

Configuration I: Forward and Backward Finite Difference with Multiple Neighbourhood Points

Here, u and d are divided into 11 equal points in the range $[-1, 1]$. Each point of u was taken as a reference point and the interval between each successive point was divided into 10. These subdivisions were used as neighbourhood points. For each reference point, d was varied over its entire range. Precisely, the edge reference points have 10 neighbours while the 9 inner points each have 20 neighbourhood points (considering backward and forward neighbours) as illustrated in Figure 5-2.

So in summary, the following were considered

- 11 reference points in the range $[-1, 1]$
- 10 neighbourhood points each for boundary references and 20 for inner references
- 11 disturbance points in the range $[-1, 1]$
- Number of data points, N_p is given by the expression

$$N_p = [bn + 2n(N - b)]n_d \quad (5-20)$$

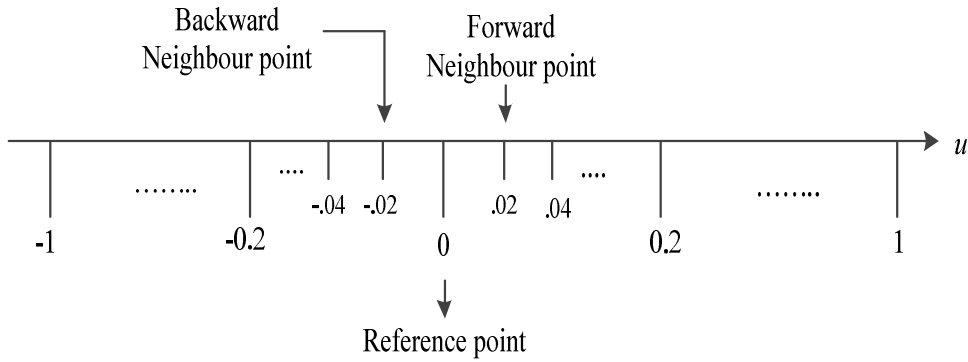


Figure 5-2: Reference and Neighbourhood Points for Configuration 1

- Where N is number of reference points, n is number of neighbour points, b is number of boundaries and n_d the number of disturbance divisions. So, for this case, $b = 2$, $n = 10$, $N = 11$ and $n_d = 11$. Therefore, using Equation (5-20), $N_p = 2200$

This novel method was compared to NCO approximation (Ye et al., 2012) and local methods. CVs found using NCO approximation method are denoted by C_{1NCO} and C_{2NCO} for first and second order polynomials respectively, while that resulted from using local method is as C_{local} .

The two CVs obtained using the developed data-driven methods are

$$C_1 = 0.9838y_1 - 0.9850y_2 + 0.0837 \quad (5-21)$$

and

$$C_2 = 0.2500y_1^2 - 0.0037y_1y_2 + 0.9844y_1 - y_2 + 0.0000 \quad (5-22)$$

with R^2 -values of 0.9867 and 0.9949 respectively. Comparing this to NCO approximation method, CVs obtained are for first-order model

$$C_{1NCO} = y_1 - 0.9809y_2 + 0.0981 \quad (5-23)$$

and second-order model

$$C_{2NCO} = 0.2500y_1^2 - 2.976x10^{-17}y_1y_2 + y_1 - y_2 \quad (5-24)$$

with R²-values of 0.9903 and 1.0000 respectively.

Applying local SOC method to the toy problem, the following CV was obtained

$$C_{local} = y_1 - y_2 \quad (5-25)$$

If the bilinear term in Equation (5-24) is ignored, C_{2NCO} is the true gradient and hence its loss is 0. Knowing that at optimal operation point, the obtained CV functions must all equal to zero and therefore, by substituting the measurements y_1 and y_2 according to Equation (5-12) in the CV functions (Equations (5-21) - (5-25)), equivalent feedback control laws can be obtained as summarized in Table 5-1.

Table 5-1: Comparison between Data-Driven SOC and other Methods

CV	Control Law Equivalent to	Average Loss
C_1	$1.9976 - 2.0305\sqrt{1.0503 - 0.9702d}$	0.0054
C_2	1.0159d	4.2135×10^{-5}
C_{1NCO}	$2.03894 - 2.03894\sqrt{1.0962 - 0.9621d}$	0.0038
C_{2NCO}	d	0
C_{local}	$2.0 - 2.0\sqrt{1 - 0.25d}$	0.0935

It can be observed from Table 5-1 that the proposed method provides self-optimizing CV with a better performance than local SOC without the much needed effort to determine the gradient equation as with NCO approximation.

Having seen the superb performance of the proposed method, it is worth investigating ways in improving it further. To this regards, effects of numbers of

reference points, N and neighbourhood points, n on the method's efficacy is studied next.

Configuration 2: Forward and Backward Finite Difference with Single Neighbourhood Point

In this configuration, combination of forward and backward finite differences is used as in Configuration 1. Here, N is increased from 11 (Configuration 1) to 21 while n is reduced from 10 to 1. The following are the parameters used:

- 21 reference points in the range $[-1, 1]$
- One neighbourhood point each for boundary references and two for inner references
- 11 disturbance points in the range $[-1, 1]$
- Therefore, using Equation (5-20), number of data points, N_p for this configuration is 440. The arrangement of references and neighbours for this configuration is shown in Figure 5-3.

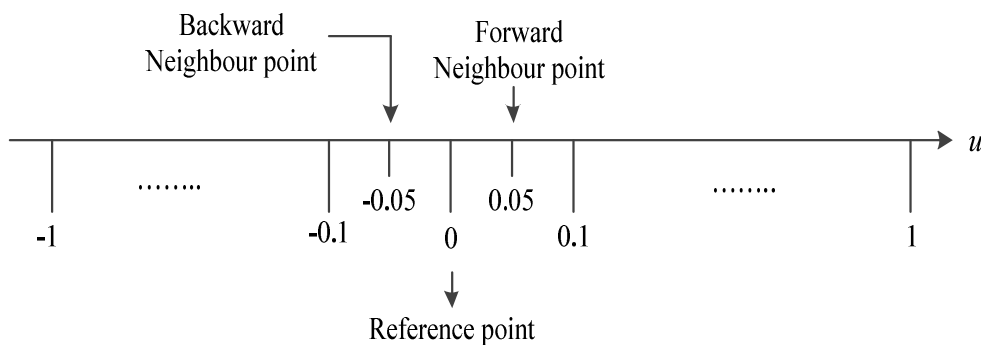


Figure 5-3: Reference and Neighbourhood Points for Configuration 2

Table 5-2 summarises the findings for the proposed method.

Table 5-2: Data-Driven SOC – Configuration 2

		First-Order Polynomial	Second-Order Polynomial
Coefficients	θ_1	0.9963	0.2500
	θ_2	-0.9860	-0.0009
	θ_3	0.0826	0.9964
	θ_4	-	-1.0000
	θ_5	-	0.0000
	Control Law	$2.0209 - 2.0284\sqrt{1.0741 - 0.9722d}$	$1.0036d$
	Average Loss	0.0046	2.1600×10^{-6}
	R²	0.9915	0.9992

Comparing this configuration with only 440 data points and Configuration 1 where N_p is 2200, it can be concluded that increasing the number of reference points helps in improving the performance of the methods. However, using multiple neighbours does not have effect on the performance. This is because, the CV function is only evaluated at reference points, and more neighbourhood points do not contribute further information to the CV function evaluation. A simple finite difference can provide similar but more consistent results than multiple neighbourhood points. For this reason, we have considered all data points as reference points in Configuration 3.

Configuration 3: Forward and Backward Finite Difference with Reference Points used as Neighbours

In this set up, all available sampling points are used as reference points with one neighbour point each for boundary references and two for inner references. There was no subdivision in the references to obtain neighbours, but the reference points were actually used as the neighbourhoods. For this case, we have

- 101 reference points in the range $[-1, 1]$
- One neighbourhood point each for boundary references and two for inner references
- 11 disturbances
- N_p is therefore 2200 as computed from Equation (5-20). This shown in Figure 5-4:

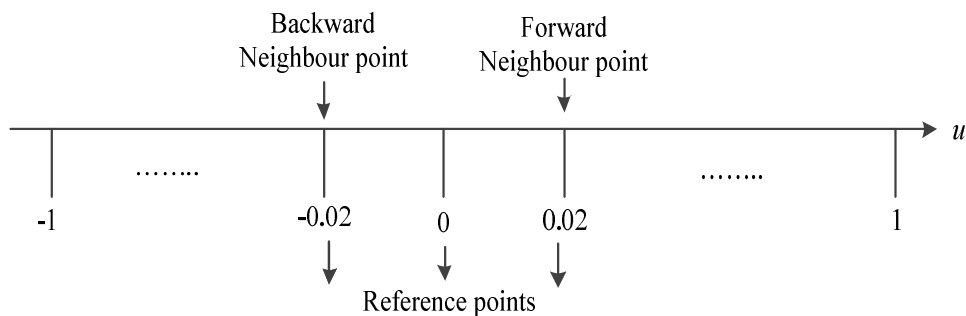


Figure 5-4: Reference and Neighbourhood Points for Configuration 3

Results obtained for this configuration are shown in Table 5-3. Comparing this case with configuration 1 of equal data points (2200), a tremendous improvement was made with reduction in loss for the second-order model of up to 99.96%.

In all the above configurations, a combination of forward and backward differences is used (Equations (5-3) and (5-4)). In the next configuration, the method was tested for central difference only, Equation (5-5).

Table 5-3: Data-Driven SOC – Configuration 3

		First-Order Polynomial	Second-Order Polynomial
Coefficients	θ_1	0.9997	0.2500
	θ_2	-0.9863	-0.0001
	θ_3	0.0822	0.9997
	θ_4	-	-1.0000
	θ_5	-	0.0000
	Control Law	$2.0272 - 2.0278\sqrt{1.0805 - 0.9728d}$	$1.0013d$
	Average Loss	0.0044	1.5000×10^{-8}
	R²	0.9924	0.9999

Configuration 4: Central Finite Difference with Reference Points used as Neighbours

Here central difference scheme is employed with the aim to improve the performance over a mix of forward and backward differences. For central difference, Equation (5-20) is modified as

$$N_p = (N - b)n_d \tag{5-26}$$

The following were used

- Six sampling points in the range [-1, 1]
- 11 disturbance points in the range [-1, 1]
- Using Equation (5-26), $N_p = 44$

Obtained results are shown in Table 5-4.

Table 5-4: Data-Driven SOC – Configuration 4

		First-Order Polynomial	Second-Order Polynomial
Coefficients	θ_1	0.5000	0.2500
	θ_2	-0.4980	0.0000
	θ_3	0.0249	0.5000
	θ_4	-	-0.5000
	θ_5	-	0.0000
	Control Law	$2.0080 - 4.0543\sqrt{0.2701 - 0.2433d}$	d
	Average Loss	0.0077	0
	R²	0.9973	1.0000

It is interesting to note from Table 5-4 that using only six sampling points, a zero loss for second-order polynomial was recorded. This justifies the importance for selecting a right model structure.

In some practical situations, there are instances that the disturbance is totally unknown. In the next configuration we will test the robustness of the method by ranking the variables according to the effect of disturbance. In Configuration 6, the disturbance was assumed to be unknown.

Configuration 5: Variables Ranking using Separable Rule

Disturbance information was used to ensure the finite difference is calculated between data points at the same disturbance. In this configuration, ranking is used to sort variables based on the effect of disturbance on J . Here, J'_k s are ranked according to their magnitude when disturbance is changed. All measurements were also ranked according to the order of J . For this configuration, the following were employed:

- 201 sampling points in the range [-1, 1]
- 11 disturbance points in the range [-1, 1]
- Using Equation (5-26), $N_p = 2189$

The following regression parameters and losses were obtained (Table 5-5)

Table 5-5: Data-Driven SOC – Configuration 5

		First-Order Polynomial	Second-Order Polynomial
Coefficients	θ_1	0.5000	0.1215
	θ_2	-0.4797	0.0000
	θ_3	0.0396	0.5000
	θ_4	-	-0.862
	θ_5	-	0.0000
	Control Law	$2.0846 - 4.1693\sqrt{0.2690 - 0.2301d}$	$5000 - 10000\sqrt{0.2500 - 0.0009724d}$
	Average Loss	0.0032	1.2696×10^{-4}
	R²	0.9780	0.9850

The results in Table 5-5 indicate that even if the disturbance is totally unknown, we can still achieve acceptable loss if we have large sufficient data. The question is, can we improve the ranking method so as to obtain an excellent performance similar to Configuration 4 performance? This is answered in the next configuration where random disturbance is used but following a particular rule for sorting

Configuration 6: Variables Ranking with Monotonicity Rule

To improve the performance of the ranking method, an appropriate variable needs to be selected for sorting. The selection is done by following a certain rule. The rule actually used is monotonicity of the measurements and objective functions to disturbance. For the toy example, the cost function is square to disturbance while measurement y_1 is independent of the disturbance. In the case of y_2 , all its values are well distributed; hence it is used as the sorting variable. The method is further validated by using randomised disturbance between -1 and 1. Central difference scheme was used.

- Six sampling points in the range [-1, 1]
- 11 random disturbance points in the range [-1, 1]
- N_p is therefore 44 using Equation (5-26) .

The results for this case are summarised in Table 5-6 which proved the concept of using monotonicity as a rule to selecting sorting variable; with only 6 sampling points, a zero loss was achieved even with random disturbance points. However, the monotonicity rule has some setbacks; in practice, we may not know which of the variables is monotonous to disturbance. Furthermore, two or more variables can be monotonous. Hence, it is recommended to find out a numerically realizable algorithm for choosing a sorting variable.

Table 5-6: Data-Driven SOC – Configuration 6

		First-Order Polynomial	Second-Order Polynomial
Coefficients	θ_1	0.5000	0.2500
	θ_2	-0.4935	0.0000
	θ_3	0.0244	0.5000
	θ_4	-	-0.5000
	θ_5	-	0.0000
	Control Law	$2.0276 - 4.0527\sqrt{0.2623 - 0.2435d}$	d
	Average Loss	0.0066	0.0000
	R²	0.9964	1.0000

Configuration 7: Separable Rule for Random Disturbance

This setup uses separable rule as in Configuration 5 but here random disturbances were generated using

- 201 sampling points in the range [-1, 1]
- 11 disturbance points in the range [-1, 1]
- N_p is therefore 2189 by using Equation (5-26)

Refer to Table 5-7 for the results summary.

Table 5-7: Data-Driven SOC – Configuration 7

		First-Order Polynomial	Second-Order Polynomial
Coefficients	θ_1	0.4991	0.1220
	θ_2	-0.4805	0.0003
	θ_3	0.0396	0.4994
	θ_4	-	-0.4886
	θ_5	-	0.0000
	Control Law	$2.0774 - 4.1623\sqrt{0.2681 - 0.2309d}$	$1664.6667 - 3333.3333\sqrt{0.2494 - 0.0002932d}$
	Average Loss	0.0033	7.7893×10^{-5}
	R²	0.9820	0.9901

The results shown in Table 5-7 indicate that the separable variable approach does work but not as perfect as configuration 6. This is because the ranking has some inherent error when the disturbance value is within some certain range.

5.2.1.2 Constrained Static Optimization

Most processes are constrained in one way or the other (Walter, 2014). However, the methodology presented in Section 5.2.1.1 does not consider constraints directly but are satisfied during data collection. This might be time consuming for large scale problems. Here, the method is extended to solve constrained optimization problems where the constraint equations are considered explicitly in the formulation. For this method, the compressed reduced gradient does not need to be determined analytically but evaluated using simulated or operational data through finite difference scheme.

The optimization problem is of the form

$$\begin{aligned} & \min_{\mathbf{u}} J(\mathbf{u}, \mathbf{d}) & (5-27) \\ \text{s. t. } & \mathbf{g}(\mathbf{u}, \mathbf{d}) = 0 \end{aligned}$$

Compressed reduced gradient given in Equation (2-37) which is repeated here as (Ye et al., 2013a)

$$\nabla_{cr} J = \frac{\partial J}{\partial \mathbf{u}} \mathbf{V}_2 = 0, \quad \nabla_{cr} J \in \mathbb{R}^{n_u - n_a} \quad (5-28)$$

is approximated using finite difference scheme where $\nabla_{cr} J$ is the compressed reduced gradient, \mathbf{V}_2 are $n_u - n_a$ right singular vectors, and n_u and n_a are the dimensions of \mathbf{u} and the constraints, \mathbf{g} respectively. The regression CV function is therefore given by

$$C(\mathbf{y}_k, \boldsymbol{\theta}) = \nabla_{cr} J|_k \quad (5-29)$$

In which case $\boldsymbol{\theta}$ is to be determined through regression. The following steps are followed to carry out the optimization process:

1. A set of data is collected by sampling the whole space of manipulative variables and disturbance
2. At each reference point, n_u gradients of the objective function against n_u manipulative variables, $\frac{\partial J}{\partial \mathbf{u}}$ and $n_a \times n_u$ Jacobian matrix of n_a constraints against n_u manipulative variables, $\frac{\partial \mathbf{g}}{\partial \mathbf{u}}$ are calculated
3. Singular value decomposition approach is used to calculate $n_u - n_a$ $\nabla_{cr} J$ at each reference point.
4. Regression is used to fit $n_u - n_a$ controlled variables to approximate the $n_u - n_a$ $\nabla_{cr} J$ for all reference points by minimizing the value of squared 2-norm of the residual as given by Equation (5-16).

The above methodology was tested on a revised form of the toy problem studied in Section 5.2.1.1.

Modified Toy Problem

The toy example is modified to include an equality constraint and two manipulative variables. The objective function is

$$J = u_1^2 + 2u_2^2 + 4u_1u_2d - 2u_1 - 16u_2 \quad (5-30)$$

The constraint is given as

$$g = u_1 - u_2 - d \quad (5-31)$$

It was assumed that there are four available measurements

$$\begin{cases} y_1 = u_1 \\ y_2 = u_2 \\ y_3 = 2u_1 - d \\ y_4 = u_2 - 5d \end{cases} \quad (5-32)$$

The disturbance d varies in the range $[-0.25, 0.25]$ while u_1 in the range $[-1, 1]$ and u_2 in $[-2, 2]$ range.

Before formulating SOC solution to this problem, the analytical solution is first derived which will be useful for comparison with other solution techniques.

Analytical Solution to Modified Toy problem

To derive the necessary condition of optimality for this problem analytically, the following steps are taken:

- The Jacobian of the constraint is computed which is given as

$$\frac{\partial g}{\partial \mathbf{u}} = [1 \quad -1] \quad (5-33)$$

- Using singular value decomposition to obtain \mathbf{V}_2 as

$$\mathbf{V}_2 = \begin{bmatrix} 0.7071 \\ 0.7071 \end{bmatrix} \quad (5-34)$$

- The Jacobian of the objective function with respect to control is computed

$$\frac{\partial J}{\partial \mathbf{u}} = [2u_1 + 4u_2d - 2 \quad 4u_2 + 4u_1d - 16] \quad (5-35)$$

- Using Equation (5-28), the NCO is computed as

$$\nabla_{cr}J = 0.7071(2u_1 + 4u_2 + 4(u_1 + u_2)d - 18) \quad (5-36)$$

SOC Solution to Modified Toy problem

Here, both first- and second-order polynomials are used to fit the reduced gradient. For the first-order polynomial, we have for four measurements

$$C_{LR} = \theta_1 y_{1k} + \theta_2 y_{2k} + \theta_3 y_{3k} + \theta_4 y_{4k} + \theta_5 \quad (5-37)$$

and for the second-order

$$\begin{aligned} C_{PR} = & \theta_1 y_{1k}^2 + \theta_2 y_{2k}^2 + \theta_3 y_{3k}^2 + \theta_4 y_{4k}^2 + \theta_5 y_{1k} y_{2k} \\ & + \theta_6 y_{1k} y_{3k} + \theta_7 y_{1k} y_{4k} + \theta_8 y_{2k} y_{3k} + \theta_9 y_{2k} y_{4k} + \theta_{10} y_{3k} y_{4k} \\ & + \theta_{11} y_{1k} + \theta_{12} y_{2k} + \theta_{13} y_{3k} + \theta_{14} y_{4k} + \theta_{15} \end{aligned} \quad (5-38)$$

After conducting the regression, performances of different CVs were evaluated numerically using the steady-state loss function defined by Ye et al. (2013a) as

$$L = J(u_{fb}, d) - J_{opt}(d) \quad (5-39)$$

where the $J(u_{fb}, d)$ is the value of the objective function which would be obtained when the feedback control law is implemented to maintain the CV at zero while $J_{opt}(d)$ is the actual optimal, J . A Monte Carlo simulation is then carried out using 1000 randomly generated disturbances that vary within its range of values.

In order to ascertain the robustness of the proposed method, a comparison was made with NCO approximation techniques reported by Ye et al. (2013a). To use NCO method, the analytical equation of the compressed reduced gradient given in Equation (5-36) is employed.

If u_1 , u_2 and d are divided into N , n and m parts respectively, the number of data points for central difference scheme is given by

$$N_p = [(N - 2)(n - 2)]m \quad (5-40)$$

For this illustrative example, central difference scheme was employed with $N = 41$, $n = 41$ and $m = 11$. Therefore, $N_p = 16731$. Table 5-8 gives the regression parameters and losses for both data-driven SOC and NCO approximation.

The R^2 -values obtained for first-and second-order polynomials are respectively 0.9714 and 1.0000. This indicates that no higher polynomial or more rigorous model is needed to fit the compressed reduced gradient. By using the central difference scheme in approximating the Jacobians of the objective and constraint functions, the losses associated with data-driven SOC is zero for second-order polynomial. This indicates that even though, we don't have the gradient information of the process, we can use measurements alone to optimize the process.

It is recommended that the method is applied to a large scale problem and its efficiency compared to that of Section 5.2.1.1.

Although, the objectives defined in Equations (5-11) and (5-30) are functions of only the manipulative variables and disturbance, the methodologies are also applicable when the objective is a function of states, provided it (objective) can be computed.

Table 5-8: Constrained Data-Driven SOC and NCO Approximation Methods

		Data-Driven SOC		NCO Approx.	
		C_{LR}	C_{PR}	C_{LR}	C_{PR}
Coefficients	θ_1	0	0	0	0
	θ_2	0.3111	0.3111	2.9698	0.6222
	θ_3	0.3536	0	0.7071	0
	θ_4	-0.0707	0.0283	-0.1414	0.0566
	θ_5	-6.3640	0	-12.7278	0
	θ_6	-	0	-	0
	θ_7	-	0	-	0
	θ_8	-	0.1414	-	0.2828
	θ_9	-	-0.3394	-	-0.6788
	θ_{10}	-	-0.1414	-	-0.2828
	θ_{11}	-	0	-	0
	θ_{12}	-	1.4849	-	2.9698
	θ_{13}	-	0.3536	-	0.7071
	θ_{14}	-	-0.0707	-	-0.1414
	θ_{15}	-	-6.3640	-	-12.7278
Losses	Minimum	1.4490x10-6	0	5.8247x10-8	0
	Average	1.10831	0	1.0648	0
	Maximum	4.3743	0	4.3393	0
	Std. Dev.	1.0734	0	1.0383	0
	R²	0.9714	1.0000	0.9714	1.0000

5.2.2 Dynamic Optimization for Reservoir Waterflooding

The optimization problem defined in Equation (2-17) is solved here using data-driven SOC without considering inequality constraint. Equations (2-12) - (2-15) are modified for easier referencing. In reservoir waterflooding, the objective function to be maximized can be written in the following form for a total number of time steps N

$$J = \sum_{k=1}^N J^k(\mathbf{u}^k, \mathbf{y}^k, \mathbf{d}^k) \quad (5-41)$$

The contribution to J in each time step is given by J^k , where \mathbf{u}^k , \mathbf{y}^k , and \mathbf{d}^k are controls, measurements and disturbances respectively at time steps k . The reservoir models can be written in a discretized form as

$$\mathbf{g}(\mathbf{u}^k, \mathbf{x}^{k+1}, \mathbf{x}^k, \boldsymbol{\varphi}) = \mathbf{0} \quad (5-42)$$

where \mathbf{x}^k is the reservoir states vector and $\boldsymbol{\varphi}$ vector of model parameters. A change in \mathbf{u}^k , at time k will not only affect J^k directly but will affect the states \mathbf{x}^{k+1} according to Equation (5-42). The states will in turn influence the outputs, \mathbf{y}^{k+1} , through the measurement equations as

$$\mathbf{h}(\mathbf{u}^k, \mathbf{x}^k, \mathbf{y}^k) = \mathbf{0} \quad (5-43)$$

As with all other SOC procedures, optimization of reservoir waterflooding using the principles of SOC consists of two main steps; viz; offline determination of CV and then the online implementation. The offline procedures are as follow:

1. A control sequence is defined given by

$$\mathbf{u}_i^1, \mathbf{u}_i^2, \dots \dots \dots \mathbf{u}_i^N,$$

the reservoir model Equation (5-42) is solved to obtain a solution sequence

$$\mathbf{x}_i^0, \mathbf{x}_i^1, \mathbf{x}_i^2 \dots \dots \dots \mathbf{x}_i^N,$$

a measurement sequence

$$\mathbf{y}_i^0, \mathbf{y}_i^1, \mathbf{y}_i^2 \dots \dots \dots \mathbf{y}_i^N,$$

and a cost J_i

2. A perturbation is applied to the control sequence where we have

$$\mathbf{u}_{i+1}^1, \mathbf{u}_{i+1}^2, \dots, \mathbf{u}_{i+1}^N,$$

the reservoir model Equation (5-42) is then solved again to get perturbed solutions

$$\mathbf{x}_{i+1}^0, \mathbf{x}_{i+1}^1, \mathbf{x}_{i+1}^2, \dots, \mathbf{x}_{i+1}^N,$$

measurements

$$\mathbf{y}_{i+1}^0, \mathbf{y}_{i+1}^1, \mathbf{y}_{i+1}^2, \dots, \mathbf{y}_{i+1}^N,$$

and cost J_{i+1} .

3. Taylor series expansion is used to approximate the gradient of the objective function with respect to the control.

If n_u is the dimension of the control, \mathbf{u} , the gradient of the objective function with respect to \mathbf{u} at each time step considering a reference trajectory, i with a neighbourhood $i + 1$ is given by Taylor series expansion as

$$J_{i+1} - J_i = \sum_{j=1}^{n_u} \sum_{k=n+1}^N G_{i,j}^k (u_{i+1,j}^k - u_{i,j}^k) \quad (5-44)$$

where $G_{i,j}^k$ is a gradient of the objective function with respect to an input channel, i at time-step, k and n number of past histories. The aim of dynamic SOC is at all time-steps to maintain the gradient at zero. Therefore, the gradient in Equation (5-44) which is time-dependent can be replaced by a measurement function that can be used as a target CV whose value will remain constant at all time-steps irrespective of the magnitudes of the individual measurements, this is shown in Equation (5-45) as

$$J_{i+1} - J_i = \sum_{j=1}^{n_u} \sum_{k=n+1}^N C(\boldsymbol{\theta}_j, \mathbf{y}_i^k, \mathbf{y}_i^{k-1}, \dots, \mathbf{y}_i^{k-n}, u_{i,j}^k) (u_{i+1,j}^k - u_{i,j}^k) \quad (5-45)$$

where $\boldsymbol{\theta}_j$ is a parameter vector to be determined through regression.

The above procedure can be visualized clearly in Figure 5-5.

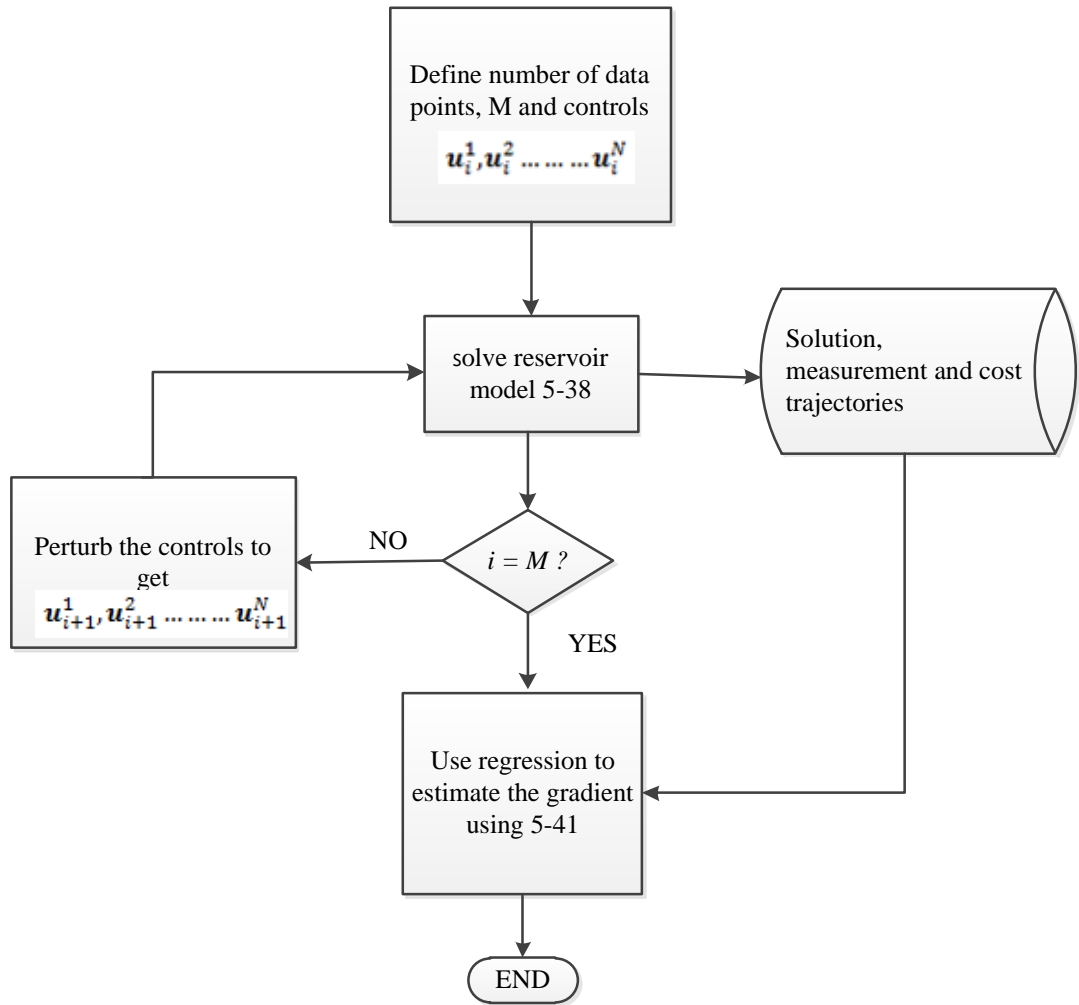


Figure 5-5: Offline Determination of CV using Dynamic SOC

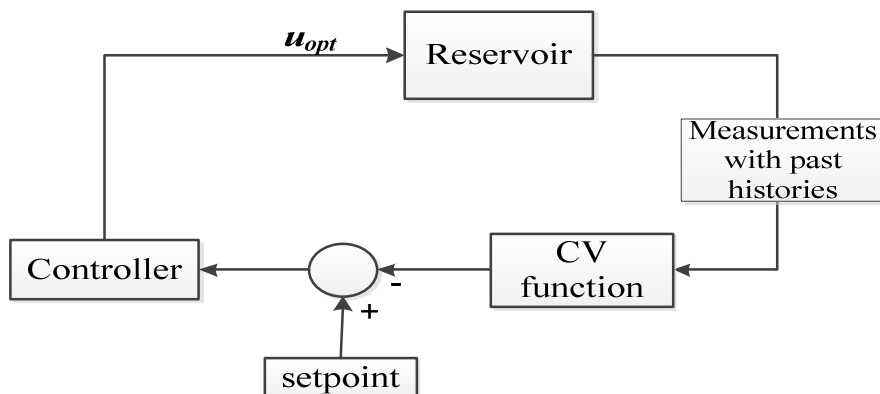


Figure 5-6: Online Implementation of Feedback Control Law

The obtained CV is implemented to the reservoir by maintaining it (CV) at zero or from which the feedback control law is derived as shown in Figure 5-6. The actual implementation of the CV starts after n time-steps where the needed past histories have been obtained.

The proposed method was tested on two categories of reservoir size. The first is the simplified reservoir size studied in Section 4.3 for easier testing of the method's efficacy. This was followed by a case of realistic reservoir size adapted from the work of Foss and Jensen (2011).

5.2.2.1 Case Study I: Simplified Reservoir Size

The reservoir sizes used in Section 4.3 for RHC approach with all uncertainty scenarios are used here to test the robustness of the developed data-driven SOC methodology in counteracting system/model mismatches and to have a basis for comparison with the former reported in the section.

Data Collection and Regression

Data used for regression to determine CV parameters, θ_j in Equation (5-45) were collected from simulations of the prediction model used in Section 4.3 which is referred to as a nominal model in this chapter. To recap its properties, the reservoir has a size of 20 m x 20 m x 5 m which was modelled using Cartesian gridding system. Each grid has a dimension of 1 m. One each of vertical injection and production wells are placed at the two opposite corners of the reservoir. These wells are perforated at each layer. Both wells are rate-constrained.

The manipulative variables (MVs) are injection and total production rates. Since voidage replacement assumption was made, that is, the total injection must equal to the total production at all time-steps, the system can therefore be regarded to have only one MV (that is, one degree of freedom, DOF). Two measurements were taken which are oil production rate, y_o and water

production rate, y_w in addition to MV, u_w , that is, water injection rate. The measurement vector can therefore be represented as

$$\mathbf{y} = [y_o \ y_w \ u_w]^T \quad (5-46)$$

The objective function used is NPV of the venture given in Equation (3-5) with all economic parameters as used in Section 3.3. With this measurement set, a linear time-series model was chosen for the CV function which is of the form

$$C = \theta_1 y_{i,o}^k + \theta_2 y_{i,w}^k + \theta_3 y_{i,o}^{k-1} + \theta_4 y_{i,w}^{k-1} + \dots + \theta_{2(n+1)} y_{i,w}^{k-n} + \theta_{2(n+1)+1} u_w^k \quad (5-47)$$

Two past histories were used ($n = 2$). The total number of coefficients to be determined is therefore $2(n + 1) + 1 = 7$.

Regressions are performed by minimizing the square of the residual given by

$$\min_{\theta} \sum_{i=1}^N ((J_{i+1} - J_i) - q)^2 \quad (5-48)$$

where q represents the right-hand side of Equation (5-45).

A feedback control law can be obtained from Equation (5-47) by setting it to zero (NCO) which can be written as ($n = 2$)

$$u_{w,fb}^k = -\theta_7^{-1} [\theta_1 y_o^k + \theta_2 y_w^k + \theta_3 y_o^{k-1} + \theta_4 y_w^{k-1} + \theta_5 y_o^{k-2} + \theta_6 y_w^{k-2}] \quad (5-49)$$

Using the nominal model, 500 solution trajectories were obtained for data collection. At each trajectory, the reservoir flooding process was simulated for a period of two years with fine time step size of one day to capture all the reservoir dynamics reasonably well. Actual optimal injection rates were used for this purpose which were slightly perturbed at each time step. So, with this set up, a 500x730 data matrix was obtained which was used to obtain the CV via regression.

CV Implementation

The obtained CV was first implemented to the nominal case and then to the other three cases with various degrees of uncertainty which include uncertainty in permeability, permeability and porosity, and geometry, size and structure. Benchmark (BM) results were also obtained from the uncertain reservoirs by solving the optimal control problem directly on the models using OC (assuming the reservoir properties are known a priori).

Losses recorded by applications of SOC and OC strategies on the uncertain reservoir models are computed by an equation similar to Equation (4-3) written as

$$Loss = \frac{J_{BM} - J_{SOC/OC}}{J_{BM}} \times 100\% \quad (5-50)$$

Similarly, increased NPV obtained by application of SOC in comparison to OC on the uncertain models is calculated as gain using

$$Gain = \frac{J_{SOC} - J_{OC}}{J_{SOC}} \times 100\% \quad (5-51)$$

Results and Discussions

The feedback control law obtained is

$$u_{w,fb}^k = -(-1.2203 \times 10^{10})^{-1} [0.0000y_o^k + 0.2245y_w^k + 1.2211y_o^{k-1} + 0.0000y_w^{k-1} + 0.0008y_o^{k-2} + 0.9968y_w^{k-2}] \times 10^{10} \quad (5-52)$$

The R-squared value is 0.9912, so no higher or more sophisticated model is required. Results for various cases of uncertainty are reported next.

Case I: Nominal Parameters

The results obtained for this case are shown in Figure 5-7 and Figure 5-8. After a period of 2 years of production the NPV obtained using OC is \$182,775 while that generated using SOC is \$182,298 which represents a loss of only 0.26% (Figure 5-7). The value of the gradient fluctuates between -9.54×10^{-7} and 9.54×10^{-7} which indicates a good performance. It can be observed from Figure 5-8 that relatively high water injection rates which average at $0.8 \text{ m}^3/\text{day}$ in the case of OC was applied right from beginning of production. This enables higher production rates from the inception. In the case of SOC, the water injection rates steadily increases from a fixed value of $0.67 \text{ m}^3/\text{day}$ to a peak value of $0.78 \text{ m}^3/\text{day}$ and then slightly drops to around $0.75 \text{ m}^3/\text{day}$ to maintain the reservoir pressure as oil is being depleted. Total productions are summarised in Table 5-9. The increased oil production in the case of OC is largely due to high water injection at the beginning of production which is associated with higher water production in comparison to SOC as well as early water break-through (difference of about 30 days).

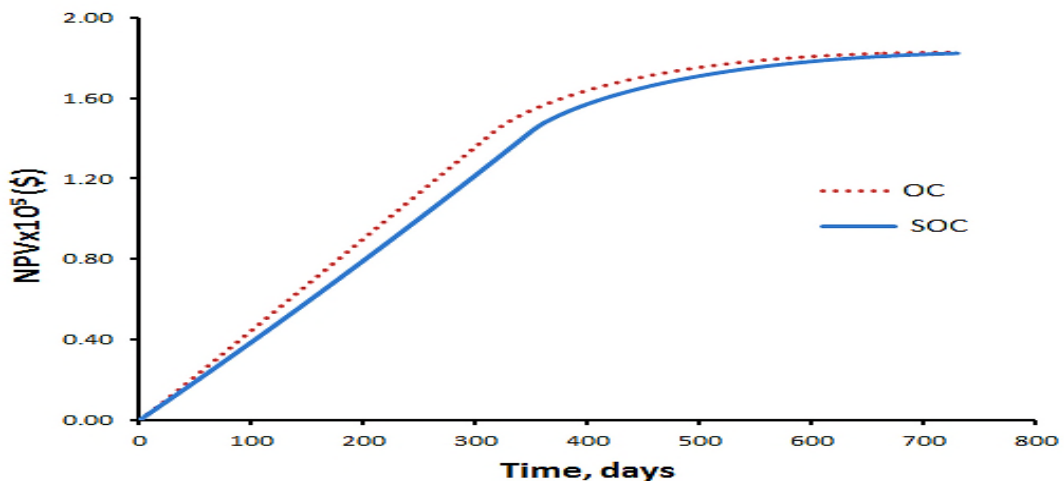


Figure 5-7: NPVs for Case I

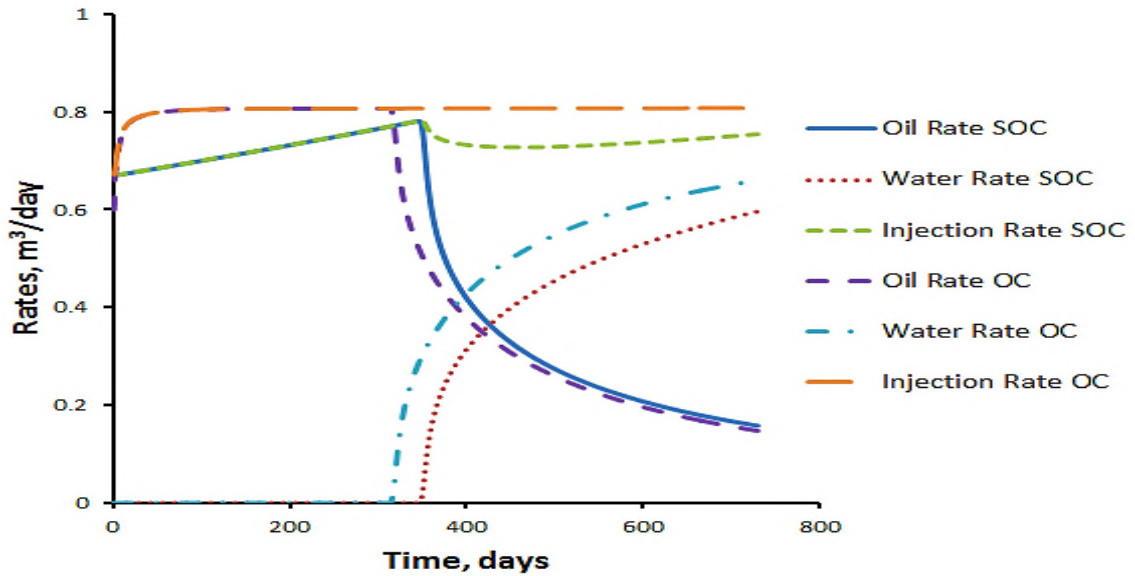


Figure 5-8: Injection and Production Rates for Case I

Table 5-9: SOC and OC Comparison for Case I

Strategy	Total Oil (m ³)	Total Water (m ³)	Time of Water Break-Through (days)	NPV (\$)
SOC	360.34	173.19	350	182,298
OC	370.69	215.91	317	182,775

Case II: Uncertainty in Permeability

To test the robustness of the feedback strategy using SOC against uncertainty in permeability, the obtained feedback control law (5-52) was implemented to the layered reservoir. The open-loop optimal solution obtained by OC in case I was also used to simulate this uncertain reservoir. Furthermore, a BM was established directly from this realization by solving the optimization problem using OC assuming a perfect knowledge of the reservoir properties. This will give the highest possible NPV since the model is assumed to be perfect. Here, SOC out performed OC with a gain of 0.21% when uncertainty is considered.

With reference to the BM, the loss by SOC and OC are 0.19% and 0.39% respectively (Figure 5-9). It can be seen from the figure that NPV generated by SOC slightly surpassed those generated by OC.

It can also be observed from Figure 5-10 that higher water injection rates were found by BM at the early stage of production than SOC and OC approaches, but this dropped quickly and became indistinguishable with OC; which helped to cut significant amount of produced water with only a slight decrease in oil production (Table 5-10), hence a better NPV. However, optimal injection settings determined by SOC strategy were at the intermediate level throughout the production period, a situation that results to a relatively higher oil production with water break-through time much earlier than OC. This can also be confirmed from Figure 5-11.

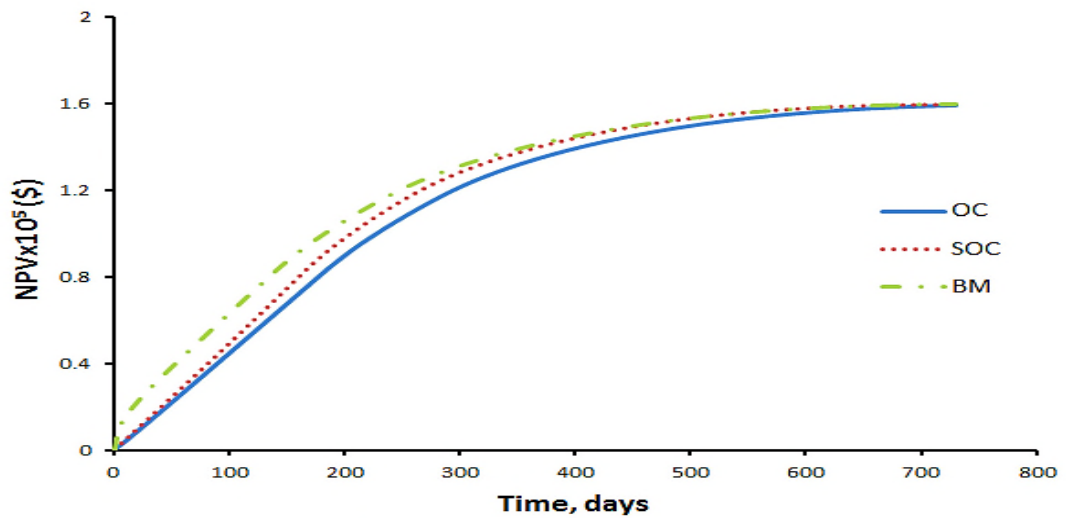


Figure 5-9: NPVs for Case II

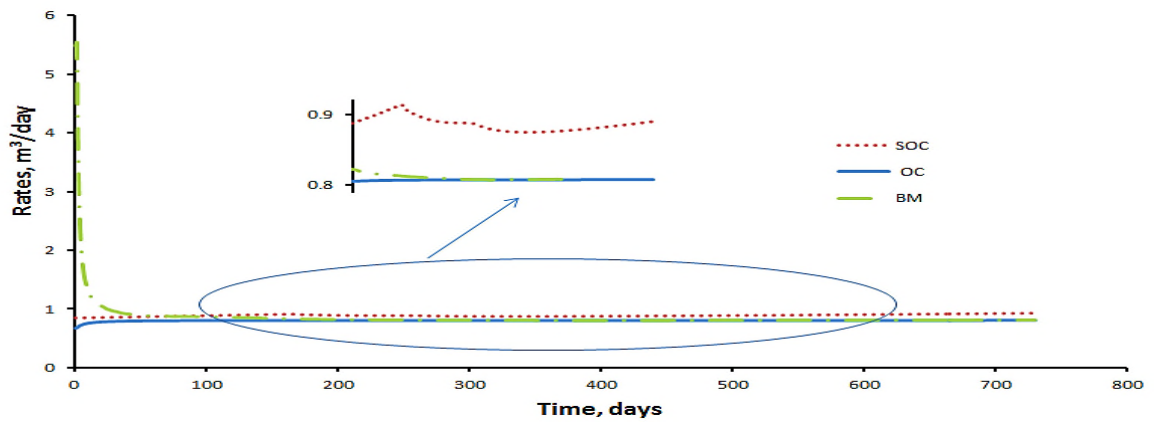


Figure 5-10: Water Injection Rates – Case II

Table 5-10: SOC and OC Comparison for Case II

Strategy	Total Oil (m ³)	Total Water (m ³)	Time of Water Break-Through (days)	NPV (\$)
SOC	348.51	301.67	166	159,427
OC	336.47	250.17	184	159,096
BM	344.28	280.33	142	159,724

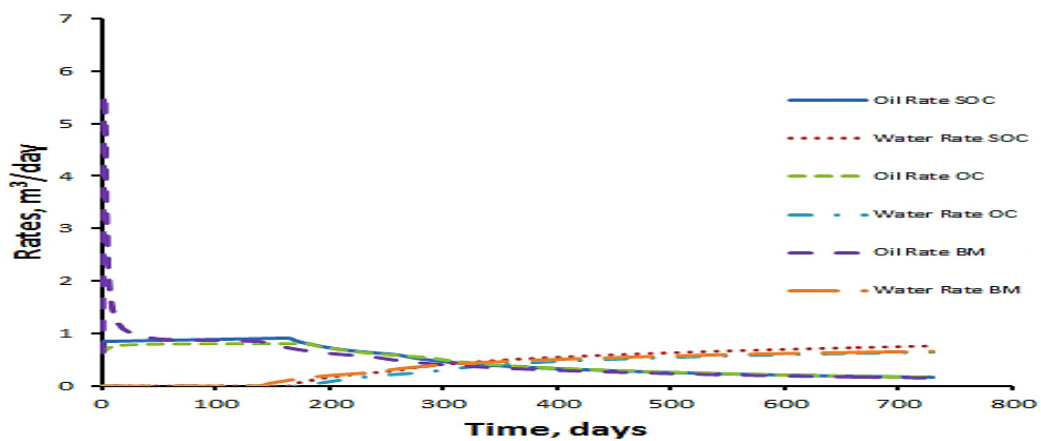


Figure 5-11: Production Rates - Case II

Case III: Uncertainty in Porosity and Permeability

Similarly, the CV and optimal solutions obtained in Case I were implemented to Case III where both permeability and porosity differed from the nominal case. This is to test the capability of the SOC method in handling unexpected reservoir behaviours that might have not been captured during data acquisition. A BM solution was also obtained. For this system/model mismatch, a higher gain in NPV of 3.16% was recorded in favour of SOC. The loss based on BM for SOC is 4.66% and 7.67% in the case of OC. The NPVs are shown in Figure 5-12.

It can also be observed from Figure 5-13 that SOC has sustained a fairly high water injection which led to an increased oil production (although with increase in water production) that gave rise to a high NPV in comparison to OC (Table 5-11). The injection settings resulted to a long oil production plateau period as shown in Figure 5-14 which confirmed the higher volume of oil produced. As a result of the rapid oil production achieved by SOC and BM approaches, early water-break through was experienced although this did not affect the NPV greatly.

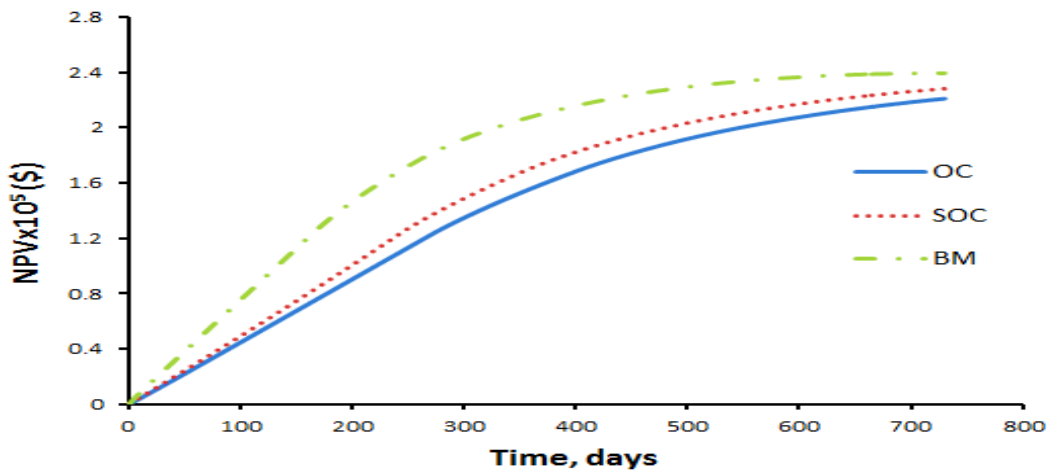


Figure 5-12: NPVs for Different Strategies - Case III

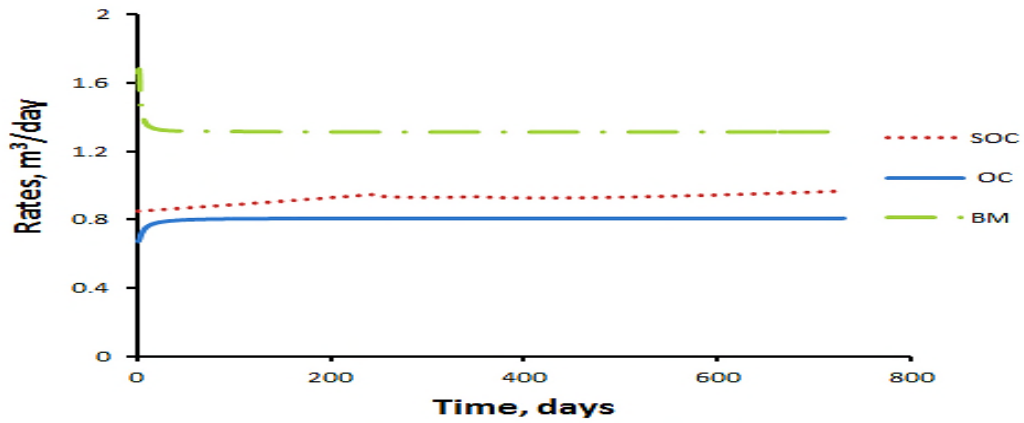


Figure 5-13: Water Injection Rates – Case III

Table 5-11: SOC and OC Comparison for Case III

Strategy	Total Oil (m ³)	Total Water (m ³)	Time of Water Break-Through (days)	NPV (\$)
SOC	452.08	222.32	244	228,116
OC	425.71	160.93	274	220,918
BM	520.0528	439.30	142	239,272

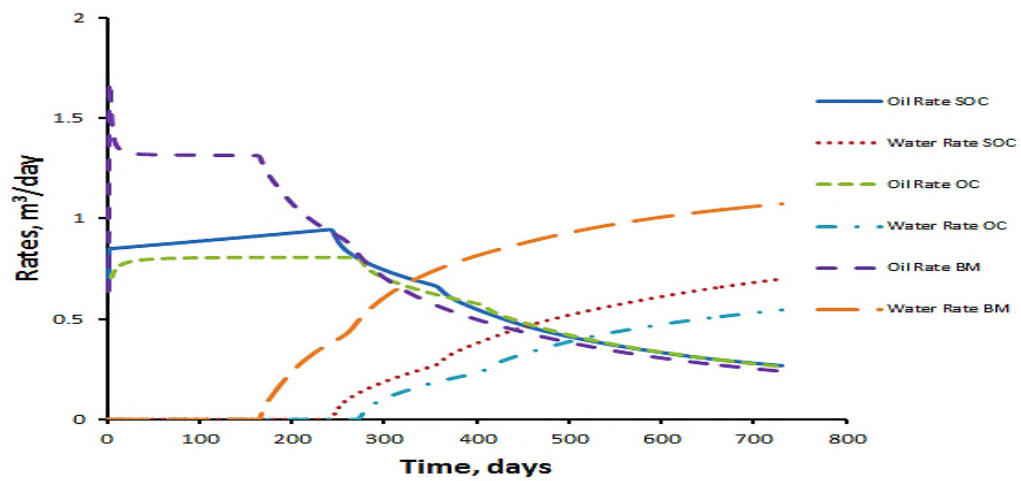


Figure 5-14: Production Rates - Case III

Case IV: Uncertainty in Reservoir Size, Geometry and Structure

After implementing the CV to Case IV and simulating it with the nominal optimal solutions, NPVs obtained are shown in Figure 5-15. Because of the very large model/system mismatch introduced in this case, a very good performance by SOC can be observed. The nominal solution turned to be completely non optimal in this case. An extremely high gain of up to 30.04% was recorded in favour of SOC. Based on the BM scenario the losses are 2.09% and 31.51% for SOC and OC respectively.

Sensing the system/model mismatches through measurements only, SOC can be seen in Figure 5-16 to adjust the injection settings so as to annul the effect. Reasonable oil production has been achieved as summarised in Table 5-12 which results to an NPV comparable to that obtained by BM. The failure of OC approach in this case can be clearly visualised from oil rate profile in Figure 5-17. If not because of the assumption of voidage replacement imposed, the reservoir may even fail to be flooded at all by OC injection settings. A very long plateau period can also be seen to be associated with SOC strategy in the figure.

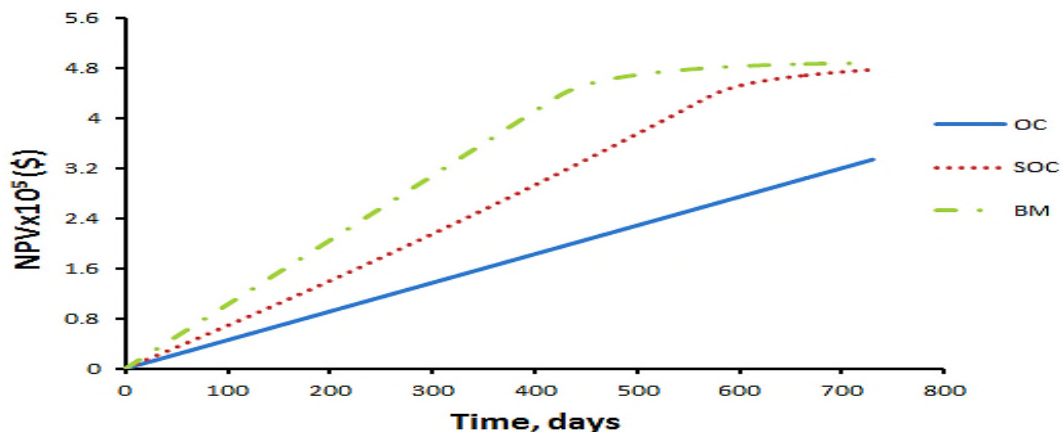


Figure 5-15: NPVs for Different Strategies- Case IV

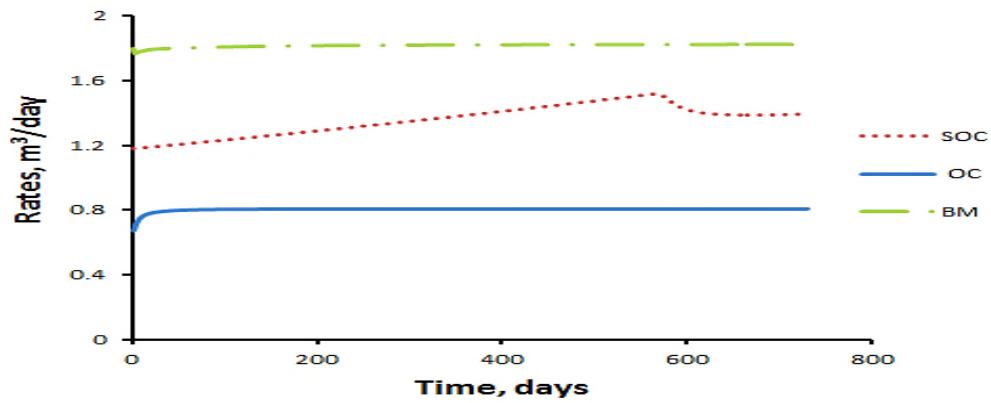


Figure 5-16: Water Injection Rates - Case IV

Table 5-12: SOC and OC Comparison for Case IV

Strategy	Total Oil (m ³)	Total Water (m ³)	Time of Water Break-Through (days)	NPV (\$)
SOC	868.29	121.35	565	477,310
OC	587.73	0.00	-	333,905
BM	944.12	381.11	418	487,520

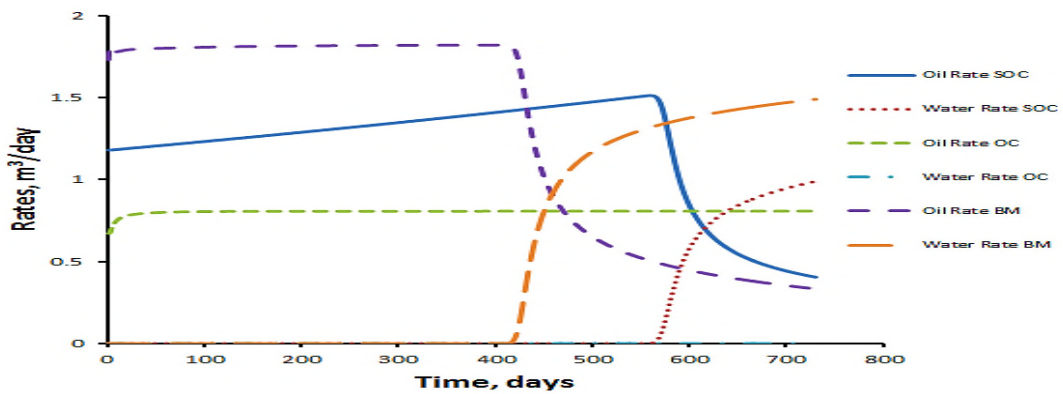


Figure 5-17: Production Rates - Case IV

The losses and gains for these cases are summarised in Table 5-13. It is clear that the relative benefits of the feedback strategy increases with increase in the intensity of uncertainty. A comparison between this method (SOC) and RHC is given in Section 5.4 for these uncertain cases.

Table 5-13: Losses and Gains for Various Cases of Uncertainty (Simple Reservoir)

		NPV(\$)	% Gain	% Loss
Case I	OC	182,775.00	-	-
	SOC	182,297.70	-	-
Case II	BM	159,723.50	-	-
	OC	159,096.40	-	0.39
	SOC	159,428.90	0.21	0.19
Case III	BM	239,271.50	-	-
	OC	220,918.20	-	7.67
	SOC	228,116.4	3.16	4.66
Case IV	BM	487,520.10	-	-
	OC	333,904.70	-	31.51
	SOC	477,309.60	30.04	2.09

5.2.2.2 Case Study II: Realistic Reservoir Size

After successfully testing the developed method on a simplistic reservoir with a nominal size of 20 m x 20 m x 5m in Section 5.2.2.1, the implementation was extended here to a realistic reservoir segment of 2250 m x 225 m x 10 m (Foss and Jensen, 2011).

Reservoir Configurations and Uncertainties

The reservoir was simulated using MRST with 30 x 3 x 1 cells. Having size of 2250 m x 225 m x 10 m, each cell is therefore 75 m x 75 m x 10 m. Two wells are drilled vertically (injection and production wells) which are located at the two ends of the reservoir. The reservoir is a two-phase system of oil and water with homogenous rock and fluid properties. It is characterised with a permeability of 400 mD and a porosity of 0.3. Other properties used are as given in Table 3-1.

The above reservoir configuration was taken as the nominal model for this case study and used to design the feedback control law. Uncertainties considered are similar to those in Section 5.2.2.1 with exception to Case III, where in the present case uncertainty in fluid properties was considered instead, typically, the shape of oil-water relative permeability curves, phase relative permeability exponents (Dilib and Jackson, 2013a). The nominal value for this parameter for both oil and water is taken as 2.0.

Data Collection and Regression

Same procedure was followed for data collection and regression as in previous case study (Section 5.2.2.1) with production period fixed to two years. Here 200 solution trajectories were obtained using a time-step size of two days. Therefore, regression was performed using 200 x 365 data matrix to obtain the required CV. After the CV was designed, it was first implemented on the nominal case and then to the other three cases with different degrees of

uncertainty. These were compared to the open-loop control solutions, OC and to the BM where all the reservoir properties were assumed to be known a priori.

Results and Discussions

Feedback control law obtained from regression using the nominal model is

$$u_{w,fb}^k = -(-4.0243 \times 10^7)^{-1}[0.0000y_o^k + 1.7216 + 4.0256y_o^{k-1} + 0.0000y_w^{k-1} + 0.0017y_o^{k-2} + 2.3041y_w^{k-2}] \times 10^7 \quad (5-53)$$

with R²-value of 0.9856.

Case I: Nominal Case

The feedback control law in Equation (5-53) was implemented on the nominal model, the performance of which was compared to that of OC approach which is shown in Figure 5-18. It can be seen from the figure that the two NPV sets are indistinguishable which confirms the effectiveness of the SOC strategy. The loss incurred as a result of the feedback implementation is only 0.11%.

The CV was well maintained around zero, hence the reason for the good performance of the SOC approach. The injection settings found was almost similar to those of OC counterparts. As is shown in Figure 5-19, the SOC's injection rate was initially lagging behind OC's, although it was on the increase till it exceeded the OC strategy. In order to put the process on the optimal path, the injection rate was forced to decline and maintained at near constant. This injection pattern has led to production profiles that are similar to those obtained using the true optimal solutions (Figure 5-19). In summary, the performance of the two strategies is given in Table 5-14.

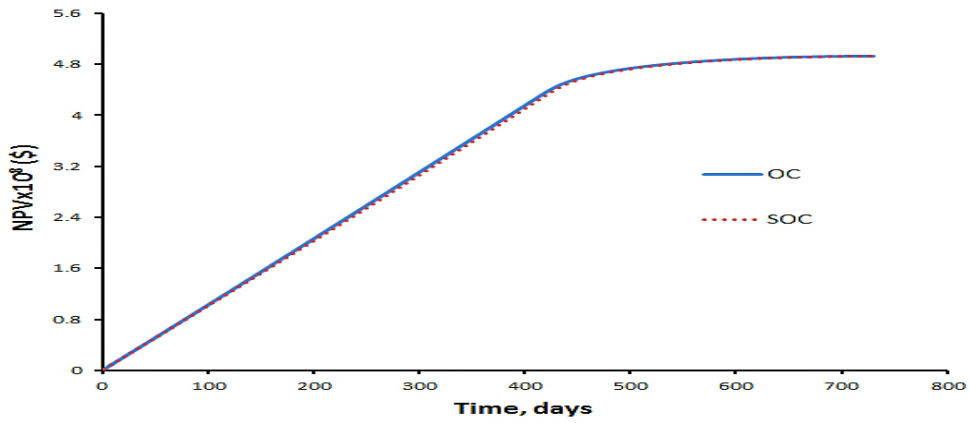


Figure 5-18: NPVs for Case I

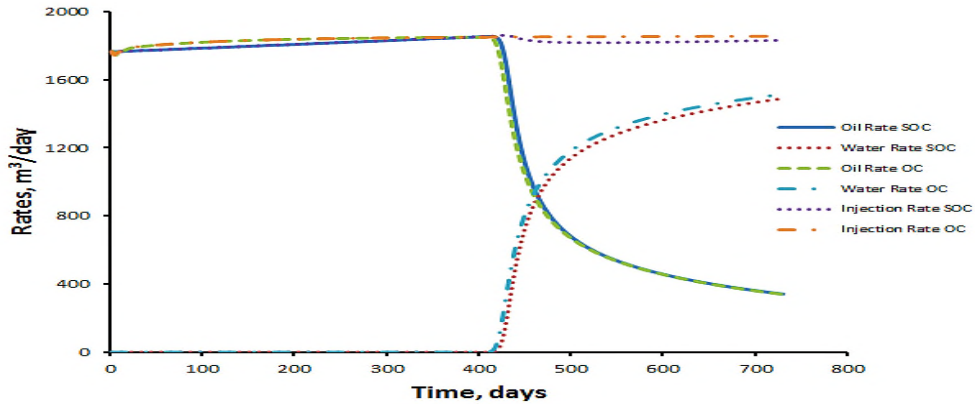


Figure 5-19: Rates Profiles for Case I

Table 5-14: OC and SOC Performance Comparison for Case I

Strategy	Total Oil (m ³)	Total Water (m ³)	Time of Water Break-Through (days)	NPV (\$)
SOC	951,305.40	372,821.70	408	492,636,353.90
OC	954,458.90	386,835.30	404	492,654,987.39

Case II: Uncertainty in Permeability

When uncertainty in permeability was introduced into the system, the benefit of feedback through SOC strategy in counteracting its (uncertainty) effect can be seen through Figure 5-20. Here, the gain is 1.03% compared to OC approach. The losses based on BM scenario are 0.028% and 1.061% for SOC and OC respectively.

This amazing performance by SOC is attributed to its injection settings whose profile is similar to that of BM approach. In particular, both injection profiles can be seen to average at 2200 m³/day; while in the case of OC, the average is about 1800 m³/day (Figure 5-21). The SOC injection rates have similar flooding effect to that of BM case which can be observed from the production profiles of oil and water in Figure 5-22. The injection rates of OC however, have produced lower amounts of oil and water with reduced NPV; the results of which are summarised in Table 5-15. Although, OC was seen to have a late water breakthrough compared to other two cases, this has not improved its relative performance in anyway.

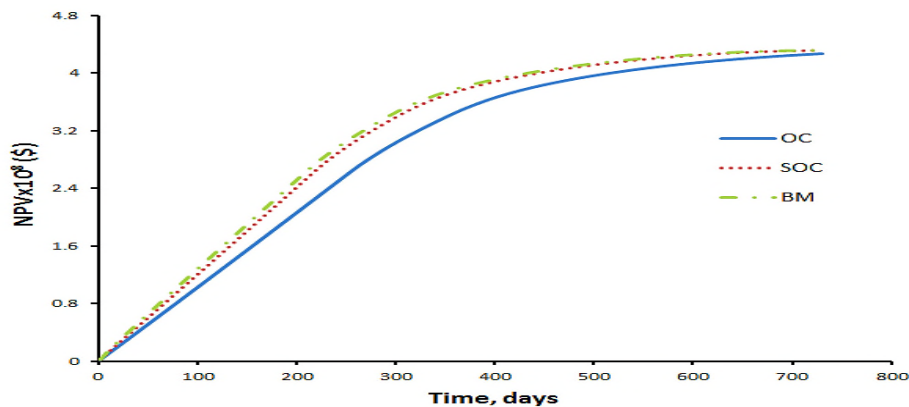


Figure 5-20: NPVs for Case II

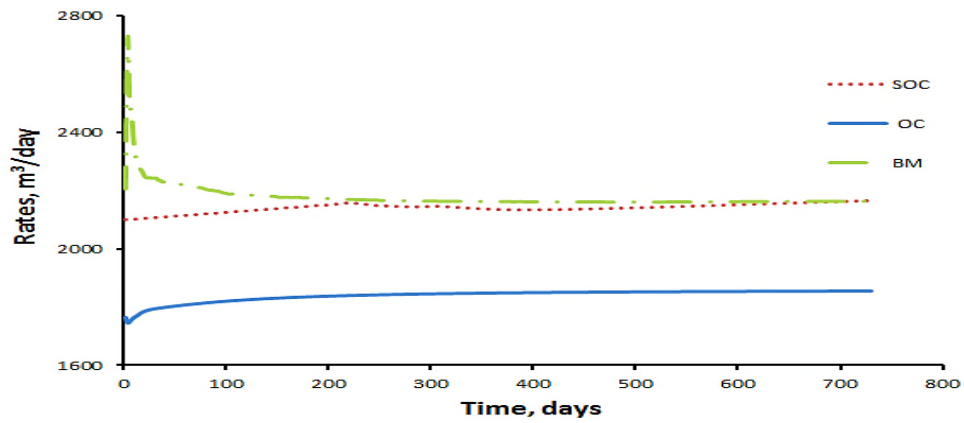


Figure 5-21: Injection Rates for Case II

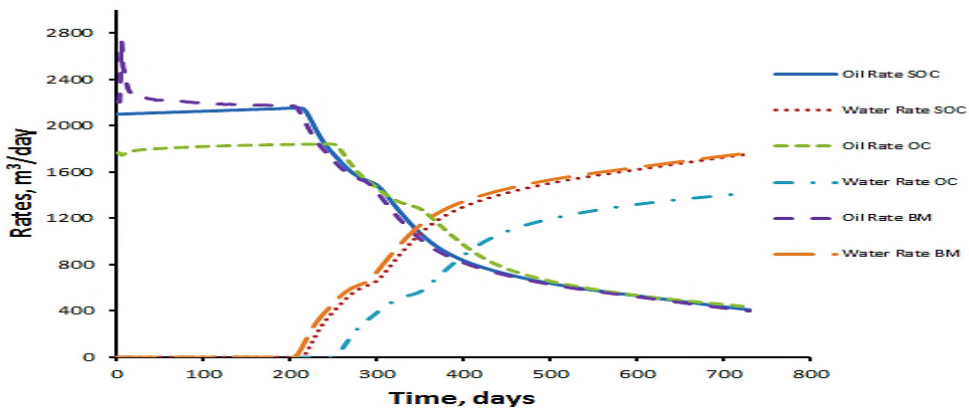


Figure 5-22: Production Profiles for Case II

Table 5-15: OC and SOC Performance Comparison for Case II

Strategy	Total Oil (m ³)	Total Water (m ³)	Time of Water Break-Through (days)	NPV (\$)
SOC	905,909.77	654,407.30	210	431,526,889.97
OC	859,567.48	481,726.65	246	427,065,786.20
BM	910,892.28	675,827.96	200	431,646,157.23

Case III: Uncertainty in Phase Relative Permeability Exponents

The nominal relative permeability exponent used is 2.0 as stated earlier. It was assumed that the actual value is 1.5. With this value, three cases of OC, SOC and BM were simulated and the NPVs generated are shown in Figure 5-23. SOC's NPV can be seen to be lagging behind that of BM from the beginning of production period which became almost equal toward the end. The losses recorded by SOC and OC approaches for this case of uncertainty are 0.39% and 1.66% respectively. A gain of 1.27% in NPV was obtained in favour of SOC.

Despite the fact that there is a wide separation between optimal injection rates found by SOC and BM, the trends are almost similar (Figure 5-24). Furthermore, with these injection settings favourable production profiles were obtained by SOC approach that led to a significant gain in comparison to OC. As can be seen from Figure 5-25, a broad oil production plateau with intermediate water production rates were realised through the former approach, a reason for a better NPV that is comparable to that obtained with an assumption of perfect reservoir knowledge. These results are highlighted in Table 5-16.

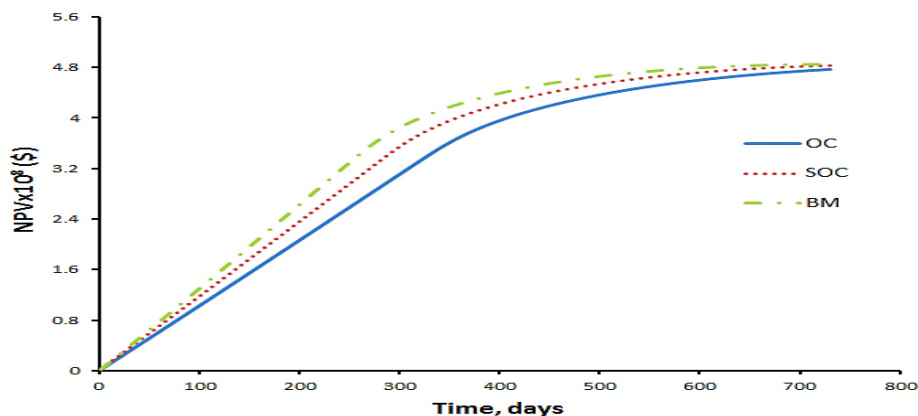


Figure 5-23: NPVs for Case III

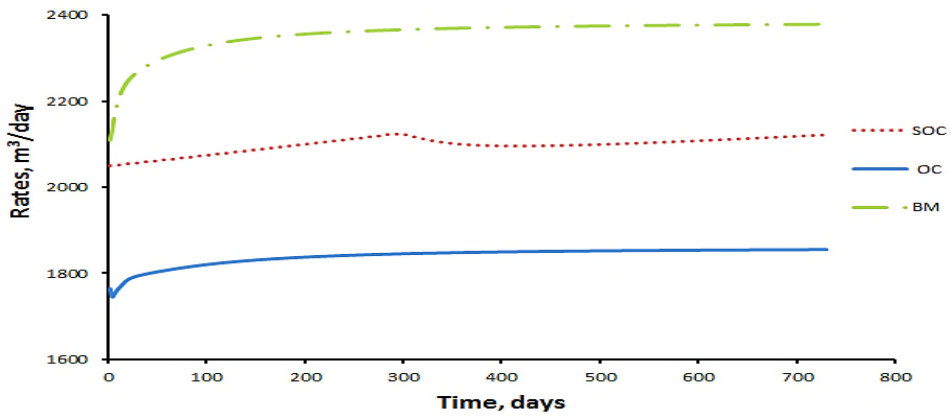


Figure 5-24: Injection Rates for Case III

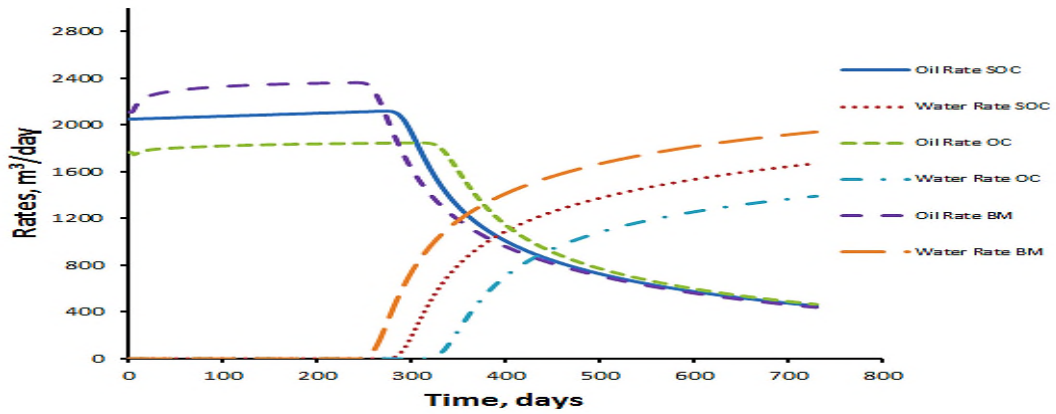


Figure 5-25: Production Rates for Case III

Table 5-16: OC and SOC Performance Comparison for Case III

Strategy	Total Oil (m ³)	Total Water (m ³)	Time of Water Break-Through (days)	NPV (\$)
SOC	974,580.53	554,721.52	266	483,011,497.29
OC	931,458.34	409,835.79	246	476,865,932.82
BM	1,011,441	705,059.45	242	484,924,572.10

Case IV: Uncertainty in Reservoir Size, Geometry and Structure

Here the truth reservoir size is 2250 m x 250 m x 2 m (smaller in size to the nominal model) but modelled with grid cells of 30 x 3 x 1 using corner point gridding system. The reservoir has a fault of 0.3 m. This structure with wells configurations is shown in Figure 4-25. Open-loop optimal control sequence was directly obtained from this reservoir which serves as the BM case. Similar comparisons performed in Cases II and III were also carried out here by applying the two approaches of SOC and OC (based on nominal model) on this truth reservoir. The NPVs obtained for the cases are given in Figure 5-26. It can be seen from the figure that OC approach is totally suboptimal for the fixed time frame of two years while SOC performance is almost similar to the BM case. Losses based on BM are 0.54% and 24.44% for SOC and OC respectively. The gain in implementing the feedback strategy is 24.03% as compared to OC. This demonstrates the robustness of the developed feedback strategy in counteracting uncertainty.

Despite the high degree of uncertainty considered in this case, the injection profile found through the application of SOC methodology mimics the BM scenario. The OC injection rates which are in the vicinity of 1800 m³/day are completely out of the optimal range for this reservoir system (Figure 5-27). This can easily be proven from oil and water production profiles shown in Figure 5-28. The OC injection setting is considered to be very high for this size of reservoir, a reason for accelerated oil production with a smaller plateau period and early water break-through characterised by very high flow rates. This results to the declining NPV shown in Figure 5-26. On the other hand, both oil and water production profiles found by SOC approach are similar to the BM scenario despite the presence of uncertainty. Table 5-17 gives a summary of the results obtained.

It is important to note that the drop in NPV generated by OC approach is due to the excessive production of water that outweighs the proceeds realisable from the produced oil. Such drop would however, not be allowed in reality as the production process will be terminated on time to prevent further financial loss.

The performance of these methods for all the cases of uncertainties considered are summarised in Table 5-18.

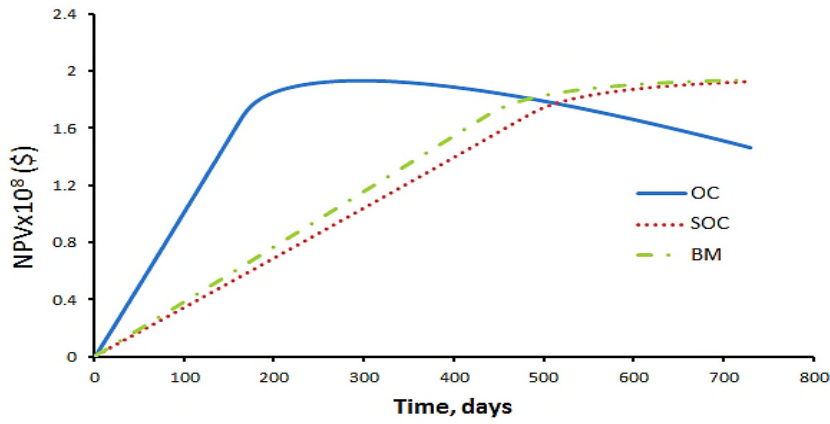


Figure 5-26: NPVs for Case IV

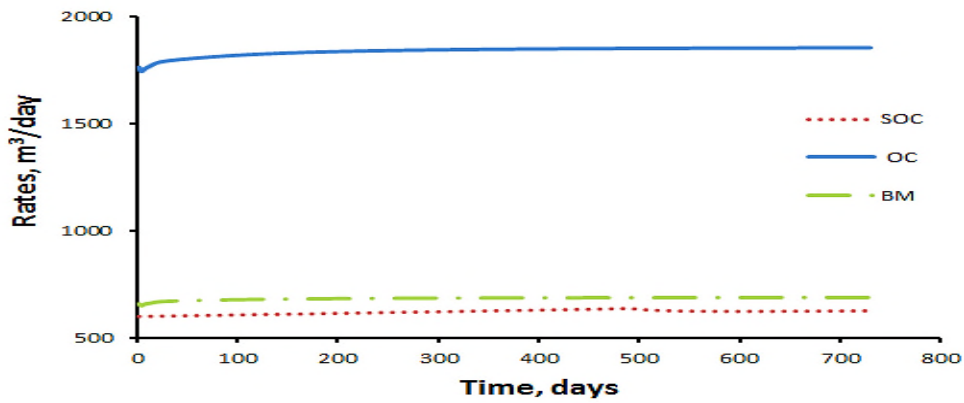


Figure 5-27: Injection Rates for Case IV

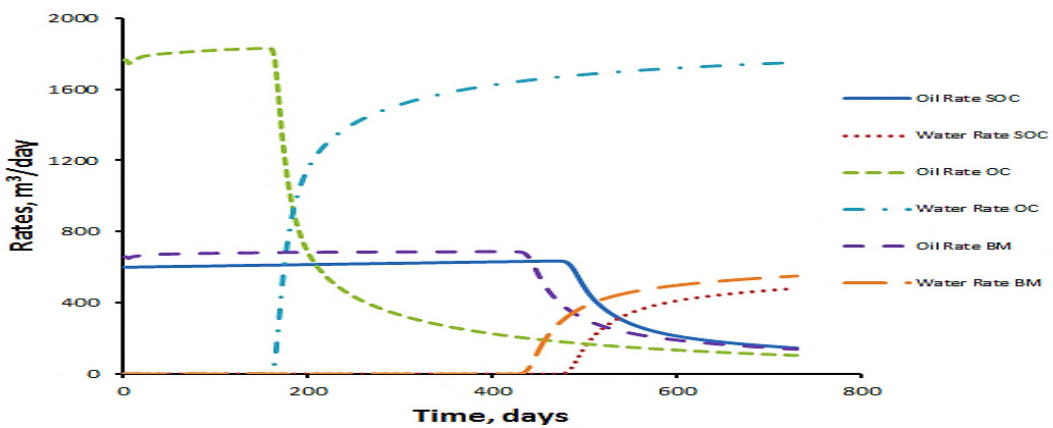


Figure 5-28: Production Rates for Case IV

Table 5-17: OC and SOC Performance Comparison for Case IV

Strategy	Total Oil (m³)	Total Water (m³)	Time of Water Break-Through (days)	NPV (\$)
SOC	360,140.80	92,219.57	237	192,693,715.20
OC	453,370.75	884,394.02	156	146,392,742.65
BM	370,103.01	128,620.17	422	193,742,723.85

Table 5-18: Losses and Gains for Various Cases of Uncertainty (Realistic Reservoir)

		NPV(\$)	% Gain	% Loss
Case I	OC	954,458.90	-	-
	SOC	951,305.40	-	-
Case II	BM	431,646,157.23	-	-
	OC	427,065,786.20	-	1.061
	SOC	431,526,889.97	1.03	0.028
Case III	BM	484,924,572.10	-	-
	OC	476,865,932.82	-	1.66
	SOC	483,011,497.29	1.27	0.39
Case IV	BM	193,742,723.85	-	-
	OC	146,392,742.65	-	24.44
	SOC	192,693,715.20	24.03	0.54

5.3 Sensitivity Analyses

The CVs formulated in the last two sections were found to be so robust and insensitive to the various uncertainties introduced. To gain an insight on the reason behind such a wonderful performance, sensitivity analyses were carried out on individual measurements (oil and water production rates) and on one of the CVs, which is actually a combination of these measurements.

To achieve the above goal, the nominal model used in Section 5.2.2.1 was simulated using the computed open-loop optimal solution under four different types of uncertainties similar to those considered earlier, which are summarised in Table 5-19.

Table 5-19: Uncertain Cases for Sensitivity Analyses

Cases	Property	Nominal Case	Uncertain Case
I	porosity	0.3	0.45
II	Permeability	Homogeneous, 100 mD	Log-normal distribution with five layers having mean values of 200, 500, 350, 700 and 250 mD from top to bottom
III	Porosity and permeability	0.3 and 100 mD	Combination of Cases I and II
IV	<ul style="list-style-type: none"> • Geometry • Size • Grid • Structure 	<ul style="list-style-type: none"> • Cartesian • 20 x 20 x 5 m³ • 20 x 20 x 5 • No fault 	<ul style="list-style-type: none"> • Corner point • 225x22.5x 1 m³ • 30 x 3 x 1 • Presence of fault with size of 0.12 m

For each of these uncertain cases, the CV from which Equation (5-52) was derived, was calculated and the corresponding measurements stored at each time step. It can be shown in Figure 5-29 that the CV was well maintained around zero for all the considered uncertainties. This has confirmed the robustness of the selected measurement combination to be used as CV. Measurements sensitivities are given in Figure 5-30 and Figure 5-31. It can be seen clearly that these individual measurements are highly perturbed when uncertain properties are introduced into the system.

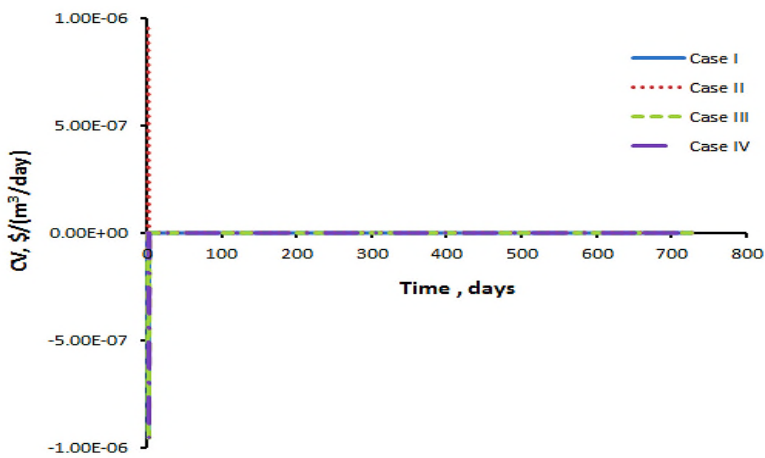


Figure 5-29: Sensitivity of CV to Uncertainties

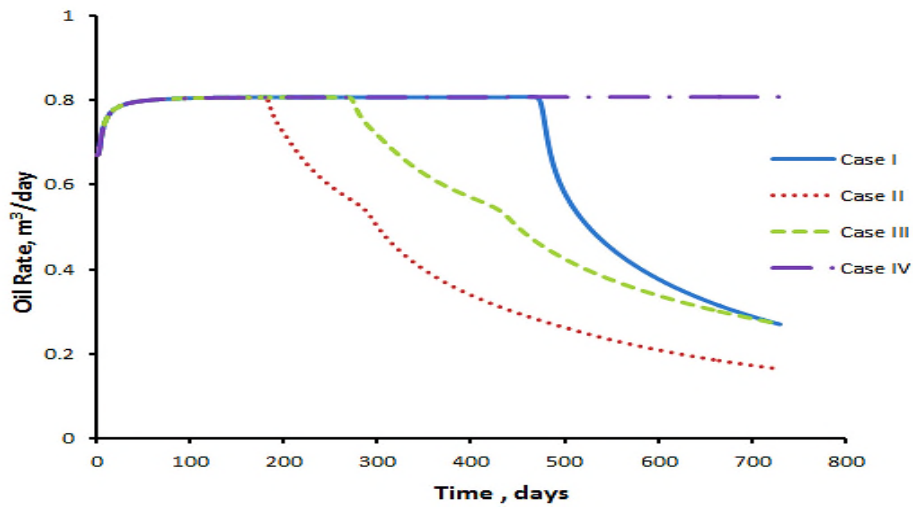


Figure 5-30: Sensitivity of Oil Production Rates to Uncertainties

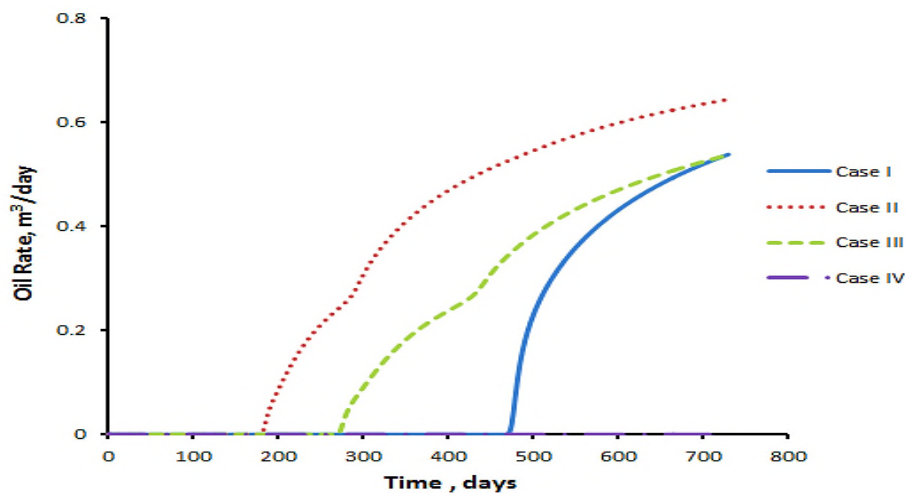


Figure 5-31: Sensitivity of Water Production Rates to Uncertainties

Now, looking at how transitions of measurements profiles occur with changing uncertain parameters, we can observe a very long oil plateau that spanned almost 500 days in Case I. However, changing the porosity to nominal value and introducing a mismatch in permeability in Case II, the plateau period was seen to drastically reduce to about 200 days. Similar explanation can be made to water production rates for these two cases where the break-through time changed sharply from 476 days to 186 days. Combining the uncertainties considered in Cases I and II, the oil plateau period has again shifted to about 300 days in Case III and water production was delayed to 277 days. Furthermore, the production profiles have taken entirely different shapes in Case IV. Here, because of the increase in reservoir size, the open-loop optimal injection trajectory has failed to sweep the expected amount of oil in the reservoir with zero water production and therefore, the oil profile has taken the shape of the injection trajectory.

Based on the above analyses and demonstrated case studies, the developed CV can be said to have satisfied the qualitative rules for CV selection as outlined by Skogestad (2000) most especially the rule that specified that “optimal value of CV should be insensitive to disturbances”, see Section 2.6.1.

5.4 Performance Comparison between SOC and RHC

Here a brief summary of the performance of the two feedback approaches developed in this work are given. The comparison is made based on the results obtained in Sections 4.3 for RHC strategy and 5.2.2.1 for SOC since same cases of uncertainty and reservoir systems were considered.

It can be seen from Table 5-20 that for the four cases, losses incurred by RHC approach are higher. In fact, an unacceptable loss of 15.21% resulted in Case IV as a result of implementing this feedback technique whereas the loss is only 2.09% for the same case by employing SOC approach. Based on these results, RHC can be said to be sensitive to model/system mismatch. The sensitivity of the formulated CV through SOC principle is however very minimal in comparison.

Table 5-20: Comparison between SOC and RHC Methods

Cases	NPV (\$)				Loss (%)	
	BM	SOC	RHC	OC	SOC	RHC
I	182,775.00	182,297.70	182,274.70	182,775.00	-	-
II	159,723.50	159,428.90	159,320	159,096.40	0.19	0.25
III	239,271.50	228,116.4	222,286.10	220,918.20	4.66	7.10
IV	487,520.10	477,309.60	413,365.02	333,904.70	2.09	15.21

5.5 Conclusions

In this chapter, a novel method of data-driven SOC was developed where the target CV is the gradient of the objective function with respect to control. The method does not require the gradient information (explicit expression of the gradient) but is computed based on data through finite difference scheme.

The concept was first developed for static optimization (both unconstrained and constrained cases) which was tested on a hypothetical case. A wonderful performance was seen with the method which is far better than local SOC. Some important points were observed in the cause of implementation of the method, some of which are

1. The more the number of reference points, the better the performance, although this has a detrimental effect on the computational time. On the other hand, the use of multiple neighbourhood points does not contribute to the superior performance of the method; this is because CV functions are only computed at reference points.
2. Using central difference scheme produced the best performance than forward and backward differences.
3. The methodology was also tested for situations where the disturbance is completely unknown. Here, variables ranking based on separable and monotonicity rules were employed to deal with the situation. Again, a tremendous performance was recorded with a loss as low as 0.00007789.
4. Application of the method to constrained scenario has also yielded excellent results with performance exactly as that of NCO approximation method which requires explicit expression of the NCO. A zero loss was achievable in this case.

The method was then extended to solve dynamic optimization problems with particular focus on waterflooding process. Implementation of the method was done on both simplistic and more realistic reservoir sizes. The feedback benefits of SOC in counteracting uncertainties in rock and fluid properties were

realised through various case studies. The following can be concluded from the study:

1. In the absence of system/model mismatch the OC approach was seen to have a better performance than SOC as expected. The difference is not significant however; the loss recorded by SOC was only 0.26% for the simplistic reservoir size and 0.11% for the real case.
2. With introduction of uncertainty of various forms and degree into the system which includes uncertainty in permeability, porosity, size, geometry, structure and shape of relative permeability curves, the developed feedback approach performed extremely well.
3. The relative performance of SOC method was observed to increase with the degree of uncertainty considered in the system. For instance, when uncertainty was considered in permeability only, gain achieved is in the range of 0.26% - 1.03%. Introducing more mismatches simultaneously in the form of reservoir size, geometry and structure, the gain was seen to shift up to 24.03% - 30.04%. Comparing this with the BM case where all properties were assumed to be known a priori, losses of only 0.54% - 2.09% were incurred by SOC as against 24.44% - 31.51% by OC.
4. In most of the cases studied, the shape of the injection trajectories found by SOC approach resemble those of the BM despite the presence of uncertainties, a situation that led to finding optimum oil and water production profiles, hence close to optimal NPVs.
5. Uncertainty is not considered in the formulation of the CVs due to complexity of oil reservoir, the robustness of the CVs is therefore entirely due to the feedback nature of the SOC strategy. With introduction of uncertainties in the CV formulation, the performance of the technique can be improved further.
6. In summary the designed CVs can be regarded as simple and robust, therefore are insensitive to uncertainties. This was also confirmed through sensitivity analyses on the CVs and individual measurements.

6 Optimal Multivariable Feedback Control for Reservoir Waterflooding

6.1 Introduction

In Chapter 5, SOC methodology for dynamic systems was developed and applied to waterflooding process. Impressive results were reported for various geological uncertainties considered. However, only systems with one manipulative variable (one degree of freedom) were considered. In the present chapter, the methodology was extended to optimize waterflooding process of higher degrees of freedom, because real oil and gas fields consist of several production and injection wells in operation and hence multivariate problems are encountered.

As was in Section 5.2.2, gradients of the objective function with respect to controls (CVs) were obtained based on a nominal model through regression. These CVs were then applied to reservoirs with different degrees of uncertainties in properties ranging from permeability, shape of relative permeability curves, and size, geometry and structure of reservoir.

The CVs were found to be robust in the presence of all the above uncertainties with performance similar to case where the reservoir properties were assumed to be known a priori. With the application of the CVs to the nominal model, only a negligible loss was incurred. Furthermore, implementation of the CVs to cases with model/system mismatch leads to a gain of up to 95% over an open-loop solution.

6.2 Data Collection and Regression

A nominal reservoir model similar to the one used in Section 5.2.2.1 was used to collect data but with slight difference in fluid properties as shown in Table 6-1. The reservoir size is 20 m x 20 m x 5 m which was modelled with Cartesian grid cells in the x, y and z directions of 20 x 20 x 5 respectively; therefore each cell is 1 m x 1 m x 1 m. There are two vertical injection (I1 and I2) and production

(P1 and P2) wells located at the corners of the reservoir (Figure 6-1). Each of the four wells is perforated at a distance of 1m vertically (five perforations for each) and is rate-constrained.

Table 6-1: Nominal Rock and Fluid Properties

Property	Value	Unit
Permeability	100	mD
Porosity	0.3	-
Oil viscosity	10	cp
Water viscosity	1	cp
Oil density	700	Kg/m ³
Water density	1000	Kg/m ³
Corey exponent		
▪ Oil	2	-
▪ Water	2	-

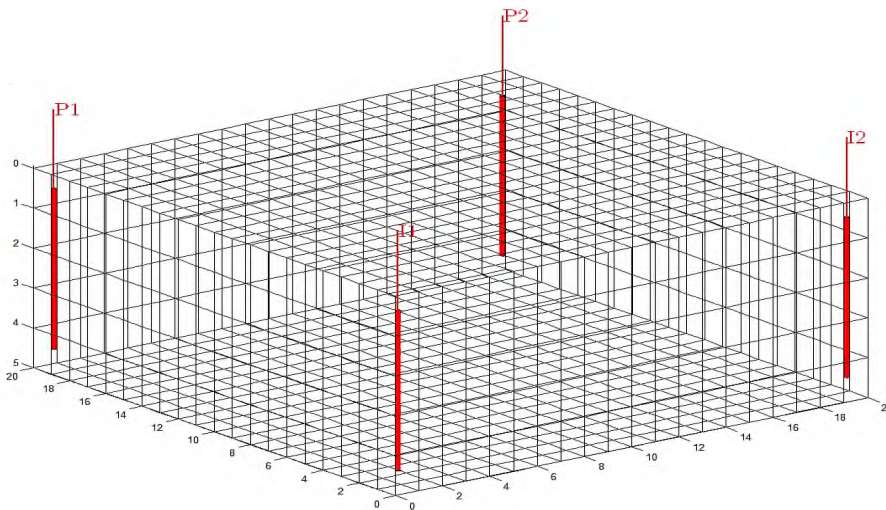


Figure 6-1: Nominal Reservoir and Wells Configuration

With this arrangement, as in previous chapter, the MVs are injection and total production rates; but with voidage replacement assumption, the MVs were reduced to two (two DOF). To be able to implement this assumption, well pairing was employed where Injector, I1 was paired with producer, P1 and I2 with P2. So, with this setup, injection rates from I1 must equal total production rates from P1 at all time-steps and likewise with I2 – P2 pairing.

The total production time was fixed to two years (730 days) with time-step of one day. At each time-step, four measurements which include oil and water production rates from wells P1 and P2 are recorded. The measurement vector is given by

$$\mathbf{y} = [y_{o1} \ y_{o2} \ y_{w1} \ y_{w2}]^T \quad (6-1)$$

where y_{o1} and y_{w1} are oil and water production rates from P1 respectively while y_{o2} and y_{w2} the respective measurements from P2. In addition to these measurements, the NPV of the process given in Equation (3-5) was also computed using same economic parameters as in Section 3.3.

The procedures outlined in Section 5.2.2 were followed. Here, 500 solution trajectories were obtained for the two MVs. For the first trajectory, the flooding process was simulated for two years using the actual optimal control solutions. The optimal controls were then slightly perturbed for subsequent trajectories. However, the controls for the first two time-steps were not perturbed because two past histories are needed ($n = 2$). Since there are two MVs for this system, Equation (5-45) can be modified as

$$J_{i+1} - J_i = \sum_{k=n+1}^N C(\boldsymbol{\theta}_1, \mathbf{y}_{1,i}^k, \mathbf{y}_{1,i}^{k-1}, \dots, \mathbf{y}_{1,i}^{k-n}, u_{1,i}^k)(u_{1,i+1}^k - u_{1,i}^k) + C(\boldsymbol{\theta}_2, \mathbf{y}_{2,i}^k, \mathbf{y}_{2,i}^{k-1}, \dots, \mathbf{y}_{2,i}^{k-n}, u_{2,i}^k)(u_{2,i+1}^k - u_{2,i}^k) \quad (6-2)$$

where $\boldsymbol{\theta}_1$ and $\boldsymbol{\theta}_2$ are parameter vectors for the two CVs to be determined through regression. The vectors of the measurements, \mathbf{y}_1 and \mathbf{y}_2 are for the respective production wells P1 and P2 given as

$$\begin{aligned} \mathbf{y}_1 &= [y_{o1} \ y_{w1}]^T \\ \mathbf{y}_2 &= [y_{o2} \ y_{w2}]^T \end{aligned} \quad (6-3)$$

In Equation (6-2), the MVs, u_1 and u_2 which are water injection rates from I1 and I2 respectively are included so that their expressions can be obtained explicitly as the feedback control laws. Each of the parameter vectors in Equation (6-2) has seven elements considering number of measurements with past histories. Modifying Equation (5-47) for each CV, we have

$$\begin{aligned} C_1 &= \theta_1 y_{o1,i}^k + \theta_2 y_{w1,i}^k + \theta_3 y_{o1,i}^{k-1} + \dots + \theta_6 y_{w1,i}^{k-2} + \theta_7 u_{1,i}^k \\ C_2 &= \theta_8 y_{o2,i}^k + \theta_9 y_{w2,i}^k + \theta_{10} y_{o2,i}^{k-1} + \dots + \theta_{13} y_{w2,i}^{k-2} + \theta_{14} u_{2,i}^k \end{aligned} \quad (6-4)$$

Regression is performed by minimizing the square of the residual according to Equation (5-48). Setting C_1 and C_2 to zero in Equation (6-4), feedback control law is obtained

$$\begin{aligned} u_{1,fb}^k &= -\theta_7^{-1} [\theta_1 y_{o1}^k + \theta_2 y_{w1}^k + \theta_3 y_{o1}^{k-1} + \dots + \theta_6 y_{w1}^{k-2}] \\ u_{2,fb}^k &= -\theta_{14}^{-1} [\theta_8 y_{o2}^k + \theta_9 y_{w2}^k + \theta_{10} y_{o2}^{k-1} + \dots + \theta_{13} y_{w2}^{k-2}] \end{aligned} \quad (6-5)$$

Where $u_{1,fb}^k$ and $u_{2,fb}^k$ are the two optimal settings of injection wells.

6.3 Uncertainty Consideration

To check the robustness of the developed CVs, four different cases of uncertainty in rock and/fluid properties with differing degree are considered. In the first case, the CVs are applied to the nominal model. The performance of such is compared with the open-loop (OC) solution. It is expected that the SOC performance will be lower than the OC since no uncertainty is introduced. Results from this case will give an initial idea of how accurate the CVs are, before they are used to counteract the effects of uncertainties.

In Case II, the size of the real reservoir was increased and random permeability field was used as in Section 3.2 which is shown in Figure 3-1. Table 6-2 shows the geological and fluid properties for the reservoir.

For Case III, the only uncertainty introduced is in the shape of relative permeability curve where the real exponents for oil and water were assumed to be 1.5 each. See Table 6-3 for details.

Table 6-2: Case II – Rock and Fluid Properties

Property	Value	Unit
Geometry	Cartesian grid	-
Grids	20 x 20 x 5	
Size	100 x 80 x 10	m
Permeability	Log-normal Distribution	mD
Porosity	0.3	-
Oil viscosity	10	cp
Water viscosity	1	cp
Oil density	700	Kg/m ³
Water density	1000	Kg/m ³
Corey exponent		
▪ Oil	2	-
▪ Water	2	-

Uncertainties in reservoir geometry, size and shape were considered in in Case IV. This case was also reported in Sections 3.2 and 5.2.2 for two wells scenario.

For this reservoir system with four wells see Table 6-4 for a detailed list of properties and Figure 6-2 for configuration.

For each of these cases, the optimal feedback control laws, Equation (6-5) are implemented; the performance of which is compared against OC solutions based on the nominal model and the ideal solutions (BM) where all the reservoir properties are assumed to be known with certainty. This is done by applying Equations (5-50) and (5-51).

Table 6-3: Case III – Rock and Fluid Properties

Property	Value	Unit
Geometry	Cartesian grid	-
Grids	20 x 20 x 5	
Size	20 x 20 x 5	m
Permeability	100	mD
Porosity	0.3	-
Oil viscosity	10	cp
Water viscosity	1	cp
Oil density	700	Kg/m ³
Water density	1000	Kg/m ³
Corey exponent		
▪ Oil	1.5	-
▪ Water	1.5	-

Table 6-4: Case IV – Rock and Fluid Properties

Property	Value	Unit
Geometry	Corner-pont grid	-
Grids	30 x 3 x 1	
Size	225 x 22.5 x 10	m
Fault size	0.3	m
Permeability	100	mD
Porosity	0.3	-
Oil viscosity	10	cp
Water viscosity	1	cp
Oil density	700	Kg/m ³
Water density	1000	Kg/m ³
Corey exponent		
▪ Oil	2	-
▪ Water	2	-

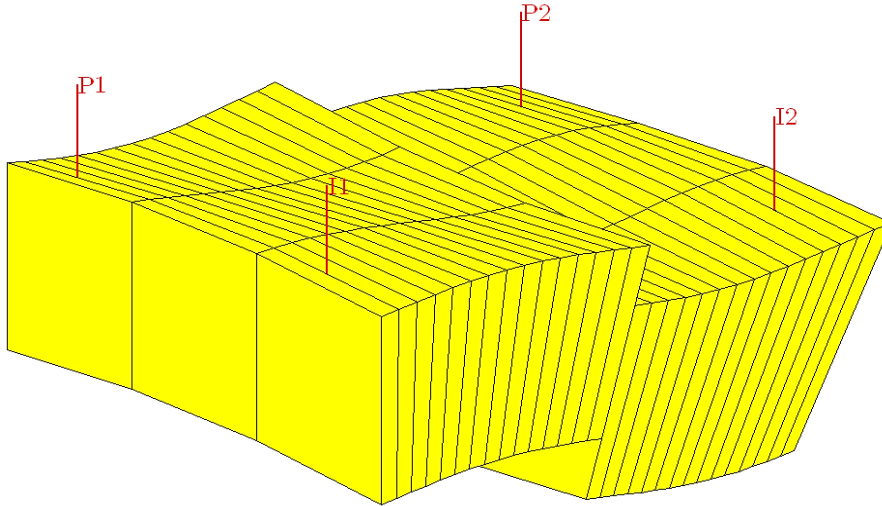


Figure 6-2: Reservoir and Wells Configuration for Case IV

6.4 Results and Discussion

6.4.1 Regression

The CV parameters obtained via regression are listed in Table 6-5. It can be seen that only three measurements out of total six are relevant in the CV functions which comprises of both oil and water production rates. The immediate past measurements ($n = 1$) are irrelevant but the current ($n = 0$) and past two ($n = 2$). However, contribution by oil production rate is more significant than water rate. An excellent regression performance with R-square value of 1.0 was obtained. This indicates that no higher-order polynomial or more sophisticated model is required. With these CVs, the two feedback control laws are:

$$\begin{aligned} u_{1,fb}^k &= 0.1436y_{o1}^k + 0.8565y_{o1}^{k-2} + 1.0005y_{w1}^{k-2} \\ u_{2,fb}^k &= 0.1435y_{o2}^k + 0.8566y_{o2}^{k-2} + 1.0005y_{w2}^{k-2} \end{aligned} \quad (6-6)$$

For an injection-production system where productions from two wells are equal, we should expect equal injection settings as suggested by Equation (6-6). Results of each case are given and discussed in Sections 6.4.2 - 6.4.5.

Table 6-5: CVs Regression Parameters

CV	Parameter	Parameter Value
C_1	θ_1	5.7929×10^{18}
	θ_2	0
	θ_3	0
	θ_4	0
	θ_5	3.4547×10^{19}
	θ_6	4.0354×10^{19}
	θ_7	-4.0335×10^{19}
C_2	θ_8	-8.4217×10^{18}
	θ_9	0
	θ_{10}	0
	θ_{11}	0
	θ_{12}	-5.0285×10^{19}
	θ_{13}	-5.8727×10^{19}
	θ_{14}	5.8700×10^{19}

6.4.2 Case I: Nominal Parameters

The optimal feedback control laws, Equation (6-6) obtained are implemented on the nominal model for a period of two years. This production strategy was compared to the true optimal solution (OC). The NPV recorded from SOC strategy is \$128,903.70 while that from OC is \$128,904.90. The loss is almost zero (0.0009593%). This shows the CVs obtained are almost perfect. The NPVs

are shown in Figure 6-3. It is clearly seen that the two performance indices are indistinguishable throughout the production period.

Figure 6-4 shows injection settings for the two approaches. The optimal injection settings for the two wells as obtained by both approaches (OC and SOC) can be seen to be equal at each time-step. This validates the accuracy of the feedback control law given in Equation (6-6). For the OC case, two regions can be identified from the injection profile; a rapidly increasing and decreasing region which spans for about 170 days from the beginning of production then followed by a constant injection regime for the remaining period. However, three distinguishing regions can be seen with SOC approach which consists of a steadily increasing phase (160 days) followed by a sharp decline phase and finally an ascending phase. Another interesting feature is that the injection rates meet just at the end of production period. It is worth to know that the variability of the injection settings found by the two approaches is almost the same with respective standard deviations of 0.004287 and 0.004351 for OC and SOC. This can also be confirmed from oil and water production profiles shown in Figure 6-5 and Figure 6-6 respectively, where it is observed that the injection settings found by the two strategies caused similar effects in oil and water production.

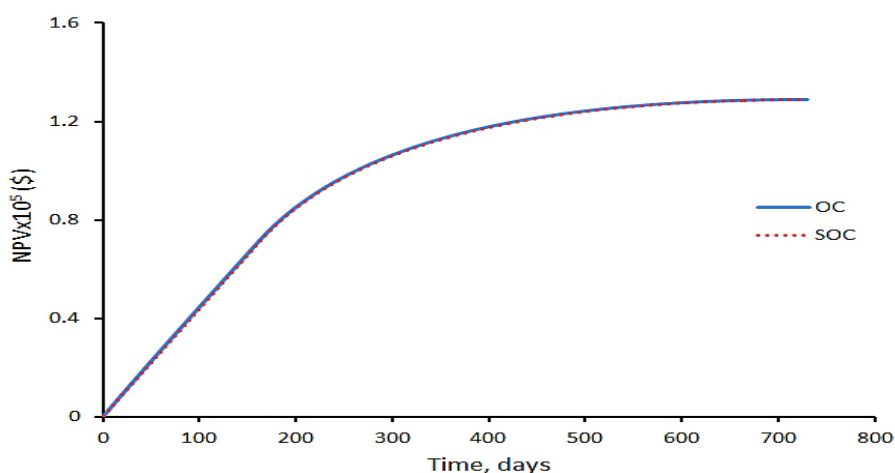


Figure 6-3: NPV for Case I – Nominal Parameters

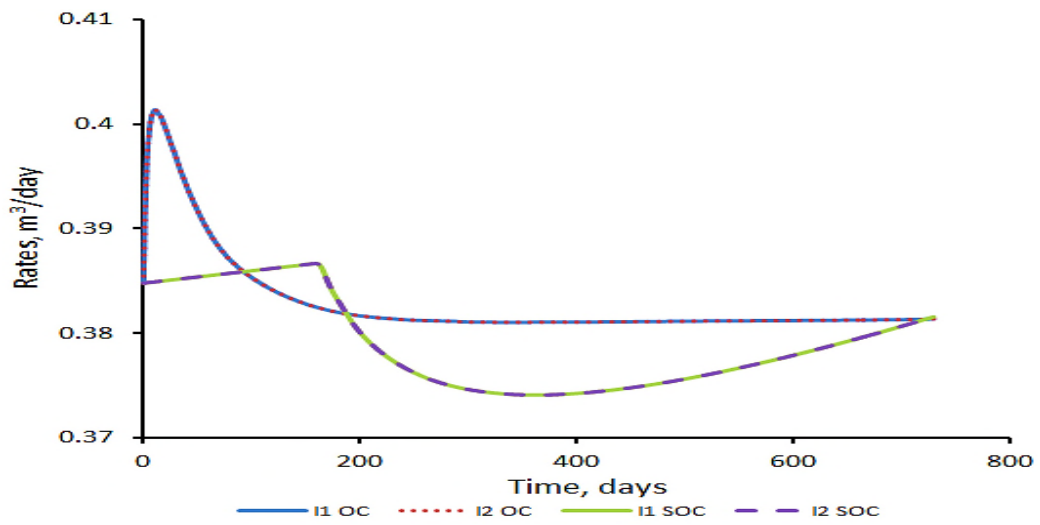


Figure 6-4: Injection Rates for Nominal Case

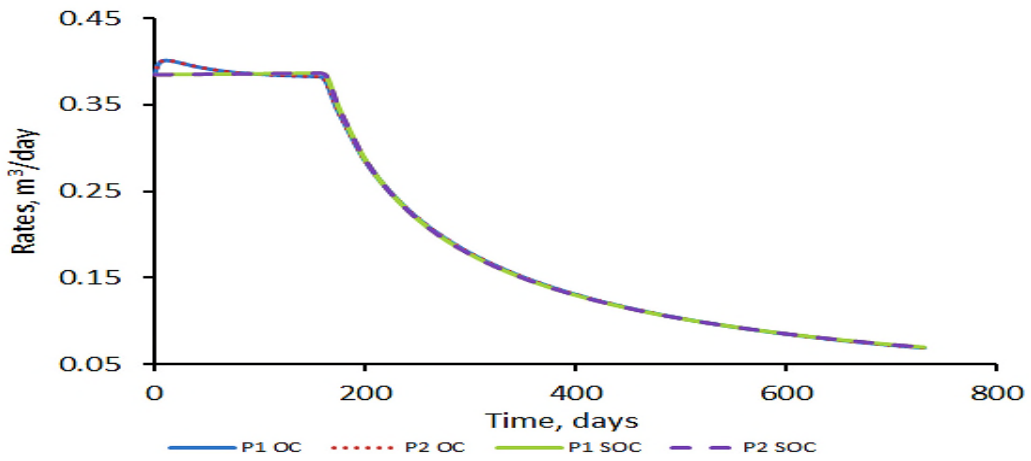


Figure 6-5: Oil Production Profiles for Nominal Case

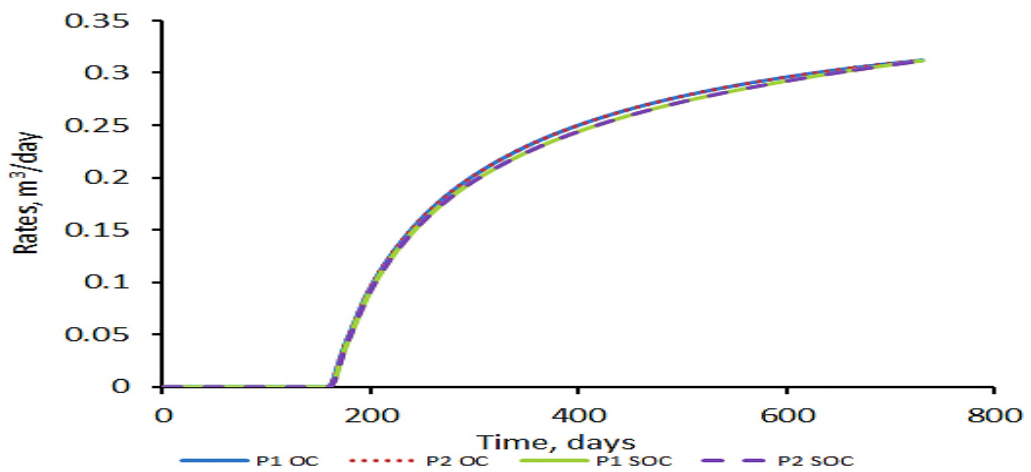


Figure 6-6: Water Production Profiles for Nominal Case

6.4.3 Case II: Uncertainty in Permeability and Reservoir Size

For this case where reservoir size is increased by 97.5% with random permeability field for each of five layers (homogeneous permeability for the nominal case), the NPVs generated are shown in Figure 6-7. It is obvious that the open-loop solution is non-optimal in this case with a loss of 93.21% when compared to BM case while performance of SOC is similar to that of BM scenario where reservoir properties are assumed to be known with perfection. The loss here is only 0.018% with a gain of 93.21% over OC approach.

Table 6-6 summarises the results for this case of uncertainties. Both total oil and water productions are higher with SOC strategy than any other case but this does not give it (SOC) a superior performance over BM because the incremental water production has to some extent annulled the benefit that can otherwise be realised from the corresponding increase in oil production. Never the less, the two NPVs (for SOC and OC) are similar. The failure of open-loop solution on this reservoir is clearer with the amount of total oil produced shown in the table (which is only 558.76 m³). However, due to the uncertainty introduced, we have seen early water break-through for both approaches of BM and SOC but this has been appropriately controlled.

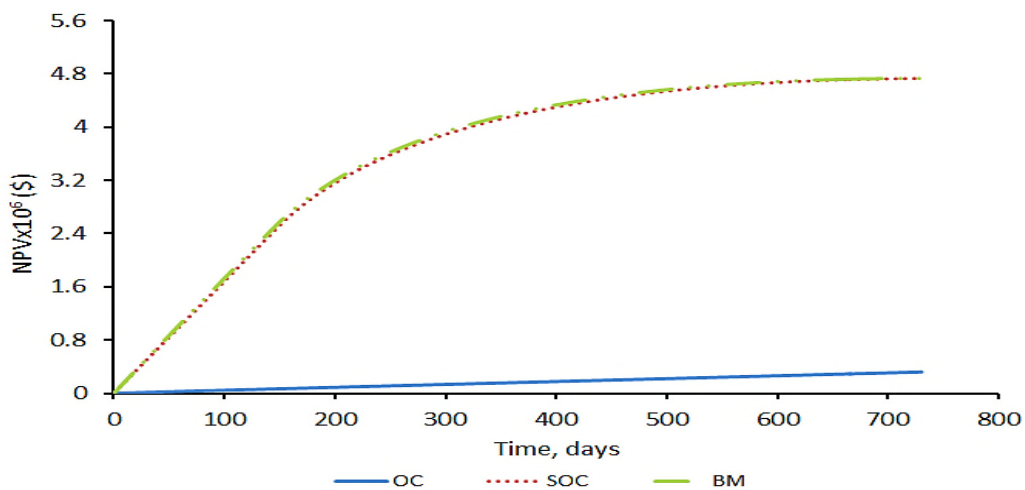


Figure 6-7: NPVs for Case II

The injection trajectories found by the three strategies are compared in Figure 6-8. It is evident that the injection requirement for this size of reservoir cannot be satisfied by the open-loop optimal solution. For the BM approach, higher proportion of water was injected mainly by well I2 while the injection rates were equally distributed between the two injectors when using SOC method; this is of course according to Equation (6-6). BM injection settings can also be seen to increase and/or decrease while nearly constant injection trajectory characterises SOC solution.

Oil production profiles for this case are shown in Figure 6-9. It is interesting to know that well I1 is communicating with well P2 likewise is well I2 with P1 for the BM case where well pairing was not considered but total voidage replacement assumption was conserved. This again has proven the robustness of the CV which was obtained on the basis of such configuration (pairing of I1 with P1 and I2 with P2) which has indeed reflected in oil production rates. A similar pattern is also observed in water production profiles shown in Figure 6-10. The preferential producer-injector communication was caused basically by the change in the reservoir geometry. Despite the disparity in well configuration in addition to huge uncertainty introduced, a very good performance index was obtained with employment of feedback strategy which is comparable to the BM performance.

Table 6-6: OC and SOC Performance Comparison for Case II

Strategy	Total Oil (m³)	Total Water (m³)	Time of Water Break-Through (days)	NPV (\$)
SOC	10,546.17	14,350.33	78	4,731,512.20
OC	558.76	0.00	-	321,245.07
BM	9,688.22	13,932.93	49	4,732,358.83

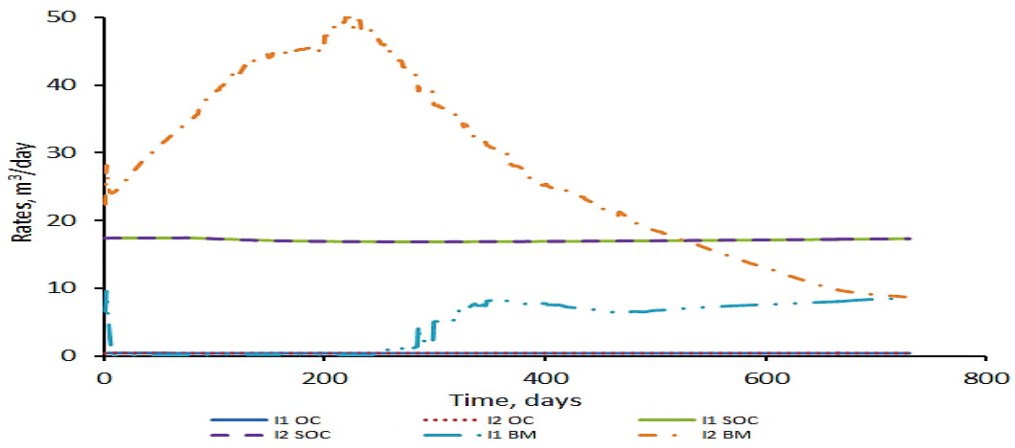


Figure 6-8: Injection Rates for Case II

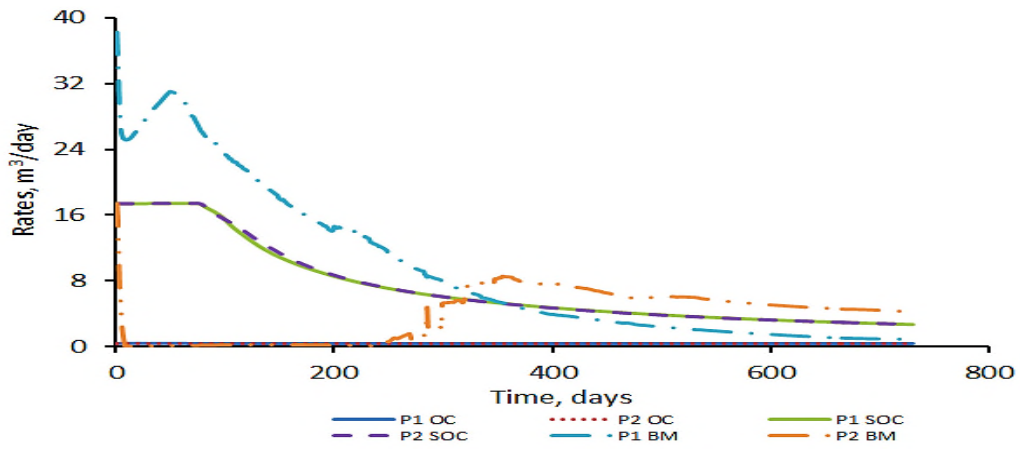


Figure 6-9: Oil Production Profiles for Case II

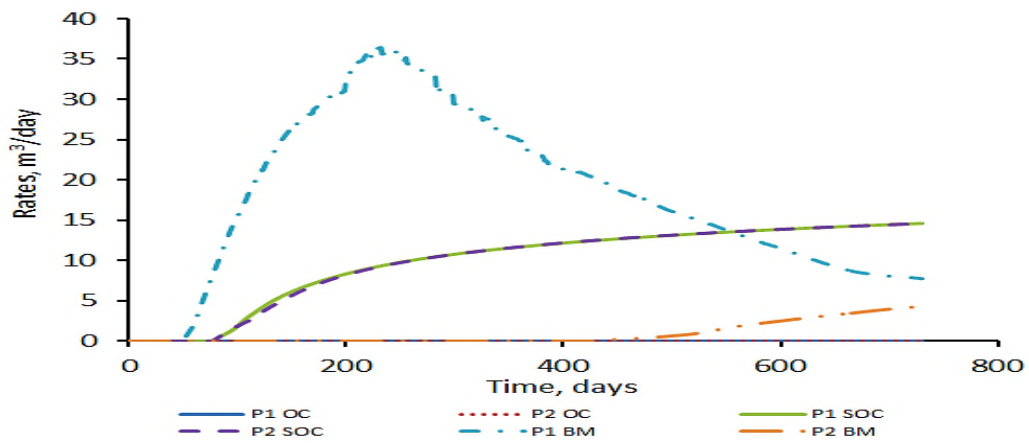


Figure 6-10: Water Production Profiles for Case II

6.4.4 Case III: Uncertainty in the Shape of Relative Permeability Curves

The nominal values of Corey exponents for both oil and water relative permeability curves are 2.0 while the real values were considered to be 1.5 each. For this uncertainty, a loss of only 0.023% was incurred as a result of SOC implementation with a gain of 0.25%. The loss is 0.27% with OC approach. Figure 6-11 shows the NPV for the three strategies. Although on the scale of the plot, not significant difference is seen, still a wide separation between OC and BM at some points is observable.

Table 6-7 gives a summary of the obtained results. A simple pattern can be established here; there is a direct correspondence between the NPV and total productions. For instance, with the BM approach, highest NPV was recorded with a similar record of oil and water productions whereas the least NPV realised from OC implementation is linked to lowest total productions. Similarly, the time of water break-through increases with an increase in NPV.

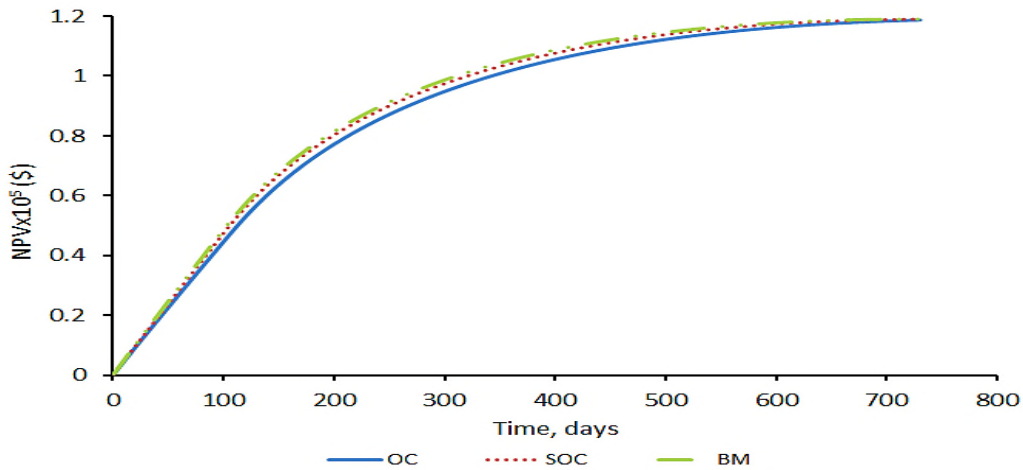


Figure 6-11: NPVs for Case III

Table 6-7: OC and SOC Performance Comparison for Case III

Strategy	Total Oil (m³)	Total Water (m³)	Time of Water Break-Through (days)	NPV (\$)
SOC	280.51	317.72	104	119,010.69
OC	272.89	285.87	111	118,710.67
BM	284.20	334.12	101	119,037.93

6.4.5 Case IV: Uncertainty in Reservoir Size, Geometry and Structure

For this huge uncertainty consideration, open-loop solution has woefully failed to optimize the waterflooding process with a loss of 95.07%. On the other hand, the optimal feedback controls obtained based on the nominal model proved to be very robust in the presence of these uncertainties with a loss of only 0.45% when compared to the BM case that assumed perfect reservoir knowledge. The SOC approach has a gain of 95.05% over the OC case. The performance indices for the strategies are compared in Figure 6-12. The figure demonstrated a total failure of OC approach for this system/model mismatch but shows the power of SOC in counteracting the uncertainties. An important feature worth considering is the resemblance SOC NPV has to that of the BM scenario after 500 days of production commencement till the end of the period.

A summary of the performances of the approaches is given in Table 6-8. The developed feedback strategy can be said to have mimicked the truth optimal solution reasonably well. This can be seen in several ways, most of which will be explored later. But it can be briefly seen in the table that both the BM and SOC approaches are associated with early water break-through time of one day. This is regarded most often as operational hiccups, however, as long as the water-cut is within some acceptable threshold as dictated by the economics, the process can be considered optimal. For whatever reason anyway, the truth optimal operational strategy is characterised by water production after a day. It is also important to note that a total oil production of only 545.99 m³ through OC

implementation has not only regarded the strategy non optimal, but also not suitable for this size of reservoir. This can be visualized more clearly from plot of injection profiles shown in Figure 6-13. Based on the BM approach, it can be seen that there is an injection requirement of up to 114 m³/day, a demand that can never be satisfied with employment of OC solution which has a maximum injection setting of 0.40 m³/day.

The most fundamental similarity in terms of operational settings between SOC and BM approaches is the near closure of Injector I1 and opening of I2 throughout the production time. A sharp increase followed by a sharp decline characterises BM injection trajectory for I2. On the other hand, an almost constant injection solution was found by SOC method which averages at 53 m³/day.

It will also be helpful to see how the injection settings influence productions from the two wells, P1 and P2. Due to the increase in reservoir size from the nominal one and perhaps the presence of fault, there is no much communication between I1 and P1 as well as between I2 and P2 for the case of BM (Figure 6-14 and Figure 6-15). However, the original well pairing was maintained by SOC strategy. Results for all the cases are given in Table 6-9.

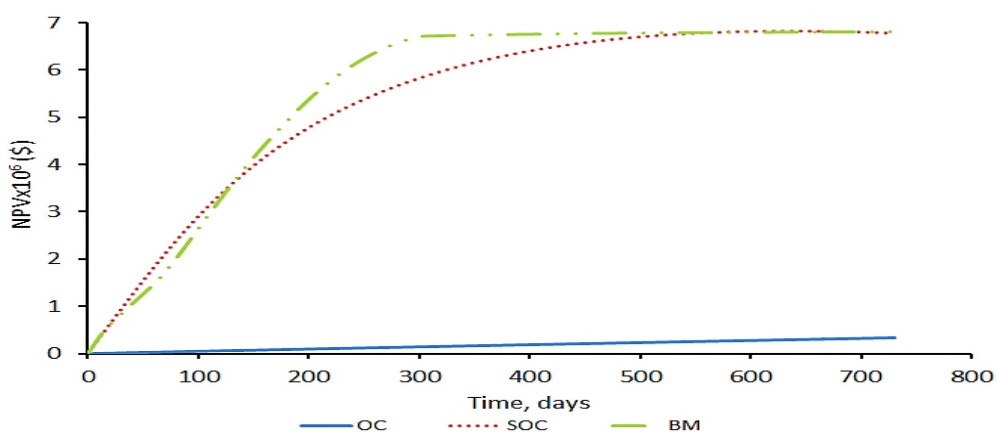


Figure 6-12: NPVs for Case IV

Table 6-8: OC and SOC Performance Comparison for Case IV

Strategy	Total Oil (m ³)	Total Water (m ³)	Time of Water Break-Through (days)	NPV (\$)
SOC	15,431.47	23,257.71	1	6,778,147.29
OC	545.99	12.77	242	335,602.48
BM	13,988.96	15,802.51	1	6,808,782.37

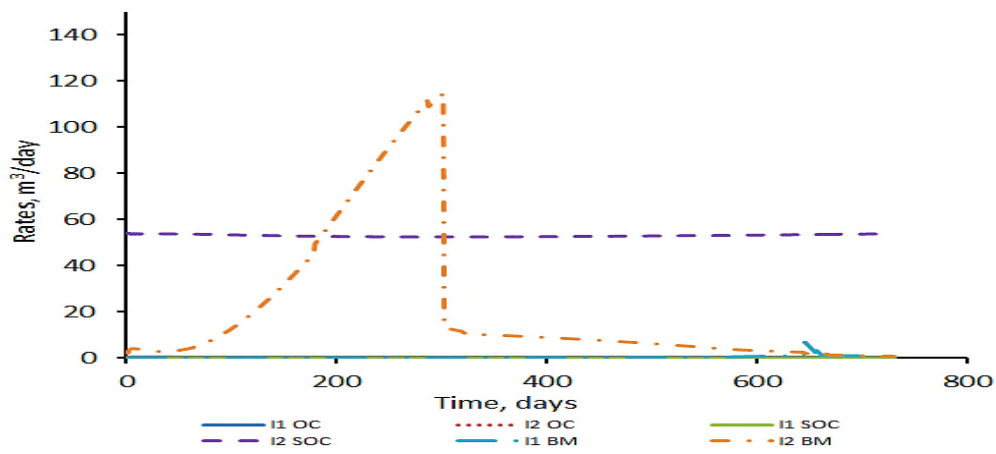


Figure 6-13: Injection Rates for Case IV

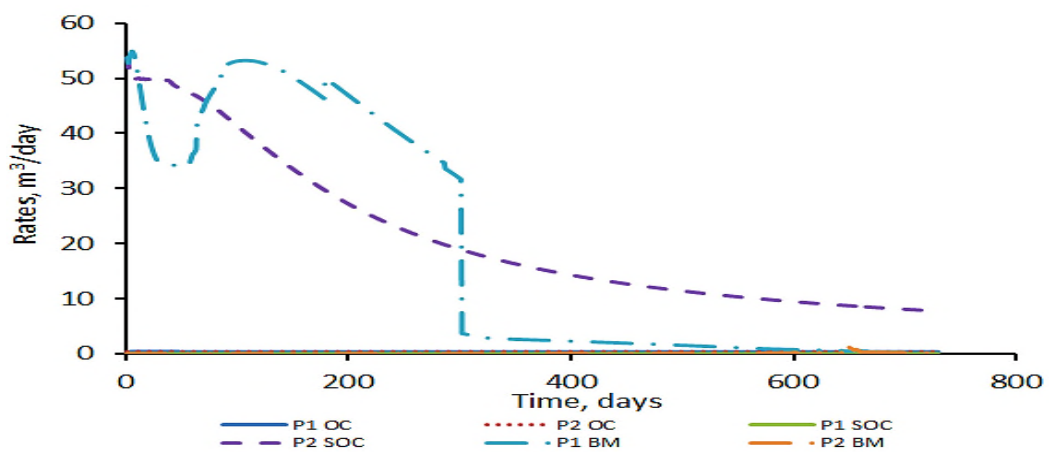


Figure 6-14: Oil Production Profiles for Case IV

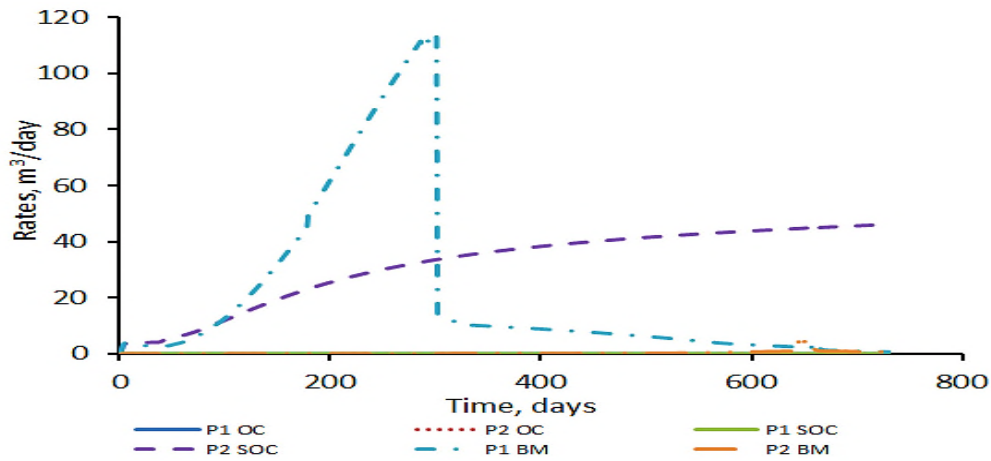


Figure 6-15: Water Production Profiles for Case IV

Table 6-9: Losses and Gains for Various Cases of Uncertainty

		NPV(\$)	% Gain	% Loss
Case I	OC	128,904.90	-	-
	SOC	128,903.70	-	-
Case II	BM	4,732,358.83	-	-
	OC	321,245.07	-	93.21
	SOC	4,731,512.20	93.21	0.018
Case III	BM	119,037.93	-	-
	OC	118,710.67	-	0.27
	SOC	119,010.69	0.25	0.023
Case IV	BM	6,808,782.37	-	-
	OC	335,602.48	-	95.07
	SOC	6,778,147.29	95.05	0.45

6.5 Conclusions

The optimal feedback control approach developed in Chapter 5 through controlled variable regression was extended here to solve multivariable waterflooding optimization problem. This task was motivated by the fact that oil and gas fields consist of several injection and production wells and therefore it become pertinent to test the novel algorithm for multivariable optimization. To achieve the objective, a reservoir with two each of injection and production wells was considered. For the purpose of CV regression, injector-producer pairing was employed, where simulated measurements made up of oil and water production rates were recorded. The data matrix was obtained via input perturbations. The gradients of the objective function with respect to controls were selected as the CVs. The CVs were then approximated with linear functions of current and past measurements (typically two past histories) which were fitted to the data via least squares regression. The robustness of the CVs was tested by initially implementing it on the nominal model and then to cases with system mismatches. Typical uncertainties introduced in the form of mismatches in reservoir and fluid properties include permeability, shape of relative permeability curves, reservoir size, geometry and structure. The performance of the SOC method was compared with open-loop solution based on optimal control theory as well as benchmark case which gives the ideal optimal solution under the assumption of complete prior knowledge of the reservoir. Extremely good results were obtained for the nominal case and cases with uncertainties which are summarised as follows:

1. The regression fitting was excellent with an R^2 index of 1.0, indicating that the linear model is satisfactorily a representative of the gradient.
2. The two feedback control laws were found to have same regression coefficients, in other words, the regression resulted to symmetrical CVs.
3. Implementing the CVs on the nominal model resulted to an almost zero loss. The true optimal injection trajectories as found through optimal control theory were identical for the two injectors. This was also the case

with SOC's solution. A similar phenomenon was observed with production profiles, an indication of the accuracy of the developed method which gave a clue of its suitability in counteracting effects of uncertainties.

4. A total failure of the open-loop solution was observed in two cases when the reservoir size is increased whereas SOC performed well with performance indices similar to the benchmark cases. Typically, a mismatch in the form of size and permeability resulted to a gain by SOC of 93.21% over OC and an incurred loss of only 0.018%. However, a very high loss of 93.21% was recorded with OC implementation. Similar results were obtained for uncertainties in reservoir size, geometry and structure. For this case, SOC gave better results with a gain of 95.07% over OC. The latter has a loss of 95.05% compared with 0.45% for the former.
5. It can be emphasised that the relative performance of SOC increases with increase in the degree of uncertainty while that of OC deteriorates in that order.
6. The designed CVs can be confirmed therefore to be robust and insensitive to the various uncertainties considered. Another point worth mentioning is that near optimal operation was achieved with the designed CVs maintaining well pairing on which basis it (CVs) was formulated whereas the true optimal solution has no such constraint.
7. In general, the optimization method presented indicated that the best CV to be selected is the gradient of the objective function and its analytical expression is not necessary to derive an operation to its optimum.

7 Conclusions and Recommendations

7.1 Conclusions

This work has presented in details methodologies of optimization of waterflooding operation with techniques to deal with reservoir uncertainties. In this section, conclusions drawn from the work reported in the main chapters, 3 - 6 are highlighted.

A detailed review on waterflooding optimization techniques has been given in Chapter 2. From the various literature surveyed, a consensus was made that the only option for optimal waterflooding operation is to introduce feedback capabilities into the optimization structure so as to annul effects of uncertainties that are inevitable to reservoir systems. With this notion, several works have been reported under the umbrella of 'Closed-Loop Reservoir Management' or CLRM. This involves updating of reservoir models using production data and subsequent online optimization based on the updated models. This approach may seem very promising but it is actually cumbersome and very difficult to be implemented in reality. However, there is a body of literature on simpler and more efficient methodology that has not been explored yet for waterflooding optimization; that is method based on the principle of self-optimizing control. This technique has been reviewed and a novel approach was proposed for optimal waterflooding process.

The optimization study of waterflooding system was started in Chapter 3. Here, performances of different smart well designs were studied for a heterogeneous reservoir system. Typically, heterogeneity in vertical permeability was considered and effectiveness of various well orientations and number of controls was critically investigated on this reservoir system. Four cases of smart well designs were compared against a nominal case which is conventional form of well completion in which control is possible only at well level. The smart well designs differ in the number of ICVs installed and/or orientation (either vertical or horizontal). Based on the performance index used, NPV of the venture, the best design was the case with highest number of ICVs while worst design was

found from the case with least number of ICVs. The improvements of these two extreme cases over the nominal design are 11.38% and 0.35% respectively. In fact, the NPV was found to be increasing with increase in number of controls. For every ICV, a more suitable flow profile is imposed along the well, so increasing the number of ICVs translates to more optimal flow trajectories and hence a better sweeping efficiency. However, installing wells with large number of ICVs will require more capital investment, a factor that has not been considered in this thesis work. Furthermore, looking at the performance of the designs from production recoveries point of view, for the type of reservoir system considered which has vertical layers each of different permeability distribution, high recovery is favoured when each layer is provided with ICVs at injection and production points. This was shown through a case where a total of 10 ICVs were installed so that injection and production perforations at each layer were equipped with control gadgets. For this case, increase in oil production over a nominal case is 7.92%. Comparing this with a case where 25 ICVs were used but without giving due consideration to the vertical layers from the production sides (horizontal producer running through the first layer), the increase is 6.70%.

A feedback control approach based on the concept of receding horizon control (RHC) was developed in Chapter 4. Two forms of RHC, fixed end (FE) and moving end (ME) were investigated. The methodology was first implemented to cases without considering model/system mismatch the performance of which was compared to that of open-loop optimal solutions (OC) based on optimal control theory. The performance of RHC was close to that of OC on several occasions, this inspired the work to be extended to uncertainties treatment. For the uncertain cases, two reservoir models were used; a prediction model and a real reservoir. Intentional mismatches in the values of some geological parameters were introduced between these two models. The prediction model was used to determine optimal injection and production settings which are subsequently implemented on the real reservoir. The real reservoir here is a synthetic reservoir model that was assumed to serve the purpose of a real field reservoir. From the comparative study of the two RHC techniques, it was found

that FE performed better than ME for all considered scenarios. The performance of ME approach is highly influenced by the length of prediction horizon. So, a considerable effort will be needed in finding an optimum prediction length when ME is to be implemented, a situation that is impractical with reservoir production. This limitation is however, not applicable to FE. Also, as part of the comparative analyses, the suitability of two performance indices, NPV and recovery, was investigated. It was confirmed that NPV is more appropriate because it takes into consideration real asset value at any point in time. Typical model/system mismatches introduced in this work include uncertainties in permeability, porosity, reservoir geometry, size, and structure. The ability of the developed RHC approach to counteract effects of these uncertainties was compared to traditional open-loop solutions with uncertainties and true optimal control solutions referred to as benchmark approach (BM). The BM is the ideal optimal solution obtained based on the assumption that all reservoir properties are known a priori. The superiority of RHC over OC was evaluated as a gain in NPV while deficit in NPV between RHC/OC and BM was regarded as a loss. Depending on the uncertainty, gains recorded are in the range of 0.14% to 19.22% while losses through RHC implementation range from 0.25% to 15.21%. For the OC approach, the loss varied from 0.39% to 31.51%. Although, a reasonable improvement over open-loop optimal control solutions has been achieved through RHC algorithm; it will be worth exploring other techniques that are less sensitive to uncertainties as well as less time consuming. This motivated the development of a novel algorithm reported in Chapter 5.

An entirely new approach to waterflooding operation optimization was reported in Chapter 5. Apart from being the only work that presented the use of self-optimizing control (SOC) principles for optimal waterflooding operation, the method is also a new practical approach to dynamic SOC. Here, the gradient of the objective function with respect to control was selected as the CV. However, it is a known fact that obtaining an explicit gradient expression of most complex systems is not trivial, and when it is available it may consist of some unmeasurable parameters. Therefore, with this point in mind, the method was

developed in such a way that analytical gradient function will not be required, but computed using finite difference scheme based on available data. The computed gradients are then fitted to a polynomial function using a regression technique. The method was first developed for static optimization case for both constrained and unconstrained scenarios. The efficacy of the method was demonstrated through theoretical case studies which were compared with existing SOC approaches. Based on the results obtained, the new technique was found to be better than local SOC method and comparable to NCO approximation technique. A point worth noting with the proposed method is that, its accuracy depends on the finite difference scheme used. Specifically, central difference was found to be most accurate. Successful application of the static method motivated its extension to solve dynamic optimization problem with particular focus to waterflooding operation. For this purpose, the gradient was proposed to be a linear function of past and current measurements, and the control(s); simulated data obtained based on a nominal model were used for function fitting. An optimal feedback control law was obtained from the regressed CV function which was used to optimise the flooding process. The control relationship was first implemented on the nominal model and then to various cases of uncertainties as discussed above. Similar to the approach adopted in Chapter 4, the performance of the dynamic SOC method was compared to those of open-loop optimal solutions as well as the true solutions (BM). The case studies were categorised into two main groups. The method was first tested on a simplistic sized reservoir studied in Chapter 4 and then to a realistic sized case. In the absence of model/system mismatch, only insignificant losses were incurred as a result of implementing the optimal feedback control. The losses are 0.26% and 0.11% for the simplistic and realistic reservoirs respectively. With introduction of uncertainties, the relative performance of SOC was seen to improve with increase in the degree of mismatches. Take for example; when uncertainty was considered in permeability only, gain achieved from implementation of the optimal feedback control was in the range of 0.26% - 1.03%. Introducing more mismatches simultaneously in the form of reservoir size, geometry and structure, the gain

was seen to increase tremendously which was 30.04% for the simplistic case and 24.03% for the real sized reservoir with respective losses of 2.09% and 0.54%. Although, uncertainty is not considered in the formulation of the CV due to complexity of oil reservoirs, the CV is still robust due to the feedback nature of the SOC strategy. However, if uncertainty will be considered in the formulation, the performance of the technique can be improved further.

The waterflooding optimization studies carried out in Chapter 5 were based on two-well reservoir system; the problem was however reduced to have a single manipulative variable (MV) as a result of imposition of total voidage replacement assumption, and wells that were constrained by rate. However, a typical waterflood field is made up of several injection and production wells and so, multivariable optimization will be required. For this reason, the dynamic SOC methodology was extended to optimize problems with higher degrees of freedom (DOF) in Chapter 6. Here, four wells were considered and with the same assumption and well constraint, the system was reduced to two DOF. Similar uncertainty scenarios were considered as in Chapter 5. Here, a near-zero loss was recorded with the implementation of the optimal feedback control solutions for the nominal case. A total failure of open-loop solutions was observed when uncertainty in reservoir size was introduced. This occurs for two different cases. However, for these same cases, the optimal feedback control solution was able to achieve optimal operational profits with only 0.018% and 0.45% worse than the true optimal controls, but 93.21% and 95.01% better than the open-loop optimal control respectively. The designed CVs can be confirmed therefore to be robust and insensitive to the various uncertainties considered. In general, the methodology presented indicated that the best CV to be selected is the gradient of the objective function and its analytical expression is not necessary to derive an operation to its optimal point.

7.2 Recommendations

A new approach to waterflooding optimization under uncertainties has been presented. However, being the first of its kind, there are still some further works that need to be carried out to ascertain its wide applicability to different reservoir systems and facilities. Two categories of future works are recommended to be carried out. The first of such are works related to physical well structure and facility size. The other category should explore different reservoir types. These are explained in details below.

On the basis of physical facility structure, the optimization methodology should be applied to cases with more number of wells. It should also be tested on other well configurations such as horizontal wells, multilateral wells, deviated wells and so on which are currently well types gaining popularity. In addition to these, it is recommended to implement the algorithm with controls focusing on ICVs instead at well level, typical of smart well control.

Currently, the work assumed incompressible reservoir fluid system. It is highly recommended to test the robustness of the obtained CVs to reservoirs with compressible fluids, such as black oil. Depending on the outcome, CVs should also be formulated for compressible fluids and comparative analyses be made.

The only source of energy considered in this work that is used in producing oil to the surface is energy derived from water injection. However, real reservoirs may have a combination of energy sources which come to play. Based on this notion, it is recommended that a systematic approach be developed that will investigate suitability of the novel technique to different reservoir drive mechanisms and its combination. The study can be conducted in this order: First, the analyses can consider energy due to fluid expansion in addition to water injection. This can be followed by adding gas cap which when expand add energy to the oil to be produced. The presence of aquifer can subsequently be added to the reservoir system. In fact, different forms of aquifer models can be considered.

REFERENCES

- Adeniyi, O. D., Nwalor, J. U. and Ako, C. T. (2008), "A Review on Waterflooding Problems in Nigeria's Crude Oil Production", *Journal of Dispersion Science and Technology*, vol. 29, no. 3, pp. 362-365.
- Ahmed, T. (2006), *Reservoir Engineering Handbook*, Third ed, Gulf Professional Publishing, Burlington, USA.
- Ahn, H., Lee, K. S., Kim, M. and Lee, J. (2014), "Control of a Reactive Batch Distillation Process using an Iterative Learning Technique", *Korean Journal of Chemical Engineering*, vol. 31, no. 1, pp. 6-11.
- Aitokhuehi, I., Durlofsky, L. J., Artus, V., Yeten, B. and Aziz, K. (2004), "Optimization of Advanced Well Type and Performance", *9th European Conference on the Mathematics of Oil Recovery (ECOMR IX)*, August 28-September 2, Cannes, France.
- Ali, S. M. F. and Meldau, R. F. (1979), "Current Steamflood Technology", *J.Petrol. Technol.*, vol. 31, pp. 1332-1342.
- Alstad, V. (2005), *Studies on Selection of Controlled Variables* (PhD thesis), Norwegian University of Science and Technology.
- Alstad, V. and Skogestad, S. (2007), "Null Space Method for Selecting Optimal Measurement Combinations as Controlled Variables", *Ind.Eng. Chem. Res.*, vol. 46, no. 3, pp. 846-853.
- Asadollahi, M. and Naevdal, G. (2009), "Waterflooding Optimization Using Gradient Based Methods", *SPE/EAGE Reservoir Characterization and Simulation Conference*, 19-21 October 2009, Society of Petroleum Engineers, Abu Dhabi, UAE.
- Asheim, H., (1987), *Optimal Control of Water Drive*, Society of Petroleum Engineers, SPE 15978-MS General.
- Asheim, H. (1988), "Maximization of Water Sweep Efficiency by Controlling Production and Injection Rates", *European Petroleum Conference*, 16-19 October 1988, Society of Petroleum Engineers, London, United Kingdom.
- Bowers, M. C., Purkale, J. D. and Gregory, M. D. (1996), "Reconciliation of Differences in Miscible Hydrocarbon Gas Floods using NMR", *SPE/DOE Improved Oil Recovery Symposium*, 21-24 April, 1996, Tulsa, Oklahoma, Society of Petroleum Engineers.

- BP plc (2014), *BP Energy Outlook 2035*, available at:
http://www.bp.com/content/dam/bp/pdf/Energy-economics/Energy-Outlook/Energy_Outlook_2035_booklet.pdf (accessed 09/29).
- Brouwer, D. R. (2004), *Dynamic Water Flood Optimization with Smart Wells using Optimal Control Theory* (PhD thesis), Technische Universiteit Delft.
- Brouwer, D. R. and Jansen, J. (2004a), "Dynamic Optimization of Waterflooding With Smart Wells Using Optimal Control Theory", *SPE Journal*, vol. 9, no. 4, pp. 391-402.
- Brouwer, D. R., Jansen, J. D., van der Starre, S., van Kruijsdijk, C. P. J. W. and Berentsen, C. W. J. (2001), "Recovery Increase through Water Flooding with Smart Well Technology", *SPE European Formation Damage Conference*, 21-22 May 2001, Society of Petroleum Engineers, The Hague, Netherlands, .
- Brouwer, D. R., N  lvdal, G., Jansen, J. D., Vefring, E. H. and van Kruijsdijk, C. P. J. W. (2004b), "Improved Reservoir Management Through Optimal Control and Continuous Model Updating", *SPE Annual Technical Conference and Exhibition*, 26-29 September 2004, Society of Petroleum Engineers, Houston, Texas, .
- Cao, Y. (2003), "Self-Optimizing Control Structure Selection via Differentiation", *Proceedings of the European Control Conference*, 1-4 September, 2003, Cambridge, U.K., pp. 445.
- Cao, Y. (2004), "Constrained Self-Optimizing Control via Differentiation", *Preprints of the 7th International Symposium on Advanced Control of Chemical Processes (ADCHEM)*, Hong Kong, pp. 63-70.
- Cao, Y. (2005), "Direct and Indirect Gradient Control for Static Optimisation", *International Journal of Automation and Computing*, vol. 2, no. 1, pp. 60-66.
- Cao, Y. and Kariwala, V. (2008), "Bidirectional Branch and Bound for Controlled Variable Selection: Part I. Principles and Minimum Singular Value Criterion", *Computers & Chemical Engineering*, vol. 32, no. 10, pp. 2306-2319.
- Capolei, A., Volcker, C., Frydendall, J. and Jorgensen, J. B. (2012), "Oil Reservoir Production Optimization using Single Shooting and ESDIRK Methods", 291 (ed.), in: *Proceedings of the 2012 IFAC Workshop on Automatic Control in Offshore Oil and Gas Production*, May 31 - June 1, 2012, Norwegian University of Science and Technology, Trondheim, pp. 286-291.

- Chen, C., Li, G. and Reynolds, A. (2012), "Robust Constrained Optimization of Short- and Long-Term Net Present Value for Closed-Loop Reservoir Management", *Society of Petroleum Engineers, SPE Journal*, pp. 849-864.
- Chen, Y. and Oliver, D. S. (2010), "Ensemble-Based Closed-Loop Optimization Applied to Brugge Field", *Society of Petroleum Engineers, SPE Journal*, no. 10.2118/118926-PA, pp. 56-71.
- Chen, Y., Oliver, D. S. and Zhang, D. (2009), "Efficient Ensemble-Based Closed-Loop Production Optimization", *Society of Petroleum Engineers, SPE Journal*, no. 10.2118/112873-PA, pp. 634-645.
- CO₂, C. (2014), *CRC for GREENHOUSE GAS TECHNOLOGIES*, available at: <http://www.co2crc.com.au/imagelibrary2/storage.html> (accessed 09/30).
- Collet, P. and Rennard, J. (2007), "Stochastic Optimization Algorithms", *arXiv preprint arXiv:0704.3780*.
- Corey, A. T. and Rathjens, C. H. (1956), "Effect of Stratification on Relative Permeability", *Journal of Petroleum Technology*, vol. 8, no. 12, pp. 69-71.
- Craig, F. J. (1971), "The Reservoir Engineering Aspects of Waterflooding", *Society of Petroleum Engineers of AIME*.
- Dahl-Olsen, H., Narasimhan, S. and Skogestad, S. (2008), "Optimal Output Selection for Control of Batch Processes", *American Control Conference, 2008*, June 11-13, 2008, Washington, USA, pp. 2870.
- Dahl-Olsen, H. and Skogestad, S. (2009), "Near-Optimal Control of Batch Processes by Tracking of Approximated Sufficient Conditions of Optimality", *Proc. of AIChE Annual Meeting*, 11 Nov., 2009, Nashville, TN.
- Dietrich, J. K. (1990), "Steamflooding in a Waterdrive Reservoir: Upper Tulare Sands South Belridge Field", *SPE Reservoir Engineering*, vol. 5, no. 03, pp. 275-284.
- Dilib, F. A. and Jackson, M. D. (2013a), "Closed-Loop Feedback Control for Production Optimization of Intelligent Wells under Uncertainty", *SPE Journal Paper 150096-PA*, pp. 345-357.
- Dilib, F. A., Jackson, M. D. and Khairullin, A. Y. (2013b), "Field Production Optimization using Closed-Loop Direct Feedback Control of Intelligent Wells: Application to the Brugge Model", *SPE Annual Technical Conference and Exhibition*, 30 September - 20 October, 2013, New Orleans, Louisiana, USA, Society of Petroleum Engineers, SPE, pp. 1-12.
- Durlofsky, L. J. and Aziz, K. (2002), "Optimization of Smart Well Control", *SPE International Thermal Operations and Heavy Oil Symposium and*

International Horizontal Well Technology Conference, 4-7 November 2002, Calgary, Alberta, Canada, .

Environmental Management in Oil and Gas Exploration and Production (2004), *Overview of the Oil and Gas Exploration and Production Process*, available at: http://www.etechnicalinternational.org/new_pdfs/lessImpact/AttAoverview.pdf (accessed Jul/04).

ExxonMobil (2014), *The Outlook for Energy: A View to 2040*, available at: <http://corporate.exxonmobil.com/en/energy/energy-outlook> (accessed 09/29).

Foss, B. and Jensen, J. P. (2011), "Performance Analysis for Closed-Loop Reservoir Management", *SPE Journal*, vol. 16, no. 1, pp. 183-190.

Fotiou, I. A., Rostalski, P., Parrilo, P. A. and Morari, M. (2006), "Parametric Optimization and Optimal Control using Algebraic Geometry Methods", *International Journal of Control*, vol. 79, no. 11, pp. 1340-1358.

Ganping, L. and Jun, H. (2011), "Iterative Learning Control for Batch Processes based on Support Vector Regression Model with Batchwise Error Feedback", *Proceedings of the 2nd International Conference on Intelligent Control and Information Processing, ICICIP 2011*, pp. 952.

Girei, S. A., Cao, Y., Grema, A. S., Ye, L. and Kariwala, V. (2014), "Data-Driven Self-Optimizing Control", *24TH European Symposium on Computer Aided Process Engineering (ESCAPE 24)*, 15-18, June, Budapest, Hungary, .

Gonzalez, K. G., Bashbush, J. L. and Rincon, A. C. (2009), "Simulation Study of Steamflooding with Horizontal Producers Using PEBI Grids", *Latin American and Caribbean Petroleum Engineering Conference*, 31 May - 3 June, 2009, Cartagena, Columbia, Society of Petroleum Engineers.

Grebenkin, I. and Davies, D. R. (2010), "Analysis of the Impact of an Intelligent Well Completion on the Oil Production Uncertainty", *SPE Russian Oil and Gas Technical Conference and Exhibition*, 26-28 October, 2010, Moscow, Russia, Society of Petroleum Engineers, SPE.

Guo, B., Lyons, W. C. and Ghalambor, A. (2007), *Petroleum Production Engineering (A Computer Assisted Approach)*, Elsevier Science & Technology Books.

Halliburton Corporation (2001), *Basic Petroleum Geology and Log Analysis*, Halliburton Corporation, Houston, United States of America.

Halvorsen, I. J., Skogestad, S., Morud, J. C. and Alstad, V. (2003), "Optimal Selection of Controlled Variables", *Ind. Eng. Chem Res.*, vol. 42, no. 14, pp. 3273-3284.

- Haupt, R. L. and Haupt, S. E. (2004), *Practical Genetic Algorithms*, Second ed, John Wiley & Sons, Inc., Hoboken, New Jersey.
- Holm, W. L. (1987), "Evolution of the Carbon Dioxide Flooding Processes", *Journal of Petroleum Technology*, vol. 39, no. 11, pp. 1,337-1,342.
- Hori, E. S. and Skogestad, S. (2008), "Selection of Controlled Variables: Maximum Gain Rule and Combination of Measurements", *Industrial & Engineering Chemistry Research*, vol. 47, no. 23, pp. 9465-9471.
- Hu, W., Umar, L. M., Xiao, G. and Kariwala, V. (2012), "Self-Optimizing Control of Constrained processes", *Journal of Process Control*, vol. 22, no. 2, pp. 488-493.
- Janert, P. K. (2013), *Feedback Control for Computer Systems*, O'Reilly Media, Inc.
- Jansen, J. D. (2011), "Adjoint-based Optimization of Multi-Phase Flow through Porous Media—A Review", *Computers & Fluids*, vol. 46, no. 1, pp. 40-51.
- Jansen, J. D., Brouwer, D. R., Naevdal, G. and van Kruijsdijk, C. P. J. W. (2005), "Closed-Loop Reservoir Management", *First Break*, vol. 23, no. 1, pp. 43-48.
- Jansen, J. D., Bosgra, O. H. and Van den Hof, P. M. J. (2008), "Model-based Control of Multiphase Flow in Subsurface Oil Reservoirs", *Journal of Process Control*, vol. 18, no. 9, pp. 846-855.
- Jansen, J., Brouwer, R. and Douma, S. G. (2009), "Closed Loop Reservoir Management", *SPE Reservoir Simulation Symposium*, 2-4 February 2009, Society of Petroleum Engineers, The Woodlands, Texas, .
- Johnny, E. (2012), *Lecture on EOR*, available at: <http://www.studyblue.com/notes/n/lecture-15-eor/deck/2637903> (accessed 09/30).
- Joshi, S., Wood, M. C., Castanier, L. M. and Brigham, W. E. (1995), "Steamflooding a Waterflooded Reservoir--Performance Evaluation and Prediction", *SPE Western Regional Meeting*, 8-10 March, 1995, Bakersfield, CA, U.S.A., Society of Petroleum Engineers, .
- Kariwala, V. and Cao, Y. (2009), "Bidirectional Branch and Bound for Controlled Variable Selection. Part II: Exact Local Method for Self-Optimizing Control", *Computers & Chemical Engineering*, vol. 33, no. 8, pp. 1402-1412.
- Kariwala, V. and Cao, Y. (2010), "Bidirectional Branch and Bound for Controlled Variable Selection Part III: Local Average Loss Minimization", *Industrial*

Informatics, IEEE Transactions on Industrial Informatics, vol. 6, no. 1, pp. 54-61.

- Let, K. P. M. S., Manichand, R. N., Suriname, S. and Serigh, R. S. (2012), "Polymer Flooding a~ 500-cp Oil", *SPE Improved Oil Recovery Symposium*, 14-18 April, 2012, Tulsa, Oklahoma, USA, Society of Petroleum Engineers.
- Lie, K., Krogstad, S., Ligaarden, I. S., Natvig, J. R., Nilsen, H. M. and Skaflestad, B. (2012), "Open-Source MATLAB Implementation of Consistent Discretisations on Complex Grids", *Computational Geosciences*, vol. 16, no. 2, pp. 297-322.
- Lorentzen, R. J., Berg, A., Naevdal, G. and Vefring, E. H. (2006), "A New Approach for Dynamic Optimization of Waterflooding Problems", *Intelligent Energy Conference and Exhibition*, 11-13 April 2006, Society of Petroleum Engineers, Amsterdam, The Netherlands.
- Lorentzen, R.J., Shafieirad, A. and Naevdal, G., (2009), *Closed Loop Reservoir Management Using the Ensemble Kalman Filter and Sequential Quadratic Programming*, Society of Petroleum Engineers, The Woodlands, Texas.
- Martin, F. D. and Taber, J. J. (1992), "Carbon Dioxide Flooding", *JPT Journal of Petroleum Technology*, vol. 44, no. 4, pp. 396-400.
- Mayne, D. Q., Rawlings, J. B., Rao, C. V. and Scokaert, P. O. M. (2000), "Constrained Model Predictive Control: Stability and Optimality", *Automatica*, vol. 36, no. 6, pp. 789-814.
- Meum, P., Tøndel, P., Godhavn, J. and Aamo, O. M. (2008), "Optimization of Smart Well Production through Nonlinear Model Predictive Control", *Intelligent Energy Conference and Exhibition*, 25-27 February 2008, Society of Petroleum Engineers, Amsterdam, The Netherlands.
- Mody, B. G. and Dabbous, M. K. (1989), "Reservoir Sweep Improvement With Cross-Linked Polymer Treatments", *Middle East Oil Show*, 11-14 March 1989, Society of Petroleum Engineers, Bahrain.
- Mungan, N. (1981), "Carbon Dioxide Flooding-Fundamentals", *Journal of Canadian Petroleum Technology*, vol. 20, no. 01, pp. 87-92.
- Muskat, M. and Wyckoff, R. D. (1933), "A Theoretical Analysis of Water-Flooding Networks", *Transactions of the AIME*, vol. 107, no. 01, pp. 62-65.
- Naevdal, G., Brouwer, D. R. and Jansen, J. -. (2006), "Waterflooding using Closed-Loop Control", *Computational Geosciences*, vol. 10, no. DOI: 10.1007/s10596-005-9010-6, pp. 37-60.

- Needham, R. B. and Doe, P. H. (1987), "Polymer Flooding Review", *Journal of Petroleum Technology*, vol. 39, no. 12, pp. 1,503-1,507.
- Odi, U. and Gupta, A. (2010), "Optimization and Design of Carbon Dioxide Flooding", *Abu Dhabi International Petroleum Exhibition and Conference*, 1-4 November, 2010, Abu Dhabi, UAE, Society of Petroleum Engineers .
- Overbeek, K. M., Brouwer, D. R., Naevdal, G. and van Kruijsdijk, C. P. J. W. (2004), "Closed-Loop Waterflooding", *9th European Conference on the Mathematics of Oil Recovery (ECOMOR IX)*, August 28 - September 2, Cannes, France.
- Pingping, S. and Wen, S. (1998), "In-Door Study of Hydrocarbon Miscible Flooding Cases", *SPE International Oil and Gas Conference and Exhibition in China*, 2-6 November, 1998, Beijing, China, Society of Petroleum Engineers.
- Qin, S. J. and Badgwell, T. A. (2003), "A Survey of Industrial Model Predictive Control Technology", *Control Engineering Practice*, vol. 11, no. 7, pp. 733-764.
- Saputelli, L., Nikolaou, M. and Economides, M. J. (2006), "Real-Time Reservoir Management: a Multi-Scale Adaptive Optimization and Control Approach", *Computational Geosciences*, vol. 10, no. 1, pp. 61-96.
- Sarma, P. (2006), *Efficient Closed-Loop Optimal Control of Petroleum Reservoirs under Uncertainty* (PhD Thesis), Stanford University .
- Sarma, P., Aziz, K. and Durlofsky, L. J. (2005), "Implementation of Adjoint Solution for Optimal Control of Smart Wells", *2005 SPE Reservoir Simulation Symposium*, 31 Jan - 2 Feb., 2005, Houston, Texas USA, SPE.
- Sarma, P., Durlofsky, L. J. and Aziz, K. (2008), "Computational Techniques for Closed-Loop Reservoir Modeling with Application to a Realistic Reservoir", *Petroleum Science and Technology*, vol. 26, no. 10-11, pp. 1120-1140.
- Sarma, P., Durlofsky, L. J., Aziz, K. and Chen, C. (2006), "Efficient Real-Time Reservoir Management using Adjoint-Based Optimal Control and Model Updating", *Computational Geosciences*, vol. 10, no. DOI:10.1007/s10596-005-9000-z, pp. 3-36.
- Sarma, P., Chen, W. H., Durlofsky, L. J. and Aziz, K. (2008), "Production Optimization with Adjoint Models under Nonlinear Control-State Path Inequality Constraints", vol. 11, no. 2, pp. 326-326-339.
- Shaw, J. and Bachu, S. (2002), "Screening, Evaluation, and Ranking of Oil Reservoirs Suitable for CO₂ Flood EOR and Carbon Dioxide

- Sequestration", *Journal of Canadian Petroleum Technology*, vol. 41, no. 9, pp. 51-61.
- Singh, S. P. and Kiel, O. G. (1982), "Waterflood Design (Pattern, Rate, and Timing)", *International Petroleum Exhibition and Technical Symposium of the Society of Petroleum Engineers*, Vol. 1, 18-26 March, 1982, Beijing, China, pp. 203-219.
- Sintef (2014a), *About SINTEF*, available at: <http://www.sintef.no/home/About-us/> (accessed 10/09).
- Sintef (2014b), *MRST Documentation Page*, available at: <http://www.sintef.com/Projectweb/MRST/> (accessed 06/28).
- Skogestad, S. (2000), "Plantwide Control: the Search for the Self-Optimizing Control Structure", *J. Process Control*, vol. 10, no. 5, pp. 487 - 507.
- Skogestad, S. (2004), "Near-Optimal Operation by Self-Optimizing Control: From Process Control to Marathon Running and Business Systems", *Comp. Chem Eng.*, vol. 29, no. 1, pp. 127-137.
- Skogestad, S. and Postlethwaite, I. (1996), *Multivariable Feedback Control: Analysis and Design*, 1st ed, John Wiley & Sons, Chichester, UK.
- Sudaryanto, B. and Yortsos, Y. C. (2000), "Optimization of Fluid Front Dynamics in Porous Media using Rate Control. I. Equal Mobility Fluids", *Physics of Fluids*, vol. 12, no. 7, pp. 1656-1670.
- Sudaryanto, B. and Yortsos, Y. C. (2001), "Optimization of Displacements in Porous Media using Rate Control", *SPE Annual Technical Conference and Exhibition*, 30 September-3 October 2001, Society of Petroleum Engineers Inc., New Orleans, Louisiana.
- Tatjewski, P. (2007), *Advanced Control of Industrial Processes: Structures and Algorithms*, Springer, London.
- Tavassoli, Z., Carter, J. N. and King, P. R. (2004), "Errors in History Matching", *Society of Petroleum Engineers, SPE*, 10.2118/86883-PA, , pp. 352-361.
- Umar, L. M., Hu, W., Cao, Y. and Kariwala, V. (2012), "Selection of Controlled Variables using Self-Optimizing Control Method", in Rangaiah, G. P. and Kariwala, V. (eds.) *Plantwide Control: Recent Developments and Applications*, First ed, John Wiley & Sons, Ltd, , pp. 43-71.
- Van Doren, J., Douma, S., Wassing, B., Kraaijevanger, H. and De Zwart, B. (2011), "Adjoint-based Optimization of Polymer Flooding", *SPE Enhanced Oil Recovery Conference*, 19-21 July, 2011, Kuala Lumpur, Malaysia, Society of Petroleum Engineers, .

- van Essen, G. M., Van den Hof, P. M. J. and Jansen, J. -. (2013), "A Two-Level Strategy to Realize Life-Cycle Production Optimization in an Operational Setting", *Society of Petroleum Engineers, SPE Journal*, no. 10.2118/149736-PA, pp. 1057-1066.
- van Essen, G., Zandvliet, M., Van den Hof, P., Bosgra, O. and Jansen, J. (2009), "Robust Waterflooding Optimization of Multiple Geological Scenarios", *SPE Journal SPE-102913-PA*, , pp. 202-210.
- Verma, K. and Giesbrecht, P. (1985), "Hydrocarbon Miscible Flood: Field Facility Design", *SPE Production Technology Symposium*, 11-12 November, 1985, Society of Petroleum Engineers, Lubbock, Texas, .
- Virnovsky, G. A. (1988), "On Optimal Control of Multiphase Porous Flow in an Oil Bed", *Comput. Math. Phys.*, vol. 28, no. 3, pp. 156-163.
- Virnovsky, G. A. (1991), "Water Flooding Strategy Design using Optimal Control Theory", *The Sixth European IOR Symposium*, 21-23 May, Stavanger, Norway.
- Völcker, C., Jorgensen, J. B. and Stenby, E. H. (2011), "Oil Reservoir Production Optimization using Optimal Control", *2011 50th IEEE Conference on Decision and Control and European Control Conference, CDC-ECC 2011*, 12 -15 December 2011, Orlando, FL, pp. 7937.
- Walter, E. (2014), *Numerical Methods and Optimization*, Springer, New York.
- Wang, C., Li, G. and Reynolds, A. C. (2009), "Production Optimization in Closed-Loop Reservoir Management", *Society of Petroleum Engineers, SPE Journal*, no. 10.2118/109805-MS, pp. 506-523.
- Wang, P. (2003), *Development and Applications of Production Optimization Techniques for Petroleum Fields* (PhD Thesis), Stanford University.
- Wei, L., Ramirez, W. F. and Qi, Y. F. (1993), "Optimal Control of Steamflooding", *SPE Advanced Technology Series*, vol. 1, no. 02, pp. 73-82.
- Ye, L., Cao, Y., Li, Y. and Song, Z. (2012), "A Data-Driven Approach for Selecting Controlled Variables", *Proceedings of 8th IFAC Symposium on Advanced Control of Chemical Processes (ADCHEM), The International Federation of Automatic Control*, 10-13 July, 2013, Singapore, Furama, Riverfront, Singapore, pp. 904-909.
- Ye, L., Cao, Y., Li, Y. and Song, Z. (2013a), "Approximating Necessary Condition of Optimality as Controlled Variables", *Ind. Eng. Chem Res.*, vol. 52, no. 2, pp. 798-808.

Ye, L., Kariwala, V. and Cao, Y. (2013b), "Dynamic Optimization for Batch Processes with Uncertainties via Approximating Invariant", *Industrial Electronics and Applications (ICIEA), 2013 8th IEEE Conference on*, 19-21 June 2013, Melbourne, VIC, IEEE, pp. 1786.

Yeten, B., Durlafsky, L. J. and Aziz, K. (2002), "Optimization of Smart Well Control", *SPE/PS-CIM/CHOA International Thermal Operations and Heavy Oil Symposium and International Horizontal Well Technology Conference*, Vol. SPE-79031-MS, 4-7 November, 2002, Calgary, Alberta, Canada, Society of Petroleum Engineers, .

Yeten, B., Durlafsky, L. J. and Aziz, K. (2003), "Optimization of Nonconventional Well Type, Location, and Trajectory", *SPE Journal*, SPE-86880-PA, vol. 8, no. 3, pp. 200-210.

APPENDICES

Appendix A Some Basic Concepts

Some properties of reservoir fluids that are important but have not been explained in detail are given. However, only oil and water properties will be considered, as only two-phase flow is assumed in the entire work. In addition to these, a detailed classification of recovery mechanisms is also given.

A.1 Properties of Reservoir Oil

Important oil properties include:

- Density
- Bubble point pressure
- Viscosity
- Surface tension
- Formation volume factor

Density: Oil density is defined as mass per its unit volume at a given temperature and pressure. Most times, specific gravity is used instead of density which is the ratio of the density of oil to that of water both measured at 60°F and atmospheric pressure.

$$\gamma_o = \frac{\rho_o}{\rho_w} \quad (\text{A-1})$$

where γ_o is specific gravity of oil, ρ_o and ρ_w are densities of oil and water respectively. Another gravity scale that is preferable in the petroleum industry is the API gravity given by

$$^{\circ}API = \frac{141.5}{\gamma_o} - 131.5 \quad (\text{A-2})$$

The API gravity for oil ranges from 47° API to 10° API for light and heavy crude oil respectively (Ahmed, 2006).

Bubble Point Pressure (p_b): This is the pressure of a hydrocarbon system at which the first gas is liberated from a liquid phase. This property is usually deduced experimentally or from available correlations developed over the years. The correlations assumed that the bubble point pressure is a function of gas solubility, R_s , gas gravity, γ_g , API and temperature. Mathematically, this can be written as

$$p_b = f(R_s, \gamma_g, API, T) \quad \text{(A-3)}$$

Many authors have proposed such correlations including Standing, Glaso, Petroski and Farshad, and so on (Ahmed, 2006).

Viscosity: This is internal resistance to fluid flow. It is an important fluid flow characteristic in porous media and pipelines. Oil viscosities are also determined experimentally through a standard procedure called PVT analysis. In the absence of experimental data, correlations are used for such purpose. Widely used correlations include Beggs-Robinson, Glaso, Chew-Conally and so on (Ahmed, 2006).

Surface Tension: This is defined as an inter-layer force between a liquid phase and its vapour phase. It is a very important property used in designing EOR projects. It is caused by differences in molecular forces in liquid and vapour phases. There are several correlations for estimating this property.

Formation Volume Factor: This is the ratio of volume of oil at reservoir conditions to its volume at standard conditions. This is expressed mathematically as

$$B_o = \frac{(V_o)_{p,T}}{(V_o)_{sc}} \quad (\text{A-4})$$

Where B_o is the formation factor of oil and V_o the oil volume.

Compressibility: It is a change in the volume of oil as a result of change in pressure given as

$$c_o = - \left(\frac{1}{V} \right) \left(\frac{\partial V}{\partial p} \right)_T \quad (\text{A-5})$$

The above expression is for isothermal system whose pressure is above the bubble point. For pressures below the bubble point, oil compressibility is defined as

$$c_o = \frac{-1}{B_o} \frac{\partial B_o}{\partial p} + \frac{B_g}{B_o} \frac{\partial R_s}{\partial p} \quad (\text{A-6})$$

Some of the correlations developed to estimate c_o at pressures above bubble point include Vasquez-Beggs, Petrosky-Farshad and McCains correlatons (Ahmed, 2006)

A.2 Properties of Reservoir Water

Water properties of interest include formation volume factor, B_w , viscosity, μ_w , compressibility, c_w , and gas solubility. These properties are either estimated experimentally or through the use of correlations. For example, Meehan correlation for water viscosity, and Brill and Beggs correlation for water isothermal compressibility.

A.3 Classification of Oil and Gas Recovery Methods

The diagram below gives a detailed classification of recovery mechanisms applied in production of oil and gas

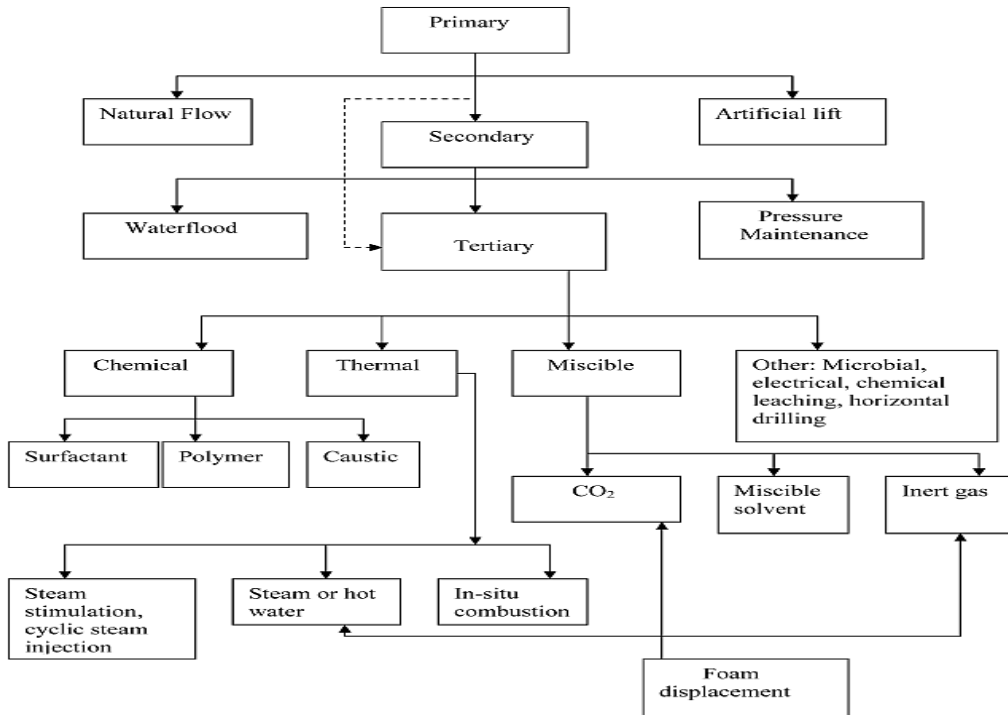


Figure A-1: Oil Recovery Methods (Adeniyi et al., 2008)

Appendix B MATLAB Reservoir Simulation Toolbox (MRST)

B.1 Introduction

The MATLAB Reservoir Simulation Toolbox is an open-source software created with the goal to develop efficient simulation approaches on the basis of accurate and robust discretisation methods. It is developed by SINTEF Applied Mathematics. SINTEF is an independent, non-commercial and largest research organisation in Scandinavia (Sintef, 2014a). MRST was first released in April 2009 with a version MRST 1.1. The latest version is MRST 2014a which was released on the 14th of May, 2014 (Sintef, 2014b). The main focus is on the development of new computational methods, the multiscale approach which will help to shift from the conventional two-point approximation methods that have convergence issues (Lie et al., 2012).

The code development of the software has been divided into two parts (Lie et al., 2012):

- MATLAB was used for prototyping and testing of new ideas.
- Compiled languages such as FORTRAN, C and C++ were used to develop solvers for high computational performance.

B.2 MRST Modules

There are two categories of modules that accompanied MRST, the core and add-on modules. The core modules provide basic functionalities and solvers for single and two-phase flows while the add-on modules are for advanced models, viewers and solvers (Sintef, 2014b).

B.2.1 Core Modules

MRST core modules include the following (Sintef, 2014b):

- Single and two-phase flow pressure and transport solvers
- Functionalities for constructing and visualising structured and unstructured grids
- Functionalities for reading and processing of corner-point grids
- Routines for physical units and properties
- Data bank for structures of reservoir grids, wells, fluids, states, objects, etc
- Stable feature set

Single-Phase Flow Solver

A single-phase flow problem in a porous medium can be represented mathematically by

$$\nabla \cdot v = q \quad (\text{B-1})$$

$$v = -\frac{K}{\mu} \nabla p \quad (\text{B-2})$$

where v is flow rate per unit cross-sectional area, K is the permeability tensor, μ is fluid viscosity and p is the pressure. However, (B-2) is commonly referred to as Darcy's Law, which is an empirical relationship between flow rate and pressure gradient of fluid in a porous medium.

The following simple steps can be followed to simulate a simple single-phase flow problem with the aid of this solver:

1. Define geometry, where grids are generated, for both structured and unstructured. For example, to generate a Cartesian grid, the following statement is used

```
G = cartGrid([nx, ny, nz]);
```

where n_x , n_y , n_z are the number of cells in the x, y and z directions respectively.

After defining the grids, it is needed to be processed so that centroids, volumes of cells, normal and areas for the faces can be computed. This can be done by the command

```
G = computeGeometry(G);
```

2. Define rock and fluid properties: the parameters involved with single-phase pressure equation are permeability and fluid viscosity. For a homogeneous permeability of 100 mD, the following command can be invoked

```
rock.perm = repmat(100*milli*darcy, [G.cells.num, 1]);
```

The viscosity is required for the computation of total mobility which is provided through a fluid object

```
fluid = initSingleFluid('mu',1*centi*poise,'rho',  
1014*kilogram/meter^3);
```

The code above indicates a viscosity of 1 cp and density of 1014 kg/m³.

3. Initialise reservoir simulator: The solutions to the flow problem are combined in a structure. Typical unknowns that are solved include, pressure, saturations and fluxes. The initial values of these are defined as

```
resSol = initResSol(G, 0.0);
```

Here the initial pressure and saturation in the entire grid cells are all equal zero where `resSol` is the solution structure.

4. Set boundary conditions (BCs): the default BC is no flow conditions on all boundaries. Other BCs can be specified such as Dirichlet and Neuman BCs.
5. Form a mimetic pressure linear system of the form

$$Ax = b \tag{B-3}$$

This can be done by simply executing the code

```
S = computeMimeticIP(G, rock);
```

6. The linear system is then solved to obtain solutions of pressures and fluxes. For an incompressible flow, this can be done as

```
resSol = solveIncompFlow(resSol, G, S, fluid, 'bc', bc);
```

7. A typical solution can be plotted for visualization as shown in Figure B-1

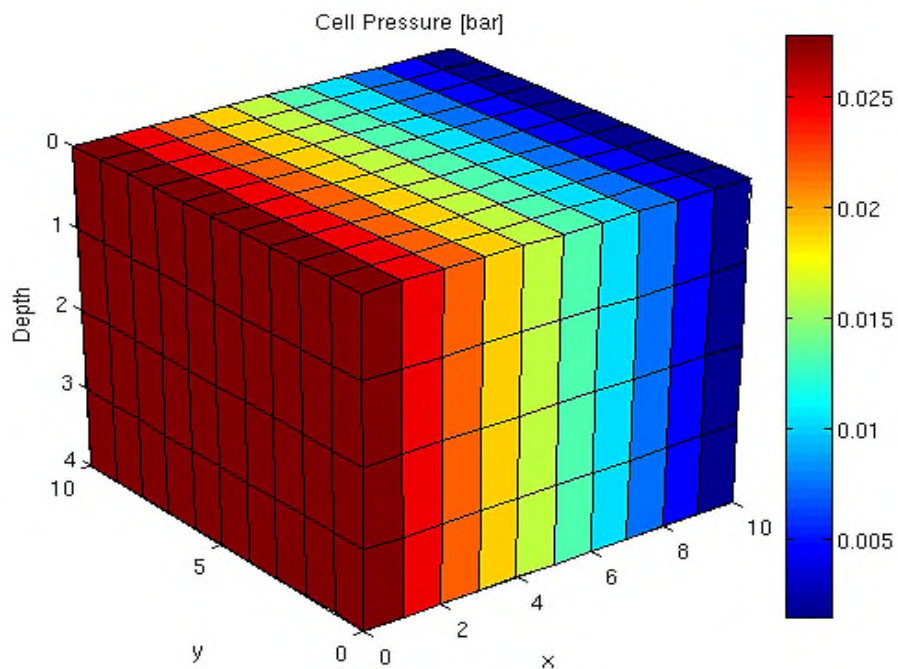


Figure B-1: Pressure Solutions (Sintef, 2014b)

Two-Phase Flow Solver

The two-phase flow problem involving oil and water only can be represented mathematically in a compact form as

$$\nabla \cdot v = q \quad (\text{B-4})$$

$$v = -\lambda K \nabla p \quad (\text{B-5})$$

Where v is the velocity and λ the mobility which is a function of saturation, S . The saturation equation can be written as

$$\phi \frac{\partial S_w}{\partial t} + \nabla \cdot (f_w(S_w)v) = q_w \quad (\text{B-6})$$

where S_w is water saturation, q_w is water source term, ϕ is rock porosity, and f_w is Buckley-Leverett fractional flow. The step-by-step procedures employed for single-phase system can be applied here. In addition the following can be performed:

- The model data can be provided as an external input file, typically, as an industrial standard ECLIPSE file. A simple syntax as the one below can be used to read model data and convert appropriate units because MRST uses SI units

```
grdecl = readGRDECL(grdecl);  
usys = getUnitSystem('METRIC');  
grdecl = convertInputUnits(grdecl, usys);
```

- Rock properties of a complex reservoir system can be plotted, for example, the permeability of a realistic reservoir can be visualised as shown in Figure B-2.

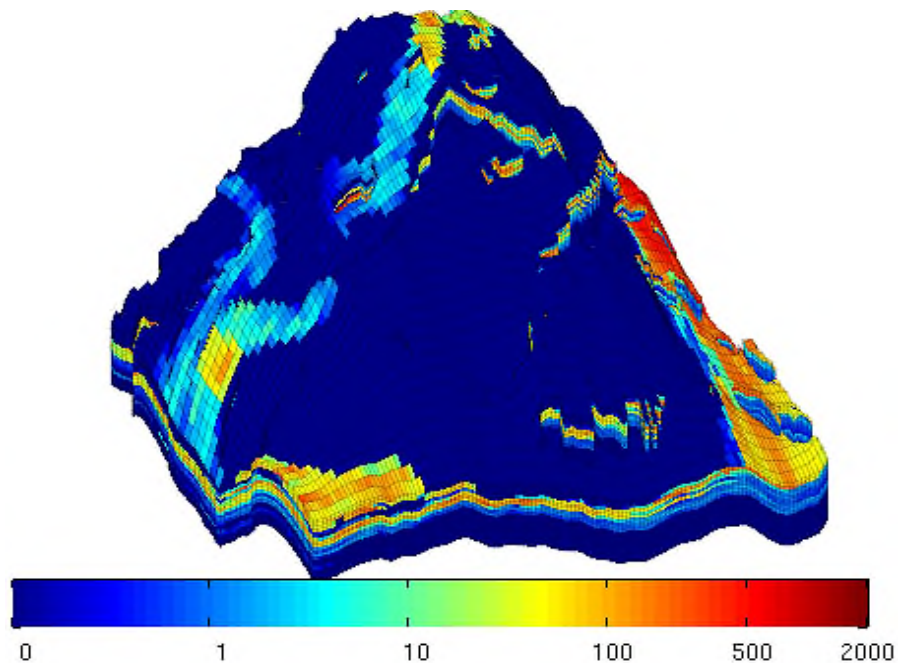


Figure B-2: Permeability Field of Realistic Reservoir (Sintef, 2014b)

- Wells can be added to the reservoir through which fluids are produced or injected. Wells are described using a Peaceman's model and can be either rate- or pressure-controlled. The following codes introduced wells into reservoir system:

```
W = addWell([], G, rock, 1 : nx*ny : nx*ny*nz, ...
            'Type', 'rate', 'Val', 1/day, ...
            'Radius', 0.1, 'Comp_i', [1, 0]);
W = addWell(W, G, rock, nx : ny : nx*ny, ...
            'Type', 'bhp', 'Val', 1*barsa, ...
            'Radius', 0.1, 'Dir', 'y', 'Comp_i', [0, 1]);
```

The codes above drilled two wells, one vertical injection well that is rate-controlled with an injection rate of 1 m³/day and a horizontal producer controlled by a bottomhole pressure fixed at 1 bar. A typical reservoir-well system can be visualised, thus

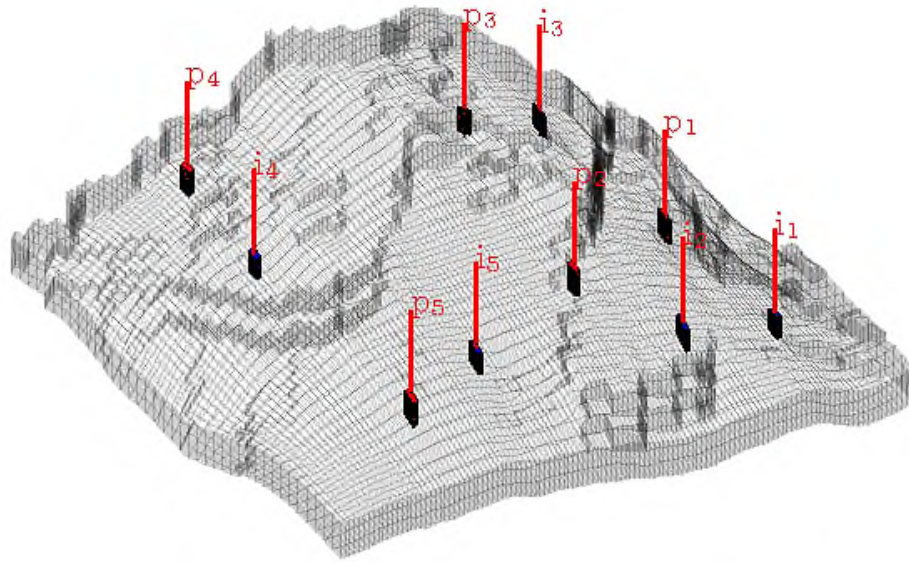


Figure B-3: A Typical Reservoir - Well System (Sintef, 2014b)

Some Grids Generated by MRST

1. Triangular grids

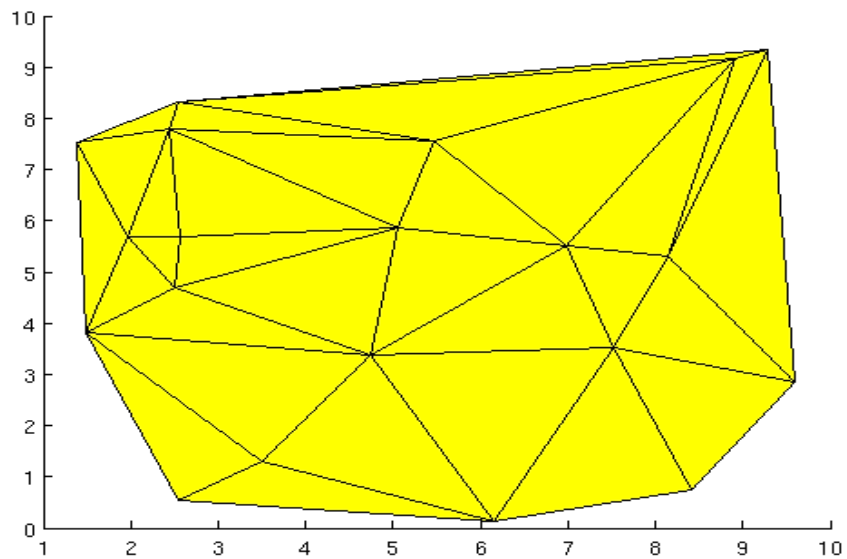


Figure B-4: Triangular Grid (Sintef, 2014b)

2. Extruded Triangular Grid

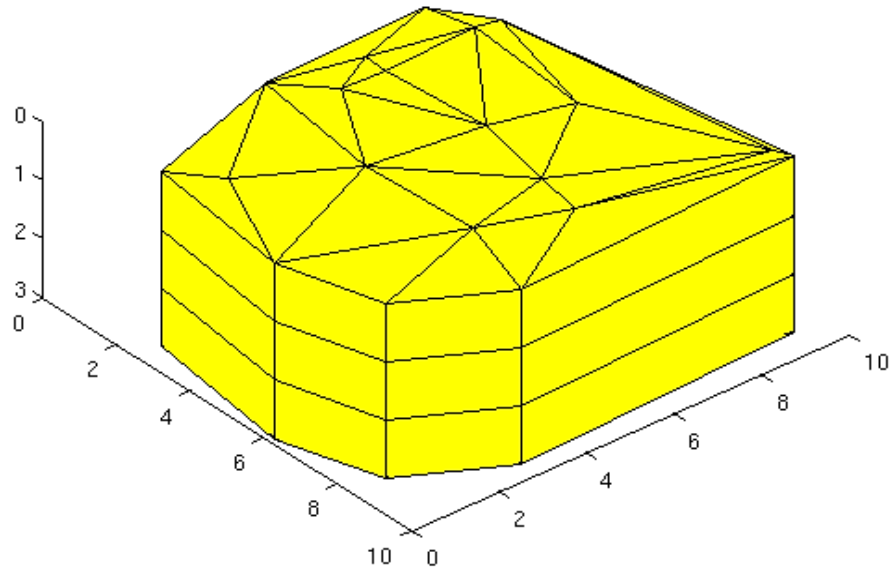


Figure B-5: Extruded Triangular Grid (Sintef, 2014b)

3. Eclipse Standard Grids (GRDECL)

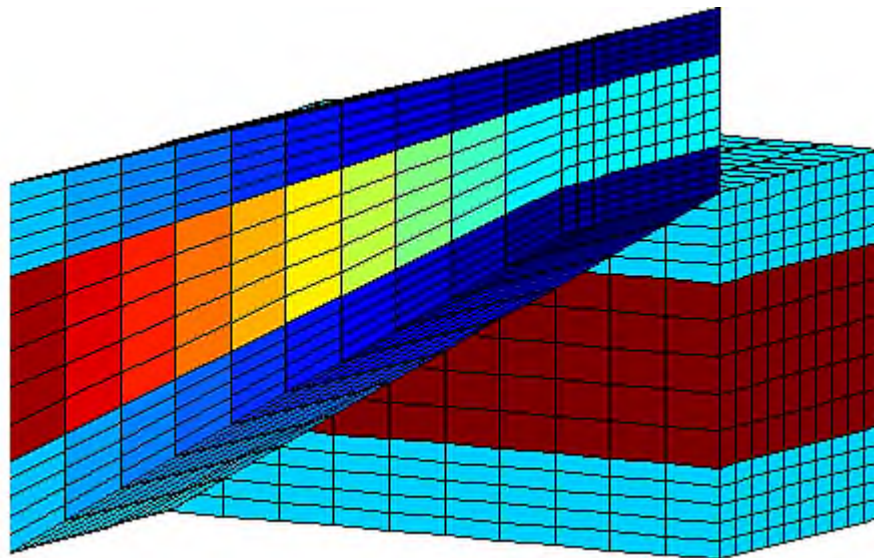


Figure B-6: GRDECL Structures (Sintef, 2014b)

B.2.2 Add-on Modules

MRST add-on modules include:

- Modifications of MRST core functionalities.
- Advanced solvers such as black-oil solver, see Figure B-7.
- Multiscale solvers and model reduction
- CO₂ modules
- Upscaling and coarsening module

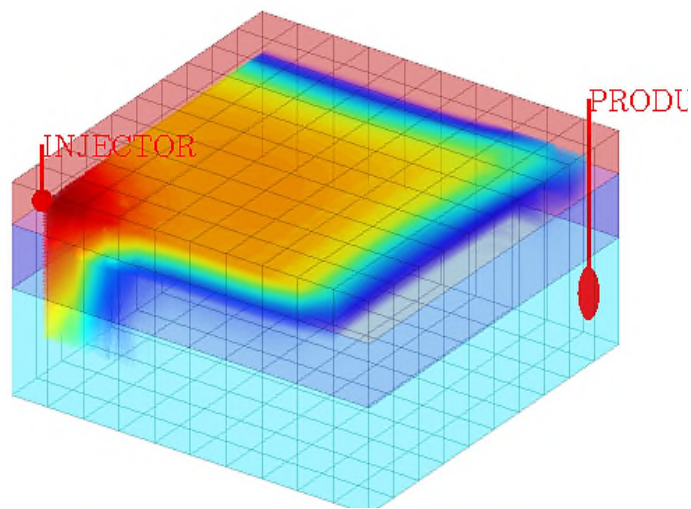


Figure B-7: Black Oil Simulation (Sintef, 2014b)

